ISSN 0021-9673

VOL. 596 NO. 2 APRIL 10, 1992

THIS ISSUE COMPLETES VOL. 596

JOURNAL OF CHROMATOGRAPHY

INCLUDING ELECTROPHORESIS AND OTHER SEPARATION METHODS

ELSEVIER

JOURNAL OF CHROMATOGRAPHY

INCLUDING ELECTROPHORESIS AND OTHER SEPARATION METHODS

Scope. The *Journal of Chromatography* publishes papers on all aspects of chromatography, electrophoresis and related methods. Contributions consist mainly of research papers dealing with chromatographic theory, instrumental development and their applications. The section *Biomedical Applications*, which is under separate editorship, deals with the following aspects: developments in and applications of chromatographic and electrophoretic techniques related to clinical diagnosis or alterations during medical treatment; screening and profiling of body fluids or tissues with special reference to metabolic disorders; results from basic medical research with direct consequences in clinical practice; drug level monitoring and pharmacokinetic studies; clinical toxicology; analytical studies in occupational medicine.

Submission of Papers. Manuscripts (in English; *four* copies are required) should be submitted to: Editorial Office of *Journal of Chromatography*, P.O. Box 681, 1000 AR Amsterdam, Netherlands, Telefax (+31-20) 5862 304, or to: The Editor of *Journal of Chromatography, Biomedical Applications*, P.O. Box 681, 1000 AR Amsterdam, Netherlands. Review articles are invited or proposed by letter to the Editors. An outline of the proposed review should first be forwarded to the Editors for preliminary discussion prior to preparation. Submission of an article is understood to imply that the article is original and unpublished and is not being considered for publication elsewhere. For copyright regulations, see below.

Publication. The *Journal of Chromatography* (incl. *Biomedical Applications*) has 39 volumes in 1992. The subscription prices for 1992 are:

J. Chromatogr. (incl. *Cum. Indexes, Vols. 551–600*) + *Biomed. Appl.* (Vols. 573–611):
Dfl. 7722.00 plus Dfl. 1209.00 (p.p.h.) (total *ca.* US$ 4880.25)

J. Chromatogr. (incl. *Cum. Indexes, Vols. 551–600*) only (Vols. 585–611):
Dfl. 6210.00 plus Dfl. 837.00 (p.p.h.) (total *ca.* US$ 3850.75)

Biomed. Appl. only (Vols. 573–584):
Dfl. 2760.00 plus Dfl. 372.00 (p.p.h.) (total *ca.* US$ 1711.50).

Subscription Orders. The Dutch guilder price is definitive. The US$ price is subject to exchange-rate fluctuations and is given as a guide. Subscriptions are accepted on a prepaid basis only, unless different terms have been previously agreed upon. Subscriptions orders can be entered only by calender year (Jan.–Dec.) and should be sent to Elsevier Science Publishers, Journal Department, P.O. Box 211, 1000 AE Amsterdam, Netherlands, Tel. (+31-20) 5803 642, Telefax (+31-20) 5803 598, or to your usual subscription agent. Postage and handling charges include surface delivery except to the following countries where air delivery via SAL (Surface Air Lift) mail is ensured: Argentina, Australia, Brazil, Canada, China, Hong Kong, India, Israel, Japan*, Malaysia, Mexico, New Zealand, Pakistan, Singapore, South Africa, South Korea, Taiwan, Thailand, USA. *For Japan air delivery (SAL) requires 25% additional charge of the normal postage and handling charge. For all other countries airmail rates are available upon request. Claims for missing issues must be made within three months of our publication (mailing) date, otherwise such claims cannot be honoured free of charge. Back volumes of the *Journal of Chromatography* (Vols. 1–572) are available at Dfl. 217.00 (plus postage). Customers in the USA and Canada wishing information on this and other Elsevier journals, please contact Journal Information Center, Elsevier Science Publishing Co. Inc., 655 Avenue of the Americas, New York, NY 10010, USA, Tel. (+1-212) 633 3750, Telefax (+1-212) 633 3990.

Abstracts/Contents Lists published in Analytical Abstracts, Biochemical Abstracts, Biological Abstracts, Chemical Abstracts, Chemical Titles, Chromatography Abstracts, Clinical Chemistry Lookout, Current Contents/Life Sciences, Current Contents/Physical, Chemical & Earth Sciences, Deep-Sea Research/Part B: Oceanographic Literature Review, Excerpta Medica, Index Medicus, Mass Spectrometry Bulletin, PASCAL-CNRS, Pharmaceutical Abstracts, Referativnyi Zhurnal, Research Alert, Science Citation Index and Trends in Biotechnology.

See inside back cover for Publication Schedule, Information for Authors and information on Advertisements.

0021-9673/92/$05.00

This issue is printed on acid-free paper.

Printed in the Netherlands

CONTENTS

(Abstracts/Contents Lists published in Analytical Abstracts, Biochemical Abstracts, Biological Abstracts, Chemical Abstracts, Chemical Titles, Chromatography Abstracts, Current Contents/Life Sciences, Current Contents/Physical, Chemical & Earth Sciences, Deep-Sea Research/Part B: Oceanographic Literature Review, Excerpta Medica, Index Medicus, Mass Spectrometry Bulletin, PASCAL-CRNS, Referativnyi Zhurnal, Research Alert and Science Citation Index)

REGULAR PAPERS

Column Liquid Chromatography

Gas Chromatography

(Continued overleaf)

Contents (continued)

In articles with more than one author, the name of the author to whom correspondence should be addressed is indicated in the article heading by a 6-pointed asterisk (*).

Journal of Chromatography, 596 (1992) 151–156
Elsevier Science Publishers B.V., Amsterdam

CHROM. 23 987

Preparation and characterization of mixed functional phase silica materials using phenyl-, butyl- or octylchlorosilane as a silylating agent

Jun Haginaka* and Junko Wakai

Faculty of Pharmaceutical Sciences, Mukogawa Women's University, 11–68, Koshien Kyuban-cho, Nishinomiya, Hyogo 663 (Japan)

(First received September 6th, 1991; revised manuscript received December 31st, 1991)

ABSTRACT

Mixed functional phase (MFP) silica materials having phenyl–diol, butyl–diol and octyl–diol phases were prepared for direct injection analysis of drugs in serum. The MFP materials were synthesized from a porous silica gel of 9 nm pore size in two steps; introduction of a hydrophobic (phenyl, butyl or octyl) phase using the corresponding trichlorosilane as a silylating agent and introduction of a glycerylpropyl (*i.e.*, diol) phase using 3-glycidoxypropyltrimethoxysilane in an aqueous medium (pH 3.5). By changing the density of the hydrophobic and hydrophilic ligands, proteins were completely recovered from the prepared MFP materials in the first injection. The MFP materials can be used for direct injection analysis of hydrophobic and hydrophilic drugs in serum.

INTRODUCTION

Recently, various types of restricted access packings or packings with surface barriers have been developed for sample clean-up or assays of drugs in biological fluids [1–3]. In previous papers [4.5], we reported a synthetic method for mixed functional phase (MFP) silica materials having phenyl, butyl or octyl groups as a hydrophobic phase and diol groups as a hydrophilic phase for direct serum injection assays of drugs. The MFP materials were prepared in three or four steps: introduction of a 3-glycidoxypropyl phase, introduction of a phenyl phase and hydrolysis of the oxirane ring to a diol phase, and three steps plus further introduction of diol phases. In the above method, phenyl-, butyl- or octylalkoxysilane was used as a silylating agent. It is difficult to introduce an octyl phase owing to the low reactivity of the corresponding alkoxysilane. Also, the packing materials obtained had the disadvantages of low column efficiency and bad batch-to-batch reproducibility. Recently, we reported an improved preparation method for an MFP material in two steps; introduction of a phenyl phase and introduction of a glycerylpropyl (*i.e.*, diol) phase [6]. The MFP materials also showed high column efficiency and good batch-to-batch reproducibility.

This paper deals with the preparation of MFP materials having phenyl, butyl or octyl groups as a hydrophobic ligand by using the corresponding trichlorosilane as a silylating agent. They were characterized by physical and retention properties and applied to direct serum injection assays of hydrophobic and hydrophilic drugs.

EXPERIMENTAL

Reagents and materials

Theobromine and bovine serum albumin (BSA) were purchased from Nacalai Tesque (Kyoto, Japan). HPLC-grade acetonitrile was purchased from Kanto Chemical (Tokyo, Japan) and 3-glycidoxypropyltrimethoxysilane, phenyltrichlorosilane, butyltrichlorosilane and octyltrichlorosilane were from Petrtarch Systems (Bristol, PA, USA). Other reagents of analytical-reagent grade and control human serum (Control Serum I) were purchased from Wako (Osaka, Japan). Phenobarbital, phenytoin,

0021-9673/92/$05.00

carbamazepine, theophylline and caffeine were kindly donated by Sankyo (Tokyo, Japan), Nippon Ciba-Geigy (Takarazuka, Japan) and Eisai (Tokyo, Japan). Develosil 90-5 silica gels (particle size 5 μm; pore size 9 nm; specific surface area 400 m^2/g) were obtained from Nomura Chemicals (Seto, Aichi, Japan).

Water purified with a Nanopure II munit (Barnstead, Boston, MA, USA) was used for the preparation of the eluent and sample solutions.

Preparation of the MFP silica materials

The MFP packing materials were prepared in two steps as shown in Fig. 1.

Introduction of a phenyl, butyl or octyl phase

Amounts of 4 g of Develosil silica gels were dried *in vacuo* over P_2O_5 at 150°C for 6 h and the dry silica gel was added to 120 ml of dry toluene. The mixture was heated at reflux until all the water had been removed as an azeotrope into a Dean–Stark-type trap. Next, 1.26, 0.40 or 0.17 ml of phenyl-, butyl- or octyltrichlorosilane (equivalent to 2.5, 1.5 or 0.45 μmol, respectively, per square metre of surface area) and 0.77, 0.47 or 0.14 ml of pyridine were added to the mixture. After refluxing for 7 h, the reaction mixture was cooled to room temperature, filtered and washed with toluene and methanol. The isolated silica gel was then dried *in vacuo* over P_2O_5 at 60°C for 2 h. The silica materials thus obtained are termed 2.5Ph, 1.5Bu or 0.45Oc silica, taking into account the number of micromoles of phenyl-, butyl- or octyltrichlorosilane per square metre of surface area used for the reaction.

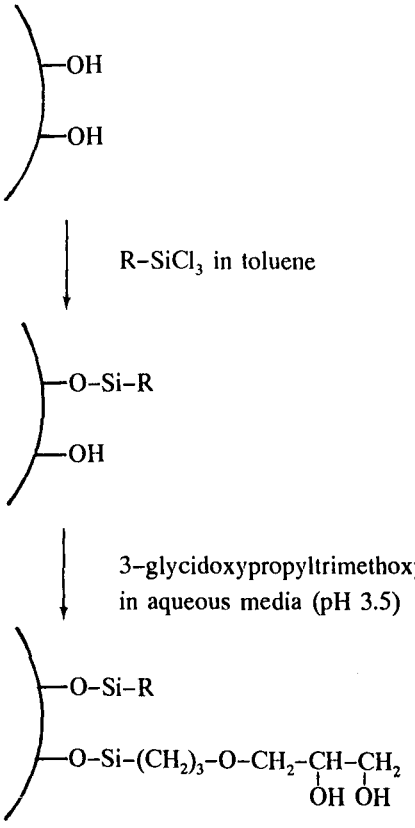

Fig. 1. Synthetic route for the MFP packing materials. R = phenyl, butyl or octyl.

Introduction of a diol phase

To 4 g of the 2.5Ph, 1.5Bu or 0.45Oc silica, 90 ml of queous solutions containing 12.0 ml of 3-glycidoxypropyltrimethoxysilane (34 μmol per square metre of surface area), the pH of which was adjusted to 3.5 by addition of perchloric acid, were added and the mixture was refluxed for 5 h. The mixture was filtered and washed with water and methanol. The isolated silica gel was dried *in vacuo* over P_2O_5 at 60°C for 2 h. The MFP silica materials thus obtained are termed 2.5Ph–34G, 1.5Bu–34G and 0.45Oc–34G silica.

Instrumentation

The reacted amounts of phenyl-, butyl- or octyltrichlorosilane and 3-glycidoxypropyltrimethoxysilane were determined by elemental analysis using an NC-80AUTO analyser (Sumika Chemical Analysis Service, Osaka, Japan).

The prepared MFP materials were packed into 100 × 4.0 mm I.D. stainless-steel tubes by conventional high-pressure slurry-packing procedures.

The chromatographic system was composed of an LC-9A pump, an SPD-6A spectrophotometer, a SIL-6B autoinjector, a C-R4A integrator and an SCL-6B system controller (all from Shimadzu, Kyoto, Japan). The eluents used are specified in the captions of the tables and figures. Detection was performed at 254 or 275 nm. All separations were carried out at ambient temperature.

Preparation of human serum samples

Drugs were dissolved in human serum at a

TABLE I

CARBON CONTENTS AND SURFACE COVERAGES OF THE MFP SILICA PACKING MATERIALS HAVING PHENYL–DIOL PHASES

Silica	Carbon content (%)	Surface coverage (μmol/m^2)	
		Hydrophobic phase	Diol phase
2.5Ph	5.33	2.12	–
2.5Ph–17G	8.94	2.12	1.49
2.5Ph–34G	9.79	2.12	2.30
2.5Ph–68G	11.63	2.12	2.68

known concentration and an appropriate volume of the serum sample was applied to the MFP material after filtration through a 0.22-μm membrane filter (Nippon Millipore, Tokyo, Japan).

Recovery of BSA from the MFP silica material

The recovery of BSA in the first injection from the MFP silica material was determined by measuring the UV absorbance at 280 nm after injection of 100 μl of BSA (10 mg/ml) sample as reported previously [6].

RESULTS AND DISCUSSION

Preparation of the MFP materials having phenyl, butyl or octyl phases as a hydrophobic ligand

Previously, we reported [6] that by using silica of 9-nm pore size as a starting material and preparation in two steps (introduction of a phenyl phase and introduction of a diol phase), the MFP packing materials obtained showed high column efficiency and good batch-to-batch reproducibility. In this study, we prepared the MFP materials having phenyl, butyl or octyl phases as a hydrophobic ligand by the same method except that phenyl-, butyl- or octyltrichlorosilane was used as a silylating agent.

Table I shows the carbon contents and surface coverages of MFP materials having phenyl–diol phases. The introduction of phenyl phases was kept constant by reaction with 2.5 μmol/m^2 of phenyltrichlorosilane with addition of pyridine as a basic catalyst. The amounts of diol phases introduced were varied by changing the amount of 3-glycidoxypropyltrimethoxysilane used for the reaction from 17 to 68 μmol/m^2.

Table II shows the average pore diameters and column efficiencies of the MFP packing materials having phenyl–diol phases and the recovery of BSA in the first injection. It was assumed that the hydrophobic phases introduced were not hydrolysed in

TABLE II

AVERAGE PORE DIAMETERS AND COLUMN EFFICIENCIES OF THE MFP SILICA PACKING MATERIALS HAVING PHENYL–DIOL PHASES AND RECOVERY OF PROTEINS

Silica	Average pore diameter[a] (nm)	Column efficiency[b] (plates per 10 cm)	Recovery of proteins in first injection[c] (%)
2.5Ph–17G	5.0	3700	90
2.5Ph–34G	5.7	4600	100
2.5Ph–68G	5.2	2600	100

[a] Measured by the inverse size-exclusion chromatographic method.

[b] Number of theoretical plates for carbamazepine under the following high-performance liquid chromatography (HPLC) conditions: column, 100 mm × 4.0 mm I.D. packed with MFP silica; eluent, 100 m*M* phosphate buffer (pH 6.9)–acetonitrile (85:15, v/v).

[c] A 100-μl portion of bovine serum albumin (10 mg/ml) was injected on to the column under the HPLC conditions as in footnote *b*.

TABLE III

CARBON CONTENTS AND SURFACE COVERAGES OF THE MFP SILICA PACKING MATERIALS HAVING BUTYL–DIOL AND OCTYL–DIOL PHASES

Silica	Carbon content (%)	Surface coverage (μmol/m^2)	
		Hydrophobic phase	Diol phase
1.0Bu–34G	7.42	0.95	2.58
1.5Bu–34G	7.42	1.76	2.03
2.5Bu–34G	7.71	2.89	1.41
0.3Oc–34G	7.16	0.35	2.58
0.45Oc–34G	7.79	0.51	2.69
0.6Oc–34G	8.61	0.79	2.74

the process of introduction of diol phases, and that diol phases were introduced as a monomeric layer. By introduction of hydrophobic and hydrophilic ligands, the average pore diameter, measured by the inverse size-exclusion chromatographic method reported by Cook and Pinkerton [7], was decreased from 9 to 5–6 nm. The recovery of proteins from the MFP materials in the first injection was 100% except for the 2.5Ph–17G silica, from which proteins were completely recovered in the second injection. The number of theoretical plates (N) was 3700, 4600 and 2600 for carbamazepine for the 2.5Ph–17G, 2.5Ph–34G and 2.5Ph–68G silicas, respectively, packed into a 100 × 4.6 mm I.D. column. Hence the amount of 3-glycidoxypropyltrimethoxysilane used for the reaction was determined to be 34 μmol/m^2.

Table III shows the carbon contents and surface coverages of MFP materials having butyl–diol or octyl–diol phases, where the amount of 3-glycidoxypropyltrimethoxysilane used for the reaction was kept constant at 34 μmol/m^2. Table IV illustrates the same data as in Table II for butyl–diol and octyl–diol phase materials.

These results reveal that the butyl- and octyltrichlorosilane used for the reaction are completely introduced into the silica surface. To recover BSA completely from the MFP materials in the first injection, the amounts of butyl-, and octyltrichlorosilane used for the reaction were 1.5 and 0.45 μmol/

TABLE IV

AVERAGE PORE DIAMETERS AND COLUMN EFFICIENCIES OF THE MFP PACKING MATERIALS HAVING BUTYL–DIOL AND OCTYL–DIOL PHASES AND RECOVERY OF PROTEINS

Silica	Average pore diameter[a] (nm)	Column efficiency[b] (plates per 10 cm)	Recovery of proteins in first injection[c] (%)
1.0Bu–34G	3.8	1400	100
1.5Bu–34G	4.6	2000	100
2.5Bu–34G	4.5	4500	30
0.3Oc–34G	5.7	2300	100
0.45Oc–34G	5.2	2800	100
0.5Oc–34G	5.1	4800	60

[a–c] See footnotes to Table II.

TABLE V

RETENTION PROPERTIES OF ANTICONVULSANT DRUGS AND METHYLXANTHINE DERIVATIVES ON THE MFP SILICA PACKING MATERIALS

Type	Compound	Capacity factor (k')		
		2.5Ph–34G	1.5Bu–34G	0.45Oc–34G
Anticonvulsant drugs[a]	Phenobarbital	1.26	0.95	0.76
	Phenytoin	4.87	3.45	2.59
	Carbamazepine	6.61	4.51	3.92
Methylxanthine derivatives[b]	Theophylline	2.57	0.86	0.75
	Theobromine	3.70	0.93	0.79
	Caffeine	6.82	1.38	1.17

[a] Capacity factors were measured under the following chromatographic conditions: eluent, 100 m*M* phosphate buffer (pH 6.9)–actonitrile (85:15, v/v); flow-rate, 0.6 ml/min.

[b] Capacity factors were measured under the following chromatographic conditions: eluent, 100 m*M* phosphate buffer (pH 6.9)–acetonitrile (23:1, v/v); flow-rate, 0.6 ml/min.

m^2, respectively. Assuming that hydrophilic phases were introduced into phenyl–diol, butyl–diol and octyl–diol materials with almost the same ligand density, the highest ligand density of phenyl phases could be obtained, resulting in complete recovery of proteins in the first injection. This is due to the length and width (*i.e.*, shape) of the substituted hydrophobic ligand on a silanol group: phenyl and butyl phases have maximum lengths of 6.28 and 6.17 Å, respectively, and maximum widths of 4.81 and 5.94 Å, respectively, according to the Sterimol parameter reported by Verloop *et al.* [8]. This indicates that to avoid interaction of hydrophobic ligands with proteins, the butyl–diol materials need a lower hydrophobic ligand density than the phenyl–diol materials when almost the same hydrophilic ligands are introduced. As octyl groups have a maximum length and width of 10.27 and 8.85 Å, respectively, the ligand density should be much smaller than with phenyl and butyl groups. If hydrophilic ligands such as polyoxyethylene groups were used instead of 3-glycerylpropyl (*i.e.*, diol) phases, a higher density of hydrophobic ligands and/or longer ligands such as octadecyl groups could be introduced, as reported by Perry *et al.* [9] and Desilets *et al.* [10] for semi-permeable surface (SPS) materials.

Retention properties of MFP materials having phenyl, butyl or octyl phases as a hydrophobic ligand

Table V shows the retention properties of anticonvulsant drugs and methylxanthine derivatives on the 2.5Ph–34G, 1.5Bu–34G and 0.45Oc–34G silicas. The anticonvulsant drugs were well retained on the all MFP packing materials, whereas 2.5Ph–34G silica was the most suitable for the separation of methylxanthine derivatives, which should be retained by hydrophobic and π-electron interactions. These retention properties were comparable to those on the MFP materials prepared in three or four steps. These results suggest that MFP materials having phenyl–diol phases could be good candidates for direct serum injection assays of hydrophobic and hydrophilic drugs.

Direct injection analysis of drugs in serum

Fig. 2A, B and C show chromatograms from the direct injection analysis of the anticonvulsant drugs phenobarbital, phenytoin and carbamazepine in human serum on the 2.5Ph–34G, 1.5Bu–34G and 0.45Oc–34G silicas, respectively. These drugs were eluted following the elution of serum proteins in the void volume, and were well separated from the background components of serum. The MFP materials prepared in two steps could be used for about 500 repetitive injections of 20-μl serum samples (total 10 ml of serum sample) without a decrease in column efficiency or increase in back-pressure.

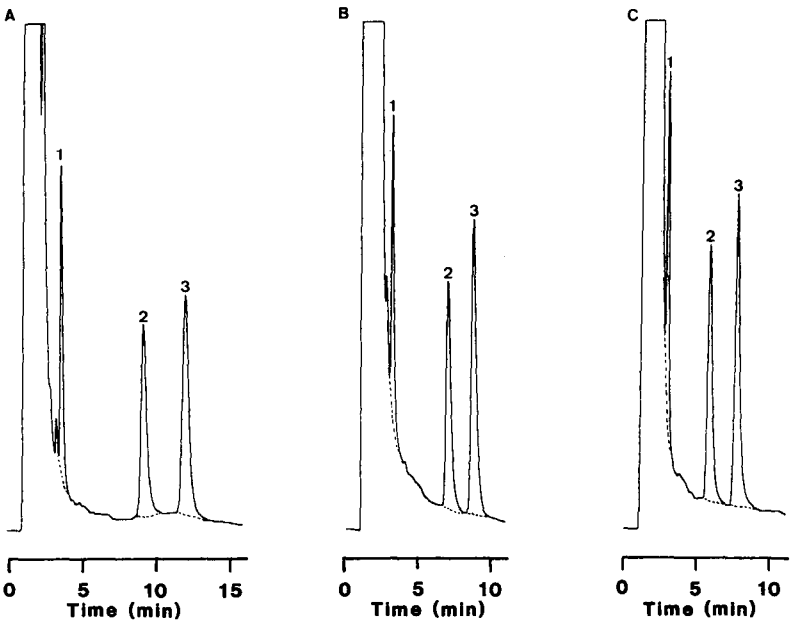

Fig. 2. Chromatograms of control serum spiked with (1) phenobarbital (20 μg/ml), (2) phenytoin (50 μg/ml) and (3) carbamazepine (10 μg/ml) on (A) 2.5Ph–34G, (B) 1.5Bu–34G and (C) 0.45Oc–34G silicas. Chromatographic conditions: column, 100 × 4.0 mm I.D.; eluent, 100 m*M* phosphate buffer (pH 6.9)–CH_3CN (10:1, v/v); flow-rate, 0.6 ml/min; detection, 254 nm; injection volume, 20 μl. Dotted lines indicate serum blank.

CONCLUSION

MFP silica materials having hydrophobic and diol phases were prepared in two steps; introduction of a hydrophobic (phenyl, butyl or octyl) phase using the corresponding trichlorosilane as a silylating agent and introduction of a diol phase using 3-glycidoxypropyltrimethoxysilane in an aqueous medium. The method can be applied to the preparation of MFP packing materials having various functionalities, and the MFP materials could be utilized for direct injection assays of drugs in serum for the purposes of therapeutic drug monitoring and biopharmaceutical studies.

ACKNOWLEDGEMENT

This work was supported in part by Grants-in-Aid from the Research Foundation for Pharmaceutical Sciences.

REFERENCES

1 J. Haginaka, *Trends Anal. Chem.*, 10 (1991) 17.
2 T. C. Pinkerton, *J. Chromatogr.*, 544 (1991) 13.
3 K. K. Unger, *Chromatographia*, 31 (1991) 507.
4 J. Haginaka and J. Wakai, *Chromatographia*, 29 (1990) 23.
5 J. Haginaka, J. Wakai and H. Yasuda, *J. Chromatogr.*, 535 (1990) 163.
6 J. Haginaka and J. Wakai, *Anal. Sci.*, submitted for publication.
7 S. E. Cook and T. C. Pinkerton, *J. Chromatogr,*, 368 (1986) 233.
8 A. Verloop, W. Hoogstraaten and J. Tipker, in E. J. Ariens (Editor), *Drug Design*, Vol. 8, Academic Press, New York, 1976, Ch. 4.
9 J. A. Perry, L. J. Glunz, T. J. Szczerba and J. D. Rateike, *LC · GC*, 8 (1990) 832.
10 C. P. Desilets, M. A. Rounds and F. E. Regnier, *J. Chromatogr.*, 544 (1991) 25.

Journal of Chromatography, 596 (1992) 157–164
Elsevier Science Publishers B.V., Amsterdam

CHROM. 23 985

Evaluation of morphological structure of packings by gel permeation chromatography

Audrius Maruška*,☆, Arūnas Šėrys, Jolanta Liesienė and Janina Urbonavičienė

Department of Organic Technology, Kaunas University of Technology, Radvilėnų 19, 3028 Kaunas (Lithuania)

Arvydas Žygas

Department of Biochemistry, Vilnius University, Čiurlionio 21, 2009 Vilnius (Lithuania)

(First received December 17th, 1990; revised manuscript received December 22nd, 1991)

ABSTRACT

Evaluation of several matrices by gel permeation chromatography (GPC) revealed that the chromatographic characteristics of packings are sensitive to the morphological structure. When closed morphology granules are used, a novel, non-classical chromatographic profile is observed. This profile is seen in chromatograms of polymeric standards and also in the calibration graph for the packing and has been termed the "skin effect". Gel filtration of polymeric standards was used to evaluate granule surface permeability and GPC process equilibrium. The use of closed morphological structure matrices for GPC is problematic because of the narrow fractionation interval and possible non-equilibrium GPC processes. Among the closed morphological structure packings, membranous granules are notable for their denser but sufficiently permeable surface. Such packings fractionate macromolecules according to molecular mass into two groups.

INTRODUCTION

Among several available means for the investigation of packings, gel permeation chromatography (GPC) is notable for the information it provides [1]. In addition, this method is valuable for its simplicity, as it can be carried out using standard chromatographic apparatus. In addition to the common characteristics of packings such as porosity and exclusion limits, it is also possible to determine the most important parameters of matrices, namely average pore size, polydispersity and specific pore surface area, by means of gel chromatographic porosimetry [2]. However, if the morphology of the granules is not fully investigated, then all of the above factors do not fully reflect the complexity of the matrix structure, or their complete chromatographic characteristics.

The morphological uniformity of a porous structure may be evaluated by means of electron microscopy [3,4]. However, there are difficulties in the preparation of soft hydrogel samples. Essential changes in porous structure may occur when the samples are dried. In order to minimize the drying effect, cryogenic preparation methods are employed for soft cellulose hydrogels (freeze-drying at the critical point). Samples may also be washed with volatile organic solvents and dried under vacuum [5].

Samples which are not dried, however, are more acceptable for the analysis of matrix porous structure. One of these methods is known as the "interuption" method [6], by which the granule morphology of ion exchangers can be qualitatively characterized. Special equipment is necessary, however, for the investigation of ion-exchange kinetics.

☆ Present address: Institut für Anorganische und Analytische Chemie, Universität Mainz, Johann-Joachim-Becher-Weg 24, 6500 Mainz-1, Germany.

0021-9673/92/$05.00

Further, the application of this method is problematic with neutral matrices.

It is worth mentioning with regard to the GPC method that it is generally accepted that the matrix morphology has a significant effect on chromatographic characteristics. However, there have been no detailed studies on the determination of the relationship between chromatographic characteristics and granule morphology, except for the work of Motozato, *et al.* [7]. They prepared granules with a denser external layer and determined their chromatographic properties.

The evaluation of the effect of matrix granule morphology on gel size-exclusion properties is reported in this paper.

EXPERIMENTAL

Apparatus

A liquid chromatograph (Kovo, Czechoslovakia) consisting of an HPP 5001 precision electromechanical pump, RIDK 102 differential refractometer, LCD 2563 UV–VIS detector and TZ 4620 linear recorder was utilized.

Materials

For packing of columns, Granocel-4, Granocel-8, Granocel-14, Granocel M-8 and Granocel MB-8 (0.07–0.2 mm fraction) were used. These matrices were developed in our laboratory. We also employed commercial packing materials: open morphological structure gel Toyopearl HW-55F (Toyo Soda, Japan) and closed morphological structure ion exchangers Ostsorb-DEAE (Spolchemie, Czechoslovakia) and DEAE-cellulose (Reanal, Hungary). The dextrans listed in Table I were used as standard polymers.

TABLE I

CHARACTERISTICS OF STANDARD POLYMERS

M_w = Mass-average molecular mass; M_n = number-average molecular mass.

Dextran	Manufacturer	M_w	M_w/M_n
T5	Serva	4700	–
T10	Pharmacia	9000	1.73
T20	Ferak	23 000	1.30
T40	Pharmacia	35 000	1.80
T70	Pharmacia	74 000	2.05
T100	Serva	129 000	1.41
T500	Pharmacia	484 000	2.46
T2000	Pharmacia	2 000 000	–
T5000–40 000	Serva	5 000 000–40 000 000	–

D-(+)-Glucose (Reakhim, USSR) was used as a low-molecular-mass (low-M_r) chromatographic standard. Bovine serum albumin (BSA) was obtained from Reanal.

Conditions

The concentration of injected sample solutions was in the range 0.3–2.0 mg/ml. The flow-rate was 7.1–42.6 ml/cm^2 · h. Chromatography of BSA was performed in 0.05 *M* Tris–HCl buffer (pH 8.35).

RESULTS AND DISCUSSION

In order to determine effect of the morphology of granules on the chromatographic characteristics of packings, cellulose matrices with a closed morphological structure, *viz.*, Granocel-4, Granocel-8, Granocel-14, Granocel M-8 and Granocel MB-8, were investigated. It was observed that the gel chromatograms of standard dextrans (Fig. 1a) obtained under normal GPC conditions (flow-rate 21.2 ml/cm^2 · h, sample concentration 2.0 mg/ml) when using a column packed with neutral cellulose matrix Granocel-8 differ from those obtained when typical gels were employed. As shown in Fig. 1, dextrans T2000 and T500 do not penetrate into the pores of Granocel-8 and are eluted with the column void volume (v_0). Lower-M_w dextrans, T70 and T40, partially penetrate into the packing. However, their elution curves are different from typical chromatograms, which exibit Gaussian curves. In spite of the monomodal M_r distribution of dextrans T70 and T40 (Pharmacia data), the chromatograms are elongated and have two more or less noticeable peaks. Further, the first chromatographic peak corresponds to the column void volume (v_0).

According to the ratio of the areas under these peaks, the amount of sample retained increases with decreasing M_r of the dextran. Injected samples of standard dextrans T20 and T10 and also glucose were almost completely retained.

Analogous separations of standard dextrans were obtained with the more porous Granocel-4 and the less porous Granocel-14 packings (data not presented). The calibration graph for Granocel-8 (Fig. 1b)

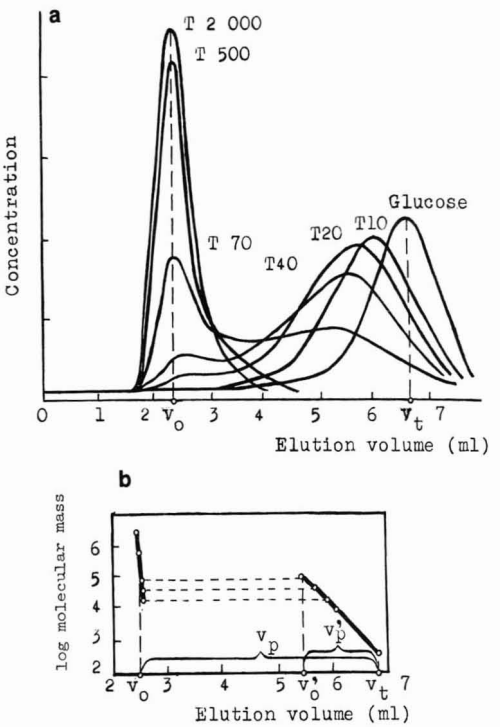

Fig. 1. (a) Chromatograms of standard dextrans obtained on the closed morphological structure cellulose packing Granocel-8 and (b) calibration graph for the packing. Flow-rate, 0.1 ml/min; detector, refractometer; column, 250 × 6 mm I.D.; sample, 0.3 ml, 2 g/l; eluent, distilled water.

shows the typical curve obtained for closed morphological structure packings. As can be seen in Fig. 1b, fractionation of polymeric standards, which is usually observed for conventional gels, does not occur within the whole interval $[v_0; v_t]$. The monotonous dependence of the elution volume v_e on the logarithm of M_w $[v_e = f(\log M_w)]$ is observed only within the interval $[v'_0; v_t]$. This interval represents only part of the whole packing pore volume v_p. Therefore, the efficiency of application of such packings for gel chromatography is always less than the efficiency of application of typical gels. In each particular case this depends on the ratio v'_p/v_p (Fig. 1b). When the magnitude of v'_p/v_p approaches unity, the "skin effect" manifests itself more subtly. As this occurs, the morphological structure and chromatographic properties of the packing differ very

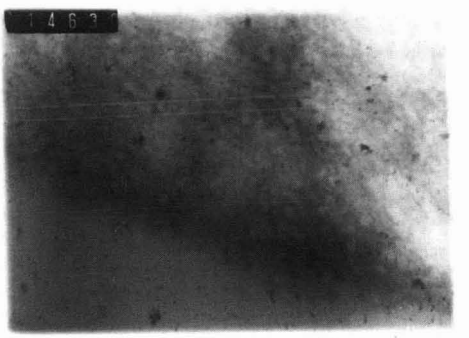

Fig. 2. Electron micrograph of Granocel-8 sphere cross-section (× 23 800).

little from the characteristics observed for typical gels.

The "skin effect" is a reflection of a specific chromatographic property of the packing which is due to the density gradient on the exterior of the granules and should be understood as a qualitative characteristic of granule morphology. The reflection of the density gradient quantitative parameters of the surface of the granules was not determined from gel chromatographic characteristics. On the other hand, qualitative determination of the morphological structure of the packing granules by means of GPC is superior because of its sensitivity. This sensitivity is observed both when there is a gradual densification of the outer layer of the granules which is indistinct and unobservable by other methods (Fig. 2). This effect is also observed when there

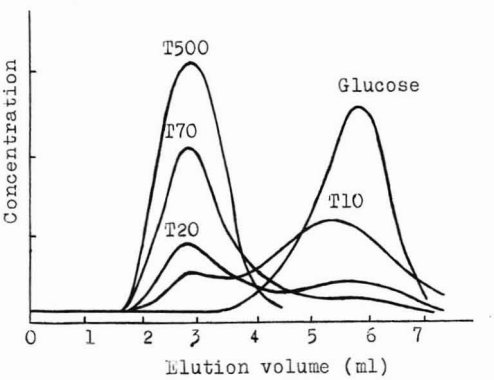

Fig. 3. Chromatograms of standard dextrans obtained on the closed morphological structure cellulose packing Granocel M-8. Flow-rate, 0.1 ml/min; detector, refractometer; column, 190 × 6 mm I.D.; sample, 0.3 ml, 2 g/l; eluent, distilled water.

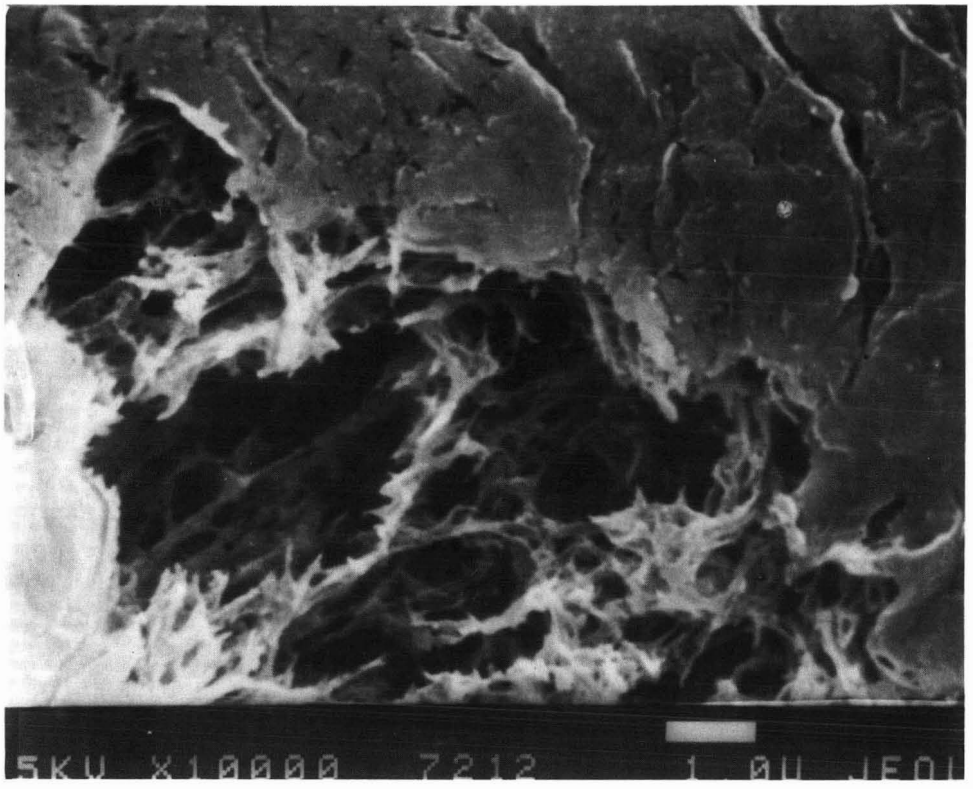

Fig. 4. Electron micrograph of Granocel M-8 granule surface and inner layers (× 10 000).

is distinct film on the granules. This film has quantitative characteristics that can be observed by microscopic methods (Figs. 3 and 4).

The "skin effect" may be observed in cellulosic matrices other than the present Granocel materials (Figs. 3, 5 and 6 in ref. 9) and also with synthetic packings, *e.g.*, Toyopearl HW-65 and Toyopearl HW-75 (Fig. 7B and C in ref. 9). A closed morphological structure is characteristic also for the ion exchangers Ostsorb-DEAE and Reanal DEAE-cellulose (Fig. 5).

The closed morphological structure of the matrices may be easily verified when the granules are subjected to mechanical grinding, *i.e.*, destroying the outer layer and obtaining easily accessible porous structure particles. After the grinding of Granocel-8 granules, for example (Fig. 6), the character of the elution curves of standard dextrans is entirely different (Fig. 7a). Typical Gaussian curves are now observed. As can be seen in Fig. 7b, the upper exclusion limit of the ground granules is increased and a linear dependence $v_e = f(\log M_w)$ is observed throughout almost the whole $[v_0; v_t]$ interval.

It is necessary to carry out this grinding procedure when there is doubt about the possible adsorption interaction of the matrix with standard polymers. As two different results are obtained under analogous conditions, the possibility of adsorption interaction may be excluded as a factor in the chromatographic behaviour of the packing. It is important to note that the gel chromatographic conditions for both intact and ground particles were identical.

In order to explain the nature of the chromatographic "skin effect", it is worth remembering that based on general GPC principles [10], every macro-

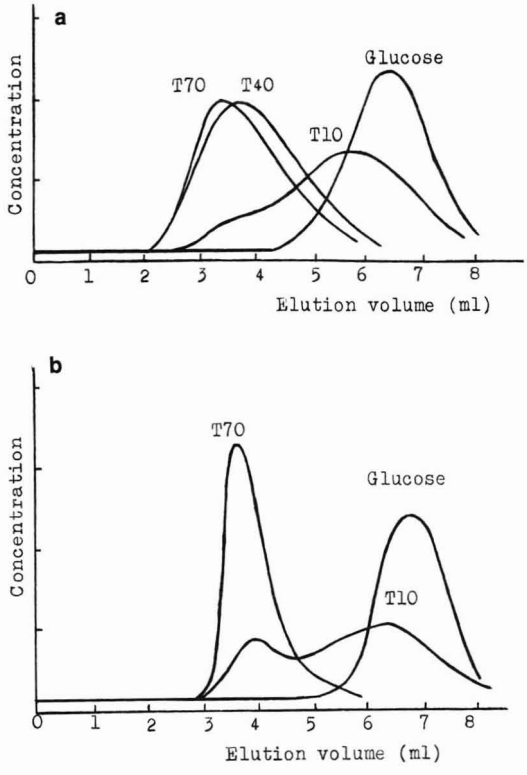

Fig. 5. Chromatograms of standard dextrans obtained on cellulose anion-exchangers: (a) Ostsorb-DEAE (column, 210 × 6 mm I.D.) and (b) Reanal DEAE-cellulose (column, 270 × 6 mm I.D.). Flow-rate, 0.1 ml/min; detector, refractometer; sample, 0.3 ml, 2 g/l; eluent, distilled water.

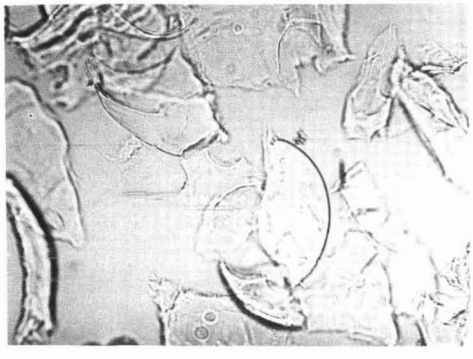

Fig. 6. Optical micrograph of ground Granocel-8 packing granules (× 90).

molecular sorption–desorption process has the following stages: (1) random macromolecules wandering in the canals of the mobile phase, due to thermal motion and hydrodynamic conditions; (2) transfer of macromolecules from the mobile phase into the stationary phase, *i.e.*, their entry into packing pores; (3) macromolecular diffusion back and forth from the external surface of the packing granules into internal canals, *i.e.*, random movement back and forth in the porous space; and (4) desorption of macromolecules, *i.e.*, their transition from the surface of the packing granules into the mobile phase.

In the process of GPC, there is no adsorption interaction between the macromolecules and the packing matrix. Therefore, stages 2 and 4 are relatively shorter than stages 1 and 3, and the kinetics of the GPC process are determined by random macromolecular motion in the mobile phase and their diffusion within granules. The denser layer on the

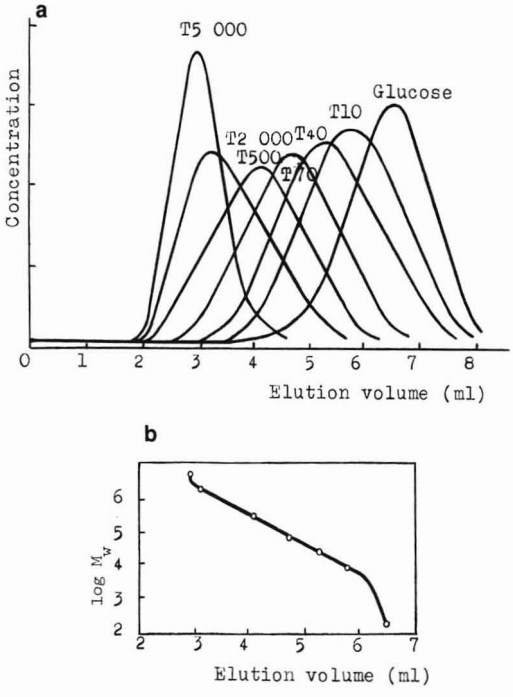

Fig. 7. (a) Chromatograms of standard dextrans obtained on the ground cellulose packing Granocel-8 and (b) calibration graph for the packing. Flow-rate, 0.1 ml/min; detector, refractometer; column, 250 × 6 mm I.D.; sample, 0.3 ml, 2 g/l; eluent, distilled water.

granule surface makes diffusion of macromolecules in and out of particles much more difficult. For this reason, the stages outlined above are prolonged, causing the chromatographic process to change.

Fig. 8 illustrates the dynamics of the separation of a macromolecular standard with a monomodal M_r distribution into two zones. This profile is not chracteristic of open morphological structure packings.

When closed morphological structure packings are used in GPC, the process may not undergo complete equilibrium owing to the poor permeability of the granules surface. This is confirmed by the experimental results for the chromatography of monodisperse protein on Granocel-8 packing (Fig. 9). Chromatography of BSA, which exibits normal chromatographic behaviour on the open morphological structure gel Toyopearl HW-55F, shows a distribution into two chromatographic peaks and separation of the protein into a wide zone when Granocel-8 was used. Also, when the concentration of the injected sample is decreased, the character of the chromatographic curve changes, *i.e.*, the relationship between the peak areas and also the position of the second peak.

The chromatograms of the polydisperse standard T70 ($M_w/M_n = 2.05$) are also essentially changed (analogous to the chromatographic curves of BSA) when different concentration samples are injected.

It should also be noted, however, that even during a non-equilibrium GPC process the sample may undergo partial fractionation according to M_r. As analysis of the collected fractions from the first and second chromatographic peaks (Fig. 10a) obtained using Toyopearl HW-55F gel has shown (Fig. 10b) these fractions are not pure with respect to M_r. The first chromatographic peak contains the higher-M_r fraction and the second contains the lower-M_r fraction. As the chromatographic process on Granocel-8 is non-equilibrium, however, refractionation of the collected fractions results in separation again into two zones (Fig. 10a). It was found that when the flow-rate was changed from 7.1 to 42.6 ml/cm^2 · h, the elution of the intermediate molecular mass

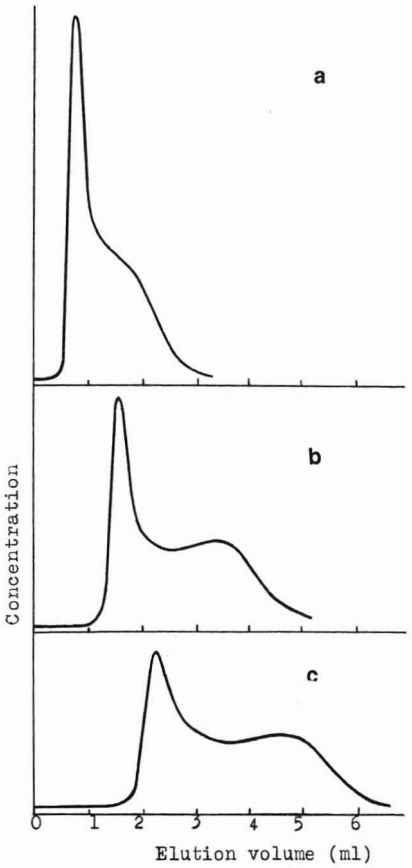

Fig. 8. Dynamics of resolution of standard dextran T70 into two chromatographic zones obtained on the cellulose packing Granocel-8 when columns of (a) 56 × 6 mm I.D., (b) 116 × 6 mm I.D. and (c) 170 × 6 mm I.D. were used. Flow-rate, 0.1 ml/min; detector, refractometer; sample, 0.3 ml, 2 g/l; eluent, distilled water.

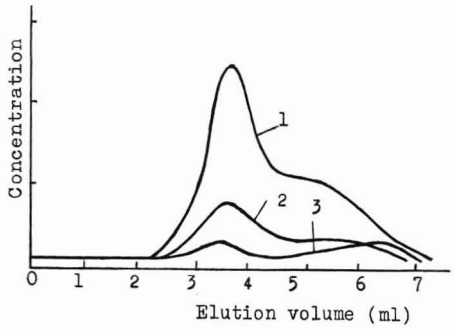

Fig. 9. Resolution of BSA when the closed morphological structure cellulose packing Granocel-8 was used. Flow-rate, 0.1 ml/min; detector, UV (254 nm); column, 250 × 6 mm I.D.; sample (0.3 ml) concentration, (1) 10 g/l, (2) 3 g/l and (3) 1 g/l; eluent, 0.05 *M* Tris–HCl buffer (pH 8.35).

dextran standards on the Granocel-8 packing occurred in different way. The change in the character of the chomatographic profiles is a same as that observed when the concentration of the injected sample is increased.

By repeated fractionation and analysis of the collected fractions of dextran standards, it was established that the equilibrium process may be partialy reached when the flow-rate and concentration of the sample are decreased. Theoretically, however, the direct cause of the non-equilibrium GPC process should be the insufficient accessibility of the granule porous structure. This depends on the ratio of the open pore surface area to the total granule surface area. The application of closed morphological structure matrices in GPC is therefore problematic not only owing to the narrow fractionation interval, *i.e.*, lower selectivity, but also to possible non-equilibrium GPC processes. In this instance the results of chromatography are very dependent on the sample concentration and the elution flow-rate. If in a common gel chromatographic process changing the sample concentration or flow-rate causes a change in the width and the height of the chromatographic peak (*i.e.*, a change in the efficiency of elution), then in a non-equilibrium gel chromatographic process a further change is observed (*i.e.*, a change in the position of the peak).

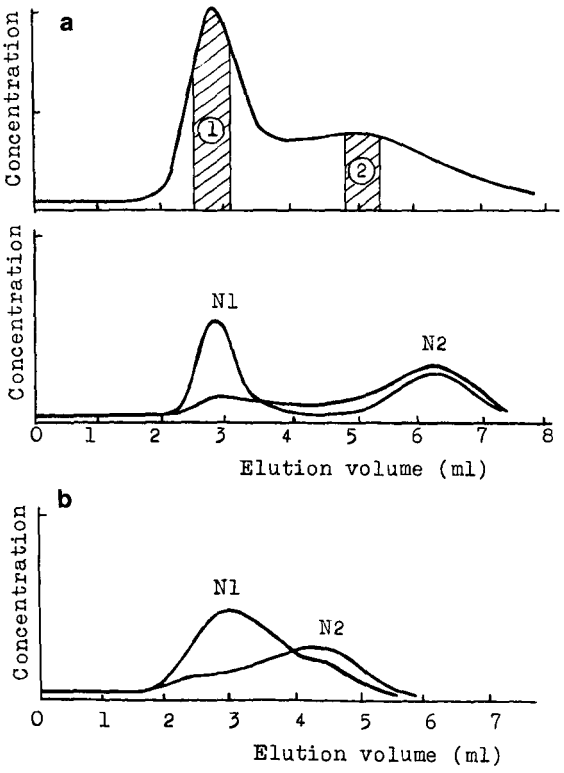

Fig. 10. (a) Collection of standard dextran T70 fractions N1 and N2 and their repeated fractionation. Packing, Granocel-8; flow-rate, 0.1 ml/min; eluent, distilled water. (b) Analysis of collected fractions N1 and N2 on the typical gel Toyopearl HW-55F. Flow-rate, 0.1 ml/min; detector, refractometer; column, 250 × mm I.D.; sample, 0.5 ml; eluent, distilled water.

Interesting chromatographic properties are characteristic of closed porous structure packings with denser but still sufficiently permeable membranes on the granule surface. In this instance macromolecules are fractionated into two groups, of lower and higher M_r the elution volumes of which correspond to the chromatographic zones v_t and v_0 (total volume and void volume), respectively. Such a chromatographic process is more similar to ultrafiltration, because the macromolecular fractionation does not show a linear dependence $v_e = f(\log M_w)$, whereas the upper and lower exclusion limits become so narrow that they almost coincide. Their value is dependent on the pores size of the granule membrane. Because of the easily accesible porous structure of the packing, this case may be treated as a limiting case. Therefore, it is worth studying this situation in more detail.

Fig. 11 illustrates chromatograms of dextrans obtained using the membranous cellulose packing Granocel MB-8. Polydisperse polymeric probes with a wide M_r distribution may be separated into two zones, as is also obtained when using Granocel-8. In this instance, however, the granule packing surface is sufficiently permeable and, as seen from repeated elution of collected fractions N1 and N2, the chromatography using this packing is an equilibrium process. It was determined by analysis of the collected fractions that they are very similar with respect to molecular mass and would be very difficult to separate using typical gels. When the typical gel chromatographic packing Toyopearl HW-55F is used, the chromatograms of fractions N1 and N2 show substantial overlapping and the peaks are separated with very low selectivity. However, when the membranous packing Granocel MB-8 is used, they are separated with maximum selectivity, *i.e.*, are eluted in the zones which correspond to the void volume and total volume of the column (Fig. 11).

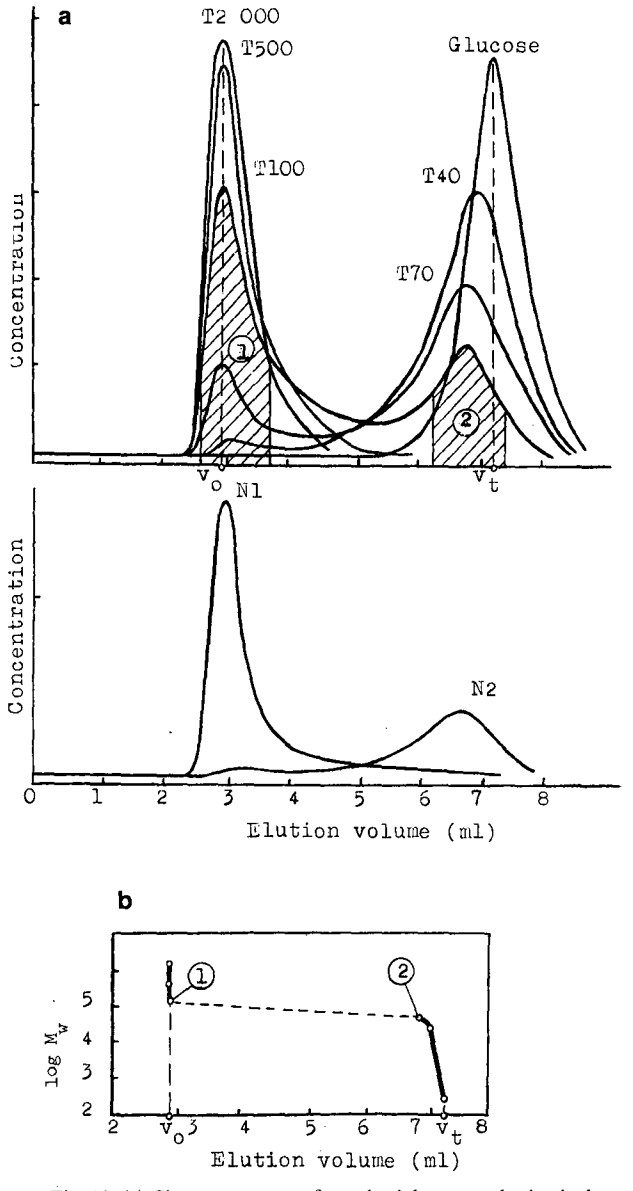

Fig. 11. (a) Chromatograms of standard dextrans obtained when the membranous cellulose packing Granocel MB-8 was used and resolution of collected standard dextran T100 fractions, and (b) Calibration graph for the packing. Flow-rate, 0.1 ml/min; detector, refractometer; column, 250 × 6 mm I.D.; sample, 0.5 ml, 2 g/l; eluent, distilled water.

CONCLUSIONS

Gel chromatographic packing characteristics are sensitive to the granule morphological structure. A closed or open morphology of the packing granules can therefore be easily determined by GPC. A closed granule morphological structure causes essential changes in the chromatographic process and the "skin effect" is reflected in chromatograms of standard polymers and also in the column packing calibration graph.

Application of a closed structure packing in GPC depends on the intensity of the "skin effect", *i.e.*, on the GPC process equilibrium, which is due to the accessibility of the porous structure, and also on the decreased fractionation selectivity.

Among the closed morphological structure packings, membranous granules are notable for their special chromatographic characteristics. These packings fractionate macromolecules according to M_r into two groups with maximum selectivity. This is due to the denser but sufficiently permeable granule surface membrane.

ACKNOWLEDGEMENTS

We are grateful to Dr. A. Boldyrev and Dr. M. Wojaczynska for help in obtaining electron micrographs.

REFERENCES

1 A. Maruška, J. Liesienė, A. Šėrys and A. Gorbunov, in A. Treimanis (Editor), *Metody Issledovania Cellulozy — Tezisy Dokladov (Methods of Cellulose Investigation — Conference Proceedings)*, Latvian Academy of Science, Riga, 1988, p. 197.
2 A. A. Gorbunov, L. Ya. Solovyova and V. A. Pasechnik, *J. Chromatogr.*, 448 (1988) 307.
3 T. G. Plachenov and S. D. Kolosencev, *Porometrya (Porosimetry)*, Khimiya, Leningrad, 1988.
4 O. I. Nachinkin, *Polimernye Microfiltry (Polymeric Microfilters)*, Khimiya, Moscow, 1985.
5 J. Peška, J. Štamberg and Z. Pelzbauer, *Cellul. Chem. Technol.*, 21 (1978) 419.
6 G. V. Samsonov and A. T. Melenevsky, *Sorbcionnye i Khromatographicheskie Metody Fiziko-Khimicheskoi Biotechnologii (Sorption and Chromatographic Methods of Physico-Chemical Biotechnology)*, Nauka, Leningrad, 1986.
7 Y. Motozato, Ch. Hirayama, M. Suga and T. Iwamoto, *Polymer*, 20 (1979) 84.
8 Sh. Kuga, *J. Chromatogr.*, 195 (1980) 221.
9 *Separation of Saccharides on Toyopearl*, Toyo Soda, Tokyo.
10 B. G. Belenky and L. Z. Vilenchik, *Khromatographiya Polimerov (Polymer Chromatography)*, Khimiya, Moscow, 1978.

Journal of Chromatography, 596 (1992) 165–171
Elsevier Science Publishers B.V., Amsterdam

CHROM. 23 970

Inclusion and fractionated release of nucleic acids using microcapsules made from plant cells

Andres Jäschke* and Dieter Cech

Department of Chemistry, Humboldt University, Invalidenstrasse 42, O-1040 Berlin (Germany)

Rudolf Ehwald

Department of Biology, Humboldt University, Invalidenstrasse 42, O-1040 Berlin (Germany)

(First received October 10th, 1991; revised manuscript received December 12th, 1991)

ABSTRACT

The encapsulation and fractionated release of nucleic acids on vesicular packing (VP) materials have been investigated. The earlier described dependence of the permeation of nucleic acid molecules through the vesicle membranes on the salt concentration is a necessary precondition for both encapsulation and fractionation. Encapsulation is achieved by applying a suitable sample onto a VP column that has been equilibrated with a high-salt buffer. In that buffer the sample molecules are permeable. Immediately after sample application, elution is started with a low-salt buffer, from which the sample molecules are excluded. At the front between the two buffers the permeability changes, and some of the sample molecules distributed inside the vesicles cannot pass through the membranes. These encapsulated molecules can be released by increasing the salt concentration in the eluent. If the encapsulated nucleic acid sample is polydisperse, a stepwise or linear increase in the salt concentration leads to a fractionated release. The fractions obtained differ in their molecular size composition.

INTRODUCTION

A certain kind of microcapsule, a vesicular packing (VP) material consisting of clusters of empty plant cells, was recently shown to be suitable as a chromatographic support [1,2]. The use of the VP material for size-exclusion chromatography of proteins and dextranes has been described. The VP material differs from conventional materials used in gel permeation chromatography (GPC) both in structure and mechanism. Whereas GPC is based on size-dependent distribution within a gel matrix, vesicle chromatography (VC) is a chromatographic type of membrane separation, where the primary plant cell wall acts as an ultrafiltration membrane and encloses the stationary liquid phase. Depending on their size and charge, the sample molecules are either permeable or not permeable. For a suitable polydisperse sample this results in the occurrence of only two peaks, which are separated by a large difference in elution volume.

The chromatographic behaviour of nucleic acids was shown to be strongly dependent on environment factors such as pH and salt concentration. Divalent cations exert an especially strong influence [3], for example, ribonucleic acid (RNA) is excluded in a slightly buffered solution at pH 7.5, but is permeable on the addition of 20 m*M* magnesium chloride. Electrostatic interactions between the phosphate groups of the nucleic acid and the carboxyl groups of the cell wall are considered to be the main reason for this change. Thus size-exclusion and ion-exclusion effects influence the chromatographic behaviour of polyanions. Anionic molecules, which could permeate according to their size, are excluded at low salt concentrations due to an additional electrostatic barrier [4]. Electrostatic influences of carboxyl groups on the cell wall permeability have

0021-9673/92/$05.00

been discussed with respect to the kinetics of anion uptake by roots and plant tissues [5], but in these instances the assumed permeability changes were quantitative. Complete prevention of cell wall permeation of anions by the ion-exclusion effect has been seen with oligonucleotides [3].

Traditionally, microcapsules are of interest for the encapsulation of macromolecules, *e.g.* enzymes. Encapsulation is usually coupled with the formation or irreversible modification of the capsule membrane [6,7]. Reversible environment dependent changes in the effective pore size of an ultrafiltration membrane were also used for the inclusion of polymers in microcapsules. Sleytr and Sara [8] have described the use of vesicular membranes reassociated from bacterial cell wall proteins for the inclusion of certain proteins by a change of the salt concentration.

The VP material differs from these vesicular membranes by the complex structure and much higher mechanical stability of the ultrafiltration membrane (plant cell wall). This paper describes the use of the reversible change of permeability of the cell wall for the encapsulation of nucleic acids inside the microcapsules and the subsequent fractionated elution of these nucleic acids by 'release chromatography'.

EXPERIMENTAL

DNA from calf thymus and herring sperm, adenosine, 2',3'-uridinemonophosphate and 2',3'-cytidinemonophosphate were obtained from Serva. RNA (not further specified) and $tRNA^{val}$ were from Boehringer Mannheim.

Oligonucleotides were synthesized on an Applied Biosystems 380A oligonucleotide synthesizer and purified as described previously [3]. The oligonucleotides, nucleotides and nucleic acids were dissolved in the appropriate buffer to give an absorbance A_{260} of 1 unit in a 200-μl volume. All other reagents were of analytical-reagent grade and were obtained from Serva and Biomol.

The VP material described by Ehwald *et al.* [1], commercially available from Serva (Vesipor) and Permselekt (Permselekt) was used.

For the encapsulation of nucleic acids, the VP material was swollen for 5 min in distilled water. It was then titrated with tris(hydroxymethyl)aminomethane to pH 7.5. This step was followed by extensive washing using a high-salt buffer (5 m*M* Tris–HCl, pH 7.5; 200 m*M* $MgCl_2$, 500 m*M* NaCl) and finally with the appropriate buffer for chromatography. Short glass columns (injection syringes with an I.D. of 16 mm) were packed conventionally. The packing was covered with filter paper. After equilibration, at least 0.1 A_{260} units of the sample were loaded onto the column. The flow-rate was controlled by a peristaltic pump (Minipuls 2, Gilson).

Chromatograms were recorded using an LKB 2238 Uvicord S II recorder operating at 254 nm.

RESULTS AND DISCUSSION

As described previously [3], for a particular size range the permeation of nucleic acids through the vesicle membranes depends on the salt concentration due to the effect of the salt concentration on the electrostatic barrier [4]. At high salt concentrations the membranes are permeable, but the nucleic acids are excluded at low concentrations. If elution with a low-salt buffer is started immediately after sample application onto a column equilibrated at high salt concentrations, some of the sample molecules (about 20–25%) remain on the column. These mol-

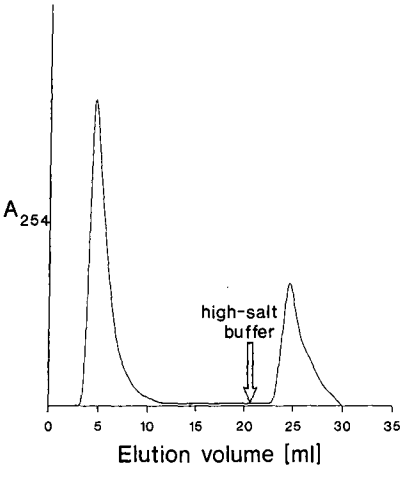

Fig. 1. Encapsulation and release of polydisperse RNA on VP material. Column dimensions, 25 × 16 mm; flow-rate 0.5 ml/min; column equilibration, high-salt buffer (1 m*M* Tris–HCl, pH 7.5; 20 m*M* magnesium chloride); sample, RNA in 50 μl low-salt buffer (1 m*M* Tris–HCl, pH 7.5); elution, first 21 ml with low-salt buffer, thereafter with high-salt buffer.

ecules are not eluted until the salt concentration in the eluent is increased (Fig. 1).

In earlier work we determined that the adsorption of nucleic acids onto VP materials does not occur at pH values above 7 [3]. Therefore, the behaviour illustrated in Fig. 1 with the salt-induced permeability changes are described as follows (Fig. 2). The column has been equilibrated with a high-salt buffer, the sample (for the sake of simplicity, a monodisperse sample in a negligibly small liquid volume) is applied and immediately thereafter elution with a low-salt buffer is started (Fig. 2, t_0). Exactly in the region where the sample is located, a steep salt gradient is formed (Fig. 2, t_1). Below a certain salt concentration, c_E, the considered sample molecule is excluded; above another (rather higher) concentration, c_P, it is completely permeable. The range between c_E and c_P corresponds to the fractionation range in VC, which is characterized by limited permeability. The molecules are partitioned between the extra-particular mobile phase and the intra-vesicular stationary phase. There is a residence time of the molecules inside the stationary phase while the mobile phase, and therefore the salt gradient, moves foreward. For this reason, the salt concentration at the vesicle membrane decreases, possibly falling below the value of c_E. In this instance the nucleic acid molecule is immobilized by inclusion in the VP material.

Some of the sample molecules pass into the zone of increasing salt concentration as they are moving faster than the eluent, as far as they do not permeate the membrane. Arriving in a region with a salt concentration $c = c_P$, the molecules become permeable and move as a peak with the same rate as the eluent. It is assumed by this model that this peak

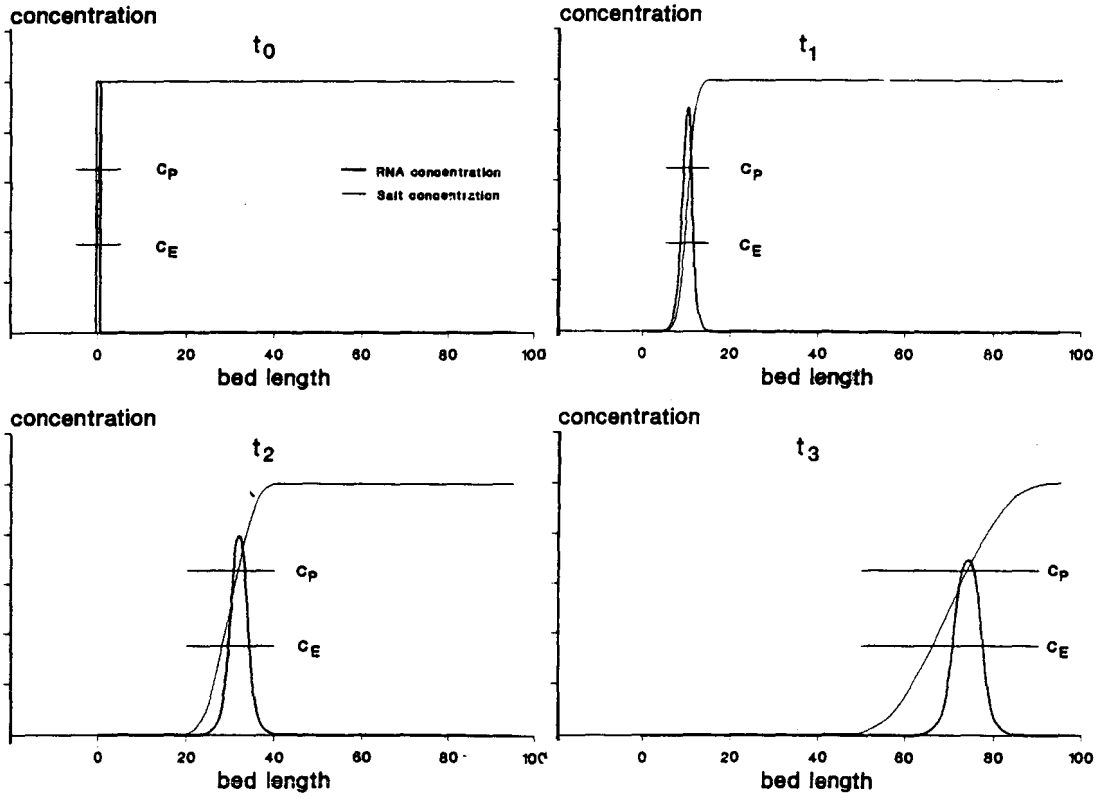

Fig. 2. Assumed concentration profiles during a chromatographic run of a monodisperse sample on a vesicle column at different times. Longitudinal section through the column: direction of the x-axis corresponds to the flow direction; RNA concentration and salt concentration are plotted as a function of the x-coordinate; x-coordinate as a percentage of the total bed length. Values for c_E and c_P chosen arbitrarily. Equilibration and elution performed in accordance with Fig. 1.

migrates ahead of the critical zone with a salt concentration of about c_E. As a result of peak dispersion, a few nucleic acid molecules may once again reach the critical zone. However, with increasing migration distance on the column the salt gradient flattens out and the conditions for inclusion become more unfavourable (Fig. 2, t_2 and t_3). The sample components not included leave the column with the salt gradient. Included molecules cannot leave the vesicles until the salt concentration in the eluent is increased above c_E.

For polydisperse samples with a suitable molecular size distribution the principle should be the same, but due to the different sizes of the molecules every species has different values for c_E and c_P.

The following results clearly show that the behaviour seen in Fig. 1 is in accordance with this explanation.

If column equilibration, sample dissolution and elution all are performed using the same buffer, nucleic acids were not held on the column either at low or high salt concentrations (Fig. 3). Obviously, not a certain salt concentration, but a change in the salt concentration is responsible for the observed immobilization.

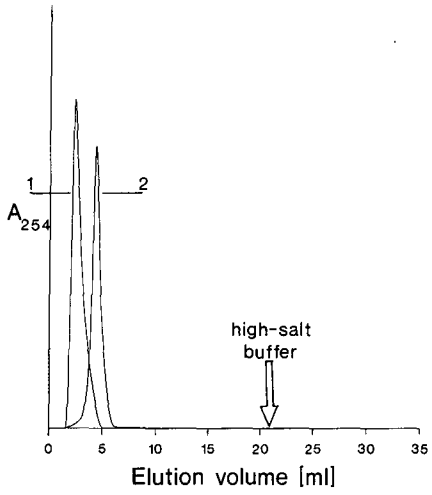

Fig. 3. Failure of immobilization at constant salt concentration. Curve 1, equilibration, sample dissolution and elution of the first 21 ml with 1 m*M* Tris–HCl, pH 7.5, then elution with 1 m*M* Tris–HCl, pH 7.5, 20 m*M* magnesium chloride. Curve 2, equilibration, sample dissolution and elution of the first 21 ml with 1 m*M* Tris–HCl, pH 7.5, 20 m*M* magnesium chloride, then elution with 1 m*M* Tris–HCl, pH 7.5, 200 m*M* magnesium chloride. Other conditions as in Fig. 1.

The retention on the column only occurs with samples, the molecules of which are excluded at low salt concentrations and which are permeable in high-salt buffer (Table I). Mononucleotides, which can permeate at high and low salt concentrations, were not encapsulated and the plasmides or ribosomal RNA which were always excluded showed no retention.

The vesicular structure of the packing material is essential for the retention. Mechanically destroyed cell wall vesicles show no retention of RNA (Fig. 4). As outlined previously [3], the destroyed material behaves like a conventional GPC material; the influence of the salt concentration on the elution volumes of nucleic acids is small. As the large isolated liquid volumes inside the VP material do not exist in the destroyed material, the sample molecules cannot be encapsulated.

The inclusion is not specific for magnesium chloride; it occurs with any other salt that influences the permeability of the cell wall for nucleic acid molecules. The effect has also been observed by using sodium chloride, potassium chloride, caesium chloride and calcium chloride; however, with monovalent cations a considerably higher concentration is necessary to include similar amounts of nucleic acids.

For small sample volumes, the bed length had no

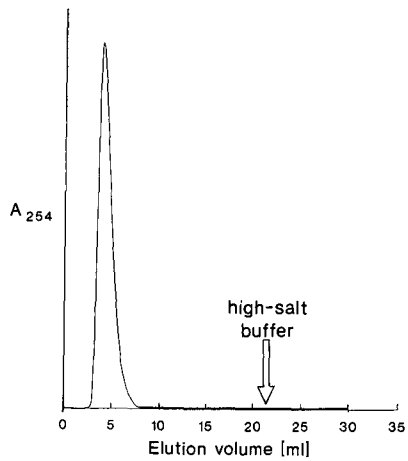

Fig. 4. Failure of immobilization with mechanically disintegrated VP material. All conditions as in Fig. 1. Destruction of the VP material was performed using a swinging mill until no intact cellular structures were detected under a microscope (magnification × 200).

TABLE I

ENCAPSULATION AND RELEASE OF NUCLEIC ACIDS, OLIGONUCLEOTIDES AND NUCLEOTIDES AS A FUNCTION OF THEIR PERMEATION BEHAVIOUR AT MAGNESIUM CHLORIDE CONCENTRATIONS OF 0 AND 20 m*M* IN 1 m*M* TRIS–HCl, pH 7.5.

Sample	Molecular weight	Permeation at 0 m*M* $MgCl_2$	Permeation at 20 m*M* $MgCl_2$	Encapsulation and release[a]
2′,3′-CMP	323	Permeating	Permeating	No
2′,3′-UMP	324	Permeating	Permeating	No
RNA from yeast[b]	< 15 000	Excluded	Permeating	Yes
DNA from herring sperm[b]	< 15 000	Excluded	Permeating	Yes
28mer oligonucleotide[c]	≈9000	Excluded	Permeating	Yes
$tRNA^{val}$ from *Escherichia coli*	≈30 000	Excluded	Excluded	No
Calf thymus DNA, native	≈5 000 000[d]	Excluded	Excluded	No
denatured[e]	≈2 500 000[d]	Excluded	Excluded	No
Plasmide pKK 161-8	≈3 000 000	Excluded	Excluded	No

[a] For evaluation of this parameter the experiment described in Fig. 1 was performed with the respective samples.
[b] Technical products, better referred to as crude mixtures of oligonucleotides.
[c] Sequence ATC TAG ATT GTG GGG GCG GCT CCC AAC A.
[d] Value represents an average of a broad molecular weight distribution.
[e] Denaturation was achieved by heating the sample for 10 min to 100°C and rapidly cooling down in an ice-bath.

significant influence on the amount of included molecules, at least in the range investigated. It is suggested that (*i*) with increasing migration distance the conditions for inclusion are less favourable due to the flattening of the gradient and (*ii*) after a few millimetres of migration all sample molecules have either been included or passed through the gradient. An efficient inclusion seems to occur only at the beginning of a chromatographic run.

If the sample is applied in a low-salt buffer and elution is performed as described earlier (see Fig. 1), an efficient inclusion can also be achieved by applying comparatively high sample volumes. As the sample molecules cannot permeate through the vesicle membranes in the sample buffer, they move faster than this buffer until they have reached the salt gradient. To obtain a high inclusion yield, the ratio between sample volume and packing volume should have a value such that the last applied sample molecules reach the zone with the critical salt concentration c_E just before this zone leaves the column. It was found experimentally that the sample volume can be as large as 60% of the packing volume for an efficient inclusion (Fig. 5). If the sample was loaded

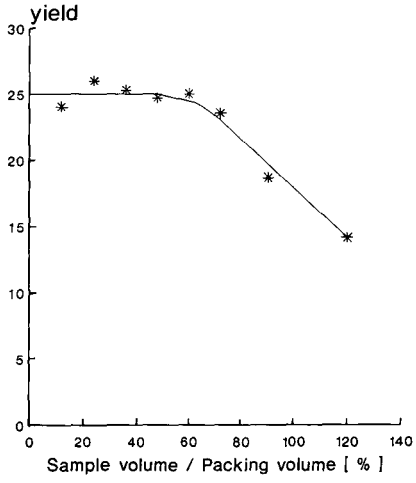

Fig. 5. Encapsulation yield as a function of the ratio between sample volume and packing volume. Yield as percentage of the released fraction compared with the total amount of RNA. Column dimensions 7.5 × 16 mm. Other conditions as in Fig. 1.

onto the column in a high-salt buffer and the above-described procedure was followed, only few molecules (about 3–5% of the RNA) were retained on the column. This is due to mixing between the high-salt sample buffer and the low-salt elution buffer at the rear side of the substance peak.

The inclusion did not lead to an absolutely durable encapsulation of all nucleic acid molecules of a polydispersed sample. The chromatograms presented here show, on closer examination, that the continuous elution of small amounts of included nucleic acids occurred at a low rate. The absorption A_{254} did not decrease to zero after inclusion, but to a value close to zero. An increase of the amount of loaded nucleic acid shows this more clearly (Fig. 6). A long elution time (20 h) with a low-salt buffer (50 packing volumes) resulted in a loss of about two-thirds of the included molecules. Thus the cell wall is not absolutely impermeable at low salt concentrations, but the permeability is decreased by some orders of magnitude.

The elution of the encapsulated molecules by permability changes can be used for the fractionation of polydisperse polymer preparations by a stepwise or continuous increase of the salt concentration. Fig. 7a shows the fractionation of polydisperse RNA in a sodium chloride step gradient. Four separated peaks were detected at the four different salt concentrations. The characterization of the collected peak fractions with respect their molecular size

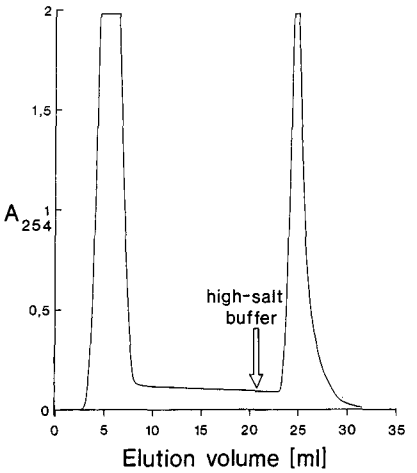

Fig. 6. Preparative encapsulation and release of polydisperse RNA. Sample volume, 1 ml. Other conditions as in Fig. 1.

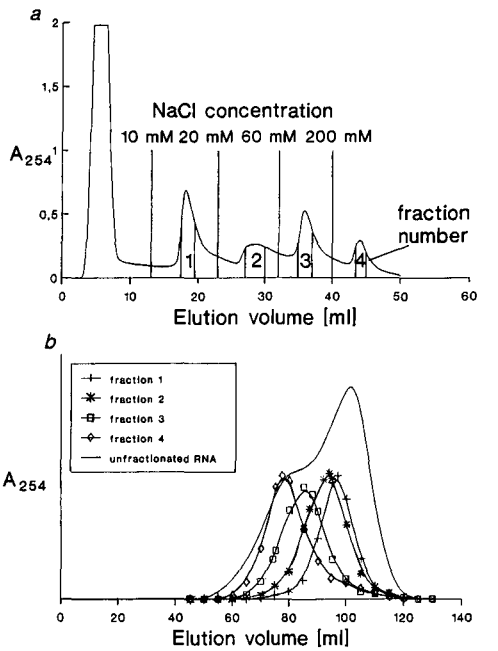

Fig. 7. (a) Preparative encapsulation and fractionated release of polydisperse RNA. Column equilibration with 5 m*M* Tris–HCl, pH 7.5, 200 m*M* sodium chloride. Sample, RNA in 1 ml of low-salt buffer (5 m*M* Tris–HCl, pH 7.5); elution, first with low-salt buffer, then stepwise increase of the NaCl concentration to the concentrations designated in the figure. All other conditions as in Fig. 1. (b) Investigation of the fractions collected in (a) using a HiLoad 16/60 Superdex 75 (preparation grade) column (600 × 16 mm) operated on a fast protein liquid chromatographic station (Pharmacia). Samples: collected fractions from (a) were concentrated by a factor of ten using a Speed Vac concentrator (Savant). Sample volume, 100 μl; eluent, 0.1 *M* Tris–HCl, pH 7.9, 0.2 *M* NaCl; flow-rate, 2 ml/min; chromatograms scaled to give an approximately equal A_{254} at peak maximum.

distribution by GPC of Superdex 75 (Fig. 7b) shows, compared with the non-fractionated RNA sample, that the elution from the VP column occurs in the order of increasing molecular size. The smaller included molecules become permeable first, while the larger molecules need higher salt concentrations for permeation. The elution of the included polydisperse RNA in a continuous linear sodium chloride gradient gave a single broad peak, whereby the mean molecular size was changing continously (chromatograms not shown).

Fractionated release similar to that shown in Fig. 7a was also observed with DNA from herring sperm and by using various salts. For the fraction-

ated release, large column lengths (high numbers of theoretical plates) are not necessary. This is a remarkable difference to GPC.

Inclusion in microcapsules and release by salt-induced permeability changes is a novel technique in nucleic acid fractionation. The method should not only apply to nucleic acids, but also to any other anionic polyelectrolyte with a suitable molecular size (distribution). Other factors influencing the permeability of cell walls for certain polymers, such as dehydration by organic solvent [9], can possibly also be used for the reported type of size fractionation. Therefore encapsulation and fractionated release might develop into a useful tool in polymer fractionation and characterization.

REFERENCES

1 R. Ehwald, G. Fuhr, M. Olbrich, H. Göring, R. Knösche and R. Kleine, *Chromatographia*, 28 (1989) 561.
2 R. Ehwald, P. Heese and U. Klein, *J. Chromatogr.*, 542 (1991) 239.
3 A. Jäschke, D. Cech and R. Ehwald, *J. Chromatogr.*, 585 (1991) 57.
4 P. L. Dubin, C. M. Speck and J. I. Kaplan, *Anal. Chem.*, 60 (1988) 895.
5 J. J. M. Hooymans, *Acta Bot. Neerl.*, 13 (1964) 507.
6 T. M. S. Chang, *Methods Enzymol.*, 44 (1976) 201.
7 H. Eikmeyer and H. J. Rehm, *Appl. Microbiol. Biotechnol.*, 20 (1984) 365.
8 U. B. Sleytr and M. Sara, *Pat.*, PCT/AT 85/00060 (1986).
9 R. Ehwald, U. Klein, A. Jäschke, D. Cech and Ch. Titel, *Pat.*, EP 0412 507 A1 (1991).

Journal of Chromatography, 596 (1992) 173–180
Elsevier Science Publishers B.V., Amsterdam

CHROM. 23 921

Membrane chromatographic systems for high-throughput protein separations

Joseph A. Gerstner

Bioseparations Research Center, Howard P. Isermann Department of Chemical Engineering, Rensselaer Polytechnic Institute, Troy, NY 12180-3590 (USA)

Richard Hamilton

Millipore Corporation, Bioseparations R, D, & E, Bedford, MA 01730 (USA)

Steven M. Cramer*

Bioseparations Research Center, Howard P. Isermann Department of Chemical Engineering, Rensselaer Polytechnic Institute, Troy, NY 12180-3590 (USA)

(First received September 17th, 1991; revised manuscript received November 8th, 1991)

ABSTRACT

This paper explores the utility of a membrane chromatographic system (MemSep) for analytical and preparative separations of biomolecules. These column systems consist of stacked disks of macroporous cross-linked regenerated cellulose membranes functionalized with ion-exchange moieties. Fluid flow through the macropores of these membranes results in rapid mass transport to and from the adsorbent surface. Elution and frontal experiments demonstrated that these systems were relatively insensitive to flow-rate. Linear gradient experiments under analytical conditions indicated that rapid separations could be readily carried out. Preparative-scale separations of proteins on ion-exchange MemSep systems were scaled-up with respect to flow-rate and mass loading with minimal adverse effect on bioproduct purity. A cation-exchange CM MemSep 1010 device was able to concentrate and purify 30 mg and 15 mg of proteins in 3 min when operated in the step and linear gradient modes, respectively. The design of these membrane chromatographic systems enables efficient gradient elution of proteins under elevated flow-rate and mass loading conditions.

INTRODUCTION

The field of preparative chromatography has seen a period of rapid growth in the last decade [1–3]. The development of novel stationary phases with increased selectivities has enabled the separation of complex mixtures of biomolecules. In addition, the use of preparative chromatographic columns in alternative modes of operation have greatly increased the throughputs attainable with these systems [4–9]. There is currently great interest in redesigning the morphology of stationary phase materials to enable rapid capture steps in the early stages of downstream processing of biopharmaceuticals. Several hollow-fiber-based membrane systems have been reported for affinity, ion-exchange and reversed-phase separations of proteins [10–12]. While these systems are potentially quite useful for bind–release separations, their use for conventional chromatographic operations have met with minimal success to date. A recent development in the chromatographic engineering field has been the emergence of perfusion chromatography [13–15]. These systems have been reported to exhibit convective fluid flow in the macropores of the support resulting in flow-rate-insensitive separations under linear

0021-9673/92/$05.00

gradient conditions. Another flow-rate-insensitive chromatographic technology is non-porous supports which have shown great utility for analytical biotechnology applications [16–23].

Although membrane systems have been used for adsorption–desorption operations for quite some time it is only recently that membrane chromatographic systems have been developed for high resolution gradient operations. Tennikova *et al.* [24] have demonstrated the utility of methacrylate copolymeric membranes for hydrophobic interaction chromatographic gradient separations of proteins. A low pressure (0–100 p.s.i.) bioseparations system consisting of stacked disks of macroporous, cross-linked regenerated cellulose membranes in a column configuration has been employed for analytical gradient chromatography [25,26]. Mass transport to and from the adsorbent surfaces in these membrane chromatographic systems is facilitated by convective transport in the macropores (12 000 Å). In this paper, we will investigate the ability of these stacked membrane chromatographic systems to carry out efficient gradient elution of proteins under elevated flow-rate and mass loading conditions.

EXPERIMENTAL

Materials

Carboxymethyl (CM) MemSep and diethylaminoethyl (DEAE) MemSep 1010 (1.0 × 2.8 cm I.D.) and 1000 (0.5 × 1.9 cm I.D.) ion-exchange membrane separation systems were supplied by Millipore (Bedford, MA, USA). Sodium acetate, sodium phosphate dibasic, sodium chloride, Tris–HCl, α-chymotrypsinogen A, cytochrome *c*, bovine serum albumin (BSA), human transferrin, human serum albumin (HSA), conalbumin, α-lactoalbumin, ovalbumin, trypsin inhibitor and lysozyme were purchased from Sigma (St. Louis, MO, USA).

Apparatus

Two chromatographic systems were employed in this work. Experimental system 1 consisted of a fast protein liquid chromatography (FPLC) system (Pharmacia-LKB Biotechnology, Uppsala, Sweden) which included a Model LCC-500-Plus controller, two Model P-500 pumps, a 0.6-ml mixer, and an MV-7 injection valve. The MemSep effluent was monitored at 280 nm by a Model UV-M detector and a Pharmacia strip-chart recorder. Fractions of the effluent were collected with a Model Frac-100 fraction collector. System 1 was used for all experiments unless otherwise noted.

Experimental system 2 consisted of a Waters 650 advanced protein purification system (Waters Chromatography Division, Millipore, Milford, MA, USA) which included a Model 600E controller, a Model 650 four buffer solvent system and a Model 484 variable-wavelength UV detector.

Procedures

Height equivalent to a theoretical plate (HETP) for MemSep. The HETP values for the DEAE and CM MemSep 1010 systems were evaluated using human transferrin and cytochrome *c*, respectively. These experiments were carried out under unretained conditions to evaluate the dispersive effects due to non-uniform fluid flow in these systems. Mobile phase conditions for the DEAE and CM MemSep analyses were 25 m*M* sodium phosphate, pH 7.5, containing 500 m*M* NaCl and 400 m*M* sodium acetate, pH 5.5, respectively.

Dynamic binding capacities of DEAE and CM MemSeps. The effect of flow-rate on the dynamic binding capacity of the DEAE MemSep 1000 was evaluated using sequential perfusions of: 44.8 ml of 1 mg/ml of HSA in 20 m*M* Tris, pH 8.0; 11.2 ml of 20 m*M* Tris, pH 8.0; and 11.2 ml of 20 m*M* Tris, pH 8.0, containing 1 *M* NaCl. Flow-rates of 1.4, 2.8, 5.6, 11.2 and 22.4 ml/min were employed. The shape of the resulting breakthrough curve as well as the total protein bound at each flow-rate was evaluated to investigate the effect of flow-rate on "dynamic" protein binding (Experimental system 2).

The binding capacities of the DEAE MemSep 1010 and the CM MemSep 1010 for BSA and lysozyme, respectively, were also determined by frontal chromatography under strongly retained conditions. 5.0 mg/ml BSA in 25 m*M* Tris, pH 8.5, and 5.0 mg/ml lysozyme in 25 m*M* sodium acetate, pH 5.5, were used for the DEAE and CM MemSeps, respectively.

Linear gradient

Anion exchange. A 5-mg amount of a protein mixture containing conalbumin, human transferrin, α-lactoalbumin, ovalbumin and trypsin inhibitor was separated using a linear gradient of 0 to 0.2 *M*

NaCl in 20 m*M* Tris, pH 8.1 on a DEAE MemSep 1010. Gradient times of 30, 20 and 10 min were employed at a volumetric flow-rate of 10 ml/min (Experimental system 2).

Effect of flow-rate. A 25-μl feed solution consisting of 3.0 mg/ml α-chymotrypsinogen A, 4.0 mg/ml cytochrome *c* and 3.0 mg/ml lysozyme in 25 m*M* sodium acetate, pH 5.5, was separated using a linear gradient of 0 to 400 m*M* sodium acetate, pH 5.5, on the CM MemSep 1010. Volumetric flow-rates of 2, 5 and 10 ml/min were employed to evaluate the efficacy of the CM MemSep in linear gradient chromatography under various flow-rate conditions. Gradient volume was held constant at 30 ml at each flow-rate by appropriate adjustment of the gradient time.

Effect of mass loading. A feed solution containing 5 mg/ml each of α-chymotrypsinogen A, cytochrome *c* and lysozyme in 25 m*M* sodium acetate, pH 5.5, was employed to evaluate the effect of mass loading on the performance of the CM MemSep 1010 operated in the linear gradient mode. Injection volumes ranging from 25 μl to 1 ml were used at flow-rates ranging from 2–10 ml/min. A linear gradient of 0 to 400 m*M* sodium acetate, pH 5.5, with a gradient volume of 30 ml was used to elute the proteins.

Linear elution studies. Linear elution chromatography of α-chymotrypsinogen A, cytochrome *c* and lysozyme was carried out at various concentrations of sodium acetate, pH 5.5, to examine the effect of salt on protein retention time. From these experiments, a plot of log capacity factor (k') *vs.* log [Na^+] was generated in order to predict appropriate "windows" of salt concentration for the step gradient experiments.

Multiple step gradients. Feed solutions of 1 ml containing 6, 15 and 30 mg total protein of α-chymotrypsinogen A, cytochrome *c* and lysozyme in 25 m*M* sodium acetate, pH 5.5, were separated by step gradient chromatography on the CM MemSep 1010 module. The CM MemSep was initially equilibrated with distilled water. The buffered protein feed solutions were introduced into the CM MemSep 1010 after which the first step change in salt concentration was performed. The subsequent step changes in salt concentration were executed when the eluting peak obtained a maximum value. All experiments were performed at a flow-rate of 5.0 ml/min. The 30-mg experiment was also carried out at a flow-rate of 10 ml/min. The following step gradients were carried out: 6 mg injection: 100, 175 and 400 m*M* sodium acetate; 15 mg injection: 90, 165 and 400 m*M* sodium acetate; 30 mg injection: 60, 150 and 400 m*M* sodium acetate.

RESULTS AND DISCUSSION

HETP for DEAE and CM MemSep

In order to evaluate the inherent efficiency of these stacked membrane chromatographic columns a traditional HETP evaluation was carried out. While the exact meaning of "plate height" in such a membrane chromatographic column is unclear, it nonetheless served as a comparative measure of efficiency in these systems. Since these modules are typically employed for gradient chromatography where adsorption–desorption kinetics have minimal effects on system efficiency, we examined the dispersion due solely to the fluid flow characteristics of the system. The resulting HETP plots for unretained human transferrin and cytochrome *c* on the DEAE MemSep and CM MemSep modules, respectively, are presented in Fig. 1. Under these conditions, the plate heights were on the order of 20 μm and were relatively insensitive to flow-rate. Thus, there appears to be minimal dispersive contributions from fluid flow irregularities in these systems under typical operating conditions of 1–10 ml/min.

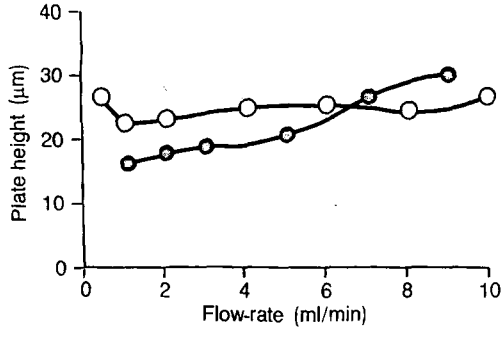

Fig. 1. Height equivalent to a theoretical plate (HETP) *vs.* flow-rate for DEAE and CM MemSeps 1010 for unretained proteins. DEAE MemSep: human transferrin (●) in 25 m*M* sodium phosphate, pH 7.5, containing 500 m*M* sodium chloride; CM MemSep: cytochrome *c* (○) in 400 m*M* sodium acetate, pH 5.5.

Binding capacity of DEAE and CM MemSeps

The effect of flow-rate on the dynamic binding capacity of the DEAE MemSep 1000 was evaluated as described in the Experimental section. The resulting chromatographic profiles are shown in Fig. 2. As seen in the figure, the breakthrough fronts were relatively sharp at flow-rates of 1.4 and 11.2 ml/min with a slightly more diffuse front occurring at 22.4 ml/min. The dynamic binding capacities of these systems remained essentially constant at approximately 35 mg as shown in Table I. Thus, these membrane chromatographic systems can be readily scaled-up with respect to flow-rate when operated in the adsorption–desorption mode.

The binding capacities of the DEAE MemSep 1010 for BSA and the CM MemSep 1010 for lysozyme were also measured by frontal chromatography as described in the experimental section. Under these strongly retained conditions, the binding capacity of the DEAE MemSep 1010 was 34.2 mg BSA. For the CM MemSep 1010, the binding capacity was 67.2 mg lysozyme. While these represent lower binding capacities than generally obtained with conventional chromatographic supports, the ability to operate at elevated flow-rates makes these systems attractive for high-throughput capture operations in downstream bioprocessing.

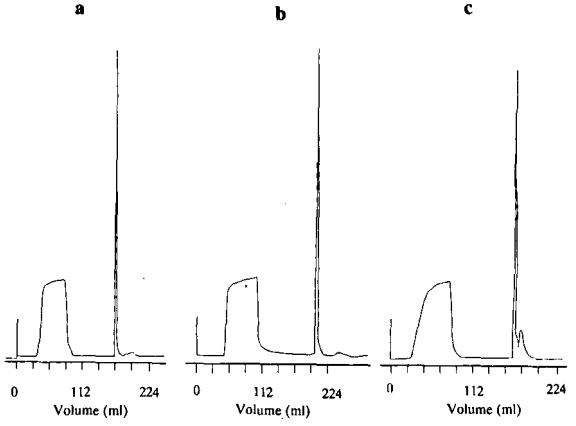

Fig. 2. Effect of flow-rate on dynamic binding capacity of the DEAE MemSep 1000. Feed: 44.8 ml of 1 mg HSA/ml in 20 m*M* Tris, pH 8.0; wash: 11.2 ml of 20 m*M* Tris, pH 8.0; eluent: 11.2 ml of 20 m*M* Tris, pH 8.0, containing 1 *M* NaCl; flow-rates: (a) 1.4, (b) 11.2 and (c) 22.4 ml/min.

TABLE I

DYNAMIC BINDING CAPACITY OF DEAE MemSep 1010 FOR HUMAN SERUM ALBUMIN

Flow-rate (ml/min)	Binding capacity (mg)
1.4	37.8
2.8	33.6
5.6	34.7
11.2	35.8
22.4	34.8

Linear gradient

The DEAE MemSep 1010 system was employed in the linear gradient mode for the analytical separation of a five-component protein mixture under various flow-rate conditions. The resulting separations for gradient runs ranging from 30 to 10 min are shown in Fig. 3. These results demon-

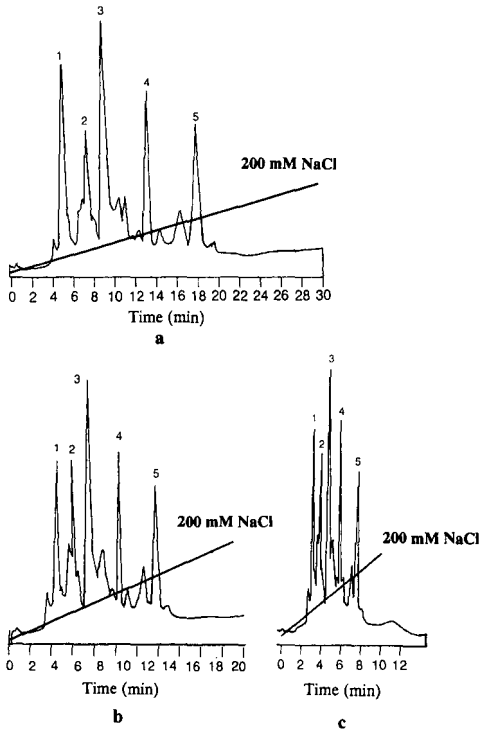

Fig. 3. Linear gradient separation of a five-component protein mixture on DEAE MemSep 1010. Feed: 1 = conalbumin; 2 = human transferrin; 3 = α-lactoalbumin; 4 = ovalbumin; 5 = trypsin inhibitor (5 mg total protein); flow-rate: 10 ml/min; gradient conditions: 0 to 200 m*M* NaCl in 20 m*M* Tris, pH 8.1, in 30 min (a), 20 min (b) or 10 min (c).

strate that these systems can indeed be employed for linear gradient separations of complex protein mixtures.

The CM MemSep 1010 column was employed in a series of linear gradient experiments to examine the effects of flow-rate and mass loading on the performance of the system. These experiments were carried out under conditions where baseline resolution of the proteins was maintained. Linear gradient conditions were established using analytical-scale protein loading (0.25 mg total protein). The resulting chromatogram, depicted in Fig. 4a, demonstrates that these cation-exchange MemSep systems can also be readily employed for linear gradient protein separations. In order to examine the effect of flow-rate in these systems, the experiment was repeated at volumetric flow-rates of 5 and 10 ml/min. The resulting chromatograms, shown in Fig. 4b and c, indicate that these analytical linear gradient separations can be readily scaled-up with respect to flow-rate with minimal adverse effect on the separation efficiency. Clearly, these ion-exchange membrane systems have significant potential for rapid analytical chromatographic applications. Furthermore, the ability to carry out rapid analytical experiments will significantly shorten method development time with these membrane chromatographic systems.

While these results indicate that the MemSep systems can be a powerful tool for analytical chromatography, in order for it to have utility for preparative separations, it must be capable of high-throughput bioseparations. Accordingly, the linear gradient experiment on the CM MemSep 1010 was repeated at mass loadings in the range of 0.75–15 mg total protein. As seen in Fig. 5, this preparative separation was readily scaled-up to 15 mg total protein with minimal adverse effect on the separation efficiency.

In an effort to further increase the throughput in this linear gradient system, the 15-mg separation was repeated at 10 ml/min resulting in the chromatogram shown in Fig. 6. The gradient time for this separation of 15 mg of proteins was 3 min. These results demonstrate that these membrane chromatographic systems can be readily employed in the linear gradient mode at both elevated mass loadings and volumetric flow-rates for high-throughput bioseparations.

Multiple step gradients

In order to establish appropriate conditions for multiple step gradient protein separations, linear

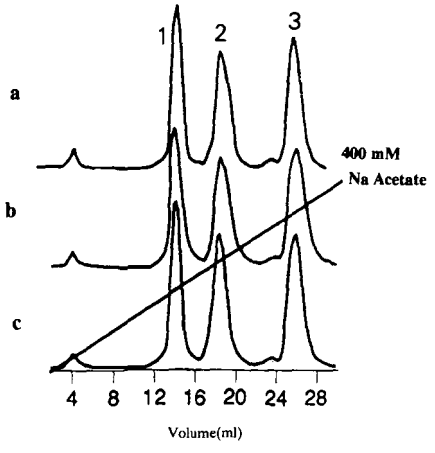

Fig. 4. Linear gradient separation of a three-component protein mixture on CM MemSep 1010. Feed: 1 = α-chymotrypsinogen A; 2 = cytochrome *c*; 3 = lysozyme (0.25 mg total protein). Gradient conditions: 0–400 m*M* sodium acetate, pH 5.5; in (a) 15 min at a flow-rate of 2.0 ml/min, (b) 6 min at a flow-rate of 5.0 ml/min or (c) 3 min at a flow-rate of 10.0 ml/min.

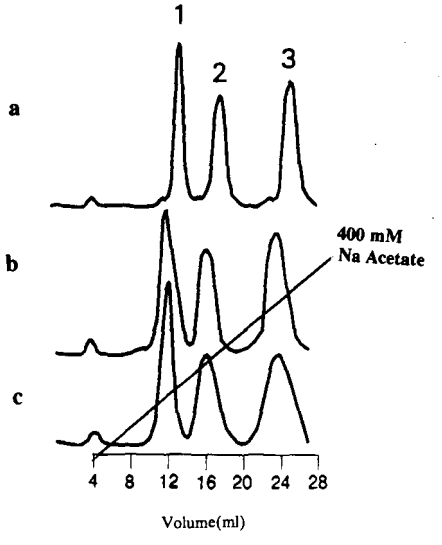

Fig. 5. Linear gradient separation of a three-component protein mixture on CM MemSep 1010 at elevated protein loadings. Feed: 1 = α-chymotrypsinogen A; 2 = cytochrome *c*; 3 = lysozyme. Gradient conditions: 0–400 m*M* sodium acetate, pH 5.5 in 15 min, flow-rate: 2.0 ml/min. Total protein loadings of 0.75 mg (a), 7.5 mg (b) and 15.0 mg (c).

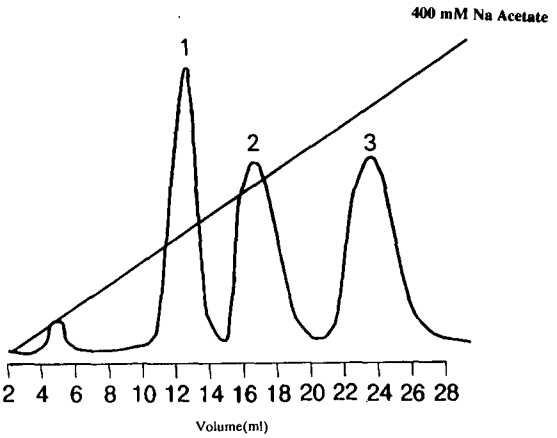

Fig. 6. Linear gradient separation of a three-component protein mixture on CM MemSep 1010 at both elevated flow-rate and protein loading. Feed: 1 = α-chymotrypsinogen A; 2 = cytochrome *c*; 3 = lysozyme (15 mg total protein). Gradient condition: 0–400 m*M* sodium acetate, pH 5.5 in 3 min, flow-rate: 10.0 ml/min.

elution studies were carried out. Various concentrations of sodium acetate were used to examine the effect of salt on the retention of α-chymotrypsinogen A, cytochrome *c* and lysozyme in the CM MemSep 1010. The resulting plot of log *k'* *vs.* log [Na^+] is shown in Fig. 7. As seen in the figure, concentrations of 100 m*M* and 175 m*M* sodium acetate result in negligible *k'* values for α-chymotrypsinogen A and cytochrome *c*, respectively. For lysozyme, any concentration above 300 m*M* sodium acetate resulted in rapid elution of the protein. Accordingly, these "windows" of salt concentration were employed in

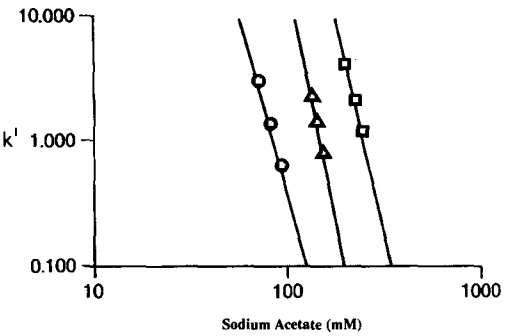

Fig. 7. Effect of salt on protein capacity factors on CM MemSep 1010. ○ = α-Chymotrypsinogen A; ▲ = cytochrome *c*; □ = lysozyme.

the multi-step gradient separation of 6 mg total protein as shown in Fig. 8a. Under these conditions, the multi-step gradient procedure resulted in complete separation of the three proteins in approximately 5 min.

The separation was then scaled-up with respect to mass loading to investigate the capacity of these systems for multiple step-gradient operation. As expected, at higher mass loadings the non-linearity of the protein isotherms resulted in elution of the proteins at lower salt concentrations. Accordingly, the step gradient conditions were appropriately modified, as the mass loading was increased, to maintain baseline separation. For a total protein loading of 15 mg, the "windows" employed for the multi-step gradient were changed to 90, 165 and 400 m*M* sodium acetate. As seen in Fig. 8b, under this mass loading, baseline separation of the proteins was achieved with a separation time of approximately 5 min.

At a protein loading of 30 mg, a significant reduction in the initial step change was required to eliminate contamination of the α-chymotrypsinogen A by the cytochrome *c*. For this mass loading, the "windows" employed for the multi-step gradient were changed to 60, 150 and 400 m*M* sodium

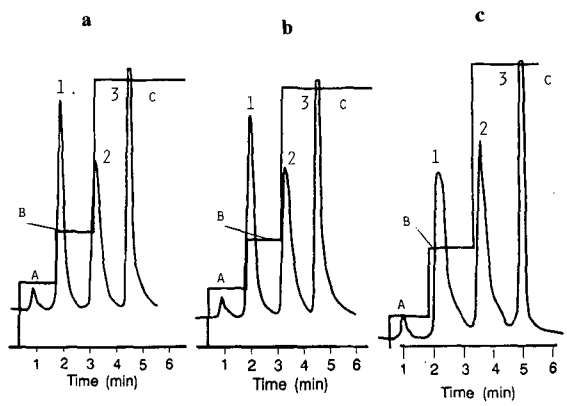

Fig. 8. Step gradient separation of a three-component protein mixture on CM MemSep 1010. Feed: 1 = α-chymotrypsinogen A; 2 = cytochrome *c*; 3 = lysozyme. Flow-rate: 5.0 ml/min. (a) Total protein: 6 mg. Gradient conditions: sequential step changes of 100 (A), 175 (B) and 400 (C) m*M* sodium acetate, pH 5.5. (b) Total protein: 15 mg. Gradient conditions: sequential step changes of 90 (A), 165 (B) and 400 (C) m*M* sodium acetate, pH 5.5. (c) Total protein: 30 mg. Gradient conditions: sequential step changes of 60 (A), 150 (B) and 400 (C) m*M* sodium acetate, pH 5.5. Flow-rate: 5.0 ml/min.

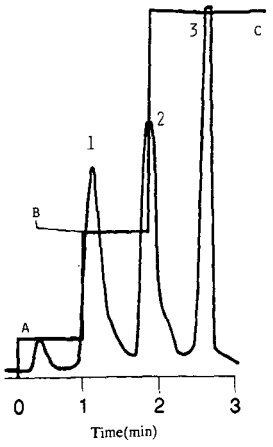

Fig. 9. Step gradient separation at elevated flow-rate and mass loading of a three-component protein mixture on CM MemSep 1010. Conditions as in Fig. 8c with the exception of flow-rate: 10.0 ml/min.

acetate. While, the reduced initial step gradient resulted in a more diffuse α-chymotrypsinogen A peak than in the previous experiments, baseline separation of the proteins was achieved with a separation time of approximately 6 min (Fig. 8c).

To further increase the throughput of these systems, the 30-mg step gradient separation was repeated at a volumetric flow-rate of 10 ml/min, resulting in the chromatogram shown in Fig. 9. Again, baseline separation of the proteins was achieved, now with a separation time of about 3 min. In fact, the bioproduct throughput could be readily increased by further optimization of the step gradient conditions as well as relaxation of the baseline resolution constraint. In addition, recovery of the feed proteins was found to be greater than 95% in all gradient experiments. If one assumes a re-equilibration time of 2 min (corresponding to 20 ml or 5 column volumes), this system would have a throughput of 360 mg purified protein/h. Thus, the CM MemSep 1010 module can be employed for high-throughput protein purification when operated in the multiple step gradient mode.

CONCLUSIONS

In this report we have demonstrated that chromatographic systems consisting of stacked adsorptive membranes can be employed for high-throughput protein purification. Linear and step gradient chromatographic separations of proteins on ion-exchange membrane systems were successfully scaled up with respect to flow-rate and mass loading with minimal adverse effect on resolution or bioproduct purity. The ability to operate these systems at elevated flow-rates enables rapid analytical chromatography as well as significantly shortened methods development time. In addition, the ability of these efficient, low-pressure systems to operate at high mass loadings in both the linear and step gradient modes of operation make these systems particularly attractive for preparative chromatographic applications.

ACKNOWLEDGEMENTS

This work was supported by Grant No. CTS-8957746 from the National Science Foundation and by Millipore Corporation.

REFERENCES

1 S. M. Cramer and G. Subramanian, in G. Keller and R. Yang (Editors), *New Directions in Sorption Technology*, Butterworth, Boston, MA, 1988, pp. 187–226.
2 G. Guiochon and A. Katti, *Chromatographia*, 24 (1987) 165.
3 E. Grushka (Editor), *Preparative-Scale Chromatography* (*Chromatographic Science Series*, Vol. 46), Marcel Dekker, New York, 1989.
4 S. M. Cramer and G. Subramanian, *Sep. Purif. Methods*, 19 (1990) 31.
5 J. Frenz and Cs. Horváth, in Cs. Horváth (Editor), *High-Performance Liquid Chromatography —Advances and Perspectives*, Vol. 5, Academic Press, Orlando, FL, 1988, pp. 211–314.
6 Cs. Horváth, in F. Bruner (Editor), *The Science of Chromatography* (*Journal of Chromatography Library*, Vol. 32), Elsevier, Amsterdam, 1985, pp. 179–207.
7 K. Veeraragavan, A. Bernier and E. Braendli, *J. Chromatogr.*, 54 (1991) 207.
8 J. Newburger and G. Guiochon, *J. Chromatogr.*, 523 (1990) 63.
9 R. S. Hodges, T. W. L. Burke and C. T. Mant, *J. Chromatogr.*, 444 (1988) 349.
10 S. Brandt, R. A. Goffe, S. B. Kessler, J. L. O'Connor and S. E. Zale, *Biotechnology*, 6 (1989) 779.
11 H. Ding, M. C. Yang, D. Schisla and E. L. Cussler, *AIChE J.*, 35 (1989) 814.
12 H. Ding and E. L. Cussler, *Biotechnol. Prog.*, 6 (1990) 472.
13 N. B. Afeyan, S. P. Fulton, N. F. Gordon, I. Mazsaroff and L. Varady, *Biotechnology*, 8 (1990) 203.
14 L. L. Lloyd and F. P. Warner, *J. Chromatogr.*, 512 (1990) 365.
15 N. B. Afeyan, N. F. Gordon, I. Mazsaroff, L. Varady, S. P.

Fulton, Y. B. Yang and F. E. Regnier, *J. Chromatogr.*, 519 (1990) 1.
16 D. J. Burke, J. K. Duncan, L. C. Dunn, L. Cummings, C. J. Siebert and G. S. Ott, *J. Chromatogr.*, 353 (1986) 425.
17 K. K. Unger, G. Jilge, J. N. Kinkel and M. T. Hearn, *J. Chromatogr.*, 359 (1986) 61.
18 Y. Kato, T. Kitamura, A. Mitsui and T. Hashimoto, *J. Chromatogr.*, 398 (1997) 327.
19 L. Varady, K. Kalghatgi and Cs. Horváth, *J. Chromatogr.*, 458 (1988) 207.
20 K. Kalghatgi, *J. Chromatogr.*, 499 (1990) 267.
21 S. Hjertén and J.-L. Liao, *J. Chromatogr.*, 457 (1988) 165.
22 J.-L. Liao and S. Hjertén, *J. Chromatogr.*, 457 (1988) 175.
23 S. Hjertén, J.-L. Liao and R. Zhang, *J. Chromatogr.*, 473 (1989) 273.
24 T. B. Tennikova, B. G. Belenkii and F. Svec, *J. Liq. Chromatogr.*, 13 (1990) 63.
25 I. M. Bird, I. H. Sadler, B. C. Williams and S. W. Walker, *Mol. Cell. Endocrinol.*, 66 (1989) 215.
26 I. M. Bird, I. Meikle, B. C. Williams and S. W. Walker, *Mol. Cell. Endocrinol.*, 64 (1989) 45.

Journal of Chromatography, 596 (1992) 181–184
Elsevier Science Publishers B.V., Amsterdam

CHROM. 23 989

Analysis of underivatized C_{12}–C_{18} fatty acids by reversed-phase ion-pair high-performance liquid chromatography with conductivity detection

Yoshiko Tsuyama*, Toshiro Uchida and Takeshi Goto

Naruto Research Centre, Otsuka Chemical Co., Ltd., 615 Satoura, Naruto 772 (Japan)

(First received October 2nd, 1991; revised manuscript received December 31st, 1991)

ABSTRACT

A rapid, simple and precise reversed-phase ion-pair high-performance liquid chromatographic method is described for the separation and determination of underivatized fatty acids (C_{12}–C_{18}) using a conductivity detector. Baseline separation of eight fatty acid standards was achieved on an octadecylsilyl column using isocratic elution with a methanol–5 m*M* tetrabutylammonium mobile phase. The method was successfully applied to the determination both of an anionic surfactant and of free fatty acids extracted from etiolated wheat shoots. The detection limit of margaric acid was *ca.* 2 ng at a signal-to-noise ratio of 3.

INTRODUCTION

The determination of free fatty acids has become important in many fields [1,2]. Although many laboratories have traditionally resolved fatty acids by gas chromatography [3], the determination of fatty acids by high-performance liquid chromatography (HPLC) seems to have become established [4–8]. Most of the available methods need derivatization for satisfactory separation and sensitivity, however, because fatty acids lack fluorescent or strongly UV-absorbing groups. Consequently, numerous types of precolumn labelling agents for HPLC have been developed [9–15].

The development of methods for the determination of underivatized long-chain fatty acids is a challenge. Separation of underivatized fatty acids has frequently been performed on octadecylsilyl (ODS) reversed-phase columns [2,16–20] using various mobile phases such as methanol–water–acetic acid [2], tetrahydrofuran–water [16] and acetonitrile–aqueous phosphoric acid [17,19,20]. Detection has been effected with refractive index [1], UV [2,17], capacitance/conductance [16] and electrokinetic detectors [18], a post-column ion-pair extraction and detection system [19], a differential thermal lens [20] and a chemiluminescence detector [21]. However, each method has drawbacks such as low sensitivity, poor resolution and long analysis time.

We have developed a rapid, simple and precise reversed-phase ion-pair HPLC method with conductivity detection for the separation and determination of underivatized fatty acids. Good separation of eight fatty acid standards was achieved by the use of a reversed-phase column, an isocratic eluent consisting of methanol–5 m*M* tetrabutylammonium (TBA) and a conductivity detector.

EXPERIMENTAL

Reagents and chemicals

Analytical-reagent-grade methanol and myristic acid were purchased from Wako (Osaka, Japan). PIC reagent A (a phosphate-buffered solution of TBA) was obtained from Waters Assoc. (Milford, MA, USA). Lauric, oleic and linoleic acids were purchased from Tokyo Kasei Kogyo (Tokyo, Japan), margaric acid from Aldrich (Milwaukee, WI, USA) and linolenic, palmitic and stearic acids from Sigma (St. Louis, MO, USA). All fatty acids were of

0021-9673/92/$05.00

the highest purity available. Lunac O-P, an anionic surfactant, was supplied by Kao (Tokyo, Japan).

Extraction of plant lipids

Wheat (*Triticum aestivum* L. *cv.* Shirasagi) seeds were sown on moistened vermiculite, germinated and grown in the dark at 25°C for 5 days. A portion (300 mg fresh weight) of shoots were cut into 1–2-cm pieces, transferred into a 10-ml vial containing 5 ml of distilled water, incubated for a further 14 h as above and homogenized in a total of 2 ml of methanol with a mortar and pestle in dim light. The fresh weight after the 14-h incubation was 330 mg. The homogenate was transferred into a 10-ml tube with a Teflon cap. Exactly 1 ml of chloroform was added and mixed well with the methanolic extract, followed by the addition of 7 ml of distilled water. The mixture was centrifuged at 2000 *g* for 5 min at 25°C. An aliquot (0.3 ml) of the chloroform layer was evaporated to dryness under a stream of nitrogen. The residue was dissolved in 30 μl of 75% aqueous methanol and an 8-μl portion was injected onto the column for fatty acid determination.

HPLC analysis

The HPLC system consisted of a CCPD pump, an IC-8010 CM conductivity detector (both from Tosoh, Tokyo, Japan) and a SIC Chromatocorder 12 (System Instruments, Tokyo, Japan). A Rheodyne Model (Cotati, CA, USA) 7125 sample injector equipped with a 20-μl loop was used for sample injection. A 150 × 4.0 mm I.D. column packed with ODS, 5-μm particle size Hitachi Gel 3056 (Hitachi Instruments Service, Tokyo, Japan) was used. The mobile phase was methanol–5 m*M* TBA (pH 7.5) (75:25, v/v) which was prepared by diluting one bottle of PIC reagent A solution with 1000 ml of distilled water, passed through a 0.45-μm filter (Fuji Photo Film, Tokyo, Japan) before use. The flow-rate was 0.8 ml/min unless stated otherwise, the column temperature being 50°C. The conductivity detector was set at sensitivity 0.01 and range 200 μS/cm. The background conductivity was 114 μS/cm. The attenuation was fixed at 8, except when the detection limit of margaric acid was estimated at 1. The minimum width, minimum height, "twice time" (the period in which the peak width is doubled) and chart speed were set at 0.1 min, 8 μV, 0 min and 2 mm/min, respectively.

RESULTS AND DISCUSSION

TBA has conventionally been used to separate organic anions as ion pairs [22–24]. A mobile phase consisting of methanol–5 m*M* TBA (75:25, v/v) efficiently separated C_{12}–C_{18} fatty acid standards (Fig. 1). Methanol–water (75:25, v/v) mixture gave a poor separation with rapid elution of the fatty acids. The retention time increased with increase in the concentration of TBA in the mobile phase. At 5 m*M* TBA the lauric acid (C12:0) and myristic acid (C14:0) peaks were segregated from the in-between system peak, and the myristic acid peak was adequately separated from the linolenic acid (C18:3) peak. At 7.5 and 10 m*M* TBA the lauric acid peak overlapped the system peak (the range was raised to 500 μS/cm only for 10 m*M* TBA having an elevated background beyond the initial setting of 200 μS/cm). Lauric acid was eluted after the system peak

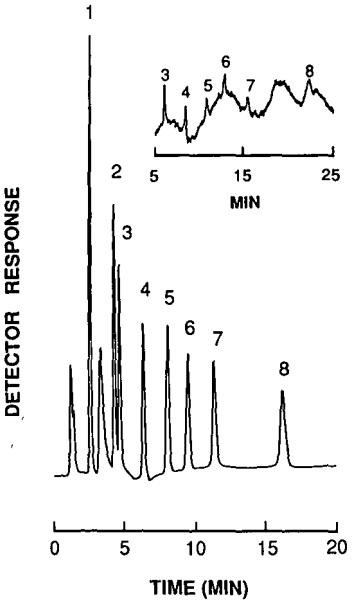

Fig. 1. Separation of free fatty acids by HPLC with conductivity detection. Mobile phase, methanol–5 m*M* TBA (pH 7.5) (75:25, v/v); flow-rate, 0.8 ml/min; oven temperature, 50°C. Detector settings: sensitivity, 0.01; range, 200 μS/cm. A 312.5-ng portion of each acid was injected. The inset shows the detection limits obtained by injecting 2 μl of 1 ppm fatty acid standards and setting the attenuation at 1 and the flow-rate at 0.6 ml/min. Peaks: 1 = lauric (C12:0) 2 = myristic (C14:0); 3 = linolenic (C18:3); 4 = linoleic (C18:2); 5 = palmitic (C16:0); 6 = oleic (C18:1); 7 = margaric (C17:0); 8 = stearic acid (C18:0).

with methanol–5 m*M* TBA (70:30, v/v), but not with methanol–5 m*M* TBA (72.5:27.5, v/v). The 70:30 eluent perfectly segregated myristic and linolenic acid, but required a longer analysis time, *e.g.*, 42.5 min for stearic acid (C18:0), whereas methanol–10 m*M* TBA (72.5:27.5, v/v) eluent yielded an almost identical chromatogram with a shorter analysis time, *e.g.*, 32.5 min for stearic acid.

As has been observed with underivatized fatty acids and their esters [17, 25], the retention time increased with increase in the number of carbon atoms and decreased with increase in the number of double bonds in the fatty acid chain (Fig. 1). The present method completely separated palmitic acid (C16:0) from oleic acid (C18:1), although the discrimination of these acids has often met with difficulty previously [1, 10, 19, 26]. Margaric acid (C17:0) was perfectly separated from the other fatty acid standards and can be used as an internal standard for fatty acid determinations.

The conductivity detector has widely been used for the detection of free fatty acids [16], ionic species and organic acids [27] and carboxylic acids and non-ionic substances [28]. The present conductimetric detection of fatty acid standards was more satisfactory with regard to both resolution and sensitivity than in a previous method [16] in which saturated C_8–C_{22} fatty acids were separated using an ODS column and tetrahydrofuran–water (45:55, v/v) as the mobile phase. The detection limit reported was 0.1 μg for capric acid (C10:0), which is higher than our detection limit given below.

Quantification of fatty acids was based on peak-area calculations, and the linearity of the method was assessed. The correlation coefficient of the regression line for each fatty acid standard ranged from 0.9995 (C16:0) to > 0.9999 (all other acids examined except lauric and myristic acids) between 43.7 ng (C16:0) and 2.66 μg (C18:3). The reproducibility of peak areas was good as shown by the small relative standard deviations (R.S.D.) of 0.75% (the largest R.S.D, obtained with 665 ng of linolenic

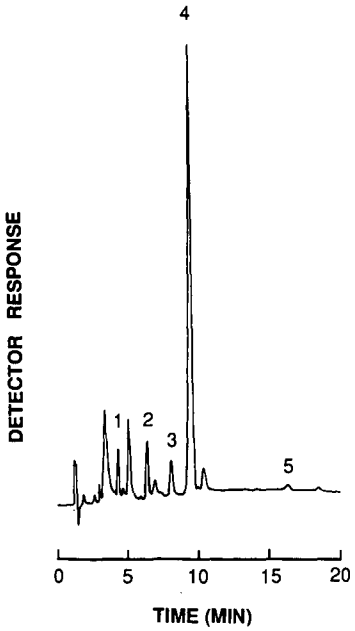

Fig. 2. Chromatogram of the anionic surfactant Lunac O-P. Lunac O-P was diluted with mobile phase to 1 mg/ml and a 2-μl portion was analysed as in Fig. 1. Fatty acids were tentatively assigned to individual peaks by comparing the retention times with those of the authentic standards in Fig. 1. Peaks: 1 = C14:0; 2 = C18:2; 3 = C16:0, 4 = C18:1; 5 = C18:0.

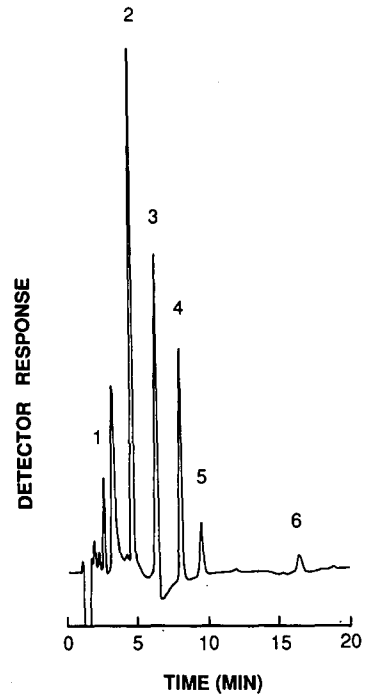

Fig. 3. HPLC profiles of lipoidal extracts from wheat shoots. Lipid fraction of dark-grown wheat shoots was analysed as in Fig. 1. See text for lipid extraction. Tentative peak identifications were made by comparing the retention times with those in Fig. 1. Peaks: 1 = C12:0; 2 = C18:3; 3 = C18:2; 4 = C16:0; 5 = C18:1; 6 = C18:0.

acid) (n = 5). The limit of detection at a signal-to-noise ratio of 3:1 was *ca.* 2 ng, based on the detectability of 1 ppm of margaric acid (2-μl injection) (Fig. 1).

The method has been successfully applied to the determination of the fatty acid contents in an anionic surfactant and in higher plant tissues, as shown in Figs. 2 and 3, respectively. Most pesticides contain surfactants as spreaders, emulsifiers or compatibility agents [29]. Therefore, exact information on the composition of a surfactant is important for pesticide formulations. Fig. 2 shows the exact compositional profile of the anionic surfactant Lunac O-P, which is reported by the manufacturer to contain mainly oleic acid, revealing that small amounts of C14:0, C18:2 and C16:0 are present. Fig. 3 shows that the main plant fatty acids were detected without interference from other lipoidal components such as carotenoids. The fatty acid profile obtained seems not too far from the galactolipid fatty acid composition of wheat shoots [30], although the linolenic acid ratio shown in Fig. 3 was low probably because of the difference between the plant tissues analysed.

The method described has several advantages: no need for derivatization, isocratic elution, good reproducibility, fairly high sensitivity and rapidity.

REFERENCES

1 J. W. King, E. C. Adams and B. A. Bidlingmeyer, *J. Liq. Chromatogr.*, 5 (1982) 275.
2 A. K. Batta, V. Dayal, R. W. Colman, A. K. Sinha, S. Shefer and G. Salen, *J. Chromatogr.*, 284 (1984) 257.
3 R. G. Ackman, *Methods Enzymol.*, 14 (1969) 329.
4 N. E. Bussell and R. A. Miller, *J. Liq. Chromatogr.*, 2 (1979) 697.
5 J. Halgunset, E. W. Lund and A. Sunde, *J. Chromatogr.*, 237 (1982) 496.
6 R. Wood and T. Lee, *J. Chromatogr.*, 254 (1983) 237.
7 E. Jüngling and H. Kammermeier, *Anal. Biochem.*, 171 (1988) 150.
8 G. Kargas, T. Rudy, T. Spennetta, K. Takayama, N. Querishi and E. Shrago, *J. Chromatogr.*, 526 (1990) 331.
9 H. D. Durst, M. Milano, E. J. Kikta, Jr., S. A. Connelly and E. Grushka, *Anal. Chem.*, 47 (1975) 1797.
10 S. A. Barker, J. A. Monti, S. T. Christian, F. Benington and R. D. Morin, *Anal. Biochem.*, 107 (1980) 116.
11 I. Yanagisawa, M. Yamane and T. Urayama, *J. Chromatogr.*, 345 (1985) 229.
12 M. Yamaguchi, S. Hara, R. Matsunaga, M. Nakamura and Y. Ohkura, *J. Chromatogr.*, 346 (1985) 227.
13 H. Miwa, C. Hiyama and M. Yamamoto, *J. Chromatogr.*, 321 (1985) 165.
14 J. D. Baty, R. G. Willis and R. Tavendale, *J. Chromatogr.*, 353 (1986) 319.
15 Y. Yasaka, M. Tanaka, T. Shono, T. Tetsumi and J. Katakawa, *J. Chromatogr.*, 508 (1990) 133.
16 Y. Hashimoto, M. Moriyasu, E. Kato, M. Endo, N. Miyamoto and H. Uchida, *Mikrochim. Acta*, 2 (1978) 159.
17 M. I. Aveldano, M. VanRollins and L. A. Horrocks, *J. Lipid Res.*, 24 (1983) 83.
18 B. K. Glod and W. Kemula, *J. Chromatogr.*, 321 (1985) 433.
19 J. F. Lawrence and C. F. Charbonneau, *J. Chromatogr.*, 445 (1988) 189.
20 S. R. Erskine and D. R. Bobbitt, *Anal. Chem.*, 61 (1989) 910.
21 H. Kawasaki, N. Maeda and H. Yuki, *J. Chromatogr.*, 516 (1990) 450.
22 K.-G. Wahlund, *J. Chromatogr.*, 115 (1975) 411.
23 S. J. Soldin and J. G. Hill, *Clin. Chem.*, 26 (1980) 291.
24 M. Janecek and K. Slais, *J. Chromatogr.*, 471 (1989) 303.
25 M. Özcimder and W. E. Hammers, *J. Chromatogr.*, 187 (1980) 307.
26 H. Kaneda, Y. Kano, M. Kamimura, T. Osawa and S. Kawakishi, *J. Agric. Food Chem.*, 38 (1990) 1363.
27 H. Small, T. S. Stevens and W. C. Bauman, *Anal. Chem.*, 47 (1975) 1801.
28 K. Tanaka and J. S. Fritz, *J. Chromatogr.*, 409 (1987) 271.
29 C. G. McWhorter, in R. H. Hodgson (Editor), *Adjuvants for Herbicides*, Weed Science Society of America, Champaign, IL, 1982, pp. 10–25.
30 J. B. St. John, *Plant Physiol.*, 57 (1976) 38.

Journal of Chromatography, 596 (1992) 185–195
Elsevier Science Publishers B.V., Amsterdam

CHROM. 23 973

Separation of monoacylglycerols by reversed-phase high-performance liquid chromatography

B. G. Semporé and J. A. Bézard*

Unité de Nutrition Cellulaire et Métabolique, Université de Bourgogne, B.P. 138, 21004 Dijon Cedex (France)

(First received April 18th, 1991; revised manuscript received December 22nd, 1991)

ABSTRACT

Reversed-phase high-performance liquid chromatography on a thermostated octadecylsilyl column was used to separate complex mixtures of monoacylglycerols formed by chemical deacylation of natural oil triacylglycerols. Acetonitrile–water mixtures were used for elution of the underivatized monoacylglycerols and a differential refractometer was used for their detection. The order of elution of monoacylglycerols in complex mixtures varies as a function of the chain length, unsaturation, positional isomerism, analysis temperature and eluent water concentration. The peak areas were representative of the amounts of monoacylglycerols detected. The method can be applied to compositional analysis and to the collection of non-contaminated fractions for further stereospecific analysis.

INTRODUCTION

Theoretically the simplest method for studying the stereospecific distribution of the fatty acids in triacylglycerol molecules is to determine the fatty acid profile of the three *sn*-1-, *sn*-2- and *sn*-3-monoacylglycerol isomers, formed by a deacylation procedure. The prerequisite is to use a deacylation technique which produces "representative" monoacylglycerols, *i.e.*, whose fatty acid profiles are exactly those expected from the fatty acid distribution in the triacylglycerol molecules. This means that the deacylating reagent should not have undesirable specificities for certain fatty acids or triacylglycerols, for certain positions in the triacylglycerol molecules, and should not promote acyl migration from one position to another, during or after hydrolysis.

Mammalian pancreatic lipase which specifically catalyses the hydrolysis of primary ester linkages (*sn*-1 and *sn*-3) in triacylglycerols [1] has been widely used in studying the fatty acid distribution at the *sn*-2-position of triacylglycerols. However, its specificity precludes the formation of *sn*-1- and *sn*-3-monoacylglycerols. In general, enzymatic deacylation procedures do not produce representative monoacylglycerols for the three positions of the glycerol moiety.

Chemical deacylation by a Grignard reagent has been widely used to produce representative diacylglycerols, especially *sn*-1,2(2,3)-diacylglycerols. Those were then utilized to study the fatty acid distribution at the *sn*-1- and *sn*-3-positions of triacylglycerols by Brockerhoff's enzymatic method [2–4] or by physical methods in which the diacylglycerol isomers were separated by high-performance liquid chromatography (HPLC) as chiral derivatives [5] or by HPLC on a chiral column [6–8].

However, the *sn*-1(3)- and *sn*-2-monoacylglycerols formed by Grignard deacylation could not be used as their fatty acid composition was not representative of the original triacylglycerol structure [9]. Extensive isomerization seemed to occur between *sn*-1(3)- and *sn*-2-isomers in both directions.

The possibility of optimizing the reaction conditions in order to minimize the extent of isomerization to an acceptable level cannot be discarded. In this regard we have examined the possibility of separating monoacylglycerols by HPLC both in the reversed-phase mode and in the presence of a chiral phase. Previously Maruyama and Yonese [10] devel-

0021-9673/92/$05.00

oped reversed-phase HPLC methods for the separation and determination of saturated and unsaturated simple underivatized monoacylglycerols. However, these methods were not entirely convenient for the simultaneous determination of the homologous distribution and the ratio of positional isomers of monoacylglycerols. Kondoh and Takano developed an original detection method for acylglycerols which they applicated to the simultaneous determination of mono-, di- and triacylglycerols [11] and then to mixtures of monoacylglycerols [12]. Homologous series and positional isomers of monoacylglycerols were well separated but the detection method involves destruction of monoacylglycerols and does not allow their collection for further analysis.

To study further the stereospecific distribution of fatty acids in triacylglycerols, we first developed the HPLC separation of complex mixtures of monoacylglycerols according to the nature of the constituent fatty acid (chain length and unsaturation) and to its positioning [*sn*-1(3)- and *sn*-2-monoacylglycerols]. Analyses were principally carried out on underivatized monoacylglycerols.

Some experiments were performed on monoacylglycerols derivatized with 3,5-dinitrophenyl isocyanate. These urethane derivatives are used in chiral-phase HPLC analyses of monoacylglycerol stereoisomerism [13].

EXPERIMENTAL

Samples

Optically active *sn*-3-monopalmitoylglycerol (*sn*-3-16:0) was obtained from Fluka (Buchs, Switzerland). *rac*-1-monopalmitoylglycerol (*rac*-1-16:0), *rac*-1-monostearoylglycerol (*rac*-1-18:0), *rac*-1-monooleoylglycerol (*rac*-1-18:1) and *rac*-1-monolinoleoylglycerol (*rac*-1-18:2) were purchased from Serdary (London, Ontario, Canada), as were optically inactive *sn*-2-isomers, namely *sn*-2-monopalmitoylglycerol (*sn*-2-16:0) and *sn*-2-monooleoylglycerol (*sn*-2-18:1). These monoacylglycerols were used without prior purification.

Natural source monoacylglycerols were prepared by Grignard degradation with ethylmagnesium bromide [14,15] and by pancreatic lipase hydrolysis [16,17] of triacylglycerols. Those were isolated from complex mixtures of peanut oil and cottonseed oil triacylglycerols by combined argentation thin-layer chromatography (TLC)–reversed-phase HPLC [18]. The fractionated triacylglycerols submitted to partial deacylation were palmitoyldioleoylglycerol (16:0 18:1 18:1), trioleoylglycerol (18:1 18:1 18:1), palmitoyloleoyllinoleoylglycerol (16:0 18:1 18:2), dioleoyllinoleoylglycerol (18:1 18:1 18:2), oleoyldilinoleoylglycerol (18:1 18:2 18:2) from peanut oil and palmitoyloleoyllinoleoylglycerol (16:0 18:1 18:2) from cottonseed oil (no distinction is being made among the *sn*-1-, *sn*-2- and *sn*-3-positions of these triacylglycerols). Monoacylglycerols formed by chemical or enzymatic deacylation of triacylglycerols were isolated by TLC on silica gel G (Merck, Darmstadt, Germany) impregnated with 5% (w/w) boric acid to prevent izomerization [19].

Preparation of monoacylglycerol urethane derivatives

The procedure used to prepare the urethane derivatives of monoacylglycerols was derived from that described by Oi and Kitahara [20] for chiral alcohols and adapted to monoacylglycerols by Takagi and co-workers [13,21]. A 20-μmol amount of monoacylglycerol (6–8 mg) was dissolved in 450 μl of dry toluene in a 0.5-ml glass vial with a PTFE-lined screw-cap, then 45 μmol (*ca.* 10 mg) of 3,5-dinitrophenyl isocyanate powder (Sumitomo, Osaka, Japan) and 45 μl of dry pyridine were added. The mixture was heated at 70°C for 1 h in an oven (or left for 3 h at ambient temperature) with occasional shaking.

At the end of the reaction, the mixture was cooled, the solvent was removed under nitrogen and the resulting urethane derivatives were dissolved in 0.2 ml of chloroform and purified by TLC on a silica gel 60 F_{254} precoated plate (20 × 20 cm, 0.25 mm thick layer) from Merck. The plates, containing a fluorescence indicator, were previously activated at 110–120°C for 1 h. They were developed twice with hexane–ethylene dichloride (or dichloromethane)–ethanol (40:15:3, v/v/v).

Crude urethane derivatives were alternatively purified by reversed-phase HPLC instead of TLC. In this instance, at the end of the derivatization procedure the mixture was decanted. The limpid upper phase was filtered through hyperfine glass-wool into another vial. The solvent was evaporated under nitrogen and the urethane derivatives were dissolved in chloroform for storage, in acetonitrile

or in the mixture used as the mobile phase for reversed-phase HPLC fractionation, *i.e.*, acetonitrile–water (95:5 or 90:10, v/v). Purification was carried out isocratically at ambient temperature (*ca.* 20°C).

Liquid chromatography

HPLC analyses were performed using a Model 6000 A solvent-delivery system (Waters, Milford, MA, USA) connected either to an R 401 differential refractometer or to a Model 450 variable-wavelength UV detector (Waters). The column was a stainless-steel prepacked 250 mm × 4 mm I.D. Hibar LiChroCART HPLC cartridge, LiChrospher 100 CH-18/II Super (4-μm particles) column purchased from Merck. A Guard-Pak precolumn, LiChroCART 4-4 filled with LiChrosorb 100 RP-18 (Merck), was attached to the column inlet. The mobile phase was acetonitrile–water in various proportions (80:20, 85:15, 90:10 and 95:5, v/v), depending on the monoacylglycerol mixtures to be analysed. It was delivered at a constant flow-rate of 1.0 or 1.2 ml min^{-1}. The analysis temperature was ambient (*ca.* 20°C) or a constant thermostatically controlled temperature [22].

Acetonitrile (Hypersolv "far UV") was obtained from BDH (Poole, UK). Water was doubly distilled. Solvents were filtered through a Millipore membrane (pore size 0.5 μm) and the HPLC solvent mixture was vacuum degassed for 2 min before use.

Peak areas were measured by means of an Enica 21 integrator–calculator (Delsi, Suresnes, France).

Gas chromatography

The fatty acid composition of the underivatized monoacylglycerols recovered from the hydrolysis products and that of the HPLC-collected monoacylglycerol urethane derivatives was determined by gas chromatography (GC) of the methyl esters prepared with methanol–boron trifluoride [23]. The analyses were carried out on a Becker-Packard Model 417 gas chromatograph equipped with a laboratory-made 30 m × 0.4 mm I.D. glass capillary column coated with Carbowax 20M (Applied Science Labs., State College, PA, USA) at a constant temperature of 195°C and a nitrogen flow-rate of 3 ml min^{-1}. The apparatus was equipped with a Ros injector [24] (Spiral, Dijon, France) and a flame ionization detector. Peak areas were measured with an Enica 21 integrator–calculator (Delsi). Calibration factors were calculated using standard mixtures of fatty acids (Nu-Chek Prep, Elysian, MN, USA).

Definitions

Monoacylglycerols were characterized by their partition number (*PN*), calculated from the equation [1]

$$PN = CN - 2\,DB$$

where *CN* is the number of carbon atoms in the acyl chains and *DB* the number of double bonds.

Chromatographic separations were characterized by three parameters: the retention time, generally corrected from the column void volume (t_R); the separation factor (α) between two successive peaks 1 and 2 (in the elution order), expressed as the ratio t_{R_2}/t_{R_1} [25]; and the resolution factor (R_s) calculated from the equation [25]

$$R_s = 2\,(t_{R_2} - t_{R_1})/(w_2 + w_1)$$

where t_R is the retention time and w the peak width at the baseline. For $R_s \geqslant 1$ two peaks are reasonably well separated.

RESULTS AND DISCUSSION

Separation of monoacylglycerols as urethane derivatives

Reversed-phase HPLC can separate a mixture of monoacylglycerol isomers into two groups, the optically inactive *sn*-2-monoacylglycerols and the optically active group of the two *sn*-1- and *sn*-3-isomers eluted together [12]. Separation of the two enantiomers in the latter can be achieved by HPLC in the presence of a chiral phase as monoacylglycerol urethane derivatives [13,21].

Chiral-phase HPLC separation of enantiomers generally cannot be applied directly to *sn*-2- and *sn*-1(3)-isomers resulting from chemical deacylation of natural triacylglycerols because of their complexity. A previous fractionation by reversed-phase HPLC according to chain length and unsaturation should be carried out.

To simplify this double-step analysis and to minimize the isomerization of underivatized monoacylglycerols, we first checked the possibility of fractionating by reversed-phase HPLC the natural complex mixture of monoacylglycerols in the obliga-

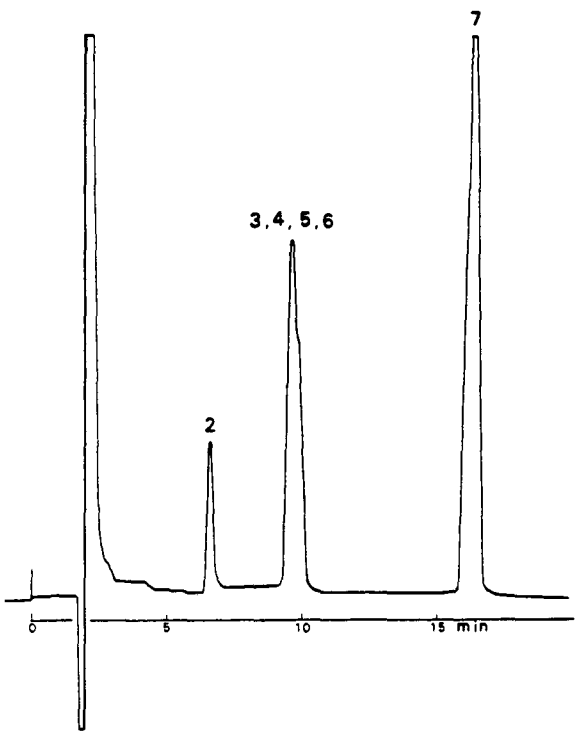

Fig. 1. HPLC separation of a mixture of standard isomeric monoacylglycerols (2 = *rac*-1-18:2; 3 = *sn*-2-18:1; 4 = *sn*-2-16:0; 5 = *rac*-1-18:1; 6 = *rac*-1-16:0; 7 = *rac*-1-18:0) as 3,5-dinitrophenyl isocyanate derivatives on an RP-18 column. The numbering of the different monoacylglycerols separated is done with respect of the elution order after reversed-phase HPLC separation of the total monoacylglycerol isomers analysed in this work as derivatives, *i.e.*, 1 = *sn*-2-monolinoleoylglycerol (*sn*-2-18:2); 2 = *sn*-1(3)- or *rac*-1-monolinoleoylglycerol [*sn*-1(3)- or *rac*-1-18:2]; 3 = *sn*-2-monooleoylglycerol (*sn*-2-18:1); 4 = *sn*-2-monopalmitoylglycerol (*sn*-2-16:0); 5 = *sn*-1(3)- or *rac*-1-monooleoylglycerol [*sn*-1(3)- or *rac*-1-18:1]; 6 = *sn*-1(3)- or *rac*-1-monopalmitoylglycerol [*sn*-1(3)- or *rac*-1-16:0]; 7 = *sn*-1(3)- or *rac*-1-monostearoylglycerol [*sn*-1(3)- or *rac*-1-18:0]. Analytical conditions: stainless-steel column (250 mm × 4 mm I.D.) packed with 4-μm octadecylsilyl (C_{18}) reversed-phase material; eluent, acetonitrile–water (95:5, v/v) at 1.2 ml min^{-1}; isocratic analysis at ambient temperature *ca.* 21°C; refractive index detection.

tory form of urethane derivatives prior to further separation of the enantiomers by chiral-phase HPLC. Six groups of urethane derivatives were studied. They were first injected separately on to the RP-18 column and then together.

Fig. 1 shows the results obtained with the synthetic mixture of the six groups of isomers. The resolution factors calculated from the corrected retention times of the monoacylglycerols injected individually indicated that for monopalmitoylglycerols the two groups of isomers [(*sn*-2 and *sn*-1(3)] were poorly separated, the calculated resolution factor R_s being only 0.56. For monooleoylglycerols, separation was just achieved (R_s = 1.00). Moreover, for the same group of isomers [*sn*-2 or *sn*-1(3)] the separation of monooleoyl- and monopalmitoylglycerol was very poor, because for the *sn*-2-isomers the retention time were 9.4 and 9.5 min, respectively, and hardly more different for the *sn*-1(3)-isomers, 9.7 and 10 min, respectively. On the other hand, in the chromatogram in Fig. 1 the four isomers [*sn*-2- and *sn*-1(3)-16:0, *sn*-2- and *sn*-1(3)-18:1] eluted almost together in the second peak (marked 3, 4, 5, 6).

Modifications of the analytical conditions (temperature, nature and flow-rate of the eluent) did not really improve the separations. This is the reason why previous fractionation of monoacylglycerol complex mitures was carried out by reversed-phase HPLC as underivatized monoacylglycerols.

Separation of underivatized monoacylglycerols

In preliminary experiments, various analytical conditions were checked: pure acetonitrile, pure propionitrile, mixtures of acetonitrile with different proportions of acetone, propionitrile and water were tested as mobile phases; and pure acetone, acetonitrile, chloroform and mixtures of these three solvents in different proportions were checked for dissolution of the monoacylglycerols samples.

The results showed that the best separations were obtained with a mixture of acetonitrile and water as the mobile phase and when the sample was dissolved in pure acetonitrile. These optimum conditions were similar to those observed previously [10,12].

Elution order. Fig. 2 shows the separation obtained in analysing a mixture of the three isomers *sn*-1-, *sn*-2- and *sn*-3- of monopalmitoylglycerol by reversed-phase HPLC at ambient temperature. Under all conditions only two peaks appeared on the chromatograms. Separate injections of commerc ial *rac*-1- and *sn*-2-monopalmitoylglycerols showed that the *sn*-2-isomer was first eluted and that the two *sn*-1- and *sn*-3-isomers were later eluted together. This elution pattern was also verified with monooleoylglycerols (Fig. 3) and monolinoleoylglycerols (Fig. 5).

Effect of solvent. The effect of increasing the

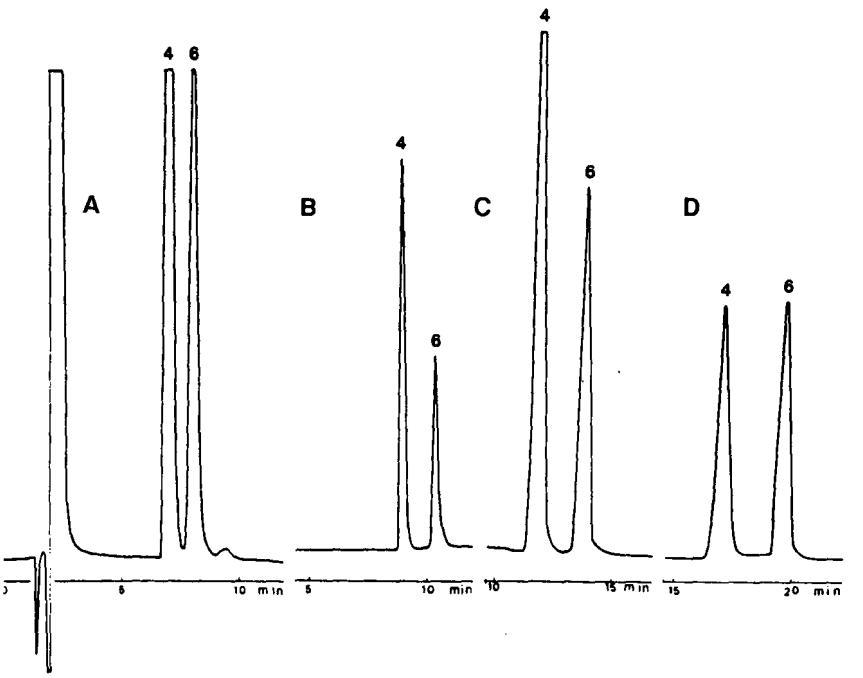

Fig. 2. HPLC separations of two standard mixtures (A–C, mixture 1; D, mixture 2) of *sn*-2- and *rac*-1-monopalmitoylglycerols (peaks 4 and 6, respectively) on an RP-18 column with different mixtures of acetonitrile–water [(A) 95:5, (B) 90:10, (C) 85:15, (D) 80:20, v/v] as the mobile phases. Analysis at ambient temperature (*ca.* 19–20°C); flow-rate, 1.2 ml min^{-1}; other conditions as in Fig. 1.

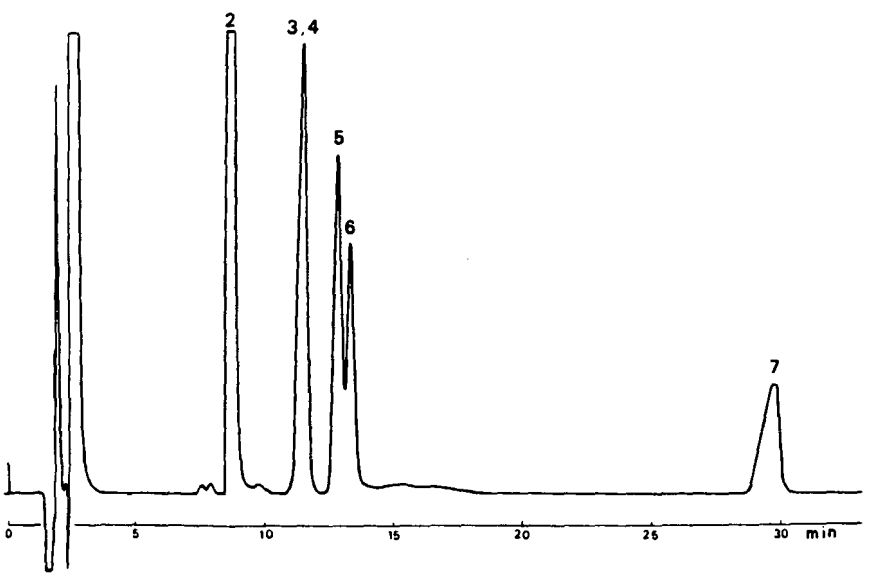

Fig. 3. RP-18 HPLC separation of a mixture of standard underivatized monoacylglycerols at ambient temperature (*ca.* 19°C). (2) = *rac*-1-18:2; (3, 4) = *sn*-2-18:1 and *sn*-2-16:0; (5) = *rac*-1-18:1; (6) = *rac*-1-16:0; (7) = *rac*-1-18:0. Mobile phase, acetonitrile–water (85:15, v/v); flow-rate, 1.2 ml min^{-1}; refractive index detection.

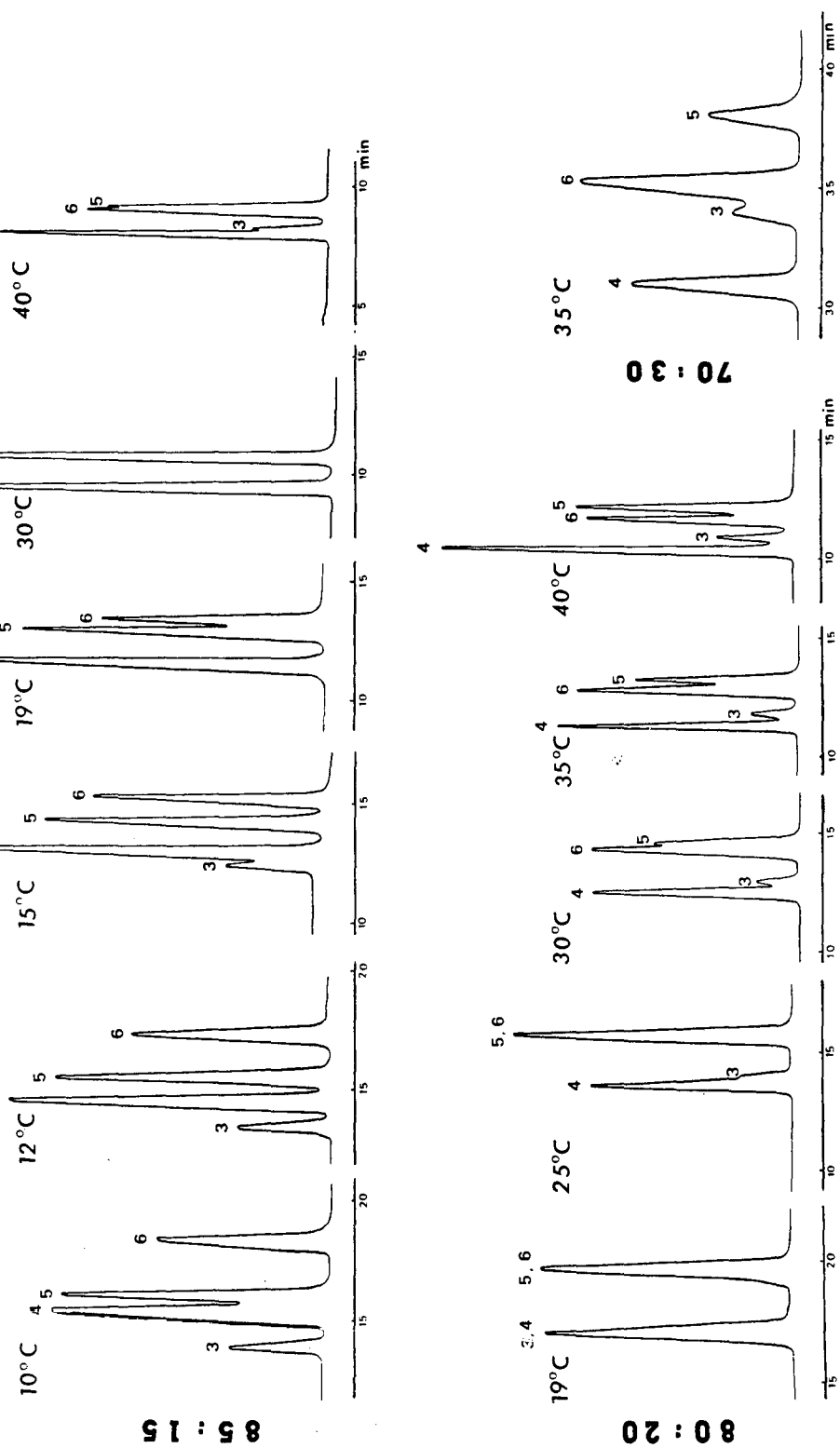

Fig. 4. RP-18 HPLC isocratic separations of a mixture of underivatized monoacylglycerols (3 = *sn*-2-16:0; 5 = *rac*-1-18:1; 6 = *rac*-1-16:0) at ambient (19°C) and different thermostatically controlled temperatures (10–40°C) and with different mobile phases [acetonitrile–water (85:15, 80:20 and 70:30, v/v], as indicated. Flow-rate, 1 ml min^{-1} for the other analyses. Other conditions as in Fig. 1.

proportion of water (5, 10, 15 and 20%) in the mobile phase on the separation of the two groups of isomers [*sn*-2-16:0 and *sn*-1(3)-16:0] is illustrated in Fig. 2.

An increase in the proportion of water greatly increased the retention times of both groups of isomers and in the same proportion. The effect was more pronounced at higher proportions of water (almost a 50% increase in retention time when the water content was increased from 15 to 20%, whereas the retention time increase was only *ca.* 30% when the water content was increased from 5 to 10%).

The separation factor between the two peaks was hardly affected (1.16 to 1.18) by varying the solvent polarity, indicating that the retention times of the two peaks were similarly affected. In contrast, the resolution factor between the two peaks increased considerably (from 1.65 to 3.00) with an increase from 5 to 10% of water in the mobile phase. The resolution factor then slightly decreased (2.39 at 15% of water and 2.77 at 20%), showing that the peak widths increased more rapidly than retention times above 10% of water. At this water concentration the resolution was sufficiently improved for pure fractions of monoacylglycerol isomers to be collected for further stereospecific analysis.

Fig. 3 illustrates the separation obtained in the HPLC analysis of a more complex mixture of monoacylglycerol isomers. The synthetic mixture contained *rac*-1-monolinoleoylglycerol (*rac*-1-18:2), *rac*-1-monooleoylglycerol (*rac*-1-18:1), *rac*-1-monopalmitoylglycerol (*rac*-1-16:0), *rac*-1-monostearoylglycerol (*rac*-1-18:0), *sn*-2-monooleoylglycerol (*sn*-2-18:1) and *sn*-2-monopalmitoylglycerol (*sn*-2-16:0). The mixture was analysed at ambient temperature and with acetonitrile–water (85:15, v/v) as the mobile phase.

Separate injection of the different isomers present in the synthetic mixture showed that the first-eluted peak corresponded to a mixture of *sn*-1- and *sn*-3-18:2, which were not separated. The second peak contained the two *sn*-2-isomers of monopalmitoyl- and monooleoylglycerols, which were not separated. They form a critical pair (similar partition number). The two components of *rac*-1-16:0 and -18:1, also constituting a critical pair, were partially separated (resolution factor 0.86). The *rac*-1-18:0 was eluted very late in 29 min, but the two *sn*-1- and *sn*-3-isomers were not separated. This very long retention time implies that with monoacylglycerols of longer chain length (20:0, 22:0, 24:0) such as those encountered in peanut oil triacylglycerols after partial deacylation, the solvent polarity should be decreased and/or the analysis temperature should be increased to reduce the retention times. Even under these conditions, the resolution factors between homologous monoacylglycerol isomers would be acceptable, when considering the resolution observed between the last two peaks in the chromatogram.

In addition to the impossibility of separating the *sn*-1- and *sn*-3-isomers of monoacylglycerols, the only problem encountered in the mixture analysis was the separation of the two critical pairs of monopalmitoyl- and monooleoylglycerols in both series of *sn*-2- and *sn*-1(3)-isomers. The resolution was studied by modifying the analysis temperature.

Effect of temperature. A mixture of the two series of monopalmitoyl- and monooleoylglycerols was analysed at increasing temperature from 7.5 to 40°C with acetonitrile–water (85:15, v/v) as the mobile phase, by using the thermostating device described previously [22]. Fig. 4 shows that at 12°C the two critical pairs in both isomer series were completely separated within the reasonable time of 18 min. The observed elution order was *sn*-2-18:1, *sn*-2-16:0, *sn*-1(3)-18:1, *sn*-1(3)-16:0. This elution order was different from that obtained by Takano and Kondoh [12] on an octylsilyl column (C_8) with an acetonitrile–water mobile phase, *viz.*, *sn*-2-16:0, *sn*-1(3)-16:0, *sn*-2-18:1, *sn*-1(3)-18:1. The resolution between peaks was also better under our analytical conditions.

Fig. 4 (top) also shows that when the analysis temperature was increased the retention of monopalmitoylglycerols decreased more rapidly than that of monooleoylglycerols in both series of isomers. At 30°C the same isomers of the two monoacylglycerols were eluted together. At higher temperature (40°C) the elution order of the two monoacylglycerols was the reverse of that observed at 12°C, and resolution was poorer. The separation can be greatly improved by combining an increase in solvent polarity and an increase in analysis temperature, as illustrated in Fig. 4 (bottom). With acetonitrile–water (80:20, v/v) the separation between the same isomers of the two different monoacylglycerols increased with increas-

ing temperature and at 40°C the four isomers were better separated with a more polar mobile phase with a similar sequence of elution (peaks 4, 3, 6, 5).

As shown qualitatively in Fig. 4, the calculated resolution factors indicated that the resolution between the two *sn*-2- (peaks 3 and 4) and the two *sn*-1(3)-18:1 and -16:0 isomers (peaks 5 and 6) decreased when the analysis temperature was increased whereas the reverse was true for *sn*-2-16:0 (peak 4) and *sn*-1(3)-18:1 (peak 5).

With the second more polar acetonitrile–water mixture (80:20, v/v), the resolution between isomer pairs (peaks 3 and 5 and peaks 4 and 6) greatly increased with increase in temperature.

Considering the overall results, it is clear that two optimum temperatures exist for the separation of critical pairs of monoacylglycerols (at least for 16:0 and 18:1) depending on the proportion of water in the mobile phase: a low temperature (12°C) for the lower proportion of water, with the elution order *sn*-2-18:1, *sn*-2-16:0, *sn*-1(3)-18:1, *sn*-1(3)-16:0 and a higher temperature (at least 40°C) for the higher proportion of water with a different elution order, *sn*-2-16:0, *sn*-2-18:1, *sn*-1(3)-16:0, *sn*-1(3)-18:1.

In practice, a low analysis temperature can be recommended for short-chain or unsaturated monoacylglycerols, which are fairly soluble in the usual solvents. Conversely, temperatures higher than ambient are more convenient for long-chain monoacylglycerols, especially when they are saturated. However, high analysis temperatures raise the problem of isomerization. Takano and Kondoh [12] observed an increased isomerization of *sn*-2- to *sn*-1(3)-monoacylglycerols at temperatures higher than 30°C, precluding quantitative analyses. The solution could be to increase the proportion of water in acetonitrile in order to obtain the same resolution at 30°C as at 40°C with a less polar mobile phase.

Application to natural monoacylglycerol mixtures

The purpose of this work was to fractionate by HPLC pure monoacylglycerol isomers for further stereospecific analysis as urethane derivatives by chiral-phase HPLC. The mixtures of isomers to be fractionated would be isolated by TLC from the chemical deacylation products of natural oil triacylglycerols.

For this reason, the analytical conditions studied above were applied to the following natural mixtures of monoacylglycerols. One mixture (A) was isolated after deacylation of peanut oil palmitoyldioleoylglycerol (16:0 18:1 18:1). It contained the four groups of isomers: *sn*-2- and *sn*-1(3)-monopalmitoyl- and -monooleoylglycerols. One mixture (B) resulted from deacylation of peanut oil palmitoyloleoyllinoleoylglycerol (16:0 18:1 18:2). It contained the six groups of isomers: *sn*-2- and *sn*-1(3)-monopalmitoyl-, -monooleoyl- and -monolinoleoylglycerols. Two mixtures (C and D) were obtained from deacylation of peanut oil dioleoyllinoleoylglycerol (18:1 18:1 18:2) and oleoyldilinoleoylglycerol (18:1 18:2 18:2), respectively. They contained the same four groups of isomers: *sn*-2- and *sn*-1(3)-monooleoyl- and monolinoleoylglycerols, but in different proportions.

The analyses were carried out at (A) 12.5°C, (B) 12°C and (C and D) 19°C with acetonitrile–water (85:15, v/v) as the mobile phase. Fig. 5 illustrates the separations obtained. Table I reports data which quantify the separations observed between two successively eluting peaks for the three analysis temperatures. The three chromatograms show a good resolution of the four or the six isomers present in the mixtures within relatively short retention times, less than 20 min in all instances.

The separation between two successive peaks was complete in all instances. The poorest separation was observed for the critical pair *sn*-2-18:1 and *sn*-2-16:0. However, the resolution factor (Table I) was 1.43 at 12.5°C (mixture A) and 1.45 at 12°C (mixture B). These good separations allow the collection of the separated fractions with minor cross-contamination for subsequent analysis of the *sn*-1(3)-isomers by chiral-phase HPLC to separate the two *sn*-1- and *sn*-3-monoacylglycerol enantiomers.

In the three mixtures, the proportions of the different isomers could be calculated from peak areas, assuming the latter is proportional to the mass of a compound. Such a determination was not made because the extent of isomerization cannot yet be determined. However, we can make interesting qualitative observations.

In mixture A (Fig. 5A), resulting from deacylation of 16:0 18:1 18:1, the 16:0 was rarely esterified at the *sn*-2 position (small amount of *sn*-2-16:0) to the benefit of 18:1. The peak areas of the monooleoylglycerols were roughly twice those of the mono-

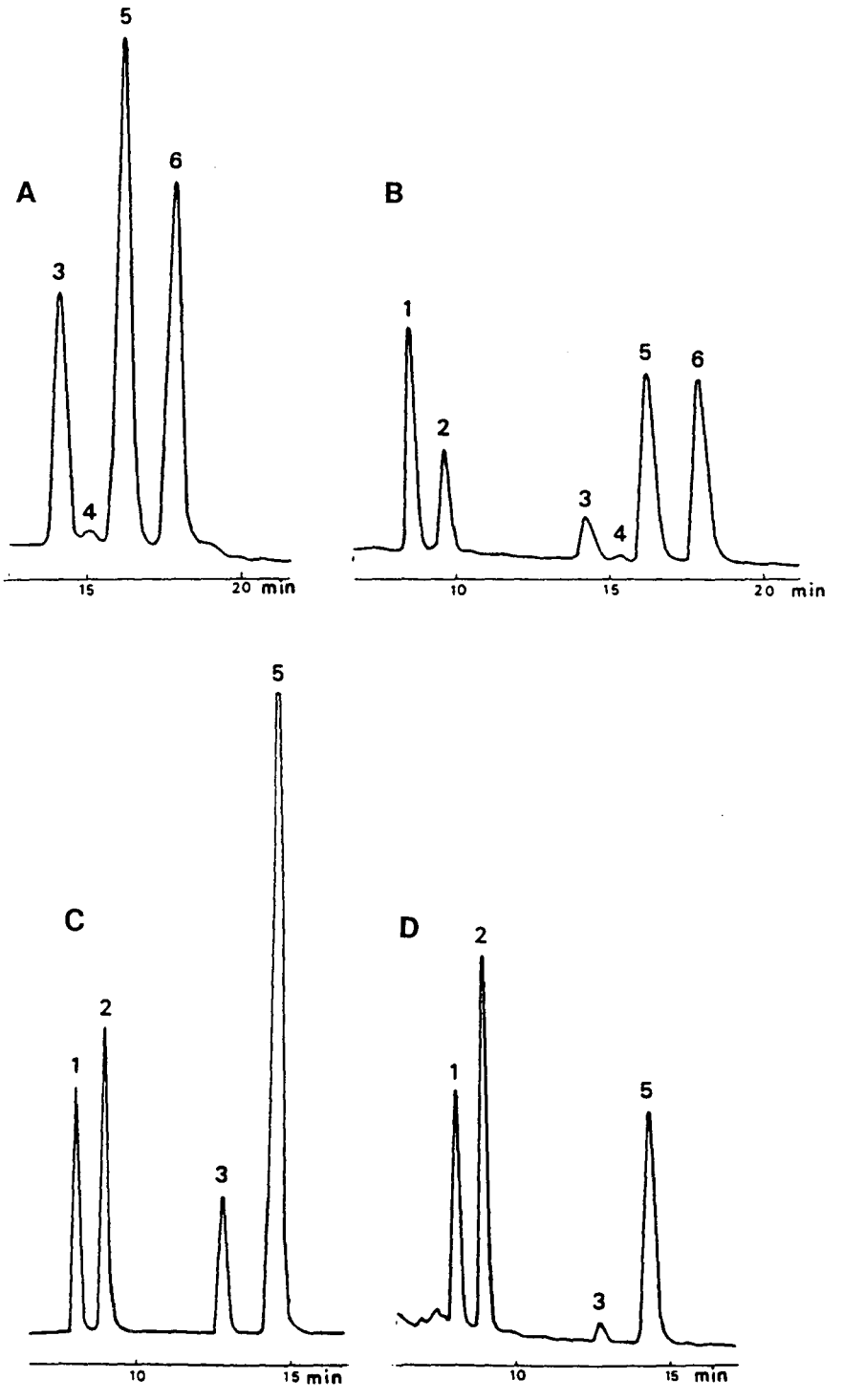

Fig. 5. RP-18 HPLC separations of mixtures of underivatized monoacylglycerols obtained after Grignard degradation of natural peanut oil triacylglycerols: (A) 16:0 18:1 18:1, (B) 16:0 18:1 18:2, (C) 18:1 18:1 18:2 and (D) 18:1 18:2 18:2. (A) Mixture of 3 = *sn*-2-18:1; 4 = *sn*-2-16:0; 5 = *sn*-1(3)-18:1; 6 = *sn*-1(3)-16:0. (B) Mixtures of 1 = *sn*-2-18:2; 2 = *sn*-1(3)-18:2; 3 = *sn*-2-18:1; 4 = *sn*-2-16:0; 5 = *sn*-1(3)-18:1; 6 = *sn*-1(3)-16:0. (C and D) Mixtures of 1 = *sn*-2-18:2; 2 = *sn*-1(3)-18:2; 3 = *sn*-2-18:1; 5 = *sn*-1(3)-18:1. Mobile phase, acetonitrile–water (85:15, v/v); flow-rate, 1.2 ml min^{-1}; analysis temperatures, (A) 12.5°C, (B) 12°C and (C and D) 19°C (ambient).

TABLE I

SEPARATION OF NATURAL MIXTURES OF MONOACYLGLYCEROL ISOMERS BY REVERSED-PHASE HPLC

Triacylglycerol[a]	16:0, 18:1, 18:1				16:0, 18:1, 18:2						18:1, 18:1, 18:2			
Monoacylglycerol[b]	*sn*-2-18:1	*sn*-2-16:0	*sn*-1(3)-18:1	*sn*-1(3)-16:0	*sn*-2-18:2	*sn*-1(3)-18:2	*sn*-2-18:1	*sn*-2-16:0	*sn*-1(3)-18:1	*sn*-1(3)-16:0	*sn*-2-18:2	*sn*-1(3)-18:2	*sn*-2-18:1	*sn*-1(3)-18:1
Temperature[c]	12.5°C				12°C						19°C			
Retention time (min)[d]	13.4	14.4	15.5	17.1	7.6	8.6	13.3	14.3	15.3	17.0	7.3	8.2	12.0	13.7
Separation factor[e]		1.07	1.08	1.10		1.14	1.54	1.08	1.07	1.11		1.12	1.47	1.14
Resolution factor[f]		1.43	1.54	1.79		1.87	6.76	1.45	1.36	2.00		2.43	9.11	3.17

[a] Triacylglycerols isolated from peanut oil by combined argentation TLC–reversed-phase HPLC.
[b] Monoacylglycerol isomers formed by chemical deacylation of the isolated triacylglycerols.
[c] Analysis at thermostated (12 and 12.5°C) and ambient (19°C) temperatures.
[d] Retention times corrected for the column void volume.
[e] Ratio of the corrected retention times of two successives peaks 1 and 2 (t_{R_2}/t_{R_1}).
[f] Calculated from the equation $R_s = 2\,(t_{R_2} - t_{R_1})/(w_2 + w_1)$, where t_R is the retention time and w the peak width at the baseline of two successive peaks 1 and 2.

palmitoylglycerol, *i.e.*, in proportion to the two acids in the original triacylglycerol.

The same remarks can be made for the localization of 16:0 in the triacylglycerol 16:0 18:1 18:2 (mixture B) and the roughly similar proportions of the three monoacylglycerols and the three fatty acids in the triacylglycerol (1:1:1).

As for mixture C, despite the affinity of 18:2 for the *sn*-2 position in triacylglycerols of vegetable origin, the proportion of *sn*-2-18:2 is lower than that of *sn*-2-18:1. The reason is that two molecules of 18:1 were in competition with one molecule of 18:2 for this position. The observed specificities of 16:0, 18:1 and 18:2 for the *sn*-2 position of peanut oil triacylglycerols confirm those generally observed for vegetable triacylglycerols [1].

Quantitative analysis

In stereospecific analyses of triacylglycerols by means of the monoacylglycerols formed by chemical

TABLE II

COMPOSITION OF NATURAL *sn*-2-MONOACYLGLYCEROL MIXTURES BY GC ANALYSIS OF FATTY ACIDS AND HPLC ANALYSIS OF MONOACYLGLYCEROLS

Fatty acid[a]	Triacylglycerol[b]									
	16:0 18:1 18:1		16:0 18:1 18:2		18:1 18:1 18:2		18:1 18:2 18:2		16:0 18:1 18:2	
	GC[c]	HPLC[c]	GC[c]	HPLC[c]	GC[c]	HPLC[c]	GC[c]	HPLC[c]	GC[c]	HPLC[c]
16:0	4.1	4.0	1.7	1.8	0.6	–	0.8	–	3.1	3.2
18:1	95.6	96.0	19.8	20.2	43.4	43.7	11.8	11.7	38.9	37.3
18:2	–	–	78.1	78.0	55.7	56.3	87.1	88.3	57.7	59.5

[a] Triacylglycerols isolated by combined argentation TLC–reversed-phase HPLC from peanut oil (first four triacylglycerols) and from cottonseed oil (last triacylglycerol).
[b] Traces of 16:1 (<0.1%) and 18:0 (<0.4%) were also found by GC analysis of fatty acids. Results are expressed as fatty acid mol%.
[c] *sn*-2-Monoacylglycerols formed by chemical deacylation of the triacylglycerols were isolated by TLC, analysed by HPLC and their fatty acids analysed by GC.

deacylation, one should know the exact relative proportions of the *sn*-2- and *sn*-1(3)-isomers separated by reversed-phase HPLC before analysing the *sn*-1(3)-isomers by chiral-phase HPLC for enantiomer composition. The easiest way to determine the relative proportions of the *sn*-2- and *sn*-1(3)-isomers is from peak areas, provided that the latter are proportional to mass.

To examine the possibility of using peak areas to calculate isomer composition, the following experiment was performed. Four triacylglycerols isolated from peanut oil (16:0 18:1 18:1, 16:0 18:1 18:2, 18:1 18:1 18:2 and 18:1 18:2 18:2) and one isolated from cottonseed oil (16:0 18:1 18:2) were submitted to chemical deacylation. The *sn*-2-monoacylglycerol fraction was isolated by borate-impregnated silica TLC [19]. An aliquot was analysed for fatty acid composition by GC as methyl esters. Another aliquot was analysed by HPLC and the composition was determined from peak areas.

The results reported in Table II show that the two series of figures are very similar, the variations not exceeding 4%.

As the GC analysis of fatty acids can be considered to be very accurate, the results reported here demonstrate that the same is true when the monoacylglycerol composition is calculated from peak areas.

CONCLUSIONS

This work has shown that monoacylglycerols can be completely separated by reversed-phase HPLC according to chain length and unsaturation and partially according to positional isomerism, as the *sn*-2-isomers were separated from the *sn*-1(3)-isomers. Peak areas are representative of the amount of compounds detected by their refractive indices (within the range tested). The *sn*-1(3)-isomers can be collected with minor contamination to be analysed further for *sn*-1- and *sn*-3-isomer composition by chiral-phase HPLC.

REFERENCES

1 C. Litchfield, *Analysis of Triglycerides*, Academic Press, New York, London, 1972.
2 H. Brockerhoff, *J. Lipid Res.*, 6 (1965) 10.
3 H. Brockerhoff, *J. Lipid Res.*, 8 (1967) 167.
4 H. Brockerhoff, *Lipids*, 6 (1971) 942.
5 P. Laakso and W. W. Christie, *Lipids*, 25 (1990) 349.
6 Y. Itabashi, A. Kuksis, L. Marai and T. Takagi, *J. Lipid Res.*, 31 (1990) 1711.
7 Y. Itabashi, A. Kuksis and J. J. Myher, *J. Lipid Res.*, 31 (1990) 2119.
8 B. G. Semporé and J. A. Bézard, *J. Chromatogr.*, 557 (1991) 227.
9 M. Yurkowski and H. Brockerhoff, *Biochim. Biophys. Acta*, 125 (1966) 55.
10 K. Maruyama and C. Yonese, *J. Am. Oil Chem. Soc.*, 63 (1986) 902.
11 Y. Kondoh and S. Takano, *J. Chromatogr.*, 393 (1987) 427.
12 S. Takano and Y. Kondoh, *J. Am. Oil Chem. Soc.*, 64 (1987) 1001.
13 Y. Itabashi and T. Takagi, *Lipids*, 21 (1986) 413.
14 W. W. Christie and J. H. Moore, *Biochim. Biophys. Acta*, 176 (1969) 445.
15 W. W. Christie and J. H. Moore, *Biochim. Biophys. Acta*, 210 (1970) 46.
16 F. E. Luddy, R. A. Barford, S. F. Herb, P. Magidman and R. W. Riemenschneider, *J. Am. Oil Chem. Soc.*, 41 (1964) 693.
17 F. H. Mattson and R. A. Volpenheim, *J. Lipid Res.*, 2 (1961) 58.
18 J. A. Bézard and M. A. Ouédraogo, *J. Chromatogr.*, 196 (1980) 279.
19 A. E. Thomas, III, J. E. Scharoun and H. Ralston, *J. Am. Oil Chem. Soc.*, 42 (1965) 789.
20 N. Oi and H. Kitahara, *J. Chromatogr.*, 265 (1983) 117.
21 T. Takagi and Y. Ando, *Lipids*, 25 (1990) 398.
22 M. Narce, J. Gresti and J. Bézard, *J. Chromatogr.*, 448 (1988) 249.
23 H. T. Slover and E. Lanza, *J. Am. Oil Chem. Soc.*, 58 (1979) 933.
24 A. Ros, *J. Gas Chromatogr.*, 3 (1965) 252.
25 L. R. Snyder and J. J. Kirkland, *Introduction to Modern Liquid Chromatography*, Wiley, New York, 2nd ed., 1979.

Journal of Chromatography, 596 (1992) 197–202
Elsevier Science Publishers B.V., Amsterdam

CHROM. 23 971

High-performance liquid chromatography and post-column derivatization with diphenyl-1-pyrenylphosphine for fluorimetric determination of triacylglycerol hydroperoxides

Kazuaki Akasaka, Setsu Ijichi, Kenji Watanabe, Hiroshi Ohrui and Hiroshi Meguro*

Department of Food Chemistry, Faculty of Agriculture, Tohoku University, Tsutsumidorui-Amamiyamachi, Aoba, Sendai 981 (Japan)

(First received September 13th, 1991; revised manuscript received December 10th, 1991)

ABSTRACT

Triacylglycerol monohydroperoxides (TG-mHPO) were selectively detected at the picomole levels after post-column reaction with diphenyl-1-pyrenylphosphine (DPPP). TG-mHPO were separated on two types of reserved-phase columns, an ODS column and a phenylated silica gel column, which were useful for determining TG-mHPO at their molecular species levels and their class levels, respectively. After the separation, DPPP solution was mixed with the eluent followed by reaction in a stainless-steel coil 20 m × 0.5 mm I.D. at 80°C, then the fluorescence intensity of DPPP oxide was measured ($\lambda_{ex.}$ 352 nm, $\lambda_{em.}$ 380 nm). Using these systems, TG-mHPO were determined in the range 2–1000 pmol. The relative standard deviations were 2.3–2.8%.

INTRODUCTION

Recently, lipid peroxidation has attracted much attention as one of the factors causing certain diseases and ageing [1–4]. In lipid peroxidation, hydroperoxides are produced both enzymatically and non-enzymatically. Several methods have been proposed for determining small amounts of hydroperoxides in foods and biological materials [5–8]. These methods, however, have some problems with reard to sensitivity, selectivity, complexity or interference from other components.

Recently, luminol and isoluminol chemiluminescence method have been reported as highly sensitive and selective high-performance liquid chromatographic HPLC post-column detection methods for lipid hydroperoxides [9,10]. An electrochemical detection system has also been used for this purpose [11]. These methods, however, have the drawback of unsuitability of organic solvents for HPLC separation.

Recently, we reported that a series of arylphosphines, prepared by replacing one phenyl group of triphenylphosphine with an aromatic fluorophore, have no fluorescence but their oxides possess strong fluorescence [12], diphenyl-1-pyrenylphosphine (DPPP) oxide giving the strongest fluorescence intensity. This reagent made it possible to determine lipid hydroperoxides selectively with high sensitivity. Some applications of the reagent to the determination of lipid hydroperoxides have been reported [13–15]. In this paper, we describe the application of the reagent to the HPLC post-column determination of triacylglycerol hydroperoxides.

EXPERIMENTAL

Chemicals

Diphenyl-1-pyrenylphosphine was synthesized as described previously [12]. Other reagents used were of special or super-special pure grade (Wako, Osaka, Japan). Trilinolein, trilinolenin and triolein were purchased from Sigma (St. Louis, MO, USA). Methylene blue, triphenylphosphine and solvents

0021-9673/92/$05.00

such as methanol, 1-butanol, acetone and chloroform were purchased from Wako and *tert.*-butylhydroxytoluene (BHT) from Tokyo Kasei Kogyo (Tokyo, Japan). The solvents for dissolving or extracting the samples contained 0.03% of BHT as an antioxidant.

Margarine, butter and mayonnaise products and salad oils were purchased locally. Vegetable oils were purchased from Nacalai Tesque (Kyoto, Japan).

Preparation of hydroperoxides and hydroxides

Trilinolein, trilinolenin and vegetable oils were autoxidized at room temperature in the dark for 12–72 h. Triolein was photooxidized in the presence of 0.1–0.3 m*M* methylene blue in ethanol. They were used after purification to triacylglycerol (TG) monohydroperoxides (mHPO) using silica gel column chromatography [16]. Their hydroperoxide contents were determined by spectrofluorimetry [13]. They were stored in a refrigerator at −25°C as a solution in chloroform–methanol (1:1).

Trilinolein hydroxides were prepared by reducing the hydroperoxides with triphenylphosphine in chloroform–methanol (1:1) at 0°C for more than 1 h and used without purification.

Separation and detection of hydroperoxides

Two systems were used to separate TG hydroperoxides. In the first system (system A), the analytical column used was TSK-gel ODS 80Tm (5 μm) (150 mm × 4.6 mm I.D.) (Tosoh, Tokyo, Japan; eluted with 1-butanol–methanol (10:90, v/v). In the other system (system B), a Develosil Ph-5 (5 μm) column (150 mm × 4.6 mm I.D.) (Nomura Chemical, Aichi, Japan) and methanol–water (95:5, v/v) eluent were used. The flow-rate of the eluent was 0.6 ml/min in both systems.

The post-column derivatization and the detection conditions were same in both systems. The HPLC eluent was monitored by UV detection at 210 or 235 nm prior to the post-column reaction with DPPP. The eluent was mixed with DPPP reagent [3 mg in 400 ml of acetone–methanol (1:3, v/v)], which was kept in an ice-bath in the dark. The flow-rate of the reagent solution was 0.3 ml/min and the mixture was passed through a 20 m × 0.5 mm I.D. reaction coil (stainless steel) at 80°C followed by another coil (0.5 m) in a water-bath at 20°C. Detection was performed by monitoring the fluorescence intensities at 380 nm with excitation at 352 nm. The mobile phase and the reagent solution were degassed by ultrasonic treatment under reduced pressure before use.

Sample preparation

Edible oils (200–400 mg) were diluted to 20 ml with chloroform and aliquots were used as samples. Commercially available mayonnaise, butter and margarine extracts were prepared in the following manner. To 0.3–1 g of the sample, 0.5 ml of water was added. Lipids were extracted from the mixture with two 1.5-ml portions of chloroform–methanol (2:1) followed by dilution to 5 ml with chloroform. Aliquots of 10 μl were injected into the HPLC system. The sample size could be minimized to less than 1 mg by reducing the scale of the procedure.

Equipment

The HPLC pump used was a CCPM multi-pump (Tosoh), which pumped both the mobile phase and the reagent solution with a single system. The reaction oven was an RE-8000 reactor. The detectors used were a UV-8000 spectrophotometer and an FS-8000 spectrofluorimeter (Tosoh). The data processor used was an SC-8010 (Tosoh) or a Chromatocoder 12 (System Instrument, Tokyo, Japan).

RESULTS AND DISCUSSION

The mechanism of the reaction of hydroperoxides with DPPP was described previously [12,13]. Hydroperoxides oxidized DPPP quantitatively to a strongly fluorescent oxide. The reaction proceeded in many organic solvents, such as methanol, ethanol, acetonitrile, ethyl acetate, chloroform, benzene and hexane, suggesting that all these solvents can be used as the mobile phase in HPLC. It was also possible to add water to the mobile phase up to 10%. The addition of larger amounts of water made DPPP insoluble in the reaction mixture. DPPP was less reactive to dialkyl peroxides, and not reactive to unoxidized fatty acids, hydroxy acids and their esters [13]. Therefore, they do not interfere in the determination of hydroperoxides.

Fig. 1 shows the chromatograms of a mixture of trilinolein and its monohydroperoxides (a,b) and a mixture of trilinolein and its hydroxide (c). Both unoxidized and hydroxylated trilinoleins gave

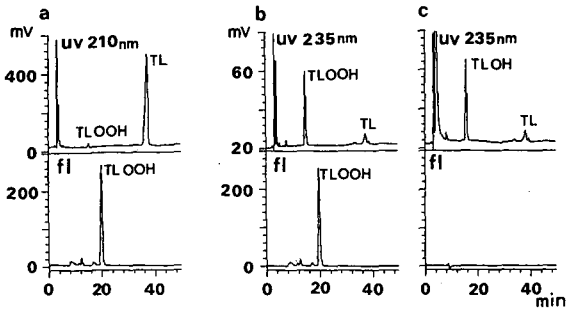

Fig. 1. HPLC of trilinolein and its hydroperoxy and hydroxy derivatives with system A. Sample: (a) and (b) trilinolein (TL, 50.0 nmol) + hydroperoxides (TL-OOH, 214 pmol); (c) TL (50.0 nmol) + hydroxide (TL-OH; 214 pmol).

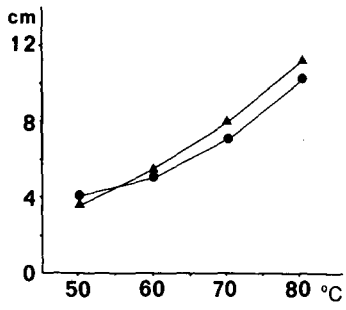

Fig. 3. Effect of reaction temperature on the peak height of trilinolein-mHPO (107 pmol) in (▲) system A and (●) system B.

peaks with UV monitoring, but no peak with spectrofluorimetry (7). On the other hand, the trilinolein-mHPO gave peaks with both UV and spectrofluorimetric detection. These results demonstrate that spectrofluorimetric detection is specific to hydroperoxides. The inclusion of a UV detector prior to the post-column reaction may be not essential for this system.

Fig. 2 shows the effect of the flow-rate of DPPP solution on the peak height of trilinolein-mHPO. The peak was higher at lower flow-rates, but the peak height variations was largest at 0.2 ml/min because it was difficult to maintain a constant flow-rate. This effect was clearer in system B than A. Fig. 3 and Table I show the effects of reaction temperature and reaction coil length on the peak height, respectively. The peaks became higher with increase in the reaction temperature and with the use of a longer coil without raising the baseline noise levels. The peaks were about 25% higher in a stainless-steel coil than in a PTFE coil. This may be attributed to the difference in their thermal conductivities. Therefore, the reaction was conducted in a 20-m stainless-steel coil at 80°C in our systems.

Table II shows the effect of the concentration of the reagent solution. The peaks became higher with increase in the reagent concentration. However, the signal-to-noise ratio was not improved with increase in concentration because of the increase in the baseline noise level. We selected the 3 mg per 400 ml solution as the reagent solution. Although the peak height decreased on addition of acetone to the reagent solution, acetone–methanol (1:3) was used as the solvent in our systems because of the improvement in the stability against oxidation of DPPP by the oxidant in the solution. Methanol would be less useful as a solvent for the reagent solution because the baseline noise level was doubled after keeping the reagent solution for 1 day at −25°C. Therefore, it was neccesary to prepare the

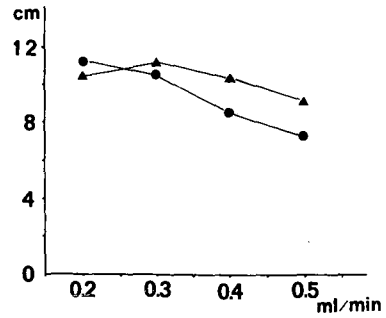

Fig. 2. Effect of flow-rate of the reagent solution on the peak height of trilinolein-mHPO (107 pmol) in (▲) system A and (●) system B.

TABLE I

EFFECT OF REACTION COIL LENGTH ON THE PEAK HEIGHT OF TRILINOLEIN-mHPO (107 pmol)

Coil	Length (m) (× 0.5 mm I.D.)	Peak height (cm)	
		System A	System B
PTFE	10	5.40	3.90
Stainless steel	4	3.75	2.08
	10	6.47	5.20
	20	11.39	10.40

TABLE II

EFFECT OF CONCENTRATION OF THE REAGENT SOLUTION ON THE PEAK HEIGHT OF TRILINOLEIN-mHPO (107 pmol)

System	Parameter	Concentration of DPPP (mg per 400 ml)		
		1.5	3.0	6.0
A	Peak height (cm)	5.41	11.20	19.36
	Relative noise level	1.0	1.4	2.0
B	Peak height (cm)	5.43	10.48	14.50
	Relative noise level	1.0	1.2	1.6

solution just before use when methanol was used as the solvent. With the use of methanol, the peak was 20–35% higher than with acetone–methanol (1:3). The fluorescence intensity of DPPP oxide was only 5% stronger in methanol than in acetone–methanol (1:9). The decrease in the peak height in acetone–methanol was partly attributed to this effect, but the main reason is the lower reactivity of DPPP with hydroperoxides in the solvent system.

In system A, the ODS column, one of the most popular reversed-phase columns, was used for the separation of TG-mHPO. As shown in Fig. 1, trilinolein-mHPO were detected as a single peak by spectrofluorimetry and determined in the range 2.1–1000 pmol (r = 0.999). The relative standard deviation of the peak area was 2.3% (107 pmol, n = 6).

Trilinolein-mHPO were not composed of a single molecular species but a mixture of some positional isomers which had a hydroperoxy group at different positions. However, these isomers were hardly separated by this system. On the other hand, as shown in Fig. 4, several peaks were observed in a mixture of TG-mHPO which were prepared by autoxidation of vegetable oils and subsequently purified by silica gel column chromatography. The peaks between 14 and 35 min should be the TG-mHPO composed of various fatty acids with different partition numbers (PN) (Partition numbers are defined by the equation PN = TC − 2DB, where TC and DB are the numbers of total carbon atoms and double bonds of fatty acids of which the TG is composed, respectively; for TG, there is a linear relationship between PN and log t_R, where t_R is the retention time). As shown in Fig. 5, six model TG-mHPO showed linear relationships between PN and log t_R as for TG [17]. This means that the TG-mHPO species could be roughly predicted from their retention times and the fatty acid compositions in the same way as for TG.

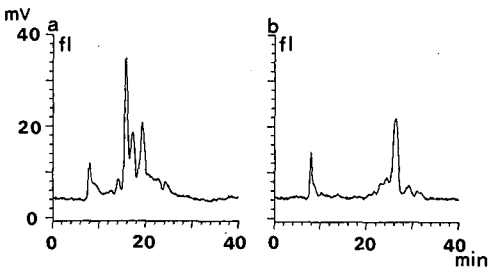

Fig. 4. HPLC of TG-mHPO in vegetable oils with system A. Sample: (a) TG-mHPO in linseed oil (296 pmol); (b) TG-mHPO in olive oil (166 pmol).

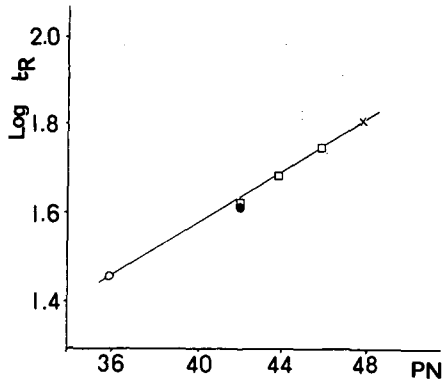

Fig. 5. Relationship between partition number of TG-mHPO and log t_R. The HPLC conditions used were the same as in system A except for the reaction coil length (10 m). Sample: trilinolenin-mHPO (PN = 36, ○), trilinolein-mHPO (PN = 42, ●), triolein-mHPO (PN = 48, ×) and TG-mHPO (PN = 42, 44 and 46, □) prepared from TG after separation at each PN on an ODS column.

In system B, a phenylated silica gel column was used as an analytical column. The separation patterns of TG-mHPO with this column were different from those with the ODS column. The difference would be due to the different characteristics of phenyl and alkyl groups. Fig. 6 shows typical chromatograms of TG-mHPO. The peaks of TG-mHPO in vegetable oils were broader and, in some instances, showed a small difference (less than 1

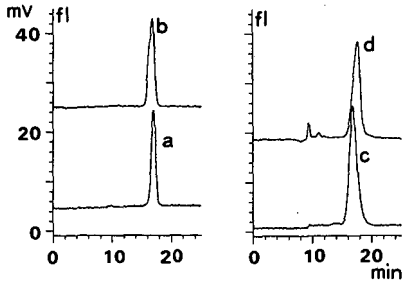

Fig. 6. HPLC of TG-mHPO with system B. Sample:(a) trilinolein-mHPO (45.5 pmol), (b) trilinolenin-mHPO (55.0 pmol), (c) TG-mHPO in linseed oil (100 pmol), (d) TG-mHPO in olive oil (82.8 pmol).

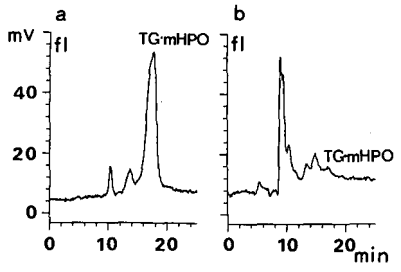

Fig. 7. HPLC of hydroperoxides in a salad oil (a, TH = 153 pmol) and a margarine extract (b, TH = 69.0 pmol) with system B.

min) between their retention times. This suggests that TG-mHPO which had different PN did not have exactly the same retention time, but almost. In practice, TG-mHPO gave a single peak regardless of their fatty acid compositions. This allowed us to determine TG-mHPO at the class level. Table III shows the peak-area ratio of trilinolein and vegetable oil-mHPO. Although there was a *ca.* 10% variation between them, it was almost possible to use the calibration graph of trilinolein-mHPO for TG-mHPO in vegetable oils. The ratio for triolein-mHPO was smaller than the others, which could be attributed to the lower reactivity of triolein-mHPO with DPPP.

Using the proposed method, TG-mHPO was determined in the range 2–300 pmol. The relative standard deviation of the peak area of trilinolein-mHPO was 2.8% (45.5 pmol, $n = 6$).

Fig. 7 shows the chromatograms of a salad oil and an extract from a food sample. Before TG-mHPO several peaks were detected. Judging from their retention times, they were probably the bis- or trishydroperoxides of TG or lower molecular weight hydroperoxides such as hydroperoxides of free fatty acids, mono- or diacylglycerols and degradation products of TG-mHPO. Total hydroperoxides (TH) were determined from the total peak area using the calibration graph of trilinolein-mHPO. They agreed with the results obtained by the batch method ($r = 0.997$, $n = 10$) [18]. Recoveries of added TG-HPO from the vegetable oils and the foods were 95–102% ($n = 6$). Although the composition of the injection solvent seemed unsuitable for a reversed-phase system, there was no problem with injections of up to 10 μl.

TABLE III

RELATIVE PEAK AREA OF TG-mHPO WITH SYSTEM B

Lipid hydroperoxide	Relative peak area
Trilinolein-mHPO	1.00
Trilinolenin-mHPO	1.00
Triolein-mHPO	0.71
Safflower oil-mHPO	1.10
Corn oil-mHPO	1.10
Cottonseed oil-mHPO	1.04
Soybean oil-mHPO	0.94
Linseed oil-mHPO	1.01
Olive oil-mHPO	0.94
Peanut oil-mHPO	0.88
Rapeseed oil-mHPO	1.04
Sesame oil-mHPO	1.07

CONCLUSIONS

Lipid hydroperoxides were detected at picomole levels with high selectivity using the proposed post-column derivatization system. The use of the phenylated column made it possible to determine TG-mHPO at their class levels and the total hydroperoxides in vegetable oils and some food extracts. The method should be useful for studying the initial stage of lipid peroxidation and for checking food quality based on its high sensitivity, selectivity and peak separation patterns. Moreover, the method should be useful for determining TG hydroperoxide in biological materials.

ACKNOWLEDGEMENT

This work was supported in part by a Grant-in-Aid for Scientific Research from the Ministry of Education, Science and Culture, Japan.

REFERENCES

1 J. Glavind, S. Hartmann, J. Clemmesen, K. E. Jessen and H. Dam, *Acta Pathol. Microbiol. Scand.*, 30 (1952) 1.
2 T. Yoshikawa, K. Yamaguchi, M. Kondo, N. Mizukawa, T. Ohta and K. Hirakawa, *Arch. Gerontol. Geriatr.*, 1 (1982) 209.
3 T. Nakayama, M. Kodama and C. Nagata, *Agric. Biol. Chem.*, 48 (1984) 571.
4 D. Harman, in W. A. Pryor (Editor), *Free Radicals in Biology*, Vol. V, Academic Press, New York, 1982, pp. 255–275.
5 C. H. Lea, *Proc. R. Soc. London, Ser. B*, 108 (1931) 175.
6 T. Asakawa and S. Matsushita, *Lipids*, 15 (1980) 965.
7 K. Yagi, *Biochem. Med.*, 15 (1976) 212.
8 S. Hara, M. Shida and Y. Totani, *J. Jpn Oil Chem. Soc.*, 37 (1988) 119.
9 T. Miyazawa, K. Yasuda and K. Fujimoto, *Anal. Lett.*, 21 (1988) 1033.
10 Y. Yamamoto, M. H. Brodsky, J. C. Baker and B. N. Ames, *Anal. Biochem.*, 160 (1987) 7.
11 K. Akasaka, T. Suzuki, H. Ohrui and H. Meguro, *Anal. Lett.*, 20 (1987) 731.
13 K. Akasaka, T. Suzuki, H. Ohrui and H. Meguro, *Anal. Lett.*, 20 (1987) 797.
14 K. Akasaka, H. Ohrui and H. Meguro, *Anal. Lett.*, 21 (1988) 965.
15 H. Meguro, K. Akasaka and H. Ohrui, *Methods Enzymol.*, 186 (1990) 157.
16 K. Sohde, S. Izutani and S. Matsusita, *Agric. Biol. Chem.*, 37 (1973) 17979.
17 R. D. Platter, G. F. Spencer and R. Kleiman, *J. Am. Oil Chem. Soc.*, 54 (1977) 511.

Journal of Chromatography, 596 (1992) 203–209
Elsevier Science Publishers B.V., Amsterdam

CHROM. 23 940

Purification of serine hydroxymethyltransferase from *Bacillus stearothermophilus* with ion-exchange high-performance liquid chromatography

Hiroshi Ide*, Kaoru Hamaguchi, Satoyuki Kobata, Akira Murakami, Yoshiharu Kimura and Keisuke Makino

Department of Polymer Science and Engineering, Kyoto Institute of Technology, Matsugasaki, Sakyo-ku, Kyoto 606 (Japan)

Masahumi Kamada

Reagent Division, Kanto Chemical Co. Inc., 11-1 Nihonbashi Honcho 4-Chome, Chuo-ku, Tokyo 103 (Japan)

Shigemi Miyamoto, Tsutomu Nagaya and Kouichi Kamogawa

Research and Development Center, Nippon Zeon Co. Ltd., 1-2-1 Yako, Kawasaki-ku, Kawasaki 210 (Japan)

Yoshikazu Izumi

Department of Biotechnology, Faculty of Engineering, Tottori University, Koyama-minami, Tottori 680 (Japan)

(First received October 11th, 1991; revised manuscript received December 11th, 1991)

ABSTRACT

The gene of serine hydroxymethyltransferase (SHMT) of a thermophilic bacterium *Bacillus stearothermophilus* was expressed in *Escherichia coli*, and SHMT was successfully purified from the crude extract of *E. coli* in two steps while maintaining the enzymatic activity. The purification steps involved ammonium sulphate precipitation followed by high-performance liquid chromatographic separation using the anion-exchange column Fractogel EMD DEAE-650(S). In addition to the DEAE column, three other types of anion- and cation-exchange columns were also studied for their ability to separate SHMT, and the performances of the four columns were compared.

INTRODUCTION

L-Serine is a key starting material for the enzymatic synthesis of a series of industrially important amino acids such as L-tryptophan, L-tyrosine and L-cysteine, and for the synthesis of manu pharmaceuticals [1–4]. Accordingly, the production of L-serine at low cost is indispensable for successful applications of the synthetic methods. Amino acids are generally synthesized by a chemical, fermentation or enzymatic method. The enzymatic method has the advantage that optically pure amino acids can be specifically produced in a short time. Furthermore, the fact that some of the key enzymes responsible for the amino acid synthesis are made available in fairly large amounts using recombinant DNA technology has made the enzymatic method more attractive.

Serine hydroxymethyltransferase (SHMT) (EC 2.1.2.1) catalyses the interconversion of glycine and L-serine (reaction, Fig. 1) [5,6]. The physiological role of SHMT is to transfer the β-carbon of L-serine

0021-9673/92/$05.00

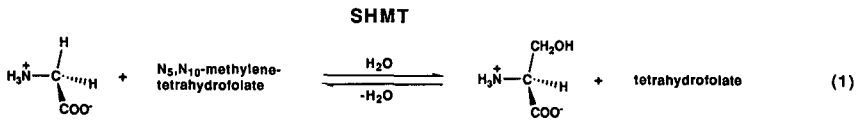

Fig. 1. Interconversion of glycine and L-serine catalysed by serine hydroxymethyltransferase (SHMT) (reaction 1).

to tetrahydrofolate, thereby providing the biosynthesis of amino acids and nucleic acids in cells with one-carbon units. However, reaction 1 catalysed by SHMT is reversible, and glycine can be stereospecifically converted to L-serine using the backward reaction of reactin 1. A multicopy plasmid carrying the *Escherichia coli glyA* gene encoding SHMT has been placed in a *Klebsiella aeronenes* strain and SHMT obtained from the strain has been used to produce L-serine [7,8]. Recently, the SHMT gene of a thermophilic bacterium *Bacillus stearothermophilus* has been cloned and expressed in *E. coli* [9]. The use of thermostable SHMT has the potential to make it possible to operate bioreactors for the production of L-serine at elevated temperatures, thereby avoiding possible contamination by sundry bacteria. However, the purification procedure for thermostable SHMT which is necessary for preliminary characterization of the enzyme before its application to the bioreactors has not been established.

In this paper, we report the application of high-performance liquid chromatography (HPLC) to the purification of SHMT of *B. stearothermophilus* from the crude extract of *E. coli* harbouring a plasmid encoding the SHMT gene. The enzyme can be purified to near homogeneity in two steps from the crude extract while maintaining the activity.

EXPERIMENTAL

Expression of SHMT gene in E. coli cells

Construction of an SHMT expression vector (pMS046) in which the SHMT gene of *B. stearothermophilus* was inserted in the *SmaI* site of pUC18 will be published elsewhere [9]. A host JM101 was transformed with pMS046 following the method of Sambrook *et al.* [10]. Transformed cells were grown in an LB medium containing ampicillin (50 μg/ml) with shaking at 37°C for 21 h. Cells were collected by centrifugation at 2400 *g* for 15 min. To confirm the expression of the SHMT gene in the transformant, proteins were analysed by sodium dodecyl sulphate -polyacrylamide gel electrophoresis (SDS-PAGE) as follows: harvested cells (≈ 1 mg) were resuspended in GTE buffer (50 μl) containing glucose (9 g/l), Tris (25 m*M*) and EDTA (10 m*M*) and disrupted by 0.2 *M* NaOH–1% SDS (50 μl). After centrifugation at 22 000 *g* for 20 min, the supernatant (50 μl) was analysed by SDS-PAGE.

For SDS-PAGE, samples were denatured by brief heating at 100°C in the presence of SDS and 2-mercaptoethanol and subjected to electrophoresis on a 12.5% stacking polyacrylamide gel. Electrophoresis was performed at a constant voltage (2 V/cm). Gels were stained by Coomassie brilliant blue, destained and photographed.

Purification

Preparation of crude enzyme. Cells were grown and harvested as described above and resuspended in five volumes of a 1% glycine solution. The harvested cells were disrupted by sonication with an Astrason Model XL2020 ultrasonic processor (Heat Systems, Farmingdale, NY, USA) (output 475 W, 12 × 10 s with 20-s interval) at 0°C. Cell debris was removed by centrifugation at 16 000 *g* for 12 min and the supernatant recovered (fraction I).

Ammonium sulphate precipitation. Solid ammonium sulphate was added stepwise to fraction I (typically 50 ml) and precipitates recovered by centrifugation at 30, 50, 60 and 70% saturation, respectively. Each protein fraction obtained by the ammonium sulphate precipitation was dissolved in a 1% glycine solution (2 ml). The resulted solutions were assayed for activity and analysed by SDS-PAGE (see *Expression of SHMT gene in E. coli cells*). The fractions (30–60% saturation) containing SHMT were combined (fraction II).

Ion-exchange HPLC. Fraction II was purified by ion-exchange HPLC. Four types of Fractogel EMD ion-exchange columns (150 × 10 mm I.D., particle size 25–40 μm) (Merck, Darmstadt, Germany), including TMAE-650(S) (strong anion exchange),

DEAE-650(S) (weak anion exchange), SO_3^--650(S) (strong cation exchange) and COO^--650(S) (weak cation exchange) were tested for their ability to separate SHMT. HPLC separation was performed using a liquid chromatograph consisting of a Model L-6000 pump (Hitachi, Tokyo, Japan) and a Model L-3000 photodiode-array three-dimensional detector (Hitachi, Tokyo, Japan). Gradient elution was carried out at a flow-rate of 1 ml/min using 20 m*M* phosphate buffer (pH 7.5) (eluent A) and 20 m*M* phosphate buffer (pH 7.5) containing 1 *M* NaCl (eluent B). The gradient profiles used are shown in the figures by broken lines. All HPLC operations were performed at room temperature. SHMT purified by HPLC is designated as fraction II (for detail, see under results and discussion).

Determination of activity

SHMT catalyses not only the interconversion of glycine and L-serine (reaction 1 but also the conversion of β-phenylserine to benzaldehyde (reaction, Fig. 2) [11]. As benzaldehyde has a distinctive absorption band at 250 nm (ε = 15 000), reaction 2, catalysed by SHMT, can be easily followed by measuring the increase in absorbance at 250 nm. In a typical assay, the reaction mixture (2 ml) for the determination of the enzymatic activity contained an appropriately diluted enzyme solution (100 μl), β-phenylserine (0.5 m*M*), pyridoxal phosphate (PLP, 50 μ*M*) and phosphate buffer (125 m*M*, pH 7.5). Incubation was performed at 25°C for 15 min. UV spectra were taken using the same assay mixture as a reference except that the enzyme solution was omitted in the reference misture. One unit is defined as an activity that produces 1 μmol of benzaldehyde per min under these conditions.

The protein concentration was determined by the method of Lowry *et al.* [12]. UV spectra were measured on a DU-68 spectrometer (Beckman, Palo Alto, CA, USA) with a 50-μl microcell.

RESULTS AND DISCUSSION

SDS-PAGE analysis of proteins produced in *E. coli* cells was first performed to confirm the overproduction of SHMT. For JM101 transformed with pMS046 carrying the SHMT gene, a distinctively intense band was observed (Fig. 3, lane 4), but it was not present for JM101 without transformation or JM101 transformed with a control plasmid pUC19 carrying no insert (Fig. 3, lanes 2 and 3). The calculated molecular weight based on the migration distance was 45 000 (Fig. 4), which was very close to that reported for a subunit of *E. coli* SHMT (molecular weight 46 500 [13], 45 265 [14]), whose active form is a dimer consisting of two identical subunits. These results strongly suggest that the SHMT gene was expressed in the *E. coli* cells transformed with pMS046.

A crude extract (fraction I) was prepared from JM101/pMS046 and the enzymatic activity of fraction I was determined as described under Experimental. The amount of benzaldehyde fromed by SHMT increased linearly with time up to 15 min (data not shown). The specific activity of fraction I was 0.010 U/mg. Fraction I was treated with ammonium sulphate and precipitates were analysed by SDS-PAGE. SHMT was precipitated in the fractions with ammonium sulphate concentrations between 30 and 60% saturation. The precipitated crude SHMT in these fractions was dissolved in a 1% glycine solution and the fractions were combined (fraction II). The specific activity of fraction II was 0.012 U/mg.

For analytical purposes, fraction II was diluted ten-fold and 100 μl of the sample (0.114 mg as protein) were separated by HPLC equipped with a weak anion-exchange Fractogel EMD DEAE-650(S) column. Fig. 5 shows a typical chromatograph obtained. To analyse the major peaks 1–4 in the chromatogram, fraction II was applied to

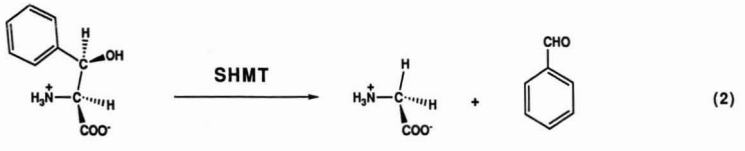

Fig. 2. Conversion of β-phenylserine to benzaldehyd catalysed by SHMT (reaction 2).

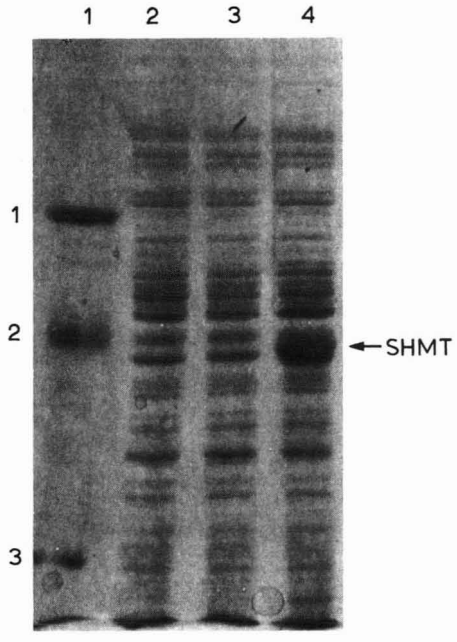

Fig. 3. SDS-PAGE analysis of proteins produced in *E. coli* cells. Lane 1, molecular weight marker [1, bovine serum albumin (molecular weight 66 000); 2, ovalbumin (45 000); 3, trypsinogen (24 000)]; lane 2, JM101; lane 3, JM101 transformed with a control plasmid pUC19; lane 4, JM101 transformed with PMS046 bearing the SHMT gene.

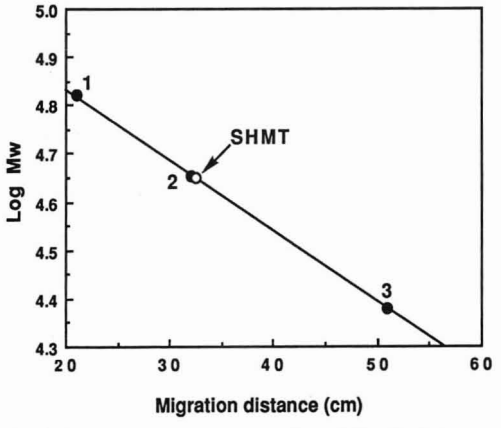

Fig. 4. Molecular weight determination of SHMT of *B. stearothermophilus*. The molecular weight of SHMT (open circle) was determined by SDS-PAGE on a 12.5% slab gel with reference proteins of known molecular weights (1, bovine serum albumin; 2, ovalbumin; 3, trypsinogen). Data points were taken from Fig. 3.

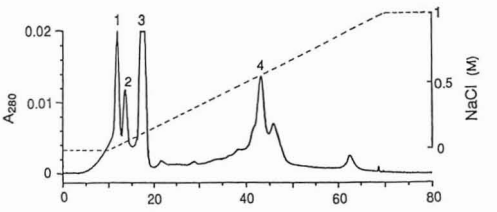

Fig. 5. HPLC analysis of crude SHMT. Fraction II obtained by ammonium sulfate precipitation was diluted ten-fold and 100 μl of the sample (0.114 mg as protein) were injected. Column, Fractogel EMD DEAE-650(S) (150 × 10 mm I.D.); eluent A, 20 m*M* phosphate buffere (pH 7.5); eluent B, 20 m*M* phosphate buffer (pH 7.5) containing 1 *M* NaCl; gradient, 0% B (0–10 min), 0–100% B (10–70 min), 100% B (70–80 min); flow-rate 1 ml/min.

HPLC system without dilution (100 μl, 1.14 mg as protein) and peaks 1–4 were collected. There was no significant change in an elution profile arising from the increase in the load of the sample (data not shown). When the activity of each peak was assayed, only peak 4 showed any activity. According to the colour development by Lowry's method, peaks 1–3 contained small amounts of proteins compared with peak 4 containing SHMT. For more efficient separtion of SHMT, fraction II was concentrated by ultrafiltration and 100 μl of the sample (4.3 mg as protein) were separated by HPLC using a slightly modified gradient (Fig. 6a). Eluted fractions were collected every minute and assayed for protein concentration and enzymatic activity. By comparison of the elution peaks of SHMT (peak 4 in Fig. 5 and the peak indicated by SHMT in Fig. 6a), it can be seen that the separation of the last half of peak 4 in Fig. 5 was improved with the modified gradient in Fig. 6a. It is also clear that the major contaminating species eluted between 5 and 20 min had strong UV absorption at 280 nm, but contained very small amounts of proteins (Fig. 6b). These results indicate that the DEAE column can efficiently remove contaminating components other than protein which are not detectable in SDS-PAGE analysis. The eluted fractions containing SHMT were pooled (fraction III). The specific acticity of fraction III was 0.031 U/mg.

When the UV spectrum of fraction III was measured, a weak absorption band was observed around 425 nm (Fig. 7). By comparison with the spectrum of authentic PLP, the absorption was as-

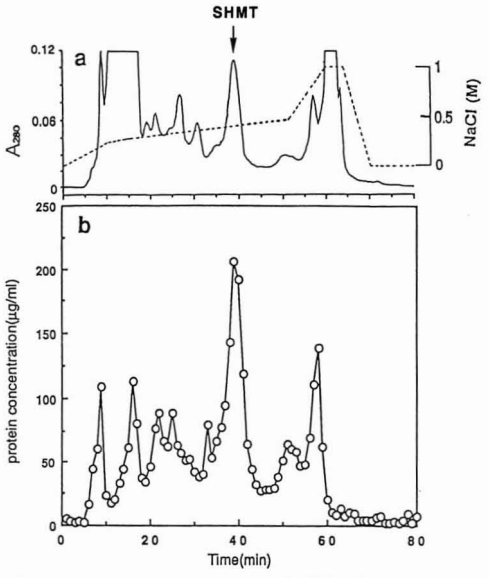

Fig. 6. HPLC elution profiles of crude SHMT monitored by (a) absorption at 280 nm and (b) protein concentration. Fraction II was concentrated by ultrafiltration and 100 μl of the sample (4.3 mg as protein) were injected. (b) Eluted fractions were collected every minute and assayed for protein concentration by the method of Lowry *et al.* [12]. Column, Fractogel EMD DEAE-650(S) (150 × 10 mm I.D.); eluent A, 20 m*M* phosphate buffer (pH 7.5); eluent B, 10 m*M* phosphate buffer (pH 7.5) containing 1 *M* NaCl; gradient 0–25% B (0–10 min), 25–50% B (10–50 min), 50–100% B (50–60 min), 100% B (60–70 min), 100–0% B (70–80 min); flow-rate 1 ml/min.

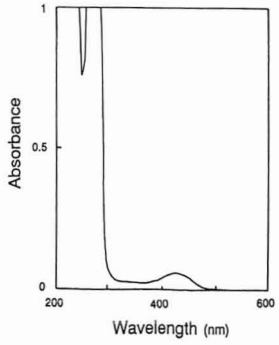

Fig. 7. UV spectrum of purified SHMT. SHMT purified with the DEAE column (fraction III) was concentrated by ultracentrifugation and the UV spectrum was measured.

signed to PLP bound to SHMT. It has been reported that SHMT purified from eukaryotic and prokaryotic cells contains PLP as a co-factor. The ratio of the adsorptions at 425 nm (PLP) and 280 nm (protein) determined for fraction III was 0.04, which was considerably smaller than those (0.11–0.23) reported for SHMT purified from various origins [15–18]. This implied that PLP was released from the SHMT holoenzyme during HPLC separation, and that purified SHMT in fraction III was present in part in the form of an apoprotein. Thus the apparent recovery of the SHMT activity after the HPLC separation was as low as 21% (Table I). To explore the possibility of reconstituting the enzymatic activity, fractions II and III were incubated with PLP (0.5 m*M*) at 42°C for 2 h, and the enzymatic activity was assayed. For fraction II obtained by the ammonium precipitation, no increase in the specific activity was observed after incubation (Table I). In contrast, the specific activity of fraction III obtained by the HPLC separation increased approximately fivefold, and the total activity of fraction III after reconstitution was virtually the same as that of the loaded sample. These results clearly indicate that the partial release of PLP from SHMT occurred during the HPLC separation; however, full enzymatic activity could be reconstituted by the post-reaction incubation with PLP. The interaction between the negatively charged phosphate group of PLP and the anion-exchange matrix in the DEAE column must be responsible for the release of PLP from the enzyme.

It has been also confirmed by SDS-PAGE analysis of fractions I–III that the HPLC purification with the DEAE column is a very effective step for the purification of SHMT (Fig. 8). Although a few minor bands were still noticeable in the SDS-PAGE analysis of fraction III, SHMT was purified to near homogeneity after the HPLC purification.

When SHMT was prepared by this method, the increase in the specific activity was at most fifteenfold: the specific activities of fractions I, II and III were 0.010, 0.012 and 0.147 (after reconstitution), respectively. This is because the specific activity of the crude extract (fraction I) was already high due to the overproduction of SHMT in *E. coli* cells bearing plasmid pMS046. However, the major contaminating components other than protein, as wel as proteins, were able to be efficiently removed by this method, as shown in Fig. 4.

TABLE I

PURIFICATION OF SHMT WITH FRACTOGEL EMD-DEAE-650(S) COLUMN

Fraction II concentrated by ultrafiltration (100 μl, 4.3 mg as protein) was separated on the DEAE column and the enzymatic acitvity was assayed as described under Experimental.

Sample	Fraction	Total activity (U)	Recovery of activity (%)	Specific activity (U/mg)
Before HPLC purification	II	0.052	100	0.012
	II + PLP[a]	0.048	92	0.011
After HPLC purification	III	0.011	21	0.031
	III + PLP[a]	0.051	98	0.147

[a] Fraction II or III incubated with PLP to reconstitute SHMT holoenzyme.

In addition to the weak anion-exchange column (described above), three other types of ion-exchange columns, including Fractogel EMD TMAE-650(S) (strong anion-exchange), SO_3^--650(S) (strong cation exchange) and COO^--650(S) (weak cation exchange) were tested for their ability to separate SHMT using fraction II (4.3 mg as protein). Elution peaks containing SHMT were identified by independent injections of marker SHMT purified by the DEAE column (fraction III). The elution profile for the strong anion-exchange column (TMAE) was similar to that for weak anion exchange column (DEAE) shown in Fig. 4, so that major contaminating specied were eluted in an early region of the gradient (retention time 7–15 min). Based on this result, it is concluded that the strong anion-exchange column (TMAE) can essentially separate SHMT as well as the weak anion-exchange column (DEAE). In contrast, the weak and strong cation-exchange columns did not separate SHMT as well as the anion-exchange columns. A typical elution profile obtained with the weak cation-exchange column [COO^--650(S)] is shown in Fig. 9, and a similar profile was obtained for the strong cation-exchange column [SO_3^--650(S)]. Most of the components present in the injected samples were eluted in the front regions of the gradient for both the cation-exchange columns. SHMT was found to be eluted in the first major peak (marked by an asterisk in Fig. 9) under these conditions. As the integrated areas of the first peaks containing SHMT were too large to account for SHMT alone, it is

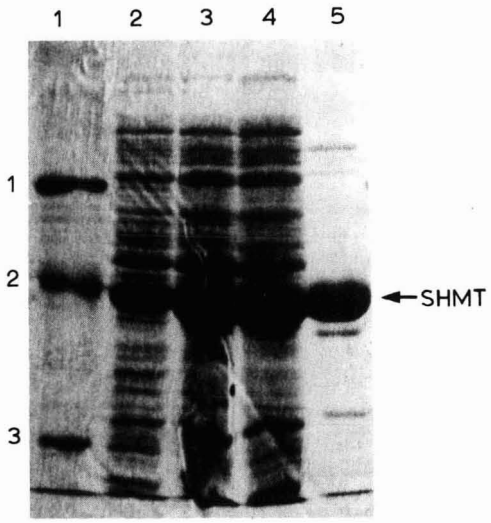

Fig. 8. SDS-PAGE analysis of fractions I–III. Lane 1, molecular weight marker (see Fig. 1 for numbers); lane 2, crude extract of JM101/pMS046 prepared by the alkaline SDS method (see under Experimental); lane 3, fraction I (crude extract); lane 4, fraction II (ammonium sulfate precipitate); lane 5, fraction III (HPLC purified fraction).

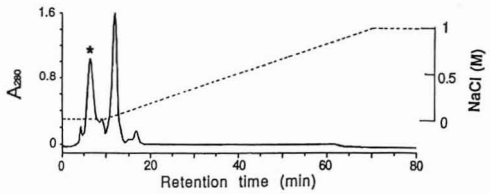

Fig. 9. Separation of crude SHMT by a weak cation-exchange column. Sample, concentrated fraction II (100 μl, 4.3 mg as protein); column, Fractogel EMD COO^--650(S) (150 × 10 mm I.D.). Other HPLC conditions were as in Fig. 5. SHMT was eluted in the peak marked by an asterisk.

evident that contaminating components were co-eluted with SHMT with these columns.

In summary, the SHMT gene of *B. stearothermophilus* has been expressed in *E. coli*, and the enzyme has been efficiently purified from the crude extract by HPLC with a weak anion-exchange column [Fractogel EMD DEAE-650(S)]. Release of PLP bound to the SHMT holoenzyme as a co-factor occurred during the HPLC separation, but a full enzymatic activity was reconstituted by post-reaction incubation with PLP. With respect to the separating ability of SHMT, the performance of a strong anion-exchange TMAE column was comparable with the DEAE column, whereas those of cation-exchange SO_3^- and COO^- columns were not so satisfactory. In conventional methods, it takes many steps to purify SHMT from various origins [11,18–20]. The application of this method using HPLC coupled with the anion-exchange columns to the purification of SHMT should facilitate the purification process.

REFERENCES

1 W. G. Bang, S. Lang, H. Sahm and F. Wagner, *Biotechnol. Bioeng.*, 25 (1983) 999.
2 W. G. Bang, U. Behrendt, S. Lang and F. Wagner, *Biotechnol. Bioeng.*, 25 (1983) 1013.
3 U. Behrendt, W. G. Bang and F. Wagner, *Biotechnol. Bioeng.*, 26 (1984) 308.
4 B. K. Hamilton, H-Y. Hsiao, W. E. Swan, D. M. Anderson and J. L. Pelente, *Trends Biotechnol.*, 3 (1985) 64.
5 R. L. Blakey, *Biochem. J.*, 61 (1955) 315.
6 L. Schirch, *Adv. Enzymol. Relat. Areas Mol. Biol.*, 53 (1982) 83.
7 H-Y. Hsiao, T. Wei and K. Campbell, *Biotechnol. Bioeng.*, 28 (1986) 857.
8 H-Y. Hsiao and T. Wei, *Biotechnol. Bioeng.*, 28 (1986) 1510.
9 S. Miyamoto, T. Nagaya, K. Kamogawa, H. Ide, A. Murakami, Y. Izumi and K. Makino, in preparation.
10 J. Sambrook, E. F. Fritsch and T. Maniatis, *Molecular Cloning, A Laboratory Manual*, Cold Spring Harbor Laboratory, Cold Spring Harbor, 2nd ed., 1989, pp. 1.74–1.110.
11 R. J. Ulevitch and R. G. Kallen, *Biochemistry*, 16 (1977) 5342.
12 O. H. Lowry, N. J. Rosebrough, A. L. Farr and R. J. Randall, *J. Biol. Chem.*, 193 (1951) 265.
13 G. Stauffer, M. D. Plamann and L. T. Stauffer, *Gene*, 14 (1981) 63.
14 M. D. Plamann, L. Stauffer, M. Urbanowski and G. Stauffer, *Nucleic. Acids Res.*, 11 (1983) 2065.
15 L. Schirch and A. Diller, *J. Biol. Chem.*, 246 (1971) 3961.
16 M. Fujioka, *Biochim. Biophys. Acta*, 185 (1969) 338.
17 S. S. Miyazaki, S. Toki, Y. Izumi and H. Yamada, *Agric. Biol. Chem.*, 51 (1987) 2587.
18 T. Masuda, M. Sakamoto, I. Nishizaki, M. Yamamoto and H. Wada, *J. Biochem.*, 101 (1987) 643.
19 V. Schirch, S. Hopkins, E. Villar and S. Angelaccio, *J. Bacteriol.*, 163 (1985) 1.
20 S. S. Miyazaki, S. Toki, Y. Izumi and H. Yamada, *Eur. J. Biochem.*, 162 (1987) 533.

Journal of Chromatography, 596 (1992) 211–216
Elsevier Science Publishers B.V., Amsterdam

CHROM. 23 962

Determination of tetracyclines in bovine and porcine muscle by high-performance liquid chromatography using solid-phase extraction

John R. Walsh*, Laurence V. Walker and Jonathan J. Webber

Regional Veterinary Laboratory, Department of Agriculture, Ballarat Road, Hamilton, Victoria 3300 (Australia)

(First received July 16th, 1991; revised manuscript received December 16th, 1991)

ABSTRACT

A method is presented for the determination of the three tetracyclines oxytetracycline, tetracycline and chlortetracyline in muscle, spiked at 100 ng/g, using high-performance liquid chromatography (HPLC). The concentration and extraction steps are carried out using Waters Environmental Sep-Pak cartridges. The principal steps involve homogenizing the sample in EDTA–McIlvaine buffer followed by centrifugation and precipitation of the supernatant using trichloroacetic acid. After further filtration and concentration on a Sep-Pak cartridge, the sample is eluted and analysed by HPLC with UV detection and confirmation by diode-array. The column used is a Nova-Pak C_{18} (4 μm) cartridge (10 cm × 8 mm I.D.). A phosphate–citrate–acetonitrile buffer, utilizing ion suppression, is the mobile phase. The analytes are detectable at levels down to 10 ng/g. The analyte identity can be confirmed at 20 ng/g by the use of diode-array detection and spectral library comparison.

INTRODUCTION

In Australia, oxytetracycline (OTC) and chlortetracycline (CTC), together with various members of the sulphonamide group, are the most widely used antibacterials in the meat-production industry. A monitor of the use of these antibiotics and their subsequent residues in food is of serious concern to consumers in the export and domestic markets. A reliable, robust and reproducible method was required for the determination of tetracyclines in muscle. The method would form part of a panel of analyses that could be used throughout Australia to monitor both domestic and export meat for the presence of a range of antibacterial residues. To this end, all equipment, chemicals and products had to be available and supported in Australia.

The maximum residue limits (MRL) in Australia are 250 ng/g for OTC and 50 ng/g for CTC. The aim of this study was to produce a method for the determination of tetracyclines that would produce consistent peak areas in tissues spiked at the 100 ng/g level. At the same time, a reasonable laboratory throughput had to be maintained. This method should permit a very favourable signal-to-noise ratio at around the MRL, such that it would be easy to quantify concentrations of analytes in muscle significantly below the stated MRLs.

Many methods have been published for the determination of tetracyclines in a number of matrices [1–8] that can be reproduced with varying degrees of success. These methods utilize a number of purification techniques: partitioning [3], ultrafiltration [7], solid-phase dispersion (SPD) [8] and solid-phase extraction (SPE) involving ion exchange [5], adsorption [4] or reversed phases (C_{18}) [1,2,6,7]. The last group can be subdivided into external, or preconcentration of the sample on a cartridge [1,6], and on-column, where the sample is directly concentrated on the analytical column [2,7]. In most of these reports, samples were spiked at 1000 ng/g, and the sensitivity was extrapolated to much lower concentrations. There are only two reports [6,7] of samples spiked at 20–100 ng/g. We believe that the re-

0021-9673/92/$05.00

coveries are not constant throughout the ranges, and it is necessary to spike samples in the required range of analysis. Other published methods appear to have a less favourable signal-to-noise ratio at these MRL levels. The method of Oka *et al.* [1] was adopted and modified by techniques that allow much higher sample loads in a smaller final sample volume. The chromatographic conditions were modified to permit the use of diode-array detection and to minimize analyte losses in the analytical column.

EXPERIMENTAL

Chemicals and materials

Environmental Sep-Pak cartridges (0.85 g, 55–105-μm C_{18}; end-capped silica; 12% carbon loading) (Waters), water purified in a Milli-Q apparatus, methanol and acetonitrile (Millipore, Milford, MA, USA). Trichloroacetic acid, ethylenediaminetetraacetic acid (EDTA), sodium salt, citric acid, disodium monohydrogenorthophosphate dihydrate, potassium dihydrogenorthophosphate, hydrochloric acid (HCl) and tetramethylammonium chloride were of analytical-reagent grade.

EDTA–McIlvaine buffer (pH 4) was prepared by dissolving 15 g of disodium monohydrogenorthophosphate dihydrate, 13 g of citric acid and 3.72 g of EDTA in water and diluting to 1 l.

Antibiotics

Oxytetracycline (OTC), tetracycline (TC) and chlortetracycline (CTC) (Sigma, St. Louis, MO, USA) were each dissolved in 0.01 *M* HCl at 0.1 mg/ml. The working solution was a mixture, prepared by dilution of 1 ml of each stock-solution 100-fold with 0.1 *M* potassium dihydrogenorthophosphate solution, containing 0.01 *M* EDTA to produce a 1000 ng/ml standard. All solutions were stored in the dark at 4°C.

Apparatus

The following equipment was used: Janke & Kunkel homogenizer using the 18N probe; Sorvall refrigerated centrifuge; 50-ml (nominal) Sorvall centrifuge tubes; 400-ml tall-form beakers; 250-, 25- and 10-ml measuring cylinders; 75-mm glass funnels; Whatman 11-cm No. 541 filter-papers; large ice-bath; magnetic stirrer; stirring bars; 50-ml polypropylene plastic syringe barrels (reservoirs); 10-ml gas-tight syringes; water vacuum pump and a simple manifold for multiple vacuum outlets.

The chromatograph used was a Varian Star system, equipped with a ternary pump (Model 9010), a diode-array UV detector (Model 9065), an autosampler (Model 9095) and a computer for control and data handling (Varian Star Software).

Method

A 35–40-g amount of trimmed meat (muscle) was homogenized with 5 ml/g of EDTA–McIlvaine buffer (4°C) using a Janke & Kunkel homogenizer (18N probe). The weight (w_1) and volume (v_1) used were recorded. The homogenate was centrifuged at 2700 *g* for 15 min at 4°C. The supernatant was collected and its volume (v_2) recorded.

A volume (v_3) of trichloroacetic acid solution (1 g/ml), equal to 10% of the supernatant volume, was slowly added to the supernatant with constant stirring. The mixture was stirred for a further 1 min, then placed in a bed of ice for 15 min. The mixture was filtered through a No. 541 Whatman filter into a 250-ml measuring cylinder and the volume (v_4) recorded.

At this point, the weight of muscle (w_2) to be loaded on to the Environmental Sep-Pak cartridge can be calculated using the equation

$$w_2 = w_1[v_2/(v_2+v_3)][v_4/(w_1+v_1)]$$

The assumption is made that the muscle is virtually all water, *i.e.*, w_1 g contributes w_1 ml, and that it all contributes to the dilution of v_1.

The Sep-Pak cartridge, conditioned with 5 ml each of methanol and then EDTA–McIlvaine buffer, is attached to a reservoir, made from the barrel of a 50-ml polypropylene syringe, supported by a clamp. The outlet of the Sep-Pak cartridge is connected to a water pump, and the sample is aspirated through at no more than 10 ml/min. When the sample has been passed through, the Sep-Pak cartridge is disconnected, flushed with 5 ml of EDTA–McIlvaine buffer and the surplus liquid blown out.

The technique of minimum volume elution is used. Into a 10-ml gas-tight syringe exactly 2 ml of a 50:50 mixture of acetonitrile and EDTA–McIlvaine buffer are aspirated. The syringe is attached to the Sep-Pak cartridge and about 0.6 ml of this eluent, or enough for one drop of liquid of eluate to appear

at the outlet, is injected. After waiting 30 s for equilibration, the remainder of the eluent is injected and the eluate is collected in a 10-ml measuring cylinder. The syringe is removed, refilled with air and reconnected to the Sep-Pak cartridge, and the remaining eluate is expelled into the measuring cylinder. The volume (v_5) (ml) in the measuring cylinder is measured. A 150-μl volume is injected into the liquid chromatograph. The equivalent weight of muscle injected is calculated as 0.15 w_2/v_5 g.

High-performance liquid chromatography (HPLC)

Solution A was 0.01 *M* citric acid–0.01 *M* dipotassiumorthophosphate and solution B was acetonitrile. The mobile phase was A–B (72:28), containing 0.005 *M* tetramethylammonium chloride and 0.1 g/l of EDTA.

The column used was a Nova-Pak C_{18} (4-μm; end-capped) cartridge (10 cm × 8 mm I.D.) with a μBondapak C_{18} guard column (Waters). The flow-rate was 2.4 ml/min. The concentrations of the analytes were quantified using the data from the 365-nm channel.

RESULTS

Muscle from a calf, known not to contain tetracycline residues, was used for the study. A blank and five replicates spiked at 100 ng/g were processed according to the preceding method.

The peaks observed were confirmed by comparison with the retention times of known standards and with the spectra in a spectral library of tetracyclines. As seen in Table I, the recoveries were 70% [relative standard deviation (R.S.D.) = 8%] for OTC, 58% (R.S.D. = 8%) for TC and 50% (R.S.D. = 10%) for CTC. Although the recovery of CTC is much lower than that of the other tetracyclines, it is easier to detect and confirm because it appears in a part of the chromatogram relatively free from other peaks. Results of spiking studies in routine laboratory analyses have been included in Table I to show the inter-assay variability.

The chromatograms for the standards, a representative spiked sample and the blank sample (negative) are shown in Fig. 1. Figs. 2 and 3 show the spectra for OTC and CTC from a representative spiked sample, together with their software-selected overlays from the library.

Two pigs were injected with therapeutic doses of either OTC or CTC. The animals were killed 24 h later and their muscle tissue was collected, in small samples, and frozen at −20°C. Samples from these pigs were later thawed and tested using the same procedure as for the spiked samples. This experiment was used to demonstrate the applicability of the method using genuine incurred residues. The chromatograms and spectra with the overlaid library matches from these tests are shown in Figs. 4–7. In fig. 5, there is a peak that corresponds to TC. It has been observed in this laboratory that in samples containing a very high concentration of

TABLE I

ANALYSIS OF SPIKED MEAT SAMPLES

A 40-g amount of each sample was processed according to the preceding method. The extracts were chromatographed isocratically [A–B (72:28)] at a flow-rate of 2.4 ml/min and quantified at 365 nm.

Parameter	Oxytetracycline	Tetracycline	Chlortetracycline
Spike level (ng/g)	100	120	100
Intra-assay (n=5)			
Average recovery (ng/g)	70	70	50
Average recovery (%)	70	58	50
S.D. (ng/g)	10	10	0
R.S.D. (%)	8	7	10
Inter-assay (n=5)			
Average recovery (%)	61	60	47
S.D. (ng/g)	12	6	10
R.S.D. (%)	19	10	21

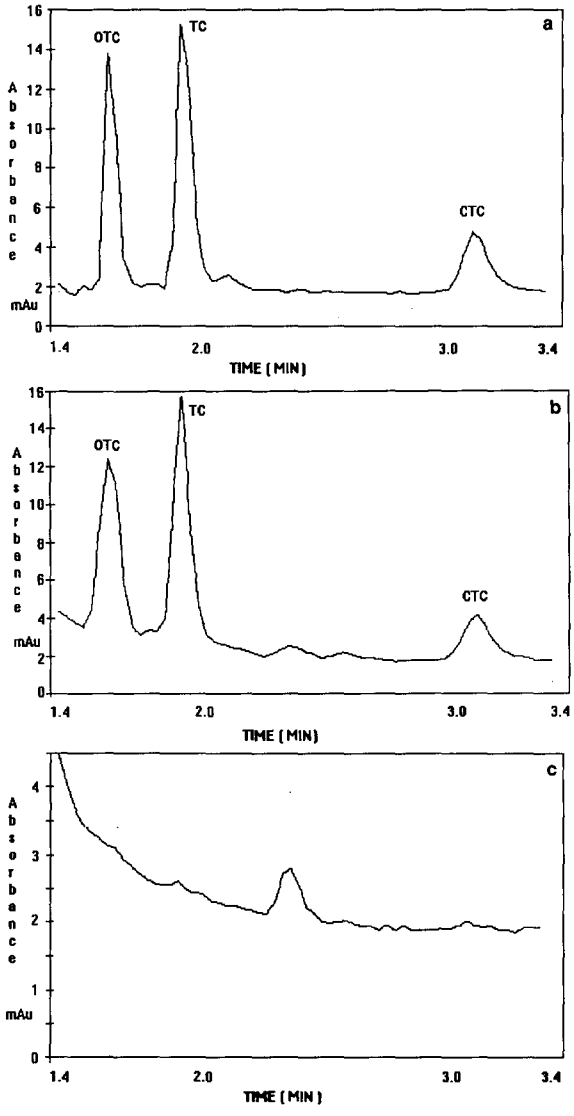

Fig. 1. (a) Chromatogram of three tetracycline standards (150 ng). (b) Chromatogram of blank meat sample spiked with three tetracyclines at 100 ng/g (150 μl). (c) Chromatogram of blank meat-sample (150 μl). HPLC conditions: Nova-Pak C_{18} column (10 cm × 8 mm I.D.); mobile phase, A–B (72:28); flow-rate, 2.4 ml/min; detection at 365 nm.

CTC in muscle or urine, some TC is also observed at varying concentrations. TC is not used in animals in Australia and its source has not been investigated.

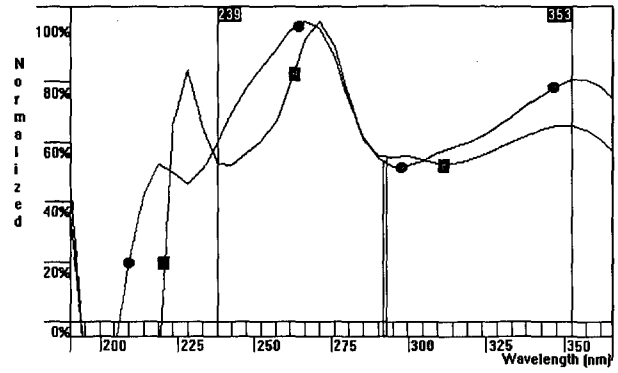

Fig. 2. (■) Diode-array spectra of spiked oxytetracycline sample and (●) oxytetracycline spectrum from the library. For experimental conditions, see Fig. 1.

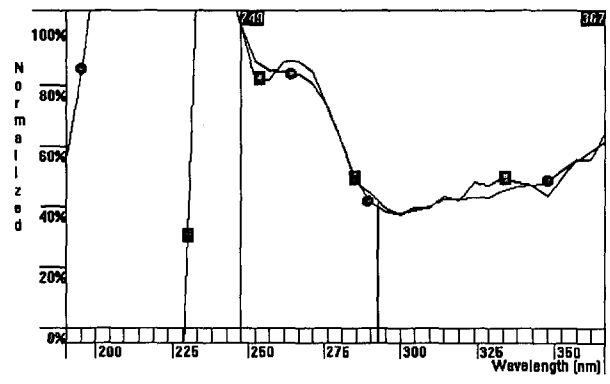

Fig. 3. (■) Diode-array spectra of spiked chlortetracycline sample and (●) chlortetracycline spectrum from the library. For experimental conditions, see Fig. 1.

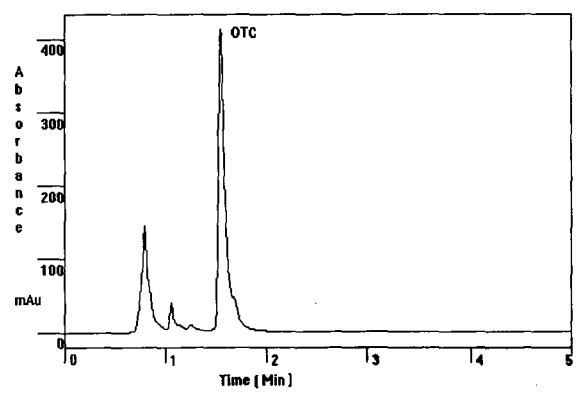

Fig. 4. Chromatogram of incurred oxytetracycline residue sample. For experimental conditions, see Fig. 1.

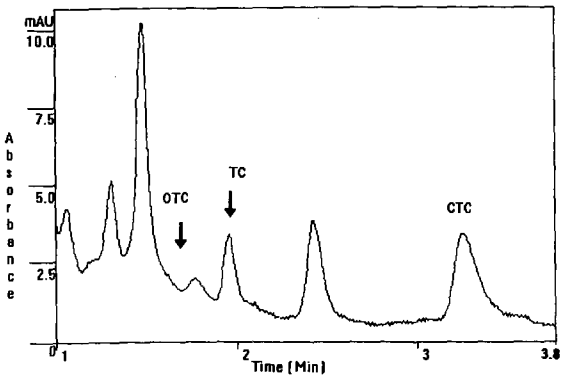

Fig. 5. Chromatogram of incurred chlortetracycline residue sample. The retention-times of OTC and TC are marked. Note the TC peak. For experimental conditions, see Fig. 1.

DISCUSSION

The method of Oka *et al.* [1] was adapted to suit our requirements, as follows: (a) a larger sample size (40 g), with connective tissue and fat carefully trimmed off; (b) larger capacity SPE cartridges (Environmental Sep-Pak); (c) removal of most extraneous compounds (proteins) that otherwise would saturate the Sep-Pak cartridge and the chromatogram and, ultimately, block the column irreversibly, no matter what house-keeping techniques are used [7]; (d) buffers that have minimum UV absorbance above 220 nm; (e) high-resolution liquid chromatographic columns [Nova-Pak C_{18} (10 cm × 8 mm I.D.)] and (f) application of the concept of minimum volume elution.

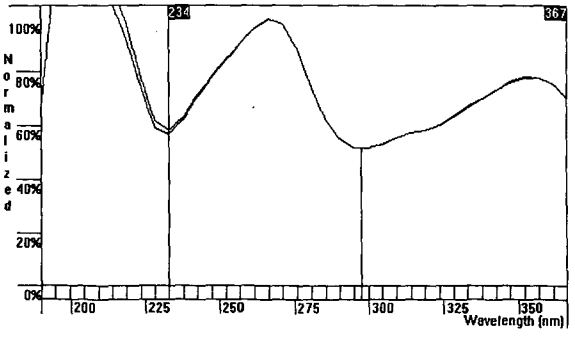

Fig. 6. Diode-array spectra of incurred oxytetracycline residue and oxytetracycline spectrum from the library. For experimental conditions, see Fig. 1.

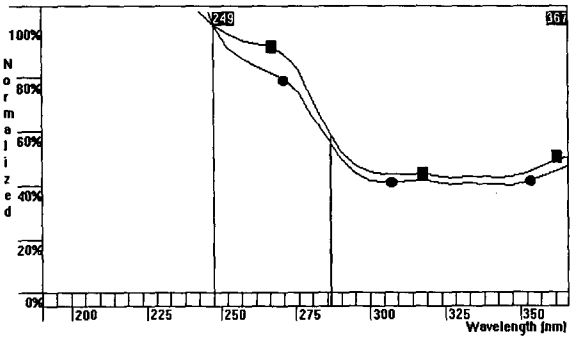

Fig. 7. (■) Diode-array spectra of incurred chlortetracycline residue and (●) chlortetracyline spectrum from the library. For experimental conditions, see Fig. 1.

Measuring the volume at each step was employed for a faster throughput. This enables supernatants to be poured off, not aspirated and re-washed a number of times. The same applies to filtrates. The time per analysis would be doubled or tripled if exhaustive extraction was used. Analyses must be carried out on the same day, as the analytes deteriorate overnight, even if frozen. The R.S.D. of inter-assay spikes (Table I) was double that of the intra-assay spikes. The larger scatter was associated with a lower mean recovery. This has been shown to be due to individual samples not being analysed within the ideal time-frame used when the method was developed. When a large number of samples (8–20) are batched, *i.e.*, the whole group goes through each step together, some samples spend a longer time in each step than is desirable. The spiked sample used in each batch was always placed last in the queue, which caused any delays to affect the spiked sample the most. Results have indicated that samples should be analysed in batches of five or less to maximize recoveries.

Elution of the analytes from the Sep-Pak cartridge in the smallest possible volume is critical to the production of useful peak areas at low concentrations of TCs.

Originally, oxalic acid [1] and methanol [2] were used in the aqueous phases, but were discarded in favour of the present mixtures in order to make diode-array library matches possible at these levels. The use of oxalic acid in the mobile phase inhibits losses of the TCs in the analytical column and connecting tubing, possibly by scavenging divalent ions. EDTA [9] was substituted when oxalic acid in

the mobile phase proved unsuitable for diode-array use. Tetramethylammonium chloride was used to improve the peak shapes via the mechanism of ion suppression [2].

At low wavelengths, the contribution of the buffer and residual matrix to the UV spectrum distorts the subject spectrum. This is very apparent below 240 nm. It can seen by the comparison of Figs. 2 and 6 for OTC and Figs. 3 and 7 for CTC that the library matches for the compounds deteriorates as the level of analyte decreases. This is a function of the greater contribution of the background to the whole spectrum relative to the analyte. The contribution of the buffer and residual matrix to the spectrum is very large compared with that of the analyte and is not constant throughout the chromatogram. It is for this reason that the library of spectra contains a number of spectra of each species created using different levels of spiking in samples. The retention time of the analyte is still the primary means of identification, with the diode-array system important in supplying a further source of confirmation. Tetracycline (TC) was originally included in the study to test its usefulness as an internal standard as it is not used in the meat-production industry. Its appearance with high concentrations of CTC has precluded its use.

In conclusion, this method has proved to be reliable and robust, and possesses the required sensitivity to detect the improper use of OTC and CTC in the meat-production industry in Australia, and it has been used for surveillance (compliance) and monitoring of tetracycline residues in over 300 animals.

REFERENCES

1 H. Oka, H. Matsumoto, K. Uno, K. Harada, S. Kadowaki and M. Suzuki, *J. Chromatogr.*, 325 (1985) 265–274.
2 W. A. Moats, *J. Chromatogr.*, 358 (1986) 253–259.
3 J. P. Sharma, E. G. Perkins and R. F. Bevill, *J. Chromatogr.*, 134 (1977) 441–450.
4 E. E. Martinez and W. Shimoda, *J. Assoc. Off. Anal. Chem.*, 71 (1988) 477–480.
5 Y. Onji, M. Uno and K. Tanigawa, *J. Assoc. Off. Anal. Chem.*, 67 (1984) 1135–1137.
6 E. J. Mulders and D. Van De Lagemat, *J. Pharm. Biomed. Anal.*, 7 (1989) 1829–1835.
7 M. H. Thomas, *J. Assoc. Off. Anal. Chem.*, 72 (1989) 564–567.
8 A. R. Long, L. C. Hsieh, M. S. Malbrough, C. R. Short and S. A. Barker, *J. Assoc. Off. Anal. Chem.*, 73 (1990) 379–384.
9 E. R. White, M. A. Carroll and J. E. Zarembo, *J. Antibiot.*, 30 (1977) 811–818.

Journal of Chromatography, 596 (1992) 217–224
Elsevier Science Publishers B.V., Amsterdam

CHROM. 23 981

Determination of alendronate in pharmaceutical dosage formulations by ion chromatography with conductivity detection☆

Eric W. Tsai*, Dominic P. Ip and Marvin A. Brooks

Merck Sharp & Dohme Research Laboratories, West Point, PA 19486 (USA)

(First received October 1st, 1991; revised manuscript received December 30th, 1991)

ABSTRACT

A method was developed and validated for the direct determination in pharmaceutical dosage formulations of alendronate, a non-chromophoric compound. It is based on the use of single-column ion chromatography with conductivity detection that obviates the need for the tedious chemical derivatization procedures that are required for UV and fluorescence detection. Diluted samples of 0.05 mg/ml were chromatographed directly on a Waters IC-Pak HR anion-exchange column or a Dionex OmniPac PAX-100 column with dilute nitric acid as the mobile phase followed by conductivity detection. The method was validated and shown to be precise, accurate and specific for the assay of alendronate in intravenous (i.v.) solution and tablet formulations. The ruggedness of the assay was studied by generating data from four different instruments. Also established was the equivalence between this method and a previously reported high-performance liquid chromatographic method with 9-fluorenylmethyl chloroformate derivatization and UV detection. Application of the method to the determination of alendronate in i.v. and tablet formulations is presented and the performances of the Waters IC-Pak HR and Dionex OmniPac columns are discussed.

INTRODUCTION

Alendronate (Fig. 1) is the monosodium trihydrate salt of 4-amino-1-hydroxybutane-1,1-bisphosphonic acid and belongs to the bisphosphonate class of drugs. The drug has important therapeutic indications in the treatment of a variety of bone diseases such as hypercalcemia of malignancy, Paget's disease and osteoporosis [1,2]. Development of an assay for this class of compounds is challenging owing to the lack of a chromophore for conventional UV or fluorescence detection. The method described here is capable of the direct measurement of alendronate in pharmaceutical dosage forms based on the use of single-column (non-suppressed) ion chromatography with conductivity detection (IC–CON method). The method obviates the need for the chemical derivatization procedures that are required when UV or fluorescence detection is applied.

Three reversed-phase high-performance liquid chromatographic (HPLC) methods involving chemical derivatization have been described for the determination of alendronate. An HPLC method utilizing precolumn derivatization of the primary amine with 9-fluorenylmethyl chloroformate

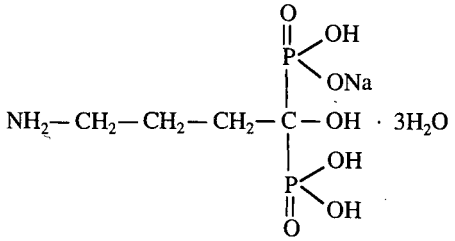

Fig. 1. Structure of alendronate.

☆ Presented at the *5th Annual American Association of Pharmaceutical Scientists Meeting, Las Vegas, NV, Nov. 1990.*

0021-9673/92/$05.00

(FMOC) for UV detection has been reported previously from our laboratory [3]. Kwong *et al.* [4] employed ion-pair chromatography and postcolumn derivatization with *o*-phthalaldehyde (OPA) for fluorescence detection. Both methods were developed for the assay of alendronate in pharmaceutical formulations. Another HPLC procedure was published by Kline *et al.* [5] for the determination of alendronate in urine by automated precolumn derivatization with 2,3-naphthalenedicarboxyaldehyde (NDA) for fluorescence detection [5]. Several HPLC methods dealing with compounds analogous to alendronate have also been reported. For example, Flesch and Hauffe [6] used precolumn derivatization with fluorescamine for fluorescence detection for the determination of Pamidronate disodium (a propyl analogue of alendronate); Daley-Yates *et al.* [7] described the use of ion chromatography, postcolumn oxidation to orthophosphate followed by conversion to a phosphomolybdate complex for the determination of the propyl analogue and several related compounds. All these procedures require either precolumn derivatization techniques that usually require extensive and tedious sample preparation or by postcolumn reactions where complicated and specialized equipment is generally necessary.

Our objective was to simplify the assay procedure by eliminating the derivatization procedure for this non-chromophoric compound. Few chromatographic methods with direct detection for bisphosphonates or related compounds have been published. Chester *et al.* [8] reported an ion-exchange chromatographic method with on-line flame photometric detection for dichloromethylene diphosphonate and Forbes *et al.* [9] described the use of an inductively coupled plasma (ICP) detector for specific phosphorus detection for Etidronate (1-hydroxyethane-1,1-bisphosphonate) disodium. These detection devices are generally not available in pharmaceutical analysis laboratories. Den Hartigh *et al.* [10] presented results obtained using ion-exchange HPLC with conductivity detection for the determination of phosphonates in pharmaceutical preparations.

This paper reports the development, validation and application of the IC–CON method for the direct determination of alendronate in intravenous (i.v.) and tablet formulations. Typical validation studies were carried out, including injection precision, linearity, specificity, recovery and method precision. Assay ruggedness was additionally addressed by generating data from four commonly used chromatographic systems. Also established was the equivalence of the IC–CON and FMOC methods by direct comparison of the analytical results. The performances of two different columns used in this work, namely Waters IC-Pak HR and Dionex OmniPac, are also discussed.

EXPERIMENTAL

Chemicals and reagents

Alendronate (MK-0217, $C_4H_{12}NO_7P_2Na \cdot 3H_2O$; mol. wt. 325.1) of pharmaceutical grade manufactured within Merck Sharp & Dohme Research Labs. (Rahway, NJ, USA) was used as an analytical standard. All solvents and reagents were used as received. Nitric acid (OPTIMA grade), acetonitrile (HPLC grade) sodium citrate, citric acid and sodium chloride (analytical-reagent grade) were purchased from Fisher Scientific (Philadelphia, PA, USA). Deionized water of at least 18MΩ purified with a Milli-Q system (Millipore, Bedford, MA, USA) was used for mobile phase, sample and standard preparations.

Equipment

Most of the development and validation work was performed on a Dionex (Sunnyvale, CA, USA) Model 4500i inert chromatographic system equipped with a Dionex pulsed electrochemical detector (conductivity mode) and a Spectra-Physics (San Jose, CA, USA) Model 8880 autosampler. Stainless-steel systems such as a Hewlett-Packard (Avondale, PA, USA) Model 1090 system connected with a Milton Roy (Riviera Beach, FL, USA) conductivity detector, Perkin-Elmer (Norwalk, CT, USA) Series 4 with Milton Roy detector and Spectra-Physics Model 8800 with Milton Roy detector were also investigated in order to establish the ruggedness of the method. A Waters (Milford, MA, USA)IC-Pak HR anion-exchange column (6 μm particle size, 75 mm × 4.6 mm I.D.) and a Dionex OmniPac PAX-100 column (8 μm particle size, 250 mm × 4 mm I.D.) were used. Mobile phases of 1.6 m*M* nitric acid and 1.76 m*M* nitric acid + 20% acetonitrile were delivered at a flow-rate of 0.5 ml/min

for the IC-Pak HR and OmniPac columns, respectively. Analyses were carried out at ambient temperature with 25-μl injections of 0.05 mg/ml alendronate. Detection by conductivity was set at negative polarity with an output range of 50 μS for the Dionex detector and 1 μS for the Milton Roy detector.

Standard solution preparation

For the assay of i.v. solutions, a standard solution was prepared by dissolving 32 mg of alendronate (equivalent to 25 mg of free acid) in 500 ml of a placebo-equivalent diluent (205.8 mg of sodium citrate + 57.6 mg of citric acid + 98.2 mg of sodium chloride dissolved in 1000 ml of water) in order to maintain an identical ionic strength between the standard and i.v. sample solutions. For the tablet assay, water was used as a diluent for preparing the standard. The standard concentration was 0.05 mg/ml in both instances.

Sample solution preparation

The i.v. solution (2.5 mg/ml) was diluted appropriately with water to yield a concentration of 0.05 mg/ml and transferred to an HPLC vial for analysis. A tablet (2.5 mg) was dispersed and sonicated in an appropriate volume of water for 5 min and diluted to 0.05 mg/ml. The resulting solution was filtered through a Millipore 0.22-μm filter unit and transferred to an HPLC vial for analysis.

Assay procedure

Generally, the system was first equilibrated with the mobile phase by injecting a standard solution until reproducible results were observed (about three injections) prior to the i.v. or tablet assay. Standard and sample solutions were injected directly.

RESULTS AND DISCUSSION

Chromatography

The concept of ion chromatography with conductivity detection has allowed the determination of ionic and non-chromophoric compounds such as alendronate with minimum sample preparation. The single-column ion chromatographic method for anion determination was introduced by Gjerde and co-workers [11,12]. By carefully choosing the anion exchanger and eluent for alendronate, the separation column can be directly coupled to a conductivity detector for direct detection. Under the IC–CON conditions described under Experimental, alendronate is eluted and directly detected by the use of an eluent of 1.6 m*M* nitric acid (pH *ca.* 2.5) as shown in Fig. 2a for the Waters IC-Pak HR column. The selection of dilute nitric acid as a mobile phase was appropriate for pH maintenance to produce predominantly monovalent (-1) charge state of alendronate so that a reasonably short retention (or ion-exchange process) was achieved. It is generally true that the greater the charge state of the sample, the later it elutes owing to its higher affinity for the anion-exchange resin. Because of the high background conductance of the nitric acid mobile phase (mainly because of H^+), the solute (alendronate) produces a decreasing or negative signal (indirect chromatographic signal, see Fig. 2) owing to its uptake of H^+. Similar results have been described by

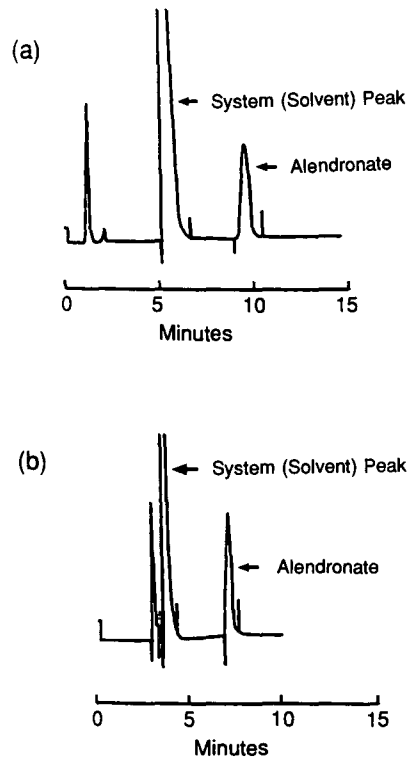

Fig. 2. Typical chromatograms of 0.05 mg/ml alendronate standard solution in water obtained with the IC–CON method on (a) the IC-Pak HR column and (b) the OmniPac column.

Gjerde and co-workers [13,14]. The greater negative deflection observed prior to the alendronate peak, a system peak, was produced from the sample water diluent [15]. This deflection is typically noted in non-suppressed ion chromatography [16] and was attenuated by the concentration of the cation present in the sample, *i.e.*, a higher cation concentration yielded a lower system peak. The use of a cation suppressor (Dionex) to reduce the H^+ concentration of the eluent and hence the background conductance for this method was attempted. This attempt was not successful owing to the simultaneous suppression of the alendronate signal, possibly related to the reduction of the H^+ concentration which was considered critical for the generation of the alendronate signal.

Fig. 2a was generated using a Waters IC-Pak HR anion-exchange column packed with trimethylammonium-functionalized polymethacrylate resin. As indicated, this column produced a relatively broad alendronate peak. Recently, a series of multi-phase columns capable of performing both reversed-phase and ion-exchange HPLC were introduced by Dionex. Experiments demonstrated that an OmniPac PAX-100 column (a highly cross-linked styrene–divinylbenzene polymeric microporous substrate with the surface functionalized by a quaternary ammonium base) with 20% of acetonitrile as an organic modifier yielded a typical chromatogram for alendronate as shown in Fig. 2b. This column has the advantage of yielding a shorter retention with a better peak shape for alendronate than the IC-PAK HR column. The performances of these two columns were preliminarily validated in terms of injection precision, linearity and method specificity for practical applications.

Validation

Injection precision for ten replicate injections of a 0.05 mg/ml standard solution (dissolved in an i.v. placebo-equivalent diluent for i.v. assay or dissolved in water for tablet assay) was satisfactory [relative standard deviation (R.S.D.) < 1% by peak height] for both the IC-Pak HR and OmniPac columns. The peak-area measurements showed higher R.S.D. values (*ca.* 2%), probably owing to the variation of area integrations with such a high background conductance. Peak-height measurements were therefore adopted to determine alendronate in this method.

The detector responses to a range of 40–160% of the assay concentration (in both i.v. and water media) was determined to be linear with $R^2 > 0.999$ for both columns. In some instances, a non-zero intercept was observed in the linearity plot, especially when peak-area measurements were used. This non-zero intercept was attributed to the background conductance drift during the experimental runs. It was less pronounced when peak-height measurements were used and had an inconsequential effect on accuracy at the assay concentration.

Method specificity utilizing the OmniPac column was demonstrated by the separation of alendronate from its aminohydroxypropyl analogue (relative retention time, t_R, = 1.16) and its thermal decomposition products obtained by melting alendronate at 260°C by differential scanning calorimetry (DSC) (two late-eluting peaks at t_R = 1.23 and 1.59). The degradation products induced by DSC melting were generated under unrealistic high temperature conditions for the purpose of illustrating method specificity only. Identification of these thermal decomposition products was not pursued. The method was also specific against components of the i.v. and tablet placebo formulations (see below). No bias was evident in each instance under the described chromatographic conditions. The validation was extended to the recovery and method precision for 2.5 mg/ml i.v. and 2.5 mg tablet formulations.

Analysis of formulations

Intravenous solution. Fig. 3 illustrates typical chromatograms obtained with the IC–CON method using the IC-Pak HR column for (a) and i.v. placebo containing citrate buffer in saline solution and (b) alendronate in an i.v. formulation. It is apparent that alendronate could be resolved from components in the i.v. placebo without any interference. The OmniPac column could not be utilized for this sample because of an interfering i.v. background, probably due to column overload owing to the amount of citrate present in the formulation. It is important to note that there was a slight difference (*ca.* 0.1 min) in the retention times (and hence peak heights) between the standard dissolved in water and the i.v. sample solution. This difference resulted in an experimental error of 2–3% when i.v. samples were analyzed against the standard solution in water. This error could be circumvented by

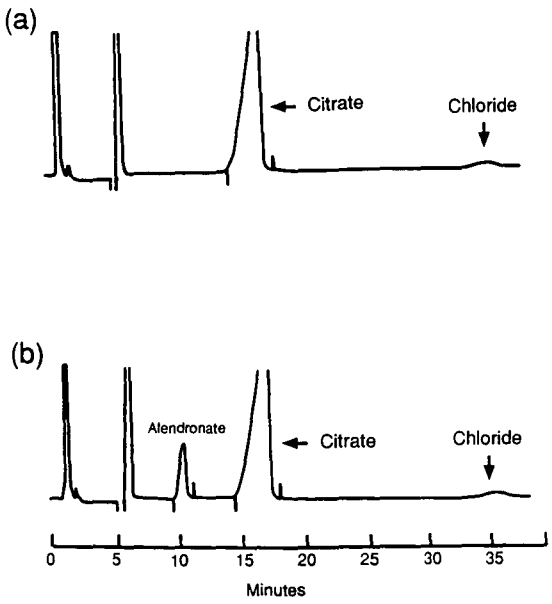

Fig. 3. Chromatograms of (a) diluted i.v. pacebo and (b) diluted i.v. sample solution obtained with the IC-Pak HR column.

matching the standard with an i.v. placebo-equivalent diluent (see Experimental) so that identical responses were observed for i.v. smaple and the "modified" standard solutions owing to their equivalent ionic strength. More accurate results could therefore be obtained. The validation data for i.v. solutions were therefore generated based on the selection of a matched standard solution.

Recovery studies were performed by spiking aliquots of a stock solution (0.1 mg/ml) of alendronate into an i.v. placebo in duplicate at 80%, 90%, 100%, 110% and 120% levels of potency followed by appropriate dilution. The results were satisfactory with a mean recovery of 100.2% and R.S.D. = 1.4% (n = 10).

The method precision was determined by analyzing ten replicate samples. Table I summarizes the mean assay results for ten samples generated by two individual analysts. For comparison purposes, the results calculated against standard in water and standard in placebo-equivalent solution are also presented in Table I. Excellent precisions were attained with R.S.D. < 1% in all instances. It is obvious that data calculated with respect to the matched standard solution yield relatively more accurate results. This observation confirms the significance and necessity for the selection of a matched standard solution for i.v. sample analysis. Also listed in Table I are the data obtained by our previously published FMOC method for establishing equivalence (see below for discussion).

Tablet formulation. For the tablet formulation, both columns demonstrated satisfactory specificity, as shown in Fig. 4, where alendronate could be separated from the placebo excipients. It is pertinent to note that the assay for tablets provides more time saving than the i.v. assay. The later is complicated by the late-eluting ionic species of citrate and chloride present in the formulation. The OmniPac column yields a better peak shape and shorter retention time than the IC-Pak HR column and is therefore more suitable for the assay of tablet forms. The validation and analytical data for 2.5 mg tablets were collected on both columns for comparison.

Recovery experiments for the tablets were performed using similar experimental conditions to those described for the i.v. solution. Results of these experiments for duplicate samples prepared at 80%,

TABLE I

METHOD PRECISION DATA AND COMPARISON BETWEEN IC-CON AND FMOC METHODS

IC-CON[a]				FMOC method[a]	
Standard in placebo		Standard in H_{2O}			
Analyst I	Analyst II	Analyst I	Analyst II	Analyst I	Analyst II
2.52 mg/ml, 100.8% (R.S.D. 0.87%)	2.52 mg/ml, 100.7% (R.S.D. 0.42%)	2.42 mg/ml, 96.8% (R.S.D. 1.06%)	2.44 mg/ml, 97.5% (R.S.D. 0.35%)	2.54 mg/ml, 101.5% (R.S.D. 0.10%)	2.54 mg/ml, 101.6% (R.S.D. 1.04%)

[a] Data are given as mg/ml found with % of label claim for 2.5 mg/ml i.v. solutions, with R.S.D. (n = 10) in parentheses.

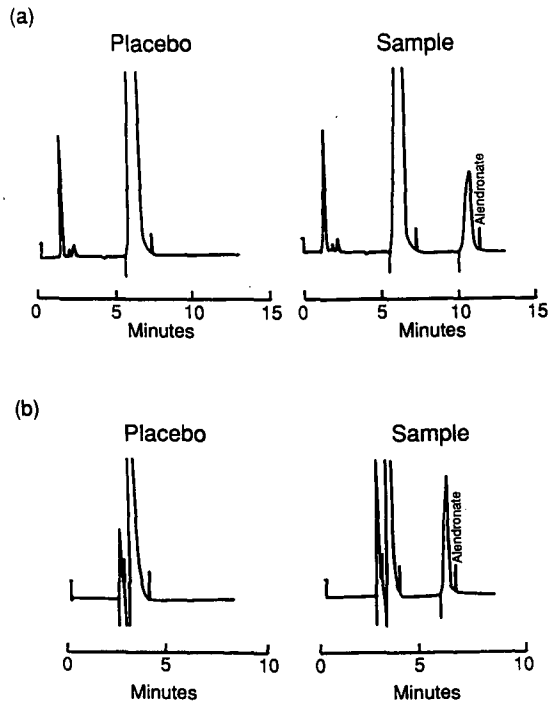

Fig. 4. IC–CON analysis of alendronate tablet formulations including placebo and sample performed on (a) the IC-Pak HR column and (b) the OmniPac column.

90%, 100%, 110% and 120% levels of potency were satisfactory with a mean recovery of 99.8% (R.S.D. 0.95%) and 100.1% (R.S.D. 0.76%) for the OmniPac and IC-Pak HR columns, respectively. All the data were calculated using a standard solution in water. Unlike the i.v. solution, the tablet formulation does not contain ionic components such as chloride and citrate anions. Hence, the choice of water as the the standard diluent for simplicity can be justified without affecting the accuracy of the assay.

Table II summarizes the uniformity in composition of ten tablets assayed using both columns for establishing the method precision. Satisfactory analytical results and precision (R.S.D. < 2%) were obtained by the IC–CON method and were consistent with those of the FMOC method. The R.S.D. (n = 10) reported for the tablet formulation represents the sum of the variations from the assay and the manufacture of the dosage form.

Based on the above validation and analytical results for i.v. and tablet dosage forms, it is concluded

TABLE II

CONTENT UNIFORMITY DATA FOR 2.5 mg TABLETS ASSAYED BY THE IC–CON AND FMOC METHODS

IC–CON method[a]		FMOC method[a]
OmniPac column	IC-Pak HR column	
2.47 mg, 98.9% (R.S.D. 0.75%)	2.47 mg, 98.7% (R.S.D. 1.80%)	2.45 mg, 97.8% (R.S.D. 0.69%)

[a] Data are given as mg found with % of label claim, with R.S.D. (n = 10) in parentheses.

that the IC–CON method is precise, accurate, specific and suitable for the assay of alendronate in the two formulations. The limit of quantification (LOQ) was also determined in order to evaluate the possible application for the measurement of drug dissolution rates. An LOQ of 0.005 mg/ml was found to be achievable with an R.S.D. of 2.9% (the limit of detection was 0.002 mg/ml with signal-to-noise ratio = 4). Although the method demonstrates an advantage in ease of sample preparation, further evaluation of the method ruggedness and method equivalence between the IC–CON and FMOC methods was conducted as discussed below.

Method ruggedness and equivalence testing

Ruggedness testing was primarily demonstrated via data (Table I) showing that the IC–CON method could be reproduced by two individual analysts, indicating that the method is operator independent. The assay ruggedness was more intensively addressed by performing similar experiments on three chromatographic systems equipped with stainless-steel tubing (see Experimental), as the Dionex inert LC system (PEEK-based flow path) was considered to be a specialized instrument. Table III summarizes data reproducibility which substantiates the performances of the four LC systems. These systems could generate a smooth baseline, comparable injection precision (R.S.D. < 1.5%, n = 10), good linearity (R^2 > 0.999) and satisfactory assay results for ten i.v. samples. Consequently, it is reasonable to conclude that the method is rugged as a specialized instrument is not required. However, it is worth noting that the Spectra-Physics Model 8800 + Model 8880 autosampler exhibits an

TABLE III

PERFORMANCES OF DIFFERENT INSTRUMENTS FOR RUGGEDNESS TESTING

HPLC system + autosampler[a]	Baseline	Injection precision (R.S.D., %)[b]	Linearity (R^2)	I.v. sample analysis[b]
Dionex + SP 8880	Smooth	0.85	1.000	100.7% of label (R.S.D. 0.43%)
SP 8800 + SP 8880	Smooth	0.98	0.999	100.9% of label (R.S.D. 0.91%)
HP 1090	Smooth	0.95	1.000	100.7% of label (R.S.D. 0.89%)
PE	Smooth	1.38	0.999	Not determined

[a] Detectors used are specified under Experimental. SP = Spectra-Physics; HP = Hewlett-Packard; PE = Perkin-Elmer.
[b] $n = 10$.

erratic baseline and unacceptable analytical results (about 2–8% error) when the system is switched from reversed-phase HPLC to ion chromatography. The problem could be eliminated by bypassing the mixer (which probably contains unknown contaminants) and passivating the flow path with 0.05 *M* nitric acid overnight, and also replacing the Vespel rotor seal in the autosampler with a Tefzel rotor seal. The exact reason for the erratic ion chromatography was not pursued. After these extensive cleaning and equilibration procedures, the Spectra-Physics system performed equally well, as indicated in Table III.

The data shown in Tables I (i.v. sample analysis) and II (tablet sample analysis) obtained with both the IC–CON and FMOC methods attest to the equivalence between these two methods. Degraded i.v. samples (*e.g.*, stressed at 80°C for 16 weeks) were also analyzed by both methods with consistent results (94.1% of theory by the IC–CON method and 93.1% of theory by the FMOC method). These data additionally support the method equivalence. In order further to demonstrate the equivalence, sixteen lots of i.v. samples were assayed by the IC–CON method and the data compared with the available FMOC results. The data obtained with the two methods do not show a significant difference and yield similar variabilities from the label concentration of 2.5 mg/ml. The IC–CON mean result was 2.51 mg/ml (R.S.D. = 1.51%) and the FMOC mean result was 2.52 mg/ml (R.S.D. = 1.62%). The difference of 0.01 mg/ml was not statistically significant (*t*-test, $P = 0.33$). Hence these results strongly support the fact that the two methods are essentially equivalent.

CONCLUSIONS

A novel IC–CON method using a Waters IC-Pak HR column has been validated and shown to be precise, accurate, specific and suitable for the assay of alendronate in i.v. solution. It is also applicable to the assay of tablets using an OmniPac or IC-Pak HR column. The former yields a sharper peak shape and shorter retention time. The method is rugged based on evidence that four different instrumental systems can perform equally well, and that equivalent results can be achieved independently by different operators using similar instrumentation. The IC–CON method has been demonstrated to be equivalent to the current FMOC method. This newly developed method can offer a direct measurement of alendronate in various dosage forms without the need for the derivatization procedures that are required with UV–VIS and fluorescence detection and hence is relatively simple. The ease of sample preparation has led us to investigate a wide range of applications of this methodology, especially for similar compounds without a derivatizable amino group such as Etidronate, where FMOC derivatization is not possible. Finally, a similar approach with indirect UV absorption detection at 230 nm due to the decrease in nitrate concentration is under investigation.

ACKNOWLEDGEMENTS

The authors thank Dr. J. H. Clair for useful statistical consultations and Mrs. L. Rittle for typing the manuscript.

REFERENCES

1 G. Heynen, P. Delwaide, O. L. M. Bijvoet and P. Franchimont, *Eur. J. Clin. Invest.*, 11 (1982) 29.
2 H. P. Sleeboom, O. L. M. Bijvoet, A. T. van Oosterom, J. H. Gleed and J. L. H. O'Riordan, *Lancet*, ii (1983) 239.
3 J. D. DeMarco, S. E. Biffar, D. G. Reed and M. A. Brooks, *J. Pharm. Biomed. Anal.*, 12 (1989) 1719.
4 E. Kwong, A. M. Y. Chiu, S. A. McClintock and M. L. Cotton, *J. Chromatogr. Sci.*, 28 (1990) 563.
5 W. F. Kline, B. K. Matuszewski and W. F. Bayne, *J. Chromatogr.*, 534 (1990) 139.
6 G. Flesch and S. A. Hauffe, *J. Chromatogr.*, 489 (1989) 446.
7 P. T. Daley-Yates, L. A. Gifford and C. R. Hoggarth, *J. Chromatogr.*, 490 (1989) 329.
8 T. L. Chester, E. C. Lewis, J. J. Benedict, R. J. Sunberg and W. C. Tettenhorst, *J. Chromatogr.*, 225 (1981) 17.
9 K. A. Forbes, J. Vecchiarelli, P. C. Uden and R. M. Barnes, in P. Jandik and R. M. Cassidy (Editors), *Advances in Ion Chromatography*, Century International Franklin, MA, 1989, p. 487.
10 J. Den Hartigh, R. Langebroek and P. Vermeij, presented at the *3rd International Symposium on Drug Analysis, Antwerp, May 1989*, abstracts, p. 114.
11 D. T. Gjerde, J. S. Fritz and G. Schmuckler, *J. Chromatogr.*, 186 (1979) 509.
12 D. T. Gjerde, G. Schmuckler and J. S. Fritz, *J. Chromatogr.*, 187 (1980) 35.
13 J. S. Fritz, D. T. Gjerde and R. M. Becker, *Anal. Chem.*, 52 (1980) 1519.
14 D. T. Gjerde and J. S. Fritz, in W. Bertsch, W. G. Jennings and R. E. Kaiser (Editors), *Ion Chromatography*, Hüthig, New York, 2nd ed., 1987, Ch. 7, p. 133.
15 D. T. Gjerde and J. S. Fritz, in W. Bertsch, W. G. Jennings and R. E. Kaiser (Editors), *Ion Chromatography*, Hüthig, New York, 2nd ed., 1987, Ch. 6, p. 93.
16 T. Okada and T. Kuwamoto, *Anal. Chem.*, 56 (1984) 2073.

Journal of Chromatography, 596 (1992) 225–232
Elsevier Science Publishers B.V., Amsterdam

CHROM. 23 986

Characterization and identification of wheat cultivars by multi-dimensional analysis of reversed-phase high-performance liquid chromatograms

Ph. Courcoux* and Th. Serot

École Nationale d'Ingénieurs des Techniques des Industries Agroalimentaires, Domaine de la Géraudière, 44072 Nantes Cedex 03 (France)

C. Larre and Y. Popineau

Institut National de la Recherche Agronomique, Domaine de la Géraudière, 44072 Nantes Cedex 03 (France)

(First received July 18th, 1991; revised manuscript received December 31st, 1991)

ABSTRACT

Reversed-phase high-performance liquid chromatography was used to identify wheat cultivars. A collection of 59 chromatograms of the gliadin fractions of samples from 18 different cultivars was analysed through multi-dimensional statistical methods. The discrimination quality of the different varieties studied makes possible a classification of the chromatograms obtained. The great variability of the chromatographic profiles and the correct repeatability of the technique used indicate that multi-dimensional analysis applied to the treatment of reversed-phase chromatograms is a reliable and relevant method for cultivar identification.

INTRODUCTION

Since Bietz's work [1] showing that cereal storage proteins can be characterized by reversed-phase high-performance liquid chromatography (RP-HPLC), many papers on the use of this method for wheat: identification [2,3], quality prediction [4–6] and genetic analysis of cereals [7] have been published. Studies have also been carried out on the computer processing of the chromatograms obtained [8]. More recently, algorithms allowing identification by comparison of an unknown sample with a database [9] have been published. Recognition is achieved by homology of the retention times of identified peaks. This method originates from work on the identification of wheat cultivars by electrophoresis [10,11].

Statistical methods and techniques of multi-dimensional data analysis are frequently used to study sets of continuous signals, especially in infrared spectrometry [12]. The application of such methods to gel permeation HPLC data has proved relevant for discriminating and identifying varieties [13]. In this work, multi-dimensional methods were used to characterize and classify different wheat cultivars by RP-HPLC of the gliadin fraction, wich has been shown to have good potential for varietal identification [14].

EXPERIMENTAL

Chemicals

Protein sequencing grade trifluoroacetic acid (TFA) was supplied by Sigma Chimie (France) and HPLC-grade acetonitrile (ACN) by Carlo Erba (Milan, Italy). HPLC-grade water was prepared with a Milli-Qplus water purification system (Millipore, Molsheim, France).

0021-9673/92/$05.00

Wheat samples

Different wheat samples were supplied by INRA Plant Breeding Station (Clermont Ferrand, France) and consisted of eighteen cultivars of common wheat: Andain (AN), Arminda (AR), Capitole (CA), Castan (CS), Courtot (CO), Fanion (FA), Festival (FE), Florence–Aurore (FL), Gavroche (GA), Hardi (HA), Lutin (LU), Maître Pierre (MP), Pistou (PI), Prinqual (PR), Récital (RE), Rex (RX), Tarasque (TA) and Thésée (TH).

Sample prepartion

After grinding the grains with a refrigerated Dangoumeau grinder, gliadins were extracted from flour with 70% ethanol and then purified by gel permeation on S300 Sephacryl gel in 0.028 *M* aluminium lactate (pH 3.6) to remove glutenin. Gliadin fractions were then dialysed against 0.1% acetic acid and freeze-dried.

The different samples corresponding to α-, β-, ω- and γ-gliadins were obtained by fractionating crude gliadins by ion-exchange chromatography on SP-Trisacryl M [15] and by hydrophobic interaction chromatographgy [16]. The fractions were dialysed, freeze-dried and characterized by polyacrylamide gel electrophoresis at pH 3.1. For chromatography, gliadins were weighed, dissolved in water–ACN (72:28) + 0.088% TFA and filtered through a 0.2-μm Millipore membrane before injection.

HPLC

Chromatography was carried out with an LDC/Milton Roy Series 4000 system. Chromatographic data were stored in an IBM-compatible microcomputer through Labnet software (Spectra-Physics).

A Vydac (Cluzeau, France) C_{18} column (15 cm × 0.46 cm I.D.) of 300 Å porosity was used to separate gliadins.

A 100-μl protein sample (5 mg/ml) was injected on to the column. The proteins were eluted with a linear gradient from water–ACN (72:28) + 0.088% TFA to water–ACN (52.5:47.5 + 0.080% TFA in 60 min. The flow-rate was 1 ml/min and protein detection was performed at 226 nm.

Two methods were used. Method A: solvent A ACN–water (15:85) +0.1% TFA and solvent B ACN–water (80:20) +0.06% TFA [1,2], gradient from 28% to 47.5% ACN in 60 min. Method B: solvent A water +0.1% TFA and solvent B ACN +0.06% TFA, gradient from 28% to 47.5% ACN in 60 min.

Statistical treatments

Prior to treatment, the chromatographic signals were truncated in order to retain only the useful part situated between 13 min and 59.8 min after the injection peak. The baseline of these chromatograms was then subtracted and their areas were adjusted to the same reference. After this reduction phase, the chromatograms all had the same surface area.

The chromatograms were then integrated by sections. On the basis of electrophoresis, thirteen sections were retained, corresponding to zones enriched in one or two gliadin components. Therefore, each chromatographic profile is described by thirteen variables corresponding to the areas of the integration zones.

The processed file is made up of 59 observations (repetitions on the eighteen cultivars) and thirteen variables (integration areas). An analysis of variance (ANOVA) and a canonical discriminant analysis (DISCRIM) were carried out in order to describe the most discriminant factors, together with a hierarchical clustering (CLUSTER with Ward's minimum variance method) allowing a tree diagram (or dendrogram) of these cultivars to be elaborated.

These treatments were performed with SAS statistical software (SAS Institute, Cary, NC, USA) on a SUN workstation and with specifically developed software.

RESULTS AND DISCUSSION

Chromatographic reproducibility assays

Preliminary tests with crude gliadins from the cultivar Hardi were carried out in order to determine the chromatographic conditions allowing the best reproducibility. In the first experiments, gliadin elution was effected according to method A, in which prediluted solvents were used. For the twelve major peaks, the average retention times, the standard deviations and the relative standard deviations were calculated for seven repetitions (Table I). It is interesting that as long as the gradient was performed with the same series of solvents A and B, the calculated standard deviation was near 0.1 min. However, the use of new solvents A and B, even

TABLE I

COMPARISON OF THE TWO CHROMATOGRAPHIC METHODS

Averages, standard deviations (S.D.) and relative standard deviations (R.S.D.) for the retention times of the twelve major peaks for seven repetitions on the Hardi cultivar. For methods A and B, see Experimental.

Peak No.	Method A			Method B		
	Average retention time (min)	S.D. (min)	R.S.D. (%)	Average retention time (min)	S.D. (min)	R.S.D. (%)
1	30.59	0.61	1.86	30.37	0.10	0.34
2	31.84	0.58	1.72	31.54	0.12	0.38
3	33.17	0.58	1.65	32.82	0.10	0.30
4	34.10	0.56	1.56	33.71	0.11	0.32
5	35.57	0.56	1.48	35.12	0.11	0.31
6	36.31	0.57	1.50	35.83	0.10	0.29
7	37.10	0.58	1.49	36.65	0.12	0.32
8	37.78	0.55	1.38	37.41	0.11	0.28
9	39.39	0.53	1.29	39.06	0.12	0.30
10	42.86	0.53	1.18	42.33	0.11	0.27
11	44.38	0.53	1.14	43.93	0.13	0.29
12	51.06	0.51	0.95	51.32	0.12	0.23

prepared under closely controlled conditions, decreased the reproducibility considerably. This led to standard deviations up to 0.51 min as indicated in Table I. This lack of reproducibility has to be related to variations in the preparation of solvents. In order to avoid such variations, another method (method B) in which solvents A and B were used pure, was applied in a second series of experiments. The relative standard deviations obtained (Table I) were six times lower than those obtained with method A. These results are in agreement with previous reports for RP-HPLC of gliadins [14] with automatic analysis.

Variability of chromatographic profiles

The subsequent elution profiles were all obtained using method B. Depending on the cultivar, about twenty peaks resulted (Fig. 1). The chromatograms can be roughly split into four zones corresponding to the four gliadin groups. Referring to the profiles of purified gliadins (Fig. 2), the less hydrophobic ω-gliadins were eluted between 13 and 24 min, the α- and β-gliadins between 24 and 40 min and the γ-gliadins between 40 and 45 min. In that zone, the γ-46 gliadin peak was identified at 43 min and that of γ-44 gliadin at 44 min. Proteins eluted after 45 min were not identified. The retention times and the acetonitrile percentages (Table II) at which the different types of gliadins were eluted are similar to those obtained by Lookhart and Albers [17].

Some chromatograms exhibited sufficient qualitative differences to be easily distinguishable. These differences mainly concerned the ω- and α-gliadin fractions.

Statistical analysis

Peak retention time and peak size are the prime characteristics in HPLC. For further analysis, each pattern was normalized. This reduction of the data minimized the protein content differences between samples. Thirteen integration sections were defined (Fig. 3) and their areas were considered as the variables of the analysis of variance. The results of this analysis carried out on these thirteen variables for the 59 observations are summarized in Table III. The sections which best discriminate the different cultivars are S1, S2, S3 and S8 with highly significant tests. From the localisation of the different groups of gliadins on a chromatogram, the sections S1, S2, S3 correspond to ω-gliadins, while S8 correspond essentially to α-gliadins. These results are in agreement with the observations of Branlard and Dardevet [18], who showed that among the four groups of gliadins, the amounts of the ω- and

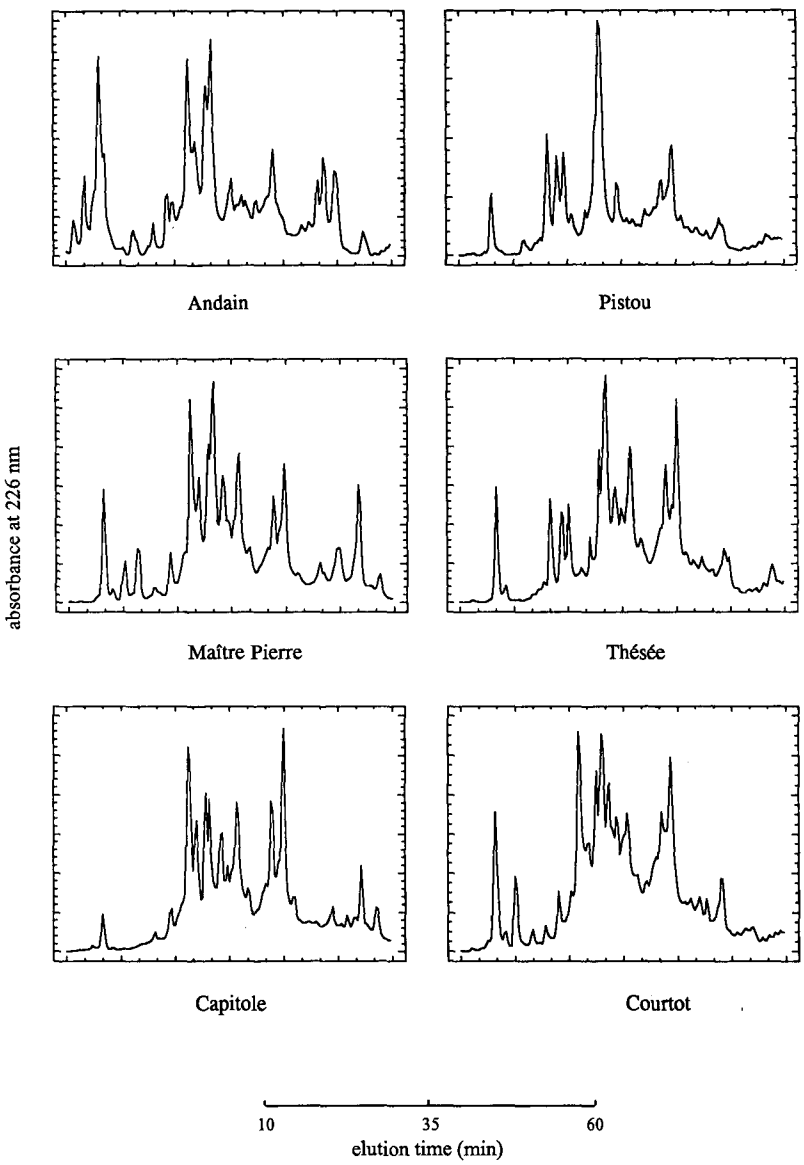

Fig. 1. RP-HPLC elution profiles of the wheat gliadin fraction of six cultivars (part situated between 13 and 59.8 min). The gradient is performed according to method B (ACN from 28% to 47.5% in 60 min); flow-rate, 1 ml/min; detection at 226 nm. The baseline has been subtracted and the surfaces adjusted to the same reference.

α-components were the most variable in 70 cultivars. Nevertheless, they observed also that the amount of each group of gliadin was strongly related to the protein content of the grains, whereas in our experiment the influence of protein content was minimized. Moreover, Autran and Bourdet [19], using electrophoretic techniques for varietal determination, pointed out the discriminating power of ω-gliadins. Nothing has been mentioned previously about α-gliadins.

Fig. 4 shows the first plane of the discriminant analysis on cultivars (this plane explains 63.8% of the total inertia). The projection nearness of profiles corresponding to repetitions of each cultivar con-

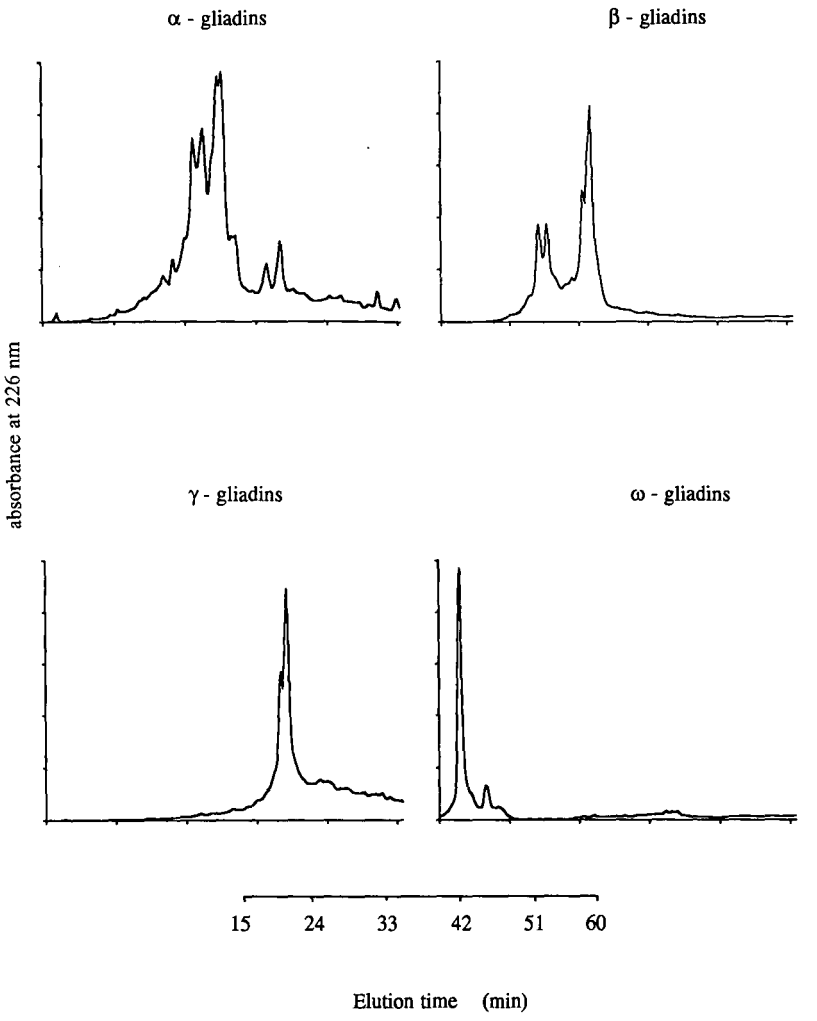

Fig. 2. Chromatograms of purified fractions. Elution conditions as in Fig. 1.

firms the very good repeatability of the chromatograms. On the other hand, great variability of the profiles can be seen, confirming visual observations with particular cultivars (Pistou, Andain) and close relationships between others (*e.g.* Maître Pierre and Fanion).

The discrimination of cultivars by DISCRIM analysis is perfect because, after resubstitution, all observations are correctly assigned to their original cultivar. This is the consequence of the good repeatability of the chromatographic technique used and of the great variability of gliadins. These results confirm the possible use of these statistical methods for the analysis and identification of French wheats based on the gliadin chromatographic profile.

Fig. 5 represents the projections of original variables on the plane of the two first canonical factors. Sections S8 and S12 are very correlated with canonical factor 1 and S1 is very correlated with canonical factor 2. These results are in agreement with those obtained previously by analysis of variance. The proteins eluted in section S12 have not been identified but, in work on the characterization of Hard Red Spring and Hard Red Winter wheats, Endo *et al.* [20] pointed out the discriminating power of the last-eluted peak. The diagram allows a more precise

TABLE II

ELUTION CONDITIONS OF THE DIFFERENT GLIADIN TYPES FOR THE STUDIED CULTIVARS

Operating conditions according to method B (see Experimental).

Peak No.	Retention time (min)	ACN (%)	Gliadin type
1	15.0	23	ω
2	19.4	34.30	ω
3	23.0	35.47	β
4	24.4	35.93	β
5	25.5	36.28	β
6	29.0	37.42	β
7	30.5	37.9	β
8	32.5	38.56	α
9	34.5	39.2	α
10	39.5	40.8	γ-16
11	40.7	41.22	γ-44
12	45–48	42.62–43.6	Not identified

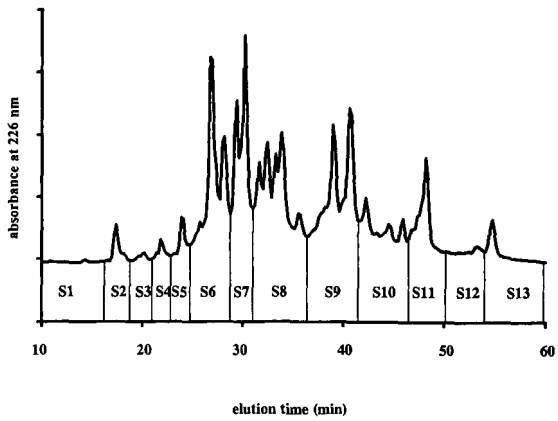

Fig. 3. Separation of the elution profile of Hardi cultivar into thirteen integration sections. Elution conditions as in Fig. 1.

interpretation of the canonical plane previously introduced. The position of the Andain cultivar on the first discriminant plane can then be explained by the wide surfaces of zones S1 and S6 and the positioin of the Pistou cultivar by the high contributions of zones S4 and S5.

Clustering of cultivars

The dendrogram resulting from a hierarchical clustering on the chromatographic profiles of the different cultivars is shown in Fig. 6. This representation helps to examine distances between cultivars and to find natural partitioning in the studied collection. The horizontal axis of the dendrogram represents a distance index measuring the similarities between cultivars. The more the linkage occurred near the leaves of the tree, the more similar are the chromatograms of the cultivars.

The originality of the Pistou and Andain cultivars is verified on the hierarchical tree produced by the CLUSTER procedure and the proximities noticed previously are confirmed. Cutting the tree at the right level allows partitioning of all cultivars into five groups the individuals of which have close profiles:

g1: Pistou;
g2: Andain;
g3: Maître Pierre, Fanion;
g4: Castan, Arminda, Thésée, Lutin;
g5: Capitole, Récital, Tarasque, Festival, Rex, Gavroche, Florence, Courtot, Hardi, Prinqual.

This partitioning shows good agreement with the positions of the cultivars on the first plane of the discriminant analysis shown previously. This dendrogram results only from the polymorphism of gliadin as revealed by RP-HPLC. It will be of interest to compare these results with genetic proximities between cultivars.

TABLE III

ANALYSIS OF VARIANCE ON THE 18 CULTIVARS

Influence of the cultivar on the areas of the 13 different sections of the 58 chromatograms.

Section	Mean square	$F(17,41)^a$
S1	29.39	414
S2	1.73	234
S3	1.78	203
S4	2.30	25
S5	6.42	113
S6	21.96	142
S7	11.43	102
S8	38.06	240
S9	22.45	44
S10	9.19	29
S11	10.00	139
S12	8.92	158
S13	2.26	5

[a] F test calculated with 17 and 41 degrees of freedom (d.f.).

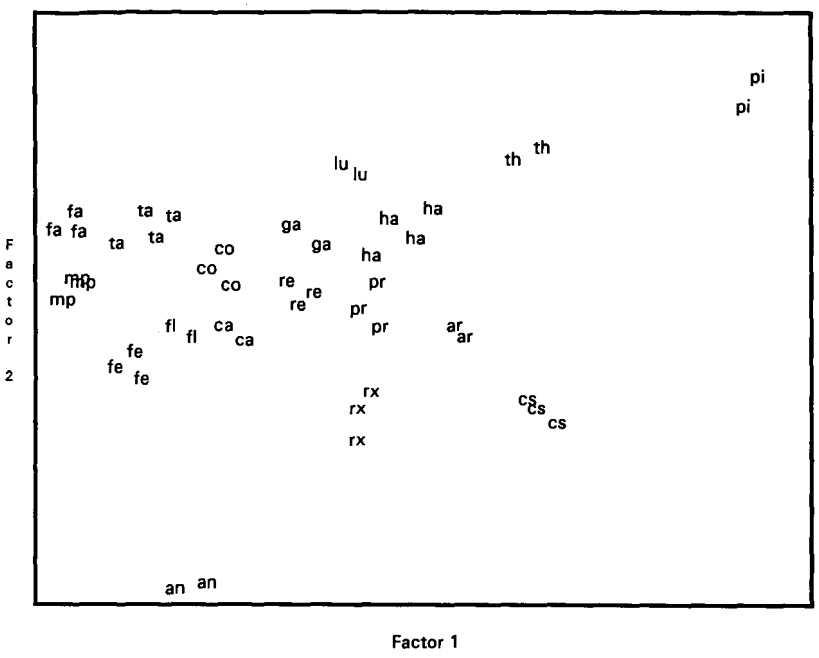

Fig. 4. First factorial plane of the discriminating analysis of cultivars. Projection of the 59 samples.

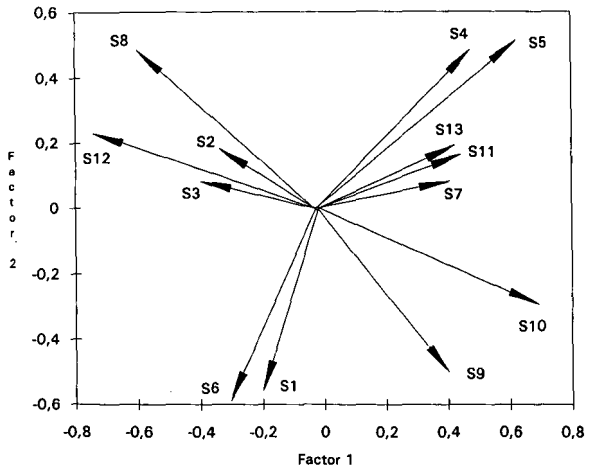

Fig. 5. Projection of the original variables (areas of the thirteen integration section) on the plane of the two first canonical factors of the discriminating analysis.

CONCLUSIONS

The different statistical analyses performed on RP-HPLC data led to coherent conclusions. Therefore, multi-dimensional analysis applied to chromatograms obtained by RP-HPLC is a method particularly suitable for the discrimination and classification of wheat cultivars. This confirms the possibility of applying statistical methods currently used for the treatment of other continuous signals, as in infrared spectrometry [12]. However, well controlled chromatographic conditions are necessary to perform statistical analysis. Nevertheless, this method needs to be validated taking into account growing year and location; such studies are in progress.

ACKNOWLEDGEMENTS

We thank Mr. J. Koenig (INRA, Clermont-Ferrand) for supplying cultivar samples and Dr. G. Branlard (INRA, Clermont-Ferrand) for stimulating discussions.

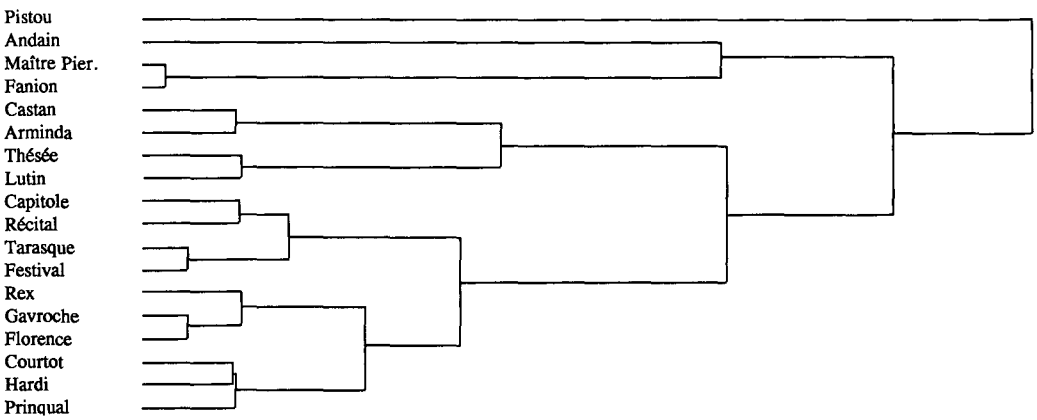

Fig. 6. Dendrogram resulting from a cluster analysis (Ward's method) on the thirteen integration sections of the eighteen cultivars.

REFERENCES

1 J. A. Bietz, *J. Chromatogr.*, 255 (1983) 219–238.
2 T. Burnouf and J. A. Bietz, presented at the *2nd International Symposium on Biochemical Approaches to Identification of Cultivars and Their Properties, Braunschweig, May 5–9, 1985.*
3 M. G. Scanlon, H. D. Sapirstein and W. Bushuk, *Cereal Chem.*, 66 (1989) 112–116.
4 F. R. Huebner and J. A. Bietz, *J. Chromatogr.*, 327 (1985) 333–342.
5 F. R. Huebner and J. A. Bietz, *Cereal Chem.*, 64 (1987) 15–20.
6 B. A. Marchylo, J. E. Kruger and D. W. Hatcher, *J. Cereal. Sci.*, 9 (1989) 113–130.
7 J. A. Bietz and T. Burnouf, *Theor. Appl. Genet.*, 70 (1985) 599–609.
8 J. A. Bietz and F. R. Huebner, in R. Lasztity and F. Bekes (Editors), *Proceedings of the 3rd International Workshop on Gluten Proteins*, World Scientific, Singapore, 1987, pp. 413–427.
9 M. G. Scanlon, H. D. Sapirstein and W. Bushuk, *Cereal Chem.*. 66 (1989) 439–443.
10 H. D. Sapirstein and W. Bushuk, *Cereal Chem.*, 62 (1985) 372–377.
11 J. C. Autran and P. Abbal, *Electrophoresis*, 9 (1988) 205–213.
12 D. Bertrand, P. Robert and W. Loisel, *J. Sci. Food Agric.*, 36 (1985) 1120–1124.
13 D. Bertrand, P. Courcoux, J. C. Autran, R. Meritan and P. Robert, *J. Chemometr.*, 4 (1990) 143–151.
14 B. A. Marchylo, D. W. Hatcher and J. E. Kruger, *Cereal Chem.*, 65 (1988) 28–40.
15 Y. Popineau and F. Pineau, *Lebensm. Wiss. Technol.*, 18 (1985) 133–135.
16 Y. Popineau and F. Pineau, *J. Cereal Sci.*, 3 (1985) 363–368.
17 G. L. Lookhart and L. D. Albers, *Cereal Chem.*, 65 (1988) 222–227.
18 G. Branlard and M. Dardevet, *J. Cereal Sci.*, 3 (1985) 329–343.
19 J. C. Autran and A. Bourdet, *Ann. Amelior. Plantes*, 25 (1975) 277–301.
20 S. Endo, K. Okada, S. Nagao and B. L. D'Appolonia, *Cereal Chem.*, 67 (1990) 480–485.

Journal of Chromatography, 596 (1992) 233–239
Elsevier Science Publishers B.V., Amsterdam

CHROM. 23 982

Determination of 7-methylbenz[*c*]acridines by capillary gas chromatography with electron-capture detection

Kunihiro Kamata*

Metropolitan Research Laboratory of Public Health, 24–1, Hyakunin-cho 3-chome, Shinjuku-ku, Tokyo 169 (Japan)

Noboru Motohashi

Department of Medicinal Chemistry, Meiji College of Pharmacy, 1–22–1, Yato-cho, Tanashi-shi, Tokyo 188 (Japan)

Roger Meyer

Herbert Laboratories, 2525 Dupont Drive, Irvine, CA 92715 (USA)

Yutaka Yamamoto

Department of Medicinal Chemistry, Tohoku College of Pharmacy, 4–4–1, Komatsushima, Aoba-ku, Sendai 981 (Japan)

(First received September 2nd, 1991; revised manuscript received December 30th, 1991)

ABSTRACT

A sensitive gas chromatographic procedure for the determination of 7-methylbenz[*c*]acridines (7-methyl-BAcs) is presented. The 7-methyl-BAcs are easily oxidized to 7-formylbenz[*c*]acridines (7-formyl-BAcs) with periodic acid in dimethyl sulfoxide. The 7-formyl-BAcs are then reacted directly with *p*-fluoroaniline by way of Schiff base formation. The Schiff bases are analyzed by gas chromatography using a 25-m HP-5 column with electron-capture detection. The electron-capture response for the Schiff bases is very sensitive and amounts down to 20 pg are easily detected. Mass spectral data for the Schiff bases obtained under electron inpact conditions are also presented.

INTRODUCTION

The analytical study of 7-methylbenz[*c*]acridines (7-methyl-BAcs) has received considerable interest as a number of these compounds, such as 7-methylbenz[*c*]acridine and 7,10-dimethylbenz[*c*]acridine, are known carcinogens in some experimental animals and are suspected carcinogens or mutagens in other species [1–5]. 7-Methyl-BAcs have been identified in a wide variety of sources, such as tobacco smoke [6,7], automobile exhausts [8,9], coal liquefaction products [10,11], petroleum products [12,13], shale oil [14], creasote oil [15], coal tar [16,17] and lake [18] and marine sediments [19]. The determination of 7-methyl-BAcs in these samples has proved to be difficult because of their low concentrations and because the widely varying samples contain a vast number of potentially interfering compounds. Analytical techniques are required that are not only extremely sensitive but also highly selective.

The determination of 7-methyl-BAcs has been carried out by different chromatographic techniques, including high-performance liquid chromatography [6,20–25] and gas chromatography (GC) [6,9,10,13,16–21,26–28]. With the latter, the best separations of 7-methyl-BAcs are achieved with capillary column GC. Generally, successful GC

0021-9673/92/$05.00

methods have used flame ionization (FID) or nitrogen-specific detection (N-FID). Although these methods are routinely used, they lack the sensitivity required for many environmental samples.

GC with electron-capture detection (ECD) has been demonstrated to be a very sensitive tool for the determination of low concentrations of a variety of compounds. Compounds with low or no electron-capture response can usually be made electron-capture sensitive by means of derivatization. However, in order to detect 7-methyl-BAcs by ECD, it is necessary to employ a derivatizing agent with the desired detectable functionality.

The purpose of this paper is to demonstrate the selectivity and highly sensitive detection of 7-methyl-BAcs by GC–ECD. It was found that the method presented here is over 100 times more sensitive than the N-FID method for the determination of 7-methyl-BAcs. Resolution differences of the Schiff bases in capillary columns with three different stationary phases are discussed. The mass spectral data for the 7-methylbenz[*c*]acridine oxide (formyl type) and Schiff base forms obtained with electron impact (EI) ionization are also presented.

EXPERIMENTAL

Materials

The following 7-methyl-BAcs were synthesized according to the literature and purified as described [20]: 7-methylbenz[*c*]acridine, 5,7-dimethylbenz[*c*]-acridine, 7,9-dimethylbenz[*c*]acridine, 7,10-dimethylbenz[*c*]acridine, 7,11-dimethylbenz[*c*]acridine, 7,9,10-trimethylbenz[*c*]acridine and 7,9,11-trimethylbenz[*c*]acridine. Stock standard solutions were prepared by dissolving each 7-methyl-BAc in dimethyl sulfoxide (DMSO) to give a concentration of 100 μg/ml. Working standard solutions were prepared by diluting the stock standard solutions with DMSO.

Periodic acid, DMSO, and *p*-fluoroaniline were purchased from Nacalai Tesque (Kyoto, Japan) and 1-chloro-9,10-diphenylanthracene (used as an internal standard) from Aldrich (Milwaukee, WI, USA). The internal standard solution for GC–ECD was prepared by dissolving 1.0 μg of 1-chloro-9,10-diphenylanthracene in 1 ml of methanol. Solvents used were of analytical-reagent grade.

Derivatization procedure

Periodic acid (30 mg) was added to a 2.0-ml aliquot of the DMSO solution (0.02–10 μg of each 7-methyl-BAc) in a 10-ml reaction vial. The reaction was allowed to proceed for 50 min at 100°C and, after cooling, the solution was transferred into a 200-ml separatoring funnel with 50 ml of water. To the separating funnel 5 ml of 0.05 *M* sodium thiosulfate was added and then the contents were back-extracted twice with 50-ml portions of diethyl ether with vigorous shaking for 5 min. The combined diethyl ether portion was washed with 25 ml of water, transferred into a round-bottomed flask and evaporated to dryness at 40°C under reduced pressure in a rotary evaporator. After addition of 2 ml of a methanolic solution of *p*-fluoroanaline (1 mg/ml), the solvent mixture was evaporated to dryness at 40°C. The flask was then heated for 20 min at 60°C. After cooling, 1 ml of the internal standard solution was added to the reaction mixture. The mixture was then analyzed by GC–ECD under the described conditions.

Gas chromatography (GC)

GC was carried out on a Varian Model 3600 gas chromatograph equipped with a ^{63}Ni electron-capture detector and a thermionic specific detector. The column was a 25 m × 0.2 mm I.D. fused-silica capillary coated with HP-5 (Hewlett-Packard) at a film thickness of 0.33 μm. The injector temperature was 300°C. A 1-μl volume of the reaction mixture was injected (splitless) at a detector temperature of 350°C and an oven temperature of 280°C. Helium as carrier gas at a flow-rate of 2.0 ml/min and nitrogen as make up gas at a flow-rate of 20 ml/min were used. The GC–thermionic specific detection (TSD) conditions were the same as the GC–ECD conditions except that the make-up gas was helium.

Gas chromatography–mass spectrometry (GC–MS)

EI ionization mass spectra were obtained on an Automass 50 mass spectrometer (JEOL) interfaced with a Hewlett-Packard Model 5890 gas chromatograph. The operating conditions for all GC–EI-MS experiments were as follows: electron energy, 70 eV; filament emission current, 0.3 nA; source temperature, 140°C; injection port temperature, 280°C; column, HP-1 (25 m × 0.2 mm I.D.), 0.33-μm film thickness; initial column temperature, 230°C for 2

min, increased at 10°C/min to a final temperature of 300°C, held for 20 min; carrier gas, helium at a flow-rate of *ca.* 1 cm^3/min.

RESULTS AND DISCUSSION

Buu-Hoi *et al.* [29] found that selenium dioxide oxidation was specific for the conversion of a methyl group at the *meso*-position into a formyl group with excellent yields. For instance, 7-methyl-, 7,9-dimethyl- and 7,9,10-trimethylbenz[*c*]acridine readily formed 7-formylbenz[*c*]acridine (64% yield), 7-formyl-9-methylbenz[*c*]acridine (50% yield) and 7-formyl-9,10-dimethylbenz[*c*]acridine (45% yield), respectively. However, these reactions require a higher yield for analytical techniques. Seven oxidation reagents (selenium dioxide, periodic acid, potassium dichromate, vanadium pentoxide, potassium permanganate, copper oxide and hydrogen peroxide) were tested for the conversion of 7-methyl-BAcs into 7-formyl-BAcs. Each yield of 7-formyl-BAc using these oxidation reagents was determined by integrating the GC–TSD area counts. It was found that the best yield of 7-formyl-BAcs was obtained by oxidation with periodic acid, and this reagent was able to attack only the methyl group on position 7. The benz[*c*]acridines without a 7-methyl group, such as benz[*c*]acridine, 8-methylbenz[*c*]-acridine, 9-methylbenz[*c*]acridine, 10-methylbenz[*c*]acridine and 11-methylbenz[*c*]acridine, are not oxidized by periodic acid.

Further, eleven organic solvents (DMSO, methanol, chloroform, hexane, tetrahydrofuran, acetonitrile, acetone, N,N-dimethylformamide, carbon tetrachloride, carobn disulfide and 1,4-dioxane) were tried to determine the differences of the reaction system in each solvent. The result was that DMSO proved to be the best solvent in periodic acid oxidation. The combination of periodic acid and DMSO to convert 7-methyl-BAcs to 7-formyl-BAcs gave essentially 100% yields.

The relationship between the amount of periodic acid in DMSO and yield of 7-formyl-BAcs was examined by changing the concentration from 0.01 to 100 mg per 10 μg of 7,9,11-trimethylbenz[*c*]acridine. Of all compounds tested, 7,9,11-trimethylbenz[*c*]acridine proved to be the most difficult to oxidize in this manner. The yield of 7-formyl-9,11-dimethylbenz[*c*]acridine increased with increasing strength of the periodic acid (between 0.01 and 20 mg) but the increased values became constant in the range 20–100 mg. From these results, the actual amount of periodic acid was chosen to be 30 mg. Fig. 1 shows the effects of the reaction time and reaction temperature on the yield of 7-formyl-9,11-dimethylbenz[*c*]acridine (the reaction time was shortened with increase in reaction temperature). Therefore, the reaction temperature and time adopted were 100°C and 50 min, respectively.

The reaction of aldehydes to form 2,4-dinitrophenylhydrazones is widely used in carbonyl group analysis, which can be followed by GC–FID [30] and GC–ECD [31,32]. The reaction between 2,4-dinitrophenylhydrazine and carbonyl compounds is extremely specific. Schiff base (2,4-dinitrophenylhydrazone) formation by aldehydes is very easy but the resulting solubility of the base is low in many solvents. In spite of the poor solubility, Schiff bases give two peaks in GC. The coupling reaction of aniline with an aldehyde forms a Schiff base in high yield. Because GC–ECD is much more sensitive to

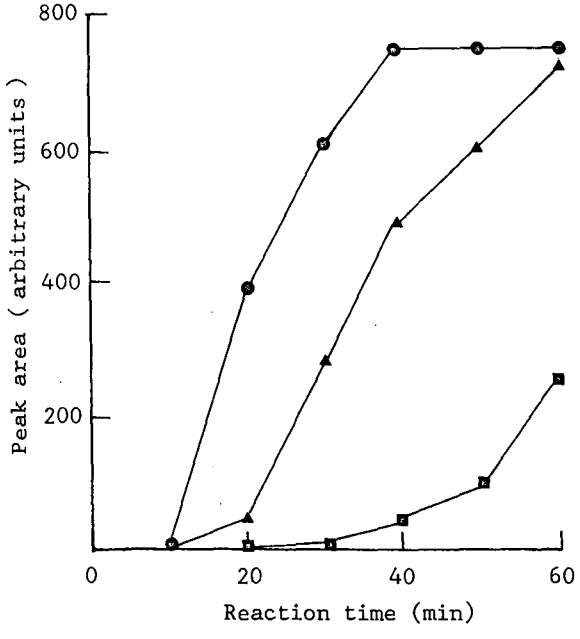

Fig. 1. Effect of reaction time and reaction temperature on the oxidation product after addition of periodic acid to 7,9,11-trimethylbenz[*c*]acridine in DMSO. To 10 μg of 7,9,11-trimethylbenz[*c*]acridine were added 30 mg of periodic acid in 2 ml of DMSO and the product was analyzed by GC–TSD, (●) at 100°C, (▲) at 80°C and (■) at 60°C.

the fluoro compounds than non-fluoro compounds, the use of fluorinated Schiff bases makes it possible to determine these compounds with much lower detection limits. In this work, *p*-fluoroaniline was chosen as a derivatizing agent to form Schiff bases with 7-formyl-BAcs. The reaction of 7-formyl-BAcs with *p*-fluoroanaline easily gives a Schiff base.

To improve the reaction efficiency of Schiff base formation with 7-formyl-BAcs and *p*-fluoroanaline, reaction times and temperatures were investigated. The reaction efficiency could be improved by increasing both the reaction time and the reaction temperature. However, the presence of solvent during the reaction resulted in a poor yield. Therefore, the solvent was first evaporated to dryness at 40°C and then formation of the Schiff base was carried out at 60°C for 20 min. The relationship between *p*-fluoroaniline concentration and yield of Schiff base with 7-formyl-BAcs was examined by varying the amount of *p*-fluoroaniline between 0.1 and 5.0 mg for amounts of 7-formyl-BAcs corresponding to 10 μg of 7-methyl-BAcs. The yield of Schiff base increased with increasing amount of *p*-fluoroaniline (0.1–1.0 mg), but remained constant in the range 1.0–5.0 mg. Consequently, the amount of *p*-fluoroaniline chosen was 2.0 mg.

The use of *p*-fluoroaniline with the Schiff base of 7-formyl-BAcs led to orders of magnitude greater sensitivity and selectivity when coupled with ECD. Whereas nanogram amounts can be determined using GC–TSD, amounts about 100 times lower can only be determined using GC–ECD.

The Schiff bases were very stable under normal laboratory conditions and no thermal decomposition products were observed in the GC analysis.

The structure of each Schiff base was confirmed by GC–MS. The mass spectra of 7-methylbenz[*c*]acridine, 7-formylbenz[*c*]acridine and the Schiff base are shown in Fig. 2. The mass spectrum corresponding to the peak obtained by oxidation of 7-methylbenz[*c*]acridine is shown in Fig. 2B with ion peaks of *m/z* 257 (M^+) and 229 $[M-28]^+$. The parent peak is at *m/z* 243 for 7-methylbenz[*c*]acridine (see Fig. 2A) and at *m/z* 257 for 7-formylbenz[*c*]acridine. All 7-formyl-BAcs generally produced the same prominent fragmentation pattern and each mass spectrum was dominated by a single unique $[M-28]^+$ fragment ion in the high-molecular-weight region.

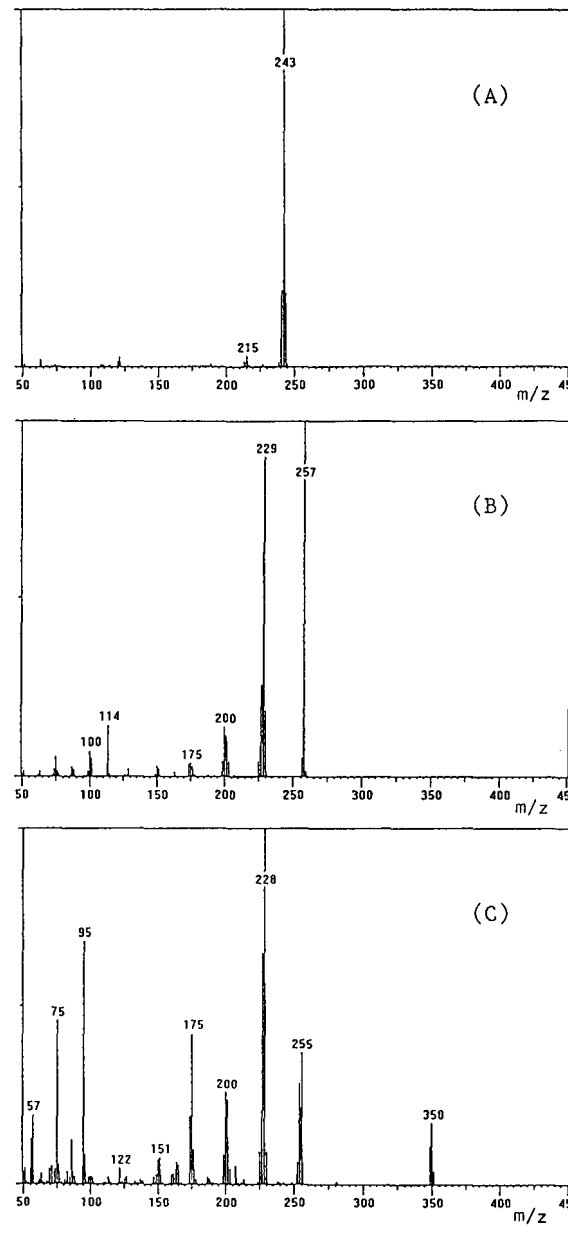

Fig. 2. EI mass spectra of (A) 7-methylbenz[*c*]acridine, (B) its oxidation product (7-formylbenz[*c*]acridine) and (C) its Schiff base.

In relation to the reaction mechanism of benzaldehyde, MacCollum and Meyerson [33] studied its synthesis with labelled-deuterium and Natalis and Franklin [34] measured the energetic values. They both concluded that the direct loss of the aldehyde

substituent with retention of charge on the fragment with oxygen occurs only to a small extent, just like the removal of carbon monoxide (CO) from the molecular ion to give $[C_6H_6]^+$ (*m/z* 78). From their conclusions, for instance, 7-formylbenz[*c*]acridine similarly showed that the $[M-28]^+$ fragment ion was formed by removal of one carbon monoxide function from 7-formylbenz[*c*]acridine. From the peak at *m/z* 229, $[M-CO]^+$, it was concluded that the product, 7-formylbenz[*c*]acridine, has a formyl substituent.

The mass spectrum corresponding to the peaks of the Schiff base is shown Fig. 2C. The molecular ion peak (M^+) with postulated *m/z* 350 and the prominent fragment ion peaks, *m/z* 255, $[M-95]^+$, and 228, $[M-122]^+$, were observed and were useful for structure assignments. The *m/z* 255 fragment ion was assigned as loss of the fluorobenzene radical, $C_6H_4F\cdot$, from the molecular ion. The base peak at *m/z* 228, $[C_{17}H_{10}N]^+$, came from the molecular ion by dissociation of $CHN-C_6H_4F$.

The proposed reaction mechanism for 7-methylbenz[*c*]acridine is shown in Fig. 3.

The chromatographic resolution of the Schiff bases was attempted on capillary columns with three different stationary phases (DB-17, HP-5 and HP-1). The retention times for seven Schiff bases on the three columns are given in Table I. All the columns were found to be suitable for the analysis of Schiff bases, but the less polar HP-1 and HP-5 columns were better than the DB-17 column. The elution order of Schiff bases was the same on all three columns. The HP-1 and HP-5 columns have similar

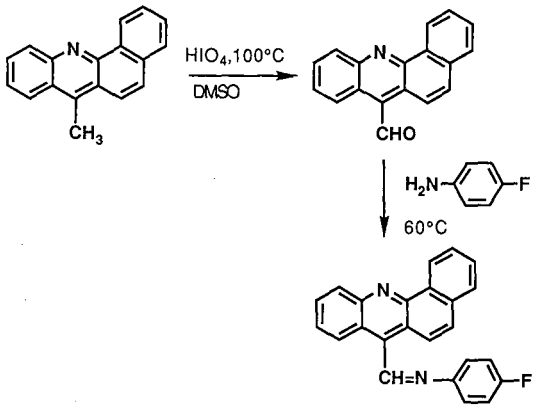

Fig. 3. Oxidation of 7-methylbenz[*c*]acridine by periodic acid and its Schiff base.

TABLE I

RETENTION TIMES OF SCHIFF BASES OF 7-METHYLBENZ[*c*]ACRIDINES ON THREE CAPILLARY COLUMNS

7-Methylbenz[*c*]acridine	Retention time (min)		
	HP-1[a]	HP-5[b]	DB-17[c]
7-Methylbenz[*c*]acridine	24.71	23.66	35.23
5,7-Dimethylbenz[*c*]acridine	31.27	28.79	42.80
7,9-Dimethylbenz[*c*]acridine	29.07	27.60	39.58
7,10-Dimethylbenz[*c*]acridine	31.90	30.22	42.86
7,11-Dimethylbenz[*c*]acridine	28.52	26.91	37.77
7,9,10-Trimethylbenz[*c*]acridine	41.64	39.22	57.25
7,9,11-Trimethylbenz[*c*]acridine	33.08	30.85	41.49

[a] 25 m × 0.20 mm I.D.; column temperature 270°C.
[b] 25 m × 0.20 mm I.D.; column temperature 280°C.
[c] 30 m × 0.25 mm I.D.; column temperature 280°C.

TABLE II

LINEAR REGRESSION DATA FOR SCHIFF BASES OF 7-METHYLBENZ[*c*]ACRIDINES

7-Methylbenz[*c*]acridine	Linear range of calibration graph (μg)	Linear equation of regression line[a]	Linearity (*r*)
7-Methylbenz[*c*]acridine	0.05–0.50	$y = 7.498x - 0.041$	0.9970
5,7-Dimethylbenz[*c*]acridine	0.05–0.50	$y = 8.580x + 0.001$	0.9992
7,9-Dimethylbenz[*c*]acridine	0.05–0.50	$y = 9.063x + 0.006$	0.9997
7,10-Dimethylbenz[*c*]acridine	0.05–0.50	$y = 7.533x + 0.014$	0.9998
7,11-Dimethylbenz[*c*]acridine	0.05–0.50	$y = 5.297x + 0.012$	0.9997
7,9,10-Trimethylbenz[*c*]acridine	0.05–0.50	$y = 8.643x + 0.181$	0.9958
7,9,11-Trimethylbenz[*c*]acridine	0.05–0.50	$y = 6.593x - 0.056$	0.9973

[a] y = Peak-area ratio; x = amount of 7-methylbenz[*c*]acridine.

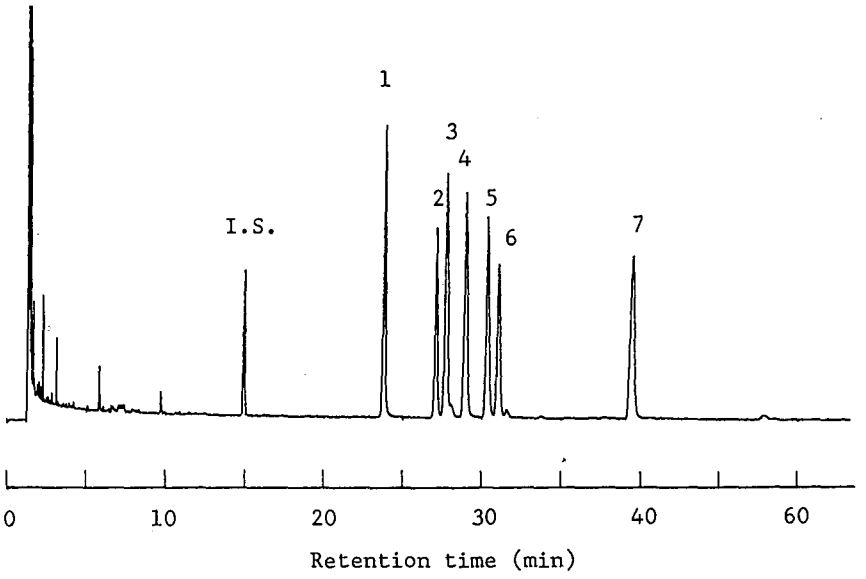

Fig. 4. GC–ECD of the Schiff bases of 7-methylbenz[*c*]acridine on the HP-5 column. For GC conditions, see Experimental. Peaks: 1 = 7-methylbenz[*c*]acridine; 2 = 7,11-dimethylbenz[*c*]acridine; 3 = 7,9-dimethylbenz[*c*]acridine; 4 = 5,7-dimethylbenz[*c*]acridine; 5 = 7,10-dimethylbenz[*c*]acridine; 6 = 7,9,11-trimethylbenz[*c*]acridine; 7 = 7,9,10-trimethylbenz[*c*]acridine; I.S. = 1-chloro-9,10-diphenylanthracene (internal standard).

resolving powers, the Schiff bases of 7-formyl-9-methylbenz[*c*]acridine and 7-formyl-11-methylbenz[*c*]acridine showed better resolution on the HP-5 than on the HP-1 column.

A typical chromatogram of seven Schiff bases is shown in Fig. 4. Each Schiff base displayed a single, symmetrical peak.

In order to test the linearity of the calibration graph, different amounts of 7-methyl-BAcs were prepared as previously described. A linear relationship was confirmed and the reproducibility was found to be satisfactory (Table II). The detection limit of 7-methyl-BAcs in this procedure was 20 pg (signal-to-noise ratio = 2).

CONCLUSION

An improved method for the determination of 7-methyl-BAcs by GC–ECD based on Schiff bases formed by the reaction of 7-formyl-BAcs with *p*-fluoroaniline was established. This method is satisfactory for the sensitive and selective determination of 7-methyl-BAcs.

REFERENCES

1 A. Laccasagne, N. P. Buu-Hoi, R. Daudel and F. Zajdela, *Adv. Cancer Res.*, 4 (1956) 315.
2 A. Laccasagne, N. P. Buu-Hoi, F. Zajdela, N. B. Giaao, P. Jacquignon and M. Dufour, *C. R. Acad. Sci., Ser. D*, 267 (1968) 981.
3 C. Liebermann, P. Lazar, I. Chouroulinkov and M. Guerin, *C. R. Seances Soc. Biol. Ses Fil.*, 162 (1968) 835.
4 B. A. Walker, E. G. Rogan and N. H. Cromwell, *Anticancer Res.*, 4 (1984) 399.
5 D. Papadsopoulo, S. Levy, V. Poirier, C. Pene, P. Markovits and M. Hurbert-Habart, *Eur. J. Cancer*, 17 (1981) 179.
6 M. E. Snook, P. J. Fortson and O. T. Cbortyk, *Beitr. Tabakforsch. Int.*, 11 (1981) 67.
7 G. Grimmer, K.-W. Naujack and G. Dettbarn, *Toxicol. Lett.*, 35 (1987) 117.
8 T. Handa, T. Yamauchi, K. Sawai, T. Yamamura, Y. Koseki and T. Ishii, *Envison. Sci. Technol.*, 18 (1984) 895.
9 P. T. Williams, K. D. Bartle and G. E. Andrews, *Fuel*, 65 (1986) 1150.
10 D. W. Later, R. A. Pelory, D. D. Mahlum, C. W. Wright, M. L. Lee, W. C. Weimer and B. W. Willson, in M. Cooke and A. J. Dennis (Editors), *Polynuclear Aromatic Hydrocarbons: Formation, metabolism and measurement*, Battelle Press, Columbus, OH, 1983, p. 771.
11 J. R. Kershaw, *Fuel*, 62 (1983) 1430.

12 J. F. McKay, J. H. Weber and D. R. Latham, *Anal. Chem.*, 48 (1976) 891.
13 G. Grimmer and K.-W. Naujack, *Fresenius' Z. Anal. Chem.*, 321 (1985) 27.
14 R. A. Pelory and M. R. Petersen, *Environ. Health Perspect.*, 30 (1979) 191.
15 N. Motohashi, K. Kamata and R. Meyer, *Environ. Sci. Technol.*, 25 (1991) 342.
16 P. Burchill, A. A. Herod, J. P. Mahon and E. Pritchard, *J. Chromatogr.*, 265 (1983) 223.
17 J. C. Lauer, D. H. Valles and D. Cagniant, *Fuel*, 67 (1988) 1446.
18 S. G. Wakeham, *Environ. Sci. Technol.*, 13 (1979) 1118.
19 C. A. Krone, D. G. Burrows, P. A. Robisch, A. J. Friedman and D. C. Mallns, *Environ. Sci. Technol.*, 20 (1986) 1144.
20 N. Motohashi and K. Kamata, *Yakugaku Zasshi*, 103 (1983) 795.
21 K. Kamata and N. Motohashi, *J. Chromatogr.*, 319 (1985) 331.
22 T. Yamauchi and T. Handa, *Environ. Sci. Technol.*, 21 (1987) 1177.
23 H. Colin, J.-H. Schmitter and G. Guiochon, *Anal. Chem.*, 53 (1981) 625.
24 A. M. Siouffi, M. Righezza and G. Guiochon, *J. Chromatogr.*, 368 (1986) 189.
25 K. Kamata and N. Motohashi, *J. Chromatogr.*, 498 (1990) 129.
26 G. Grimmer and K.-W. Naujack, *J. Assoc. Off. Anal. Chem.*, 69 (1986) 537.
27 M. L. Lee, D. L. Vassilarros, C. M. White and M. Novotny, *Anal. Chem.*, 51 (1979) 768.
28 J. M. Schmitter, I. Ignatiadis and G. Guiochon, *J. Chromatogr.*, 248 (1982) 203.
29 N. P. Buu-Hoi, M. Dufour and P. Jacquignon, *J. Chem. Soc.*, 5622 (1964).
30 K. Korolczuk, M. Daniewski and Z. Mielniczuk, *J. Chromatogr.*, 88 (1974) 177.
31 H. Kallio, R. R. Linko and J. Kaitaranta, *J. Chromatogr.*, 65 (1972) 355.
32 Y. Hoshika and Y. Takata, *J. Chromatogr.*, 120 (1976) 379.
33 J. D. McCollum and S. Meyerson, *J. Am. Chem. Soc.*, 85 (1963) 1739.
34 P. Natalis and J. L. Franklin, *J. Phys. Chem.*, 69 (1965) 2943.

Journal of Chromatography, 596 (1992) 241–249
Elsevier Science Publishers B.V., Amsterdam

CHROM. 23 968

Important design features of a system for the densitometric analysis of two-dimensional flat-bed separations

Victor A. Pollak

Department of Electrical Engineering, University of Saskatchewan, Saskatoon, Saskatchewan S7N 0W0 (Canada)

Arno Doelemeyer and Wolfgang Winkler

RWTH Aachen, Lehrstuhl für Messtechnik, Templergraben 55, 5100 Aachen (Germany)

Jörg Schulze-Clewing*

Electrical Engineering Consultant, Gerhart-Hauptmann-Strasse 21, 5653 Leichlingen 1 (Germany)

(First received October 10th, 1991; revised manuscript received December 18th, 1991)

ABSTRACT

Densitometric instruments for the analysis of one-dimensional separations employ almost universally electromechanical scanning systems. Electronic scanning has been almost universally adopted for two-dimensional work. This permits the incorporation of a number of important features which an electromechanical system cannot provide. Some of these features are specific for densitometric equipment and are not needed in other applications, and these features are discussed. Modern image processing theory was applied to densitometry and densitometry analysis of two-dimensional flat-bed separations with emphasis on electrophoresis. The described features and techniques were implemented and tested on an experimental system. Only the software aspects of that system are discussed here.

INTRODUCTION

Two-dimensional (2D) electrophoresis can provide extremely high separating powers and it is therefore mainly applied to the analysis of multi-component solutions [1]. Techniques for the examination and interpretation of the resulting separations are the focus of the initial part of this paper. Most of the discussion applies also to 2D thin-layer chromatography (TLC), although the techniques are little used in practice.

DENSITOMETRIC ASSESSMENT

Analysis of proteins, nucleotides and other complex biological substances is one of the most significant applications of 2D electrophoresis. A high-resolution electrophoretic separation may result in hundreds and even thousands of spots. Evaluation by visual inspection is then an extremely tedious and error-prone endeavour. Quantification manually with any degree of accuracy is almost impossible and computer analysis is required. The main aim of this paper is to discuss the most important features that such a system should exhibit and to describe an experimental system for implementing these features at reasonable cost.

Optical densitometry is the technique commonly used to acquire input data for the analysis. The scanning of 2D separations necessitates a number of

0021-9673/92/$05.00

features usually not found in instruments primarily designed for one-dimensional (1D) work [2]. The differences are discussed below.

The approach adopted is to regard a 2D separation as a picture and to utilize modern techniques of image processing [3]. This approach can be extended also to the analysis of 1D separations, but is of little advantage here, mainly because most current 1D densitometers employ "slit scanning" instead of "point scanning" [4].

The spatial resolution of a scanning system is determined by the number of measured data points (pixels) per unit image area. The resolution of most standard video scanners may not be sufficient for high-grade work and special designs may have to be used. Another drawback of most standard devices is an unequal resolution between the x- and y-directions. Very important is a linear grey scale of the sensor, the gamma factor of which should be unity. Gamma is the ratio of scanner output signal to the logarithm of light energy per unit area, differentially ($\gamma = \Delta u_{out}/\Delta \log E$).

Processing of the acquired input data is inevitably done on a computer, which mostly is an integral component of the analysis system. The most cost-effective solution is to use a modern microcomputer, the performance of which rivals that of mainframe computers of a decade ago at a fraction of the cost. The processing software has to be tailored to the machine employed, because programs are rarely transferrable from one type of machine to another.

IMAGE SENSORS

The most important part of an electronic picture acquisition system is the video camera and its main element, the image sensor. Semiconductor area sensors, mostly charge-coupled devices (CCDs; Fig. 1a), are currently the most cost-effective solution [5,6]. They are available with up to 1300 × 1000 pixels per device [7]. Such area sensors provide a linear resolution of up to 200 μm on a 200 mm × 200 mm object. When that is still insufficient, CCD line sensors (Fig. 1b) can be employed. They are available with more than 5000 elements in a row, yielding a linear resolution of better than 40 μm on an object plane of 200 mm × 200 mm (many suppliers, *e.g.*, Philips, Thomson-CSF, Toshiba). The resolution obtainable on smaller substrates is

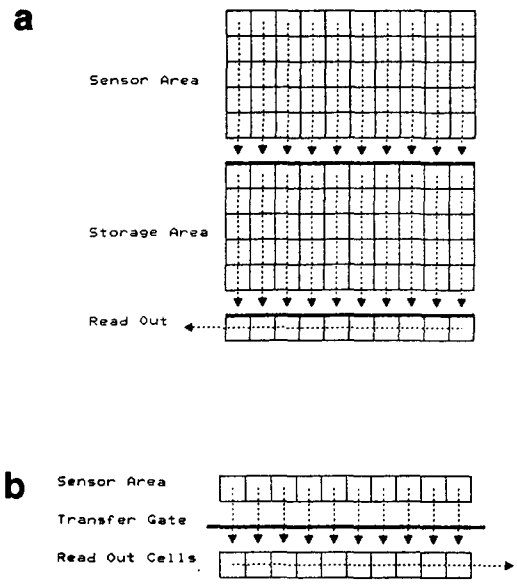

Fig. 1. (a) Disposition of a CCD area sensor with square sensing elements. During the exposure each element accumulates an amount of charge proportional to the intensity and time of illumination. The accumulated charges are usually transferred into a storage area and are then sequentially fed out line by line into an amplifier, where the charge is converted to a voltage signal. (b) Disposition of a CCD line sensor. At a given instant in time only one line of scanned image is sensed. When the charge packages are fed out, the sensor is displaced mechanically to scan the next line.

proportionally higher. Higher values than those quoted above are rarely warranted in this field. The main reason is the inevitable contamination of the background by small amounts of unwanted "garbage", which is difficult to distinguish from small spots of analysed material.

It should be noted that the practical resolution of a camera set-up is below the spatial distance of the pixels. The reason is that the modulation transfer function (MTF), a dynamic parameter, restricts the usable resolution to about 60% of the nominal value. A detailed explanation is beyond the scope here but can be found in the literature [8].

In some special cases, the available resolution can be increased by dividing the scanned image into segments which are acquired independently and then recombined in software. Another approach to raising the resolution that has proved viable is to scan the image, then to displace the sensor by half the distance between two of its neighbouring pixels

and to scan again. This displacement is usually performed by a simple piezo transducer which provides a small shift of half a pixel width with sufficient accuracy. However, the additional cost of these options is rarely warranted in systems for routine work.

When comparing line sensors with area sensors, cost and reliability are the main issues. Unless extremely high resolution is required, area sensors are generally preferable in both respects. The main advantages of line scanners, apart from their higher resolution, are simpler interfacing to the processing computer and a lower demand on its memory space. These advantages are generally more than outweighed by a significantly more complex mechanical and optical system.

MULTISPECTRAL SCANNING

Scanning at different wavelengths is an important aid for qualitative analysis. When CCD scanners are employed, the best approach to multi-spectral scanning is repeated exposure at different wavelengths of illumination. Filters or monochromators can be used to vary the sensed wavelength [2,9]. The additional time is negligible but the demand on memory space is considerable and increases the cost of the system.

The ease and speed with which spectral analysis can be carried out by electronic scanners promise to widen the field of applications of this technique. The spectral sensitivity of solid-state sensors ranges far into the infrared. This spectral range may become a useful extension of the currently used wavelengths in analysis.

LASER SCANNING

Still higher resolution than that which line sensors offer is rarely needed or even desirable. In the rare cases where still higher values are needed (*e.g.*, in some research applications), they are best achieved by laser scanning [10]. Here the scanning beam is deflected in both the x- and y-directions by mechanical or optical means. The deflecting mechanism must be built to very close tolerances, which increases the cost of the design. Also, the data acquisition time is very long. Another drawback is the fixed wavelength of all less expensive lasers. At low concentrations it is highly desirable that the operating wavelength of the densitometer coincides with the absorbance maximum of the investigated material. Laser scanners do not provide this option and are not suitable for spectral analysis.

UV SENSITIVITY

Silicon-based area sensors and line sensors are not very sensitive to UV radiation. However, sensitivity in the UV region is advantageous in many applications. Fundamental physical reasons have so far prevented the extension of the spectral sensitivity of CCD sensors into the UV region but an indirect method is possible by coating CCD sensors with a down-converting phosphor which shifts their range of sensitivity far into the UV region [11–13]. Unfortunately, the demand for UV-sensitive CCD sensors has not yet justified the large-scale production of phosphor-coated devices, which are therefore very expensive.

Another approach is the use of an image intensifier with an extended UV response in conjunction with CCD scanning. The sensitivity of the instrument is thereby significantly increased but at the price of a lower spatial resolution.

In the future, another option might be the use of pyroelectric sensors [14]. These are effectively heat sensors and their spectral sensitivity curve easily covers the whole range of wavelengths which are employed in the densitometric analysis of flat-bed separations. However, with the present state of technology the sensitivity and the spatial resolution of this type of sensor are inferior when compared with standard silicon-based CCD sensors.

OTHER HARDWARE CONSIDERATIONS

Most modern densitometers use a built-in computer as an integral part of the hardware. Often the machine serves for both the data acquisition and the subsequent analysis. An AT-class computer is mostly sufficient and leads to significant cost savings when compared with custom designs.

Many of the operations involved are fairly memory intensive. The machine selected should therefore have a sufficiently large memory bank and use a modern operating system that can handle the whole amount of memory directly. The software employed

must match the machine and its operating system. Portability of the software from one type of machine to another can rarely be assured. This caveat applies still more to specially designed hardware. Hard disks with a very large storage capacity (120 Mbyte or more) or in the extreme optical disks can be used as a data base, so that the results are available for future reference. Another quality criterion for large installations is the ability to link the complete system to an existing network such as an IEEE-488 net or higher speed links. All these devices are available at moderate cost.

PREPROCESSING

The processing operations can be divided into two functional stages. The first, the "preprocessing" stage, treats data from individual small areas as separate entities not related to data from other areas. Stage two then has the purpose of providing global information pertaining to the separation in its entirety. In many less sophisticated applications, preprocessing yields sufficient information. Only this stage will be considered here in depth. Final processing is too much application dependent to be covered in this paper.

The main operations carried out by the preprocessing stage are the following. The measured optical signals are made up of two components, one due to the optical response of the blank medium and the other to the response increment caused by the presence of separated material when a spot area is encountered. Only the latter component is useful, but its separation from the background is not always easy, because at larger concentration densities of the analyte the two components have a non-linear relationship. However, even when this non-linearity is small enough to be discounted, there are problems in isolating the response component due to the separated substance. However, the background response generally varies spatially in a random fashion, giving rise to what is called "background noise". For good accuracy and/or high sensitivity it is then necessary to take this variability into account. If the separated substance has a relatively narrow absorbance spectrum, two-wavelength (two-λ) scanning is probably the best technique for that purpose [15]. The method is described later. It is not very useful when the analyte has a broad absorbance spectrum, *e.g.*, in silver-stained protein separations. It may then be necessary to apply special techniques of signal processing.

Preprocessing can obviously be performed in many different ways, but the procedure described below seems to be both simple and efficient. Its structural organization is fairly typical although details of implementation may vary. It was adopted for the experimental system described below and performed in most respects equally well as and even better than some much more costly commercial systems used for comparison.

MEASURING MODES IN DENSITOMETRY

The first step in preprocessing is the segmentation of the picture into spotted and blank areas. High-frequency noise and other spurious signals have to be reduced to a minimum for a successful segmentation.

In the described system, a size threshold was employed to distinguish between contaminant noise and analyte signal. For partial elimination a two-step filter algorithm was used. It employs first a wide-band two-dimentional mask, then a narrow-band mask with median weighting. The mask sizes and the weighting laws were established empirically.

A special technique used fairly extensively in electrophoresis is autoradiography. Here it is also common not to examine the original separation but a photographic replica on transparent film. For quantitative analysis it is then necessary to take the gradation characteristics of the film into account.

A relatively new technique is photoacoustic spectroscopy. This holds some promise for special applications but has not yet found much acceptance in densitometry.

A detailed discussion of all these techniques and their limitations would exceed the scope of this paper. The interested reader is referred to the literature, *e.g.*, ref. 16.

DETERMINATION OF SPOTTED AREAS

A spot is defined as a contingent group of pixels which is spatially larger than an empirically chosen minimum. In the spot area the light attenuation exceeds the background attenuation $b_0(x,y)$ by at least a threshold ε. The implementation of these

simple relationships involves the solution of three by no means trivial tasks.

First it is necessary to find the mean value for $b_0(x,y)$, the attenuation of the blank medium. The procedure is given later. Pixels with attenuation values $b_s(x,y)$ more than ε above the mean value of $b_0(x,y)$ in the vicinity are judged to contain separated material if the criterion for a minimum number of contingent pixels is met.

SPOT BOUNDARIES

In principle, the contour is determined by the contingent sequence of pixels with response values which begin to increase from the background value $b_0(x,y)$ by ε or which begin to decrease by ε to $b_0(x,y)$:

$$b_s(x,y) \approx b_0(x,y) + \varepsilon \quad (1)$$

This simple approach does not lead to a reliable boundary detection in practice. Other popular methods involving the Laplace operator or direction-dependent masks are also unreliable. The main reason for the difficulties is the very shallow boundary zone without sharp transitions.

Therefore, another approach has been developed: the threshold ε is set to approximately twice the local Root Mean Square noise amplitude. Theoretical work [17] predicts that the boundary shape is approximately elliptical. An ellipse is then computed, meeting two conditions: the area of the ellipse must be equal to the area of all pixels with analyte in that cluster and the number of pixels that do not belong to the cluster must reach its minimum inside the ellipse. The synthetic contour is then overlayed on the screen for visual inspection (Fig. 2). More precise methods of contour estimation have been tested but the method described above has proven to be sufficient and the simplest to implement.

Theory also predicts an approximately Gaussian distribution of the concentration of separated material within a spot [17]. Provided that the noise floor and accordingly the threshold level ε are low, the loss due to pixels that are below ε does not significantly degrade the quantitative accuracy.

NOISE CONSIDERATIONS

The total noise components in a recording come from various uncorrelated sources. Usually the background noise of the blank medium contributes most significantly to the total noise and other sources of noise may then not have to be taken into account.

The next important noise mechanism is electronic noise from the sensor. The finite step size of the digitizer often presents an ultimate barrier if the sensor noise is kept to a minimum.

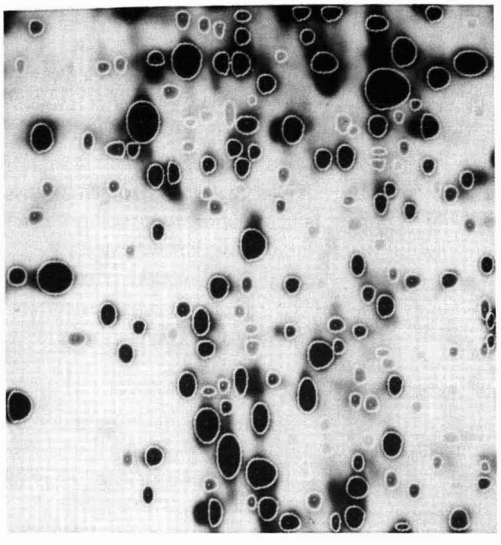

Fig. 2. Contours obtained after processing a 2D separation of cell proteins. Shown is approximately one quarter of the total picture area. Dots indicate the computed centre of gravity positions.

NOISE REDUCTION MEASURES

Low-pass filtering is a universal method and was consequently incorporated into the test system. Two stages of filtering are used, both of them employing two-dimensional masks. The first filter algorithm, with a fairly broad band pass, is mainly intended to reduce high frequency electronic noise. The second mask, with a much narrower band pass, serves for the partial elimination of background noise and other low-frequency components.

Another important feature of the system is the ability to scan the same separation repeatedly with subsequent frame averaging. This can be seen as a low-pass filter in the time domain and will only

reduce noise components that are uncorrelated in time and not those which are random in space.

The most effective method for the nearly complete elimination of background noise is the already mentioned two-lambda technique. Here the separation is scanned first at the spectral absorbance maximum of the analyte, then at a wavelength just outside its absorbance band. A pixel by pixel subtraction of the data from the two passes yields the result. The method only works if the blank medium has a flat absorbance spectrum over the range of the two wavelengths. The computational effort is not demanding.

The test system provides still another option for the reduction of background noise. Although not as efficient as the two-lambda method, it can be employed where the latter is not applicable, *e.g.* in silver-stained protein separations. The method relies on the fact that the spatial change of $b_0(x,y)$ is generally small so that for each pixel within the contour line b_0 can be approximated by linear interpolation between the values just outside the contour on both sides of the spot. For moderate demands on accuracy, the procedure can be further simplified by using the averaged value:

$$\overline{b_0(x,y_i)} \approx \tfrac{1}{2}[b_0(x_l,y_i) + b_0(x_r,y_i)] \qquad (2)$$

for all pixels on the same scan line within the spot contour, where i designates the sequential number of the respective scan line and x_l and x_r are the coordinates of the pixel on that line, which border the contour of the examined spot to the left and right, respectively.

FEATURE BASIS FOR QUALITATIVE ANALYSIS

Qualitative analysis relies to a large extent on the geometry of the spot distribution. The proposed system uses the coordinates of the centre of gravity of each spot as the characteristic feature. The determination of these parameters from the measured distribution of concentration $c(x,y)$ is computationally easy because very high accuracy is rarely needed. The quoted theory predicts an elliptical shape of the contour with the centre of gravity at the point where $c(x,y)$ and $b_s(x,y)$ reach a maximum. That maximum is generally flat and difficult to determine with any degree of accuracy. The problem can be solved with little error by replacing the coordinates of the maximum with those of the geometrical centre of the ellipse. For visual verification the centre in the experimental system is indicated on the display by a white spot. The coordinates of x_m and y_m together with the number of pixels enclosed by the contour are then considered as the characteristic set of data for each spot and compared with corresponding data from separations with known composition; x_m, y_m and the pixel counts for the individual spots are stored in long-term memory for later reference.

CORRECTION FOR GEOMETRIC DISTORTION

Evaluation of 2D separations relies very much on comparison of the examined separation with a standard or a template [18]. For this approach to provide useful results, the compared images must meet a well defined geometric correspondence. However, for reasons inherent in the separation process, the relationship between the coordinate system of individual scans can be complicated, *e.g.*, in the case of non-uniform shrinkage in the drying process. Special marker substances may be added if a substance does not contain sufficient prominent and easily identifiable components from which the geometric distortion can be computed. Constant scale differences between coordinate grids require only three markers; non-linear cases might require more markers. In the case of scale shifts the software in the test system corrects the position of the spots after the marker shifts have been identified.

QUANTIFICATION

It has to be considered that the relationship between optical response and concentration $c(x,y)$ is usually highly non-linear. Inherent linearity can only be assumed at very small values of the absorbance value $\alpha c(x,y)$, where α is the absorbance (sometimes called the extinction coefficient). Regardless of the magnitude of $\alpha c(x,y)$, a linear relationship between response and concentration can be expected for fluorescence measurements and radioassays, but for the latter only if direct measurement of the radiation is possible, which is rarely the case.

The total amount of substance in a spot is obtained by summation of $c(x,y)$ over all pixels

inside the contour. It can be seen that for a non-linear relationship between $b_s(x,y)$ and $c(x,y)$,

$$\int_A b_s(x,y) \neq \int c(x,y) \tag{3}$$

where A denotes the area for integration. It is thus evident that before summation a transform must be carried out that results in a linear relationship between the transformed response signal and the concentration.

The subject of linearization is extensively covered in the literature and a number of different transform rules have been proposed. The transform operations suggested in ref. 19 were incorporated in the software of the described test system.

For nearly transparent media such as electrophoretic gels, measurement of the optical transmittance is indicated and a logarithmic transform is then an adequate linearization operation. With strongly scattering media such as paper, transmittance is not practical and reflectance is used, and the linearizing operations are then much more involved.

STABILIZATION OF THE INTENSITY OF ILLUMINATION

Technically, the intensity of the illumination can be stabilized in different ways. The range of wavelengths required in our field is wide and therefore many densitometers are equipped with multiple light sources, each requiring an individual method of stabilization.

The system described here bypasses this difficulty by compensating for changes in the illumination intensity in the software. The intensity is measured by a separate light sensor and the output of that sensor is used by the software as a corrective scale factor. However, rapid changes in intensity cannot be taken care of in the software so that, *e.g.*, the power supply for the illumination should be a d.c. low-noise regulated source.

STREAK REMOVAL AND SEPARATION OF PARTIAL OVERLAP

Streaks can seriously affect machine reading but are not always avoidable. Destaining or similar measures can only alleviate the problem. Therefore, it is necessary to handle the effect of streaks in the preprocessing stage [20]. The elimination of partial overlap between spots uses similar software methods. Both tasks are carried out in a two-step approach outlined below.

The boundary of a cluster of pixels is checked for symmetry and size. If any asymmetry exceeds a certain limit or if the cluster is excessively large, the program assumes an anomaly and activates a subroutine. The gradient of $b_s(x,y)$ in the direction of the maximum asymmetry is computed. If the gradient is much smaller than could be expected from a Gaussian distribution, a streak is anticipated. Now the already mentioned elliptical contour is computed, but this time only taking into account areas of the spot that show normal gradients, thus excluding the streak direction. The method works well provided that the streak does not cover too much of the true spot area.

Overlap is detected by a similar test. An overlap is anticipated if the sign of the gradient in the direction of maximum asymmetry reverses and a saddle point is thus detected. Separation of overlapping spots was originally carried out by complementing the contour to both sides of the line of sign reversal to an elliptical shape. A different approach has recently been tested that additionally is capable of handling the overlap of more than two spots simultaneously. The technique employed here is erosion with subsequent dilation [21]. Erosion is normally performed independently of direction. However, there are indications that erosion enhancement in the direction of the asymmetry might be more efficient. Preliminary results are promising but a definitive conclusion has not yet been reached.

ENHANCEMENT OF DISPLAY FEATURES

Visual inspection of the scan is often the final step of the analysis. In that case feature enhancement by image processing can greatly simplify the visual examination.

A frequently employed technique for that purpose is edge enhancement. Here this method is not very useful because the software already creates a synthetic contour which is superimposed on the original contour.

Another very helpful tool is grey level transformation. Gradients in the image are artificially increased

so that the recognition of structures becomes easier. Grey levels can also be transformed into colour information as is known from satellite pictures. However, the user of such techniques must have a firm understanding of the effects of image processing. There is an extensive literature on the topic of image processing [22–27]. Pattern recognition principles can also be advantageously applied, although they are mostly targeted at applications other than densitometry [28–32].

FINAL PROCESSING

The so-far discussed preprocessing of the acquired densitometric data remains more or less unchanged regardless of the final purpose of the analysis. Final processing serves to evaluate the more global features of the acquired densitometric picture. Since the variety of tasks is great, only one of the final evaluation steps will be mentioned here. This is concerned with the comparison of the global structure of a scan with that of another one serving as a template.

The variant adopted here condenses in principle the information content of a separation into an ordered list of numerical values. The number of entries in that list is equal to the number of detected spots. However, that list can become too long to be handled efficiently, especially for biological samples. Interpretation can be facilitated by the fact that each entry consists of three values and thus can be represented by a vector in three-dimensional space. Vectorial addition of the individual entries yields a vector in multi-dimensional space which can be compared with or subtracted from the corresponding vector of a comparison separation by established mathematical procedures.

Sometimes only a fraction of the separation needs to be compared. Here the vectorial approach can also be useful, although a direct spot-by-spot comparison is then generally preferable.

TEMPLATE SELECTION

Frequently, the available advance information about the provenance of the examined sample is insufficient to select the most suitable template. It may then be necessary to investigate quickly a sometimes fairly large set of separations from storage. The vectorial approach can advantageously be employed. Separations which are to serve as templates are scanned and digitized only once. The acquired data together with the results of preprocessing are then put into library storage (mostly on hard magnetic disk) from where they are recalled when needed. Separations which are not intended to be used as templates are usually not stored in their entirely in order to limit the storage space. Storing the feature vector alone is generally adequate, more economical and facilitates search operations for retrieval. It must be considered that magnetic storage is subject to fading, and is therefore not suitable for the preservation of archival material. Optical disks offer much larger storage capacities and are not subject to fading [33].

CONCLUSIONS

The features discussed were built into an experimental system which was then used in electrophoretic separations. Emphasis was placed on a cost-effective and user-friendly realization. With very few exceptions the hardware was assembled from commercial off-the-shelf equipment around a standard AT-class computer. Only the illumination system had to be designed in detail. Therefore, a discussion of hardware details did not seem appropriate here. The software is the only aspect that was completely custom designed, but special attention was given to the possibility of using in a future version integrated mathematical packages which are not necessarily intended for densitometric use.

ACKNOWLEDGEMENTS

Most of this work was supported by a research grant from the National Science and Engineering Research Council (NSERC) of Canada. The authors are indebted to Professor Dr. D. Meyer-Ebrecht of the Institute for Measurement Techniques of the Technical University of Aachen, Germany, who made the facilities of his Institute available for this work. They also express their appreciation to Professor Dr. J. Klose of the Institute for Toxicology and Embryology of the Freie Universität Berlin for consultations and for providing actual separations for testing the system. Appreciation is also due to Professor Dr. W.

Albritton, Head of the Department of Microbiology at the University of Saskatchewan, who gave the impetus for starting the project and provided initial support for the acquisition of the necessary hardware.

REFERENCES

1 A. T. Andrews, *Electrophoresis Theory, Techniques and Biochemical and Clinical Applications*, Clarendon Press, Oxford, 1983.
2 V. A. Pollak, *Adv. Chromatogr.*, 30 (1989), Ch. 6.
3 B. F. Aycock, D. E. Weil, D. V. Sinicrope and D. L. Ilwain, *Comput. Biomed. Res.*, 14 (1981) 314–326.
4 V. A. Pollak, *J. Chromatogr.*, 393 (1987) 143–153.
5 D. F. Barbe, *Charge Coupled Devices (Topics in Applied Physics*, Vol. 38), Springer, Berlin, 1980.
6 C. H. Séquin and M. F. Tompsett, *Charge Transfer Devices*, Academic Press, New York, 1975.
7 G. J. Martin, K. H. Womack and J. H. Fisher, *A High Resolution CCD Camera for Scientific and Industrial Applications*, Company & SPIE Publication of Videk-Kodak, Canandaigua, NY, 1987.
8 D. G. Fink and D. Christiansen, *Electronics Engineers' Handbook*, McGraw-Hill, New York, 3rd. ed., 1989, Ch. 11, pp. 70–71.
9 *Vidicon Camera Tubes for the Spectral Range from the Infrared to X-Rays*, Hamamatsu, Tokyo, 1987.
10 H. Marsman and R. W. van Resandt, *Electrophoresis*, 6 (1985) 242–246.
11 M. W. Cowens, M. M. Blouke, T. Fairchild and J. A. Westphal, *Appl. Opt.*, 19 (1980) 3727–3728.
12 Technological Update, *Diagnostic Imaging Int.*, November (1988) 80.
13 M. M. Blouke, M. W. Cowens, J. E. Hall, J. A. Westphal and A. B. Christiansen, *Appl. Opt.*, 19 (1980) 3318–3321.
14 *Pyroelectric Selfscanning Infrared Detector Arrays, Application Note AN10*, Spiricon, New York, 1986.
15 V. A. Pollak, *Adv. Chromatogr.*, 30 (1989), Ch. 5.
16 V. A. Pollak, *J. Chromatogr.*, 105 (1975) 279–296.
17 V. A. Pollak, *J. Chromatogr.*, 77 (1973) 245–254.
18 V. A. Pollak, *J. Liq. Chromatogr.*, 11 (1988) 1403–1414.
19 J. Serra, *Image Analysis and Mathematical Morphology*, Academic Press, London, 1982.
20 V. A. Pollak, *J. Chromatogr.*, 77 (1973) 245–254.
21 J. Serra, *J. Microsc.*, 95, Part 1 (1972) 93–103.
22 R. C. Gonzalez and P. Wintz, *Digital Image Processing*, Addison-Wesley, London, 1987, pp. 190–200.
23 W. B. Green, *Digital Image Processing —A Systems Approach*, Van Nostrand Reinhold, New York, 1983.
24 H. C. Andrews, *Computer Techniques in Image Processing*, Academic Press, New York, 1970.
25 W. K. Pratt, *Digital Image Processing*, Wiley, New York, 1978.
26 K. R. Castleman, *Digital Image Processing*, Prentice-Hall, Englewood Cliffs, NJ, 1979.
27 E. L. Hall, *Computer Image Processing and Recognition*, Academic Press, New York, 1979.
28 R. O. Duda and P. E. Hart, *Pattern Classification and Scene Analysis*, Wiley, New York, 1973.
29 J. T. Tou and R. C. Gonzalez, *Pattern Recognition Principles*, Addison-Wesley, London, 1974.
30 T. Pavlidis, *Structural Pattern Recognition*, Springer, New York, 1977.
31 R. C. Gonzalez and M. G. Thomason, *Syntactic Pattern Recognition: an Introduction*, Addison-Wesley, London, 1978.
32 K. S. Fu, *Syntactic Pattern Recognition and Applications*, Prentice-Hall, Englewood Cliffs, NJ, 1982.
33 R. R. Freese, *Photonics Spectra*, 23, No. 10 (1989) 129–131.

Journal of Chromatography, 596 (1992) 251–264
Elsevier Science Publishers B.V., Amsterdam

CHROM. 24 016

Enzymophoresis of nucleic acids by tandem capillary enzyme reactor–capillary zone electrophoresis☆

Wassim Nashabeh and Ziad El Rassi*

Department of Chemistry, Oklahoma State University, Stillwater, OK 74078-0447 (USA)

(First received November 26th, 1991; revised manuscript received January 16th, 1992)

ABSTRACT

Enzymophoresis with coupled heterogeneous capillary enzyme reactor–capillary zone electrophoresis was developed and evaluated in the area of nucleic acids. Ribonuclease T_1, hexokinase and adenosine deaminase were successfully immobilized on the inner walls of short fused-silica capillaries through glutaraldehyde attachment. These open-tubular capillary enzyme reactors were quite stable for a prolonged period of use under operation conditions normally used in capillary zone electrophoresis. The capillary enzyme reactors coupled in series with capillary zone electrophoresis served as peak locator on the electropherogram, improved the system selectivity, and facilitated the quantitative determination of the analytes with good accuracy. Also, they allowed the on-line digestion and mapping of minute amounts of transfer ribonucleic acids, and the simultaneous synthesis and separation of nanogram quantities of oligonucleotides.

INTRODUCTION

Capillary zone electrophoresis (CZE) with its advanced instrumentation and unique selectivity has become an important microseparation technique. In CZE, and for a given set of conditions, the migration of charged species depend primarily on the sign and magnitude of their net charge and to some extent on their shape and size. Therefore, when the analytes possess the same charge-to-mass ratio and differ slightly in their size and shape, CZE is rather inadequate for their separation. In addition, as with other separation techniques, the identification of a given species in a mixture requires the use of additional means that can confirm its presence or absence, especially under coelution conditions or when no authentic standards are available. Enzymes, with their high stereospecificity in binding their substrates, are well suited to play this role.

In fact, the combination of enzymes with separation techniques has been a theme of research for many years. In 1970, Brown [1] pioneered the use of enzymes in free solution for sample pretreatment prior to chromatographic separation as a mean of peak identification, and coined the term enzymic peak-shift for the technique. On the other hand, the relative ease with which enzymes can be covalently attached or immobilized to various types of surfaces without substantial loss in their catalytic activity [2] has favored their use in solving many analytical problems [3]. One of the important applications of immobilized enzymes has been their use in pre- and post-column derivatization devices with several high-performance liquid chromatography (HPLC) techniques [3–8]. More recently, narrow-bore packed-bed trypsin reactor was introduced for the nanogram digestion of proteins prior to microcolumn liquid chromatography and capillary zone electrophoresis tryptic peptide mapping [9].

This report is concerned with the miniaturization of immobilized enzyme reactors for use in tandem with CZE. In this regard, short fused-silica capillaries with immobilized enzymes on the inner wall

☆ Presented at the *15th International Symposium on Column Liquid Chromatography, Basel, June 3–7, 1991*, lecture L53. The majority of the papers presented at this symposium have been published in *J. Chromatogr.*, Vols. 592 and 593 (1992).

0021-9673/92/$05.00

were developed for tandem heterogeneous capillary enzyme reactor–capillary zone electrophoresis (HCER–CZE). This tandem format, which is referred to as enzymophoresis, was evaluated in both the qualitative and quantitative determinations of different nucleic acids. Various HCER–CZE systems were investigated and characterized over a wide range of operation conditions including the design of the capillary enzyme reactor, the contact time of the substrates with the immobilized enzymes, the initial concentrations of the substrates, the nature of the background electrolyte and the pH. In addition, the effects of buffer additives as well as the immobilized enzymes on the magnitude and direction of the electroosmotic flow were investigated.

EXPERIMENTAL

Instrument

The instrument for capillary electrophoresis was assembled in-house from commercially available components, and resemble to previously reported systems [10,11]. It comprised two high-voltage power supplies of positive and negative polarities Models MJ30P400 and MJ30N400, respectively, from Glassman High Voltage (Whitehouse Station, NJ, USA) and a Linear (Reno, NV, USA) Model 200 UV–VIS variable-wavelength detector equipped with a cell for on-column capillary detection. The detection wavelength was set at 258 nm for sensing the various nucleic acids. The electropherograms were recorded with a Shimadzu (Columbia, MD, USA) computing integrator Model C-R3A equipped with a floppy disk drive Model FDD-1A and a CRT monitor.

Capillary columns

Fused-silica capillary columns of 50 μm I.D. and 365 μm O.D. were obtained from Polymicro Technology (Phoenix, AZ, USA). All capillaries used in this study were coated in-house with either interlocked or fuzzy polyether chains according to previously described procedures [10].

Reagents and materials

Ribonuclease T_1 (RNase T_1) from *Aspergillus oryzae* (EC 3.1.27.3), hexokinase from bakers yeast (EC 2.7.1.1), adenosine deaminase (ADA) from calf spleen (EC 3.5.4.4), transfer ribonucleic acid specific for phenylalanine ($tRNA^{Phe}$) from brewers yeast, guanylyl-(3′→5′)-adenosine (GpA), guanylyl-(3′→5′)-uridine (GpU), guanylyl-(3′→5′)-cytidine (GpC), uridylyl-(3′→5′)-guanosine (UpG), guanosine-2′:3′-cyclic monophosphate (G>p), guanosine-3′-monophosphate (Gp), adenosine-5′-triphosphate (ATP), adenosine-5′-diphosphate (ADP), adenosine (A), inosine (I), guanosine (G), uridine (U), cytidine (C), glucose and Trizma base were obtained from Sigma (St. Louis, MO, USA). L-Histidine (His), 2-[N-morpholino]ethanesulphonic acid (MES), N,N′-bis[3-aminopropyl]-1,4-butanediamine tetrahydrochloride (spermine) were from Aldrich (Milwaukee, WI, USA). γ-Aminopropyltriethoxysilane was purchased from Huls of America (Bristol, PA, USA). Reagent-grade sodium phosphate monobasic and dibasic, magnesium chloride, ammonium bifluoride, 1,3-naphthalenedisulphonic acid disodium salt, sodium acetate, phosphoric acid, hydrochloric acid, sodium hydroxide and HPLC-grade methanol were obtained from Fisher Scientific (Pittsburgh, PA, USA). Deionized water was used to prepare the running electrolyte. All solutions were filtered with 0.2-μm UniPrep syringeless filters (Fisher Scientific) to avoid column plugging.

Enzyme immobilization

Fused-silica capillaries of 15 to 25 cm long were first etched according to the procedure described by Onuska *et al.* [12]. The etched capillaries were then reacted with 10% (v/v) solution of γ-aminopropyltriethoxysilane in water at 95°C for 30 min. This step was repeated twice. Following, a 1% (v/v) solution of glutaric dialdehyde in 50 m*M* phosphate, pH 7.0, was applied to the capillary and allowed to react at room temperature for 1 h. Thereafter, a phosphate solution containing the enzyme of interest was recycled through the aldehyde activated amino-fused-silica capillaries and allowed to stand overnight. Finally, residual aldehyde reactive functions were scavenged with 50 m*M* Tris–HCl at pH 7.5. All capillaries were stored in water at 5°C.

Other procedures

In all experiments, the capillary enzyme reactors of 15 to 25 cm long were connected butt-to-butt to the separation capillaries having a polyether hydrophilic coating (*i.e.*, CZE capillary) of 64 cm total length and 30 cm to the detection point using a

PTFE tube the inner diameter of which matched the outer diameters of the two capillary columns. The enzymic reactions were carried out on-line by allowing a thin plug of the substrates to flow through the tandem capillaries either by electromigration under the influence of an applied voltage or by hydrodynamic mode (*i.e.*, gravity flow) by raising the inlet reservoir to a certain height above the outlet reservoir. In both cases, the substrates first entered the capillary enzyme reactor and were converted to products. They were further separated in the separation capillary downstream the enzyme reactor. The time required for the substrates to traverse the enzyme reactor under hydrodynamic conditions (t_i) was estimated from the following equation [13]:

$$t_i = \frac{8\eta L l}{\rho g r^2 \Delta h}$$

where η is the medium viscosity, L is the total length of the capillary, l is the distance traversed by the plug of the substrate, ρ is the electrolyte density, g is the gravitational constant, r is the inner radius of the capillary and Δh is the differential height between the electrolyte reservoirs. In all cases, the viscosity and density of the solutions were taken as that of water since the buffers used were dilute solutions of electrolytes. The calculations using the above equation agreed with the experimental migration time estimated from the chromatogram of the substrate that was allowed to flow by gravity through the tandem capillary enzyme reactor→CZE capillary. Therefore, in all the studies, the above equation gave satisfactory results in terms of the time required for the species to reach a certain distance in the capillary by hydrodynamic flow.

The running electrolyte was renewed after each run. To ensure reproducible separations the separation capillary was flushed successively with fresh buffer, water, methanol, water, and again runnning buffer. The enzyme reactor was also flushed with fresh buffer solution after each run. Both capillaries were then equilibrated with the running electrolyte for 10 min before each injection.

RESULTS AND DISCUSSION

Design of the capillary enzyme reactor

Fig. 1 is a schematic illustration of the capillary enzyme reactor. The walls of the fused-silica capillary were first roughened using a methanolic solution of ammonium bifluoride; see Experimental. This etching step is to increase the specific surface area of the capillary wall in order to achieve higher enzyme loading of the reactor. This would yield capillary enzyme reactors with higher catalytic activity, and may increase the maximum velocity, V_{max}, of the enzymic reaction. The surface roughening by ammonium bifluoride at high temperature has been recently used in our laboratory for the preparation of octadecyl capillaries for on-line preconcentration of dilute samples [14] and proved efficient in increasing the concentration of covalently attached hydrocarbonaceous ligands. Another function of the etching is to increase the surface wettability which permits the homogeneous spreading of the hydrophilic aminopropylsiliyl layer. This layer is to minimize solute–wall interactions and to provide the functional groups for the attachment of the enzyme. The HCERs thus obtained were used in series with polyether-coated capillaries.

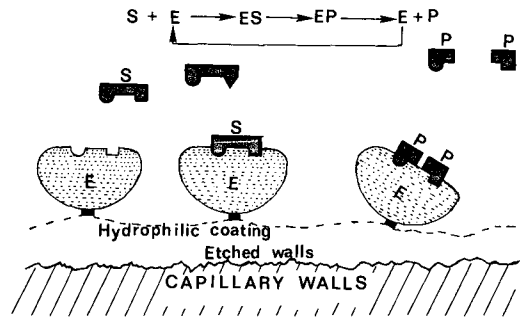

Fig. 1. Schematic illustration of immobilized capillary enzyme reactor. S = Substrate; E = enzyme; P = product.

Operational and basic principles of tandem capillary enzyme reactor-CZE

The capillary consisted of two sections connected in series via a PTFE tube. The first part is the capillary enzyme reactor and the second part is the separation capillary (*i.e.*, CZE). In all cases, the substrate(s) is first introduced as a thin plug into the capillary enzyme reactor. The catalyzed reaction takes place as the substrate(s) migrate through the enzyme reactor either by hydrodynamic flow or electromigration. Following, the reaction mixture is further separated in the CZE capillary at the same or different applied voltage than in the precolumn

enzymic derivatization reactor. To satisfy both the enzymic reaction and the separation, the background electrolyte for the reaction and separation processes can be either the same or different. Most importantly, the electrolyte for the enzymic reaction should minimize microenvironmental effects in the capillary enzyme reactor. These effects are related to electrostatic or hydrophobic interactions with the enzyme and/or the matrix [15].

Open tubular capillary enzyme reactors offer the convenience of repeated use of the enzyme without much loss of its activity, and provide enhanced storage and thermal stability for the enzyme. Furthermore, in contrary to packed-bed reactors where the substrate has to diffuse inside the pores of the packing to reach the immobilized enzyme, mass transfer in open tubular columns is of external nature (*i.e.*, bulk diffusion). This would increase the effectiveness factor η, defined as the ratio of the actual reaction rate to that obtained under conditions where no diffusional mass transfer limitations are present (*i.e.*, free solution). External mass transfer limitations, albeit small in a capillary tube, may still increase the apparent Michaelis constant K_M^{app} [16], which would result in increasing the linear dynamic range of the immobilized enzyme, and in turn benefit the analytical applications of capillary enzyme reactors.

Effect of spermine on the electroosmotic mobility

The usefulness of the catalytic activities of the various HCERs was demonstrated in the separation, identification, quantitative determination, and synthesis of nucleic acid fragments and constituents. In order to bring about the migration and separation of the various nucleic acids under investigation with coated capillaries having moderate cathodal electroosmotic flow, a means for inverting the direction of the flow was necessary so that a negative polarity mode could be utilized. This was achieved by adding spermine to the running electrolyte at low concentration.

Spermine is a biogenic tetraamine that has been successfully used as a buffer additive in the CZE analysis of polycitidines [17] with polyacrylamide-coated capillary tubes. In this study, it was thought that the spermine primary function is to reduce the net negative charge of the analytes and allow their migration and separation. To study its adsorption onto the capillary inner surface, we have measured the magnitude of the electroosmotic flow and examined its direction in the presence and absence of spermine over the pH range 3.5–7.0 using phenol as the inert tracer. The results of this study are summarized in Fig. 2. These studies were performed on an interlocked polyether-coated capillary using a running electrolyte of 25 m*M* His and 25 m*M* MES, with or without 5 m*M* spermine. In the presence of spermine, the direction of the electroosmotic flow was inverted from cathodal to anodal as shown in Fig. 2. The adsorption of spermine, which has a net positive charge of *ca.* +4 below pH 7.0, onto the capillary inner surface changed the ζ potential of fused silica from negative to positive. As can be seen in Fig. 2, the electroosmotic mobility slightly decreased upon increasing the pH in the range studied. This can be explained by both the slight decrease in the net positive charge of spermine and the increase in the ionization of surface silanols as the pH increased. Thus, spermine is a useful buffer adjunct for the analysis of negatively charged species in the negative polarity mode, since it allows the separated analytes to migrate in the same direction as that of the electroosmotic flow which in turn would yield shorter analysis time.

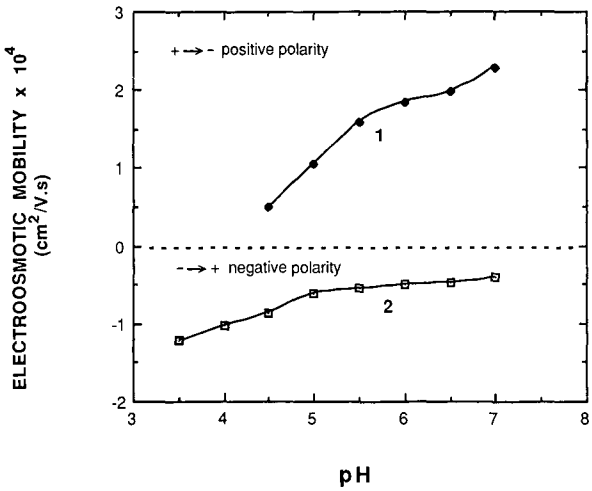

Fig. 2. Plots of the electroosmotic mobility in the absence (1) or presence (2) of spermine in the running electrolyte as a function of pH. Capillary, interlocked polyether coating, 30 cm (to the detection point), 64 cm (total length) × 50 μm I.D.; running voltage, 25 kV; background electrolyte, 25 m*M* His, 25 m*M* MES in the absence (1) or presence (2) of 5 m*M* spermine. Inert tracer, phenol.

Ribonuclease T_1 capillary enzyme reactor

Ribonuclease T_1 is a guanylic acid-specific endoribonuclease that cleaves phosphodiester bonds between 3′-guanylic acid residues and the 5′-hydroxyl groups of adjacent nucleotidyl residues [18]. In addition, under certain conditions, the enzyme acts as a ligase catalyzing the esterification of G>p with the 5′-hydroxyl group of various nucleosides to yield the corresponding dinucleotides [18,19]. Both catalytic functions of RNase T_1 were evaluated in the tandem RNase T_1 capillary enzyme reactor–CZE mode using an electrolyte system containing spermine as a buffer additive to facilitate the electrophoresis of negatively charged nucleotides, see above.

Immobilized ribonuclease T_1 as a hydrolytic enzyme. As mentioned above, RNase T_1 splits the internucleotide bonds specifically after guanylyl residues according to the following reaction schemes [18]:

$$\text{RNA} \xrightarrow[\text{Limited digestion}]{\text{RNase } T_1} \text{Oligonucleotides with terminal G>p (transphosphorylation, reversible)} \quad (1)$$

$$\text{RNA} \xrightarrow[\text{Exhaustive digestion}]{\text{RNase } T_1} \text{Oligonucleotides with terminal Gp (hydrolysis, irreversible)} \quad (2)$$

The above catalytic activity of the enzyme was demonstrated in the identification and quantitative determination of various dinucleotides using tandem RNase T_1 capillary enzyme reactor–CZE. In all experiments, the substrates were introduced as a thin plug and allowed to flow hydrodynamically through the enzyme reactor by raising the inlet reservoir to a height of 20 cm above the outlet reservoir. This corresponds to a contact time of *ca.* 16 min with the immobilized enzyme. As the plug of the reaction mixture entered the separation capillary, the enzyme reactor was disconnected and the separation capillary was inserted into the electrolyte reservoir. Thereafter, the voltage was turned on to 25 kV to bring about the separation of the reaction mixture.

As shown in Fig. 3a, a mixture of three dinucleotides namely GpU, GpA and GpC were not resolved by CZE alone using a buffer system containing 25 m*M* His, 25 m*M* MES and 5 m*M* spermine at pH 5.0. This is because these dinucleotides have approximately the same charge-to-mass ratio. As shown in Fig. 3b, with the on-line RNase T_1 capillary enzyme reactor, the dinucleotide mixture was converted to more readily separated products. Each of the three dinucleotides GpA, GpU and GpC yielded the guanosine-2′:3′-cyclic monophosphate and its corresponding nucleoside, *i.e.*, adenosine, uridine and cytidine. Hence, the three dinucleotides that coeluted as a broad peak with CZE alone were transformed into four well resolved peaks, *i.e.*, G>p, U, A and C, after a single pass through the 17 cm long RNase T_1 capillary enzyme reactor.

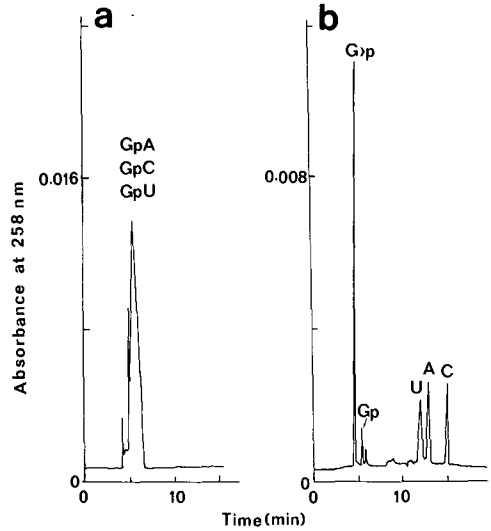

Fig. 3. Typical electropherograms of dinucleotides and their RNase T_1 digest obtained by CZE alone (a) or by tandem RNase T_1 capillary enzyme reactor–CZE (b), respectively. Capillary enzyme reactor, 17 cm × 50 μm I.D.; separation capillary, interlocked polyether coating, 30 cm (to the detection point), 64 cm (total length) × 50 μm I.D.; substrate introduction, hydrodynamic mode; enzymic reaction was carried out using gravity-driven flow; separation step, as the plug of the reaction mixture entered the separation capillary, the enzyme reactor was disconnected and the voltage was turned on to 25 kV; background electrolyte, 25 m*M* His, 25 m*M* MES, 5 m*M* spermine, pH 5.0. GpU = Guanylyl-(3′→5′)-uridine; GpA = guanylyl-(3′→5′)-adenosine; GpC = guanylyl-(3′→5′)-cytidine; G>p = guanosine-2′:3′-cyclic monophosphate; Gp = guanosine-3′-phosphate; U = uridine; A = adenosine; C = cytidine.

In another electrophoretic run, one of the three dinucleotides GpC, was replaced by UpG, a dinucleotide that is not digested by the enzyme. As expected, with CZE alone, this mixture exhibited the same electrophoretic behavior as the one in the preceding experiment, in the sense that its components could not be resolved as shown in Fig. 4a. However, after a single pass through the capillary enzyme reactor, UpG which is not split by the immobilized enzyme eluted intact, and was well resolved from the products of GpA and GpU. This feature of the capillary enzyme reactor has many practical significances. The tandem format can assess the identity of overlapping peaks and permits the simultaneous digestion and separation of the reaction mixture. Briefly, the capillary enzyme reactor functions as a peak locator by unmasking the analyte of interest on the electropherogram, and enhances the selectivity of the electrophoretic system by converting the substrates into more readily separated products.

The dinucleotide GpU, having the lowest relative rate of splitting by RNase T_1 among the other dinucleotides analyzed [20], was selected as a model substrate to evaluate the stability of the RNase T_1 capillary enzyme reactor. The reactor showed steady behavior even after prolonged storage or repeated use. Over a period of more than 2 months, the RNase T_1 capillary enzyme reactor yielded complete conversion of GpU with the liberation of G>p and U as major peaks, suggesting that the enzymic reaction occurring at the wall of the HCER is primarily a limited digestion mechanism (see reaction 1).

Another important feature of the capillary enzyme reactor is its usefulness in the quantitative determination of the dinucleotides. To demonstrate this important application of HCER, typical calibration curves for G>p and some of the nucleosides were established using 1,3-naphthalenedisulphonic acid disodium salt as the internal standard. As shown in Fig. 5, these curves were linear in the concentration range investigated. In such measurements, the G>p peak can be used for the quantitative determination of the total concentration of the dinucleotides digested by the enzyme in a given mixture, while the peak of each nucleoside can be used to estimate the concentration of its corresponding dinucleotide. In the case of only one solute analyzed, both the G>p and the nucleoside peaks are equally useful in the quantitative determination of the analyte, thus increasing the reliability of the

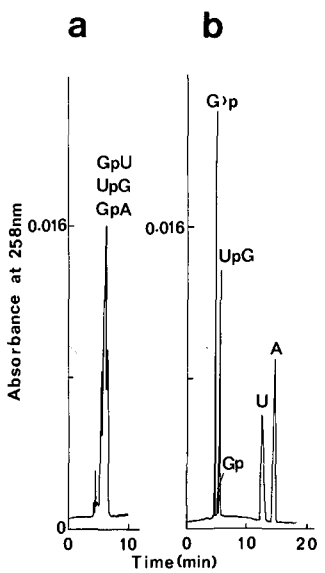

Fig. 4. Typical eletropherograms of dinucleotides and their RNase T_1 digest obtained by CZE alone (a) or by tandem RNase T_1 capillary enzyme reactor–CZE (b), respectively. UpG = Uridylyl-(3′→5′)-guanosine. Other symbols and conditions as in Fig. 3.

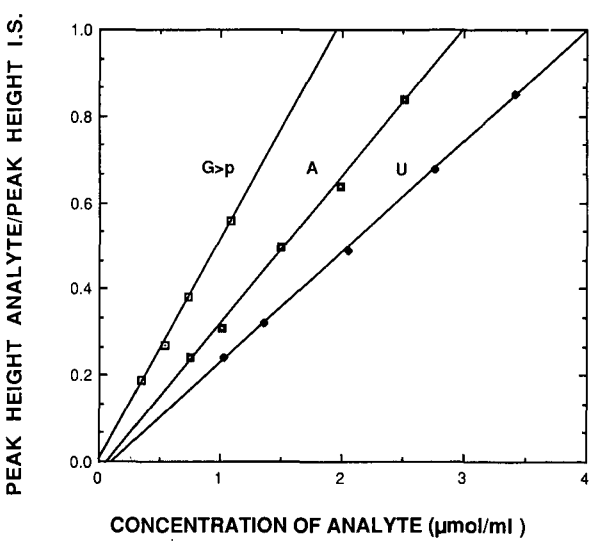

Fig. 5. Plots of the ratio of the peak height of the analyte to that of the internal standard (I.S.) as a function of the analyte concentration. Internal standard, 1,3-naphthalenedisulphonic acid disodium salt. Conditions and symbols as in Figs. 2 and 3.

method. For instance, a thin plug of an unknown solution of GpU was analyzed with the coupled capillary enzyme reactor-capillary zone electrophoresis following the same operational schemes outlined above. The calibration curves revealed on the average a concentration of 0.90 μmol/ml for G>p and 1.00 μmol/ml for U. By averaging these two values, the concentration of GpU in the unknown solution was about 0.95 μmol/ml. This illustrates the use of the capillary enzyme reactor in enhancing the reliability of quantitative determination by CZE.

In addition, the RNase T_1 capillary enzyme reactor–CZE system proved very efficient in the on-line digestion and mapping of transfer ribonucleic acid specific for phenylalanine ($tRNA^{Phe}$). The secondary structure of $tRNA^{Phe}$ is represented in Fig. 6. It comprises 76 nucleotide residues. The arrows in this figure indicate the 20 locations at which the enzyme splits the internucleotide bonds leading to the formation of 15 oligonucleotides and 1 guanosine monophosphate [21]. The digestion of $tRNA^{Phe}$ was carried out in a 20 cm long capillary enzyme reactor by allowing the substrate to contact the immobilized RNase T_1 for approximately 22 min while flowing hydrodynamically. Thereafter, the capillary enzyme reactor was disconnected and the RNase T_1 digest was mapped in the separation capillary using a running electrolyte of 0.1 *M* His, 0.1 *M* MES and 5 m*M* spermine, pH 7.0 (see Fig. 7). In this experiment, the ionic strength of the running electrolyte was increased in order to minimize electrostatic interactions between the oligonucleotide fragments and the amino-silica matrix and/or the enzyme. It can be envisioned that such format can allow (i) the quick and reproducible mapping of other native or modified tRNAs available only in minute quantities, and (ii) the conversion of ribonucleic acids to more electrophoretically manageable oligonucleotide fragments.

Immobilized ribonuclease T_1 as ligating enzyme. Another interesting feature of RNase T_1 is its ligating property. It can link cyclic G>p to a nucleoside and produce the corresponding dinucleotide. This aspect of the immobilized RNase T_1 has been previously investigated by El Rassi and Horváth [8] using tandem packed-bed enzyme reactor–high-performance displacement chromatography. To examine the effectiveness of tandem RNase T_1 capillary enzyme reactor–CZE in the synthesis and separation of ng quantities of dinucleotides, the following reaction was investigated:

$$G{>}p + U \overset{\text{RNase } T_1}{\rightleftharpoons} GpU \qquad (3)$$

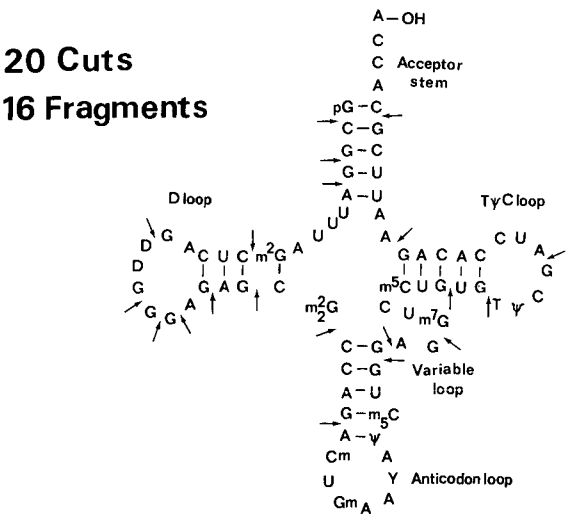

Fig. 6. Schematic representation of the secondary structure of transfer ribonucleic acid specific for phenylalanine (yeast $tRNA^{Phe}$). The arrows in this figure indicate the 20 locations at which RNase T_1 splits the internucleotide bonds.

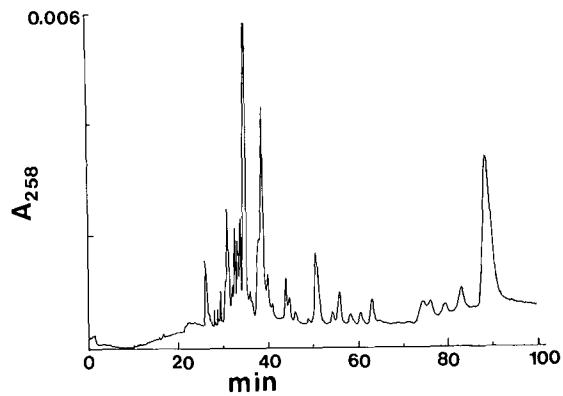

Fig. 7. On-line digestion and mapping of $tRNA^{Phe}$ by tandem RNase T_1 capillary enzyme reactor–CZE. Capillary enzyme reactor, 20 cm × 50 μm I.D.; separation capillary, interlocked polyether coating, 50 cm (to the detection point), 80 cm (total length) × 50 μm I.D.; running voltage, 15 kV; background electrolyte, 0.1 *M* His, 0.1 *M* MES, 5 m*M* spermine, pH 7.0. Substrate introduction, enzymic reaction and separation steps as in Fig. 3.

In contrary to the digestion reaction which occurs mostly in the forward direction, the ligation process requires the use of an excess of one of the reactants to drive the equilibrium towards the formation of the dinucleotide. Studies in free solution reveal that under appropriate conditions and 24 h incubation time, only 40% of G>p is transformed into GpU [22]. Fig. 8a and b illustrates typical electropherograms of the reaction mixture obtained in the absence or presence of the RNase T_1 capillary enzyme reactor, respectively. Both the enzymic and separation processes were carried out in a buffer system of 25 m*M* His, 25 m*M* MES and 5 m*M* spermine, pH 5.5. The concentration of U was 5 times that of G>p and the condensation reaction was brought about by allowing a thin plug of both substrates to contact simultaneously the immobilized enzyme by gravity-driven flow. In such mode of bisubstrate enzymic reactions, where both substrates have different electrophoretic mobilities, the enzymic reaction was best achieved using hydrodynamic flow. In fact, under electromigration conditions, the negatively charged G>p would migrate downstream the enzyme reactor while uridine being neutral would migrate behind at a slower rate, and therefore both substrates are unable to get concurrently to the enzyme active sites.

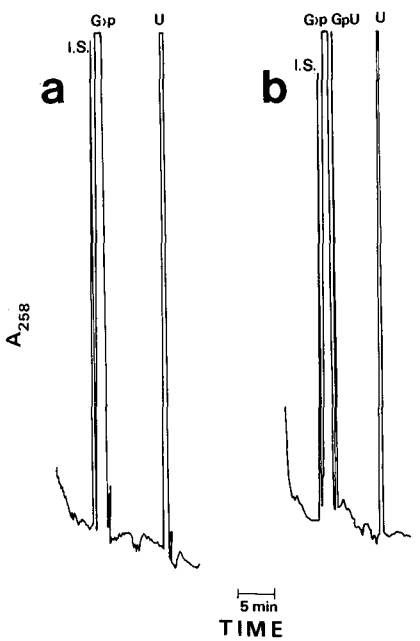

Fig. 8. Typical electropherograms of the RNase T_1 synthetic reaction mixture in the sbsence, *i.e.*, by CZE alone (a) or presence of RNase T_1 capillary enzyme reactor (b). Capillary enzyme reactor, 15 cm × 50 μm I.D.; separation capillary, interlocked polyether coating, 30 cm (to the detection point), 64 cm (total length) × 50 μm I.D.; substrate introduction, hydrodynamic mode; enzymic reaction was carried out using gravity-driven flow; separation step, as the plug of the reaction mixture entered the separation capillary, the enzyme reactor was disconnected and the voltage was turned on to 25 kV; background electrolyte, 25 m*M* His, 25 m*M* MES, 5 m*M* spermine, pH 5.5. Internal standard (I.S.), 1,3-naphthalenedisulphonic acid disodium salt. Initial concentration, [G>p] = 0.02 *M*, [U] = 0.10 *M*.

The RNase T_1 catalyzed synthesis of GpU does not go to completion as manifested by the excess substrate peaks detected after the enzymic reaction (see Fig. 8b). It was then interesting to study the effect of various operational parameters on the yield of GpU. In that regard, a calibration curve was established for GpU using 1,3-naphthalenedisulphonic acid disodium salt as an internal standard. The plot of the peak height ratio of GpU to that of I.S. *vs.* the concentration of GpU showed a linear behavior up to a concentration of 0.7 mg/ml of the analyte. This calibration curve was then used to estimate the amount of GpU produced. The yield of GpU expressed in mol% of G>p converted into GpU was determined at various pH, initial substrate concentration and contact time using a thin plug of the substrate and a single pass reactor.

The effect of the electrolyte pH on the yield of GpU was determined over the pH range 4.0 to 7.0 in an increment of 0.5 pH unit. The results obtained are illustrated in Fig. 9 by a plot of the yield of GpU *vs.* pH. In this study, the enzymic reaction was carried out using gravity-driven flow and buffers of same

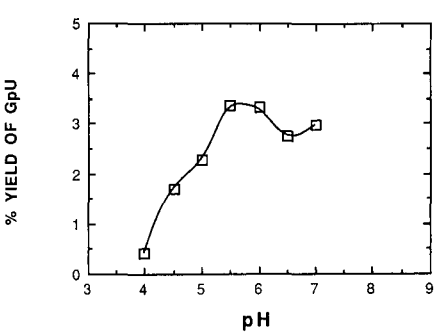

Fig. 9. Plot of the % yield of GpU as a function of the pH of the enzymic reaction. Conditions as in Fig. 8 except enzymic reaction was carried out with buffers of same composition as the running electrolyte but at various pH. See text for more details.

composition as the running electrolyte but at various pH. This means that both the capillary enzyme reactor and the separation capillary were first filled with the running electrolyte, pH 5.5 (*i.e.*, the separation pH). As the thin plug was introduced in the enzyme reactor, it was pushed through the immobilized capillary enzyme reactor with a buffer of the appropriate pH. When the reaction plug entered the separation capillary, the enzyme reactor was disconnected and the separation capillary was dipped into the separation buffer and the voltage was turned on to start the separation of the reaction mixture. Fig. 9 shows that the yield of GpU increased by a factor of 8 upon increasing the pH from 4.0 to 5.5. The optimum pH for the ligation reaction lies in the range 5.5 to 6.0 as opposed to 7.2 for the free enzyme [23]. This shift in the optimum activity of the immobilized enzyme toward more acidic pH values may be due to microenvironment effects and is in agreement with previous findings [24].

The effect of the initial substrate concentrations on the yield of GpU was investigated at pH 5.5. The initial concentrations of G>p and U were varied while keeping the molar concentration ratio of U to that of G>p equal to 5.0. These results are reported in Fig. 10. Upon increasing the concentration of G>p from 0.001 to 0.01 *M*, the yield of GpU increased from 1.2 to 4.7. However, at G>p concentrations greater than 0.01 *M* the yield of the synthesized GpU decreased monotonically. This may be explained by substrate inhibition due to system overloading. Experimental considerations such as peak overlapping limited the highest G>p concentration investigated to 0.04 *M*.

As mentioned above, the synthesis of GpU is a kinetically controlled process. Assuming Michaelis–Menten kinetics and under conditions of partial conversion, the integrated rate law can be written as [5]:

$$\frac{[P]}{[S_i]} = 1 - e^{-V_{max}\, t/K_M}$$

where [P] is the product concentration at the outlet of the reactor, $[S_i]$ is the initial substrate concentration, V_{max} is the maximum velocity of the enzymic reaction, t is the residence time of the substrate and K_M is the Michaelis constant. According to this equation, the yield of the product should increase with increasing both V_{max} and t or decreasing K_M. V_{max} has already been improved through the etching process that increases the catalytic activity of the wall. A lower K_M value will decrease the linear dynamic range of the enzyme reactor and thus limits its analytical applications. In addition, K_M cannot be controlled systematically. Thus, the simplest alternative to enhance the product yield is to increase the contact time of the substrate with the immobilized enzyme. This can be accomplished by either using longer enzyme reactor or decreasing the flow-rate for a given length of enzyme reactor. In this study, the differential height between the two electrolyte reservoirs was varied in order to obtain different gravity-driven flow-rates and consequently various contact times. Fig. 11 shows the yield of GpU *versus* the contact time of the substrates with the RNase T_1 capillary enzyme reactor. These results are in agreement with kinetic considerations. In fact, by increasing the contact time from 14 to 30 min, the yield of GpU increased by a factor of 1.5 in almost a linear

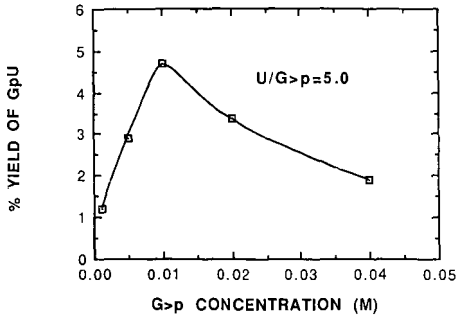

Fig. 10. Plot of the % yield of GpU as a function of the initial G>p concentration. Conditions as in Fig. 8.

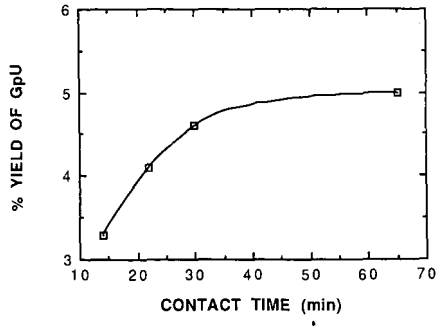

Fig. 11. Plot of % yield of GpU as a function of the contact time with immobilized RNase T_1. Conditions as in Fig. 8.

fashion and then levelled-off at higher contact times.

Besides the increase in the analysis time, a major concern of lower hydrodynamic flow velocity is its effect on the band width of the separated analytes. In open tubular systems, where longitudinal diffusion is the main source of bandspreading, longer residence time of the solute molecules leads to increased bandspreading. The number of theoretical plates of the GpU peak was measured at each contact time. These results are reported in Fig. 12 by a plot of the plate height as a function of the residence time in the enzyme reactor. As expected, the system efficiency decreased with increasing the contact time. However, increasing the contact time by a factor of 4 produced a decrease in the separation efficiency by a factor of 2 only.

It should be noted that under optimized conditions, approximately 10 ng of GpU can be produced from a single pass through the enzyme reactor. Such format employing simple CZE instrumentation can be easily automated and may prove useful in the micropreparative scale of important biochemicals, such as the synthesis of specific long oligonucleotides that are produced at low level by chemical synthesis methods. Such oligonucleotides are important in the study of mechanisms involving protein synthesis.

Hexokinase capillary enzyme reactor

Hexokinase is a relatively non-specific enzyme that catalyzes the phosphorylation of a wide variety of hexoses [25]. Its catalytic property was exploited in the HPLC separation and verification of the peak identities of ATP and ADP by treating the sample with the enzyme prior to the chromatographic separation [1]. This enzymatic reaction occurs via a random bi–bi mechanism in which the enzyme forms a ternary complex with glucose and Mg^{2+}–ATP before the start of the reaction [26]. Besides its orienting effect, the Mg^{2+} ions are thought to electrostatically shield the negative charges of the phosphate groups that would otherwise hinder the nucleophilic attack of the C(6)-OH group of glucose on the γ-phosphate of the Mg^{2+}–ATP complex. Thus, the overall net reaction is the transfer of a phosphoryl group from ATP to glucose to form glucose-6-phosphate and ADP as follows [25]:

$$\text{glucose} + \text{ATP} \xrightarrow[Mg^{2+}]{\text{HK}} \text{glucose-6-phosphate} + \text{ADP} \quad (4)$$

where HK is hexokinase.

To evaluate the immobilized hexokinase capillary enzyme reactor, ATP was introduced as a thin plug into the tandem capillaries (*i.e.*, capillary enzyme reactor–CZE), which were equilibrated with a buffer of 25 m*M* His, 25 m*M* MES and 5 m*M* spermine, pH 7.0, containing both glucose and Mg^{2+} so that the immobilized enzyme is in continuous contact

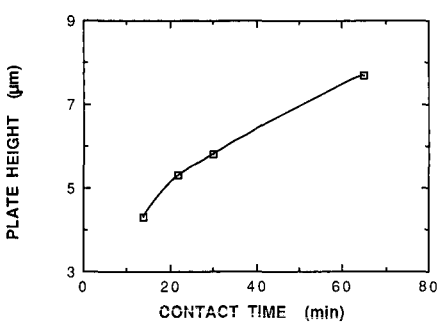

Fig. 12. Plot of the plate height of the synthesized GpU peak as a function of the contact time with the immobilized RNase T_1 enzyme. Conditions as in Fig. 8.

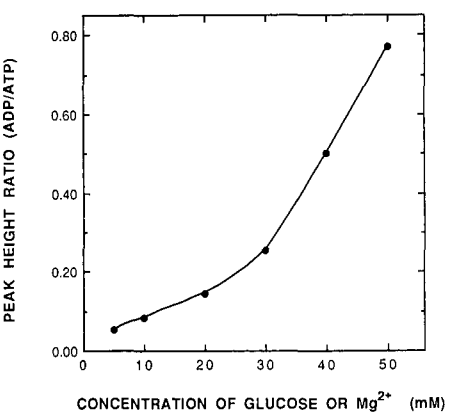

Fig. 13. Plot of the peak height ratio of ADP/ATP in arbitrary units as a function of the concentration of glucose or Mg^{2+} in the running electrolyte. Capillary enzyme reactor, 15 cm × 50 μm I.D.; separation capillary, interlocked polyether coating, 30 cm (to the detection point), 64 cm (total length) × 50 μm I.D.; substrate introduction, electromigration mode; tandem enzymic reaction–CZE was carried out at the same voltage, 25 kV; background electrolyte, 25 m*M* His, 25 m*M* MES, 5 m*M* spermine, pH 7.0 at different concentration of glucose and Mg^{2+}.

with one of the substrate (*i.e.*, glucose) and the metal ions required for the reaction. This allowed the reaction and separation to be carried out simultaneously at 25 kV. Under these conditions, the presence of spermine in the running electrolyte yielded an anodal electroosmotic flow and its effect on the magnitude and direction of the flow outweighed the influence of the immobilized enzyme on the wall of the capillary reactor. In the absence of spermine, one would expect that the electroosmotic flow to be affected primarily by the ionization of the immobilized enzyme (see below). Fig. 13 illustrates a plot of the peak height ratio of ADP/ATP in arbitrary units as a function of the concentration of glucose or Mg^{2+} in the running electrolyte. As expected, the magnitude of the conversion of ATP to ADP was a function of glucose and Mg^{2+} concentrations in the running electrolyte. As shown in Fig. 13, the peak height ratio of ADP/ATP increased by a factor of 16 upon increasing the concentrations of both glucose and Mg^{2+} by a factor of 10 (*i.e.*, from 5 to 50 m*M*). However, due to the increase in the viscosity of the buffer system at high glucose concentrations, the electrophoretic system suffered from prolonged analysis time which resulted in poor efficiency.

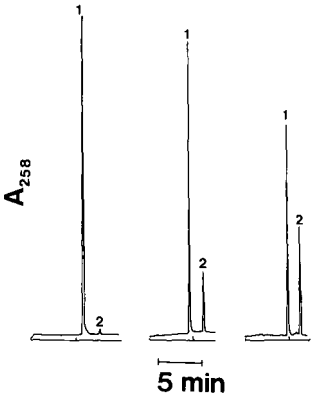

Fig. 14. Typical electropherograms of ATP (1) and ADP (2) at various contact time with the hexokinase capillary enzyme reactor. Capillary enzyme reactor, 15 cm × 50 μm I.D.; separation capillary, fuzzy polyether coating, 30 cm (to the detection point), 64 cm (total length) × 50 μm I.D.; substrate introduction, hydrodynamic mode; enzymic reaction was carried out using gravity-driven flow; separation step, as the plug of the reaction mixture entered the separation capillary, the enzyme reactor was disconnected and the voltage was turned on to 20 kV; background electrolyte, 0.1 *M* acetate containing 20 m*M* glucose and 10 m*M* Mg^{2+}, pH 5.0. Contact times of the substrate with the immobilized enzyme: left, 0 min (CZE only); middle, 10 min; right, 52 min.

In another set of experiments, ATP was allowed to migrate through the capillary enzyme reactor by a gravity-driven flow. This was aimed at studying the effect of contact time with the immobilized enzyme on the substrate conversion at constant temperature, a parameter that cannot be easily controlled when electromigration is used to vary the contact time of the substrates with the immobilized enzyme. Fig. 14 illustrates typical electropherograms of the products of the enzymic reaction at various contact time. They were carried out on a fuzzy 2000 polyether-coated capillary using 0.1 *M* acetate containing 20 m*M* glucose and 10 m*M* Mg^{2+}, pH 5.0, as the running electrolyte. Under these conditions, the electroosmotic flow was cathodal and its magnitude was relatively low. This is because the fuzzy polyether capillaries are characterized by relatively low electroosmotic flow [10], and the presence of heavy metal ions further reduced the flow [27]. This permitted the migration of the negatively charged nucleotides in the negative polarity mode without the inclusion of spermine in the background electrolyte. The electrophoretic velocity of the solutes was much greater than, and in opposite direction to, the electroosmotic flow. As can be noticed, at relatively low glucose concentration, the peak-height ratio of ADP/ATP increased almost 3 times by increasing the contact time of the substrate with the immobilized enzyme from 10 to 52 min. As in the case of RNase T_1 capillary enzyme reactor, the increase in the residence time of ATP in the enzyme reactor from 10 to 52 min, led to a drop in the separation efficiency by a factor of 2.4 and 1.8 for ATP and ADP, respectively. The tandem format hexokinase capillary enzyme reactor–CZE can be used to locate the ATP peak through its partial conversion to ADP and therefore can serve to confirm the presence or absence of ATP in a complex biological matrix.

Adenosine deaminase capillary enzyme reactor

Adenosine deaminase is a highly specific enzyme that catalyzes the deamination of adenosine to inosine with the liberation of NH_3 as follows [28]:

$$\text{adenosine} + H_2O \xrightarrow{\text{ADA}} \text{inosine} + NH_3 \qquad (5)$$

It was successfully immobilized on the inner walls

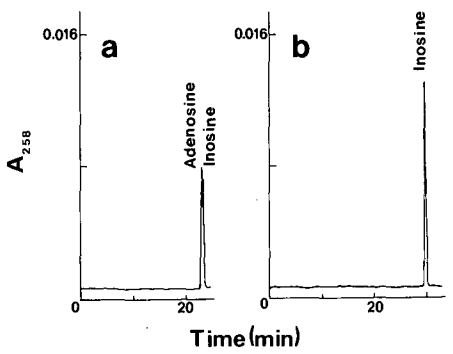

Fig. 15. Typical electropherograms of an equimolar mixture of adenosine and inosine obtained by CZE alone (a) or by tandem ADA capillary enzyme reactor–CZE (b). Capillary enzyme reactor, 15 cm × 50 μm I.D.; separation capillary, interlocked polyether coating, 30 cm (to the detection point), 64 cm (total length) × 50 μm I.D.; substrate introduction, eletromigration mode; tandem enzymic reaction–CZE was carried out at the same field strength, 190 V/cm; background electrolyte, 0.1 *M* phosphate, pH 6.5.

of a 15 cm long fused-silica capillaries as described under Experimental. The enzymic reaction was examined with a thin plug of an equimolar mixture of adenosine and inosine using 0.1 *M* phosphate, pH 6.5, as the background electrolyte. Fig. 15a and b illustrates the electropherograms of this mixture obtained on an interlocked polyether capillary in the absence or presence of the ADA capillary enzyme reactor, respectively. The enzymic reaction and the separation were carried out simultaneously at a field strength of 190 V/cm without disconnecting the enzyme reactor. Thus, the higher retention time of the inosine solute in Fig. 15b is simply the result of the extra length of the capillary enzyme reactor that the solute has to migrate. As can be seen in Fig. 15, for a short contact time of *ca.* 10 min, complete conversion of adenosine to inosine was obtained from a single pass through the reactor as manifested by the disappearance of the adenosine peak and a proportional increase in the peak height of inosine.

Since the enzymic reaction and separation were carried out simultaneously using tandem ADA capillary enzyme reactor–CZE, it was necessary to determine the effects of coupling a capillary enzyme reactor to a separation capillary both having different magnitude and sign of zeta potentials. Unlike in the case of HK capillary enzyme reactor–CZE where the direction and magnitude of the flow was mostly determined by spermine, in the case of ADA capillary enzyme reactor–CZE, the buffer did not contain any additive that would almost exclusively control the magnitude and direction of the flow. When operating the tandem capillary enzyme reactor–CZE under electromigration mode, the net electroosmotic flow of the tandem system was a function of the isoelectric point of the immobilized enzyme. In fact, as shown in Table I, at pH 6.5, *i.e.*, at pH higher than the isoelectric point of ADA (p*I* = 4.50–5.05), no significant change in the magnitude of the electroosmotic flow was observed upon connecting the capillary enzyme reactor to the separation capillary in series. However, as the pH of the running electrolyte approached the isoelectric point of the immobilized protein, a continuous drop in the electroosmotic flow was detected. The electro-

TABLE I

VALUES OF THE ELECTROOSMOTIC FLOW-RATE, EOF, AND PLATE HEIGHT, *H*, MEASURED FROM PHENOL PEAK

The measurements were performed on interlocked polyether capillaries, I-200, and tandem ADA capillary enzyme reactor-interlocked polyether capillary, ADA–I-200, at various pH values of the running electrolyte. ADA capillary enzyme reactor; 15 cm total length × 50 μm I.D., cennected to an interlocked polyether capillary of 64 cm (total length) and 30 cm to the detection point; I-200 capillary, two connected interlocked polyether capillaries of 15 and 64 cm in length, respectively; electrolytes, 0.1 *M* phosphate at different pH; field strength, 190 V/cm.

Capillary type	pH 6.50		pH 5.50		pH 5.00		pH 4.50	
	EOF (nl/min)	*H* (μm)	EOF (nl/min)	*H* (μm)	EOF (nl/min)	*H* (μm)	EOF (nl/min)	*H* (μm)
I-200	37.5	8.47	29.9	10.1	17.7	12.8	8.0	19.0
ADA–I-200	36.3	8.18	30.4	10.3	12.6	18.6	–	–

osmotic flow was reduced by 30% at pH 5.0 and at pH 4.5 there was practically no flow. This can be attributed in part to the fact that the net charge of the immobilized protein becomes positive at a pH lower than its isoelectric point. It should be noted that the unreacted amino groups of the aminopropylsilyl coating could also contribute to the reduction of the flow and inverting its direction at pH 4.5. As can be seen in Table I, the plate height measured from the peak of phenol increased from 12.8 to 18.6 μm when going from the I-200 to the ADA-I-200 capillary at pH 5.0. This is because the solute stayed longer in the ADA-I-200 capillary. This study revealed interesting fundamental points concerning the operation of capillary with immobilized enzymes on the inner walls in tandem with CZE. Since the flow was unaffected at the pH of maximum enzyme activity (*i.e.*, pH 6.5), such an arrangement can be exploited without any adverse effects on separation.

The ADA capillary enzyme reactor converted its substrate to a product that is more readily separated from other nucleosides. Fig. 16a depicts the electropherogram of a mixture of 3 nucleosides, namely cytidine, adenosine and inosine. Under these conditions both cytidine and adenosine practically coeluted but were resolved from inosine. However, after passing the mixture through the ADA capillary enzyme reactor, two well resolved peaks for cytidine and inosine were obtained (see Fig. 16b). Besides

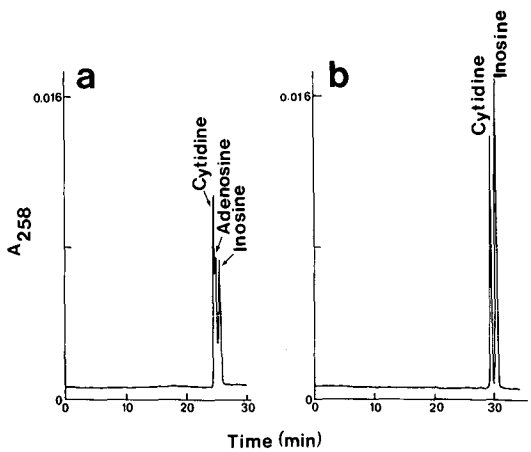

Fig. 16. Typical electropherograms of a mixture of cytidine, adenosine and inosine obtained by CZE alone (a) or by tandem ADA capillary enzyme reactor–CZE (b). Conditions as in Fig. 15.

playing the role of peak locator, the ADA capillary enzyme reactor can facilitate the quantitative determination of the analyte of interest. For instance, in situations similar to Fig. 16, the cytidine solute can be determined with good accuracy, since the previously overlapping peak of adenosine has been completely converted to inosine. In addition, the increase in the peak height of inosine can be used for the quantitative determination of adenosine.

It should be noted that the conversion of adenosine to inosine was complete even when the ADA capillary enzyme reactor was shortened to 3 cm, which correspond to a contact time of *ca.* 2 min with the enzyme reactor. From this finding, and provided that the enzymic reactions are kinetically favored, various short capillary enzyme reactors having different immobilized enzymes can be connected in series at the inlet of a separation capillary and may prove useful in the specific analysis of different solutes in a complex biological mixture.

CONCLUSIONS

In summary, the coupling of immobilized capillary enzyme reactors to capillary zone electrophoresis has proved suitable in the area of nucleic acids. The coupled format, which we refer to as enzymophoresis can be regarded as separation-based sensors with superimposed selectivities. While the enzyme provides the selective conversion of the substrates, CZE with its unique selectivity separates and detects the products. The various concepts developed and tested in this report can be transposed to electrophoretic systems involving other types of species of relevance to many areas of the life sciences and biotechnology. The enzymophoresis systems in miniature have provided the following: (i) repeated use and long term stability of enzymes, (ii) conversion of unseparable analytes to well resolved products (iii) peak identification of the analyte of interest, (iv) simultaneous synthesis and separation of ng quantities of biological species, (v) improved the reliability of CZE in the quantitative determination of analytes, and (vi) on-line digestion and mapping of biopolymers. The fact that enzymophoresis involving coupled HCER–CZE lends itself to automation will add another dimension to the capability of CZE in many areas of the life sciences.

ACKNOWLEDGEMENTS

This work was supported by the College of Arts and Sciences, Dean Incentive Grant Program at Oklahoma State University, and in part form grant No. HN9-004 from the Oklahoma Center for the Advancement of Sciences and Technology, Oklahoma Health Research Program.

REFERENCES

1 P. R. Brown, *J. Chromatogr.*, 52 (1970) 257.
2 P. Manson and D. Combes, *Methods Enzymol.*, 137 (1988) 584.
3 L. D. Bowers, *Anal. Chem.*, 58 (1976) 513A.
4 L. D. Bowers and W. D. Bostick, in F. Frei and J. F. Lawrence (Editors), *Chemical Derivatization in Analytical Chemistry*, Vol. 2, Plenum Press, New York, 1982, p. 97.
5 L. Dalgaard, *Trends Anal. Chem.*, 5 (1986) 185.
6 K. Shimada, T. Oe and T. Nambara, *J. Chromatogr.*, 492 (1989) 345.
7 L. D. Bowers and P. R. Johnson, *Biochim. Biophys. Acta*, 161 (1981) 111.
8 Z. El Rassi and Cs. Horváth, *J. Chromatogr.*, 266 (1983) 319.
9 K. A. Cobb and M. Novotny, *Anal. Chem.*, 61 (1989) 2226.
10 W. Nashabeh and Z. El Rassi, *J. Chromatogr.*, 559 (1991) 367.
11 W. Nashabeh and Z. El Rassi, *J. Chromatogr.*, submitted for publication.
12 F. I. Onuska, M. E. Comba, T. Bistricki and R. J. Wilkinson, *J. Chromatogr.*, 142 (1977) 117.
13 R. A. Wallingford and A. G. Ewing, *Adv. Chromatogr.*, 29 (1989) 1.
14 J. Cai and Z. El Rassi, *J. Liq. Chromatogr.*, in press.
15 A. D. McLaren and L. Packer, *Adv. Enzymol.*, 28 (1975) 61.
16 Cs. Horváth and J. M. Engasser, *Biotechnol. Bioeng.*, 16 (1974) 909.
17 V. Dolnik, J. Liu, J. F. Banks, Jr. and M. Novotny, *J. Chromatogr.*, 480 (1989) 321.
18 T. Uchida and F. Egami, *Methods Enzymol.*, 12 (1967) 228.
19 H. Hayashi and F. Egami, *J. Biochem (Tokyo)*, 53 (1963) 176.
20 P. R. Whitfield and H. Witzel, *Biochim. Biophys. Acta*, 72 (1963) 338.
21 L. W. McLaughlin and E. Craesen, *J. Liq. Chromatogr.*, 5 (1982) 2061.
22 K. Sato-Asano, *J. Biochem (Tokyo)*, 48 (1960) 284.
23 S. Irie, T. Itoh, T. Ueda and F. Egami, *J. Biochem (Tokyo)*, 68 (1970) 163.
24 H. Ito, M. Hagiwara, K. Takahashi and I. Ichikizaki, *J. Biochem (Tokyo)*, 82 (1977) 877.
25 W. Lamprecht and I. Trantschold, in H. U. Bergmeyer (Editor), *Methods of Enzymatic Analysis*, Academic Press, New York, 1963, pp. 543–551.
26 D. Voet and J. G. Voet, *Biochemistry*, Wiley, New York, 1990, pp. 430–431.
27 C. J. O. R. Morris and P. Morris, *Separation Methods in Biochemistry*, Wiley, New York, 2nd ed., 1976, p. 721.
28 H. Mollering and H. U. Bergmeyer, in H. U. Bergmeyer (Editor), *Methods of Enzymatic Analysis*, Academic Press, New York, 1965, pp. 491–494.

Journal of Chromatography, 596 (1992) 265–270
Elsevier Science Publishers B.V., Amsterdam

CHROM. 23 938

Determination of limiting ionic mobilities and dissociation constants of some local anaesthetics

Miroslav Polášek and Bohuslav Gaš*

Department of Physical and Macromolecular Chemistry, Faculty of Sciences, Charles University, Albertov 2030, 128 40 Prague 2 (Czechoslovakia)

Takeshi Hirokawa

Faculty of Engineering, Hiroshima University, Higashi-Hiroshima 724 (Japan)

Jiří Vacík

Department of Physical and Macromolecular Chemistry, Faculty of Sciences, Charles University, Albertov 2030, 128 40 Prague 2 (Czechoslovakia)

(First received September 24th, 1989; revised manuscript received December 9th, 1991)

ABSTRACT

The limiting ionic mobilities and thermodynamic acid dissociation constants were calculated from isotachophoretic experiments for the local anaesthetics procaine, tetracaine, lidocaine, trimecaine, bupivacaine, cinchocaine, diperodone, diocaine, cocaine, psicaine-neu, tropacocaine, amylocaine, β-eucaine and leucinocaine. The pH values at which the local anaesthetics with very similar limiting ionic mobilities can be isotachophoretically separated were determined from simulated mobility curves. The measuring apparatus employed a high-frequency contactless conductivity detector.

INTRODUCTION

Capillary isotachophoresis has already been used to separate local anaesthetics (LAs), *e.g.*, in the control of the composition of various pharmaceuticals [1–3], the determination of trimecaine in plasma [4] and separations of model mixtures [5,6] (the LAs were characterized in terms of the relative zone heights at pH 4.75, 5.4 and 6.2). Hence the determination of the mobilities and dissociation constants of these compounds would be useful not only for isotachophoresis but also for other electromigration methods. The utility of isotachophoresis as a technique for the measurement of these physicochemical constants has already been reported [7–13]. It is based on the measurement of the observed R_E values ($R_E = R_S/R_L$, where R_S is the resistance of the sample zone and R_L is the resistance of the leading electrolyte) with different leading electrolyte pH_L values.

This work was aimed at the determination of the above characteristics for fourteen LAs as the limiting ionic mobilities are not available in the literature and only a few pK values, some of them approximate, are known. On the basis of these values, experimental conditions can be found for isotachophoretic separation of the LAs, including those with very similar ionic mobilities.

EXPERIMENTAL

The isotachophoretic measurements were carried out on an apparatus with a PTFE separating capillary tube and a high-frequency contactless conduc-

0021-9673/92/$05.00

tivity detector [14–16]. The sensing electrodes of the detector are not in galvanic contact with the electrolyte inside the capillary tube, hence electrode processes which may occur on the electrodes of direct-contact conductivity detectors, especially at high pH, are prevented. The measuring cell and the part of capillary tube inside the cell were thermostated at 25°C.

It follows from the structures of the LAs that they are mostly basic, forming stable crystalline salts with acids which are readily soluble in water. The LAs used were obtained from the Faculty of Medicine, Palacký University, Olomouc, Czechoslovakia, in the form of the hydrochlorides, except for leucinocaine, which was in the form of the methanesulphate. In isotachophoretic experiments, it is often difficult to find a suitably slow terminating ion, and therefore measured LAs were used in stead of samples as the terminating electrolytes, at a concentration of 0.005 *M*. The leading ion was Na^+ in all the measurement, its concentration in the leading electrolyte being 0.01 *M* and its limiting ionic mobility assumed to be $51.9 \cdot 10^{-9}$ m^2 V^{-1} s^{-1}. Acetic acid, DL-α-alanine (both of analytical-reagent grade from Lachema, Brno, Czechoslovakia), 2-morpholinoethanesulphonic acid (Fluka, Buchs, Switzerland), 2-morpholinopropanesulphonic acid (Sigma, St. Louis, MO, USA), glycylglycine (Nutritional Biochemicals, Cleveland, OH, USA) and L-histidine (Merck, Darmstadt, Germany) were used one after another as the buffering anionic counter compounds in the leading electrolyte.

The same approach for the determination of the mobilities and pK values as described previously [7,8] was used, *i.e.*, measured R_E values were analysed by the computational program which iteratively fits the experimental data by a simulated curve using the least-squares method. Limiting ionic mobilities and pK_A values of all compounds used as input data in the calculations are listed in Table I.

The limiting anionic mobility of 2-morpholinopropanesulphonic acid has not been published previously, so it was determined isotachophoretically using system 0.01 *M* Cl^- plus ethanolamine as leading electrolyte. Ethanolamine (Sigma) was freshly distilled before measurement.

TABLE I

PHYSICO-CHEMICAL CONSTANTS USED AS INPUT DATA IN CALCULATION (25°C)

U^0 = Limiting ionic mobility (10^{-9} m^2 V^{-1} s^{-1}); pK_A = thermodynamic acid dissociation constant; HAc = acetic acid; MES = 2-morpholinoethanesulphonic acid; MOPS = 2-morpholinopropanesulphonic acid; Gly–Gly = glycylglycine; His = L-histidine; Ala = DL-α-alanine; EA = ethanolamine.

Compound	U^0	pK_A
Cl^-	−79.1[a]	−2[a]
HAc	−42.4[a]	4.756[a]
MES	−28.0[a]	6.095[a]
MOPS	−26.9[b]	7.2[c]
Gly–Gly	−31.5[d]	8.2[c]
His	−28.3[e]	9.33[e]
Ala	−32.2[e]	9.857[e]
EA	44.3[a]	9.498[a]

[a] Values taken from ref. 11.
[b] Value obtained isotachophoretically.
[c] Values taken from ref. 17.
[d] Value taken from ref. 13.
[e] Values taken from ref. 12.

RESULTS AND DISCUSSION

The results of the measurements, *i.e.*, R_E^{expti} values, together with the experimental conditions are listed in Table II. The R_E^{theor} values, effective mobilities (U_{eff}) and pH_S values in the sample zones calculated on the basis of a least-squares fit are also given. The determination of the limiting ionic mobilities (U^0) and pK_A values was performed according to the isotachophoretic steady-state model and the values obtained are given in Table III. The dissociation constants found in the literature [18,19] are also given for comparison.

When the pH_L value of the leading electrolyte is low and thus the pH_S values in the zones are also low, then the weak bases are virtually completely dissociated; the LAs are in the cationic form and the ionic mobilities equal the effective mobility (U_{eff}). The mobility curves (U_{eff} *vas* pH_S; Fig. 1a–d) were calculated for four groups of LAs according to the limiting mobilities.

It is apparent from the mobility curves that diperodone differs from the other LAs and can be separated from them in systems with a pH_L of the leading electrolyte from 6 to 7. The effective mobility of the other LAs is efficiently influenced in systems with pH *ca.* 7–8. However, LA separations at higher pH values show certain limitations. The concen-

TABLE II

OBSERVED AND CALCULATED PHYSICO-CHEMICAL VALUES FOR LOCAL ANAESTHETICS (25°C)

pH_L = Experimentally measured pH of the leading electrolyte; buffer = compound used as buffer in the leading electrolyte (abbreviations as in Table I); R_E^{exptl} = experimentally measured R_E value; R_E^{theor} = theoretically calculated R_E value; U_{eff} theoretically calculated effective mobility corrected for ionic strength (10^{-9} m^2 V^{-1} s^{-1}); pH_S = theoreticaly calculated pH in the sample zone.

LA	pH_L	Buffer	R_E^{exptl}	R_E^{theor}	U_{eff}	pH_S
Cinchocaine	4.42	HAc	2.81	2.77	17.33	4.11
	4.72	HAc	2.80	2.78	17.30	4.43
	5.62	MES	2.79	2.81	17.13	5.41
	6.25	MES	2.80	2.81	17.09	6.04
	6.60	MES	2.80	2.82	17.14	6.38
	6.87	MES	2.81	2.83	17.04	6.63
	7.11	MOPS	2.87	2.87	16.75	6.89
	7.46	MOPS	2.96	2.95	16.27	7.24
Diperodone	4.42	HAc	2.79	2.74	17.54	4.12
	4.72	HAc	2.80	2.75	17.46	4.43
	5.62	MES	2.82	2.86	16.80	5.40
	5.95	MES	2.87	2.95	16.34	5.70
	6.30	MES	3.04	3.13	15.41	5.98
	6.60	MES	3.32	3.32	14.49	6.17
	6.87	MES	3.60	3.50	13.79	6.28
Diocaine	4.42	HAc	2.70	2.70	17.83	4.13
	4.72	HAc	2.72	2.70	17.79	4.44
	6.25	MES	2.74	2.73	17.62	6.05
	6.60	MES	2.70	2.72	17.70	6.40
	6.87	MES	2.71	2.73	17.67	6.66
	7.11	MOPS	2.76	2.75	17.47	6.91
Bupivacaine	4.42	HAc	2.57	2.56	18.77	4.15
	4.72	HAc	2.57	2.57	18.73	4.46
	5.62	MES	2.58	2.59	18.56	5.43
	6.25	MES	2.58	2.60	18.47	6.06
	6.60	MES	2.59	2.61	18.46	6.39
	6.87	MES	2.65	2.64	18.28	6.63
	7.11	MOPS	2.72	2.70	17.80	6.90
	7.46	MOPS	2.85	2.83	16.96	7.23
	7.72	Gly–Gly	2.99	2.98	16.21	7.45
	7.90	Gly–Gly	3.11	3.13	15.39	7.59
Leucinocaine	5.03	HAc	2.53	2.51	19.13	4.78
	6.25	MES	2.53	2.53	18.99	6.07
	7.00	MOPS	2.54	2.54	18.93	6.82
	7.53	MOPS	2.55	2.57	18.73	7.36
	7.90	Gly–Gly	2.58	2.58	18.67	7.69
	8.12	Gly–Gly	2.63	2.62	18.38	7.90
Psicaine-neu	4.42	HAc	2.46	2.47	19.43	4.14
	5.03	HAc	2.48	2.48	19.36	4.79
	5.62	MES	2.48	2.50	19.23	5.44
	6.25	MES	2.53	2.51	19.19	6.07
	7.00	MOPS	2.56	2.54	18.92	6.82
	7.53	MOPS	2.63	2.64	18.23	7.33
Trimecaine	4.42	HAc	2.44	2.42	19.86	4.17
	5.62	MES	2.45	2.45	19.65	5.45
	6.25	MES	2.46	2.47	19.47	6.07
	6.87	MES	2.52	2.53	19.05	6.61
	7.11	MOPS	2.63	2.63	18.29	6.89
	7.46	MOPS	2.85	2.83	17.01	7.20
	7.72	Gly–Gly	3.02	3.06	15.77	7.42
	7.90	Gly–Gly	3.21	3.28	14.69	7.55
	8.24	Gly–Gly	3.81	3.81	12.65	7.76
	8.39	Gly–Gly	4.14	4.07	11.85	7.83

(Continued on p. 268)

TABLE II (*continued*)

LA	pH_L	Buffer	R_E^{exptl}	R_E^{theor}	U_{eff}	pH_S
β-Eucaine	5.03	HAc	2.36	2.34	20.54	4.80
	6.25	MES	2.37	2.35	20.42	6.09
	7.53	MOPS	2.39	2.37	20.24	7.38
	8.12	Gly–Gly	2.39	2.40	20.10	7.93
	8.67	Gly–Gly	2.48	2.51	19.11	8.41
	9.06	His	2.70	2.76	17.44	8.80
	9.33	His	3.03	2.98	16.18	8.99
	9.55	His	3.21	3.20	15.02	9.12
	9.83	His	3.48	3.48	13.81	9.24
	10.12	Ala	4.28	4.28	11.23	9.48
Tetracaine	4.42	HAc	2.35	2.31	20.77	4.19
	5.62	MES	2.36	2.33	20.59	5.46
	6.60	MES	2.38	2.35	20.50	6.42
	7.00	MOPS	2.41	2.40	20.01	6.82
	7.46	MOPS	2.50	2.52	19.04	7.26
	7.72	Gly–Gly	2.59	2.63	18.28	7.48
	7.90	Gly–Gly	2.72	2.77	17.44	7.63
	8.14	Gly–Gly	2.96	2.99	16.14	7.80
	8.39	Gly–Gly	3.27	3.26	14.78	7.95
	8.64	Gly–Gly	3.60	3.55	13.61	8.07
Lidocaine	5.03	HAc	2.34	2.29	20.97	4.81
	6.25	MES	2.33	2.34	20.57	6.08
	6.71	MOPS	2.38	2.40	20.02	6.53
	7.11	MOPS	2.50	2.52	19.05	6.89
	7.53	MOPS	2.75	2.80	17.18	7.24
	7.86	Gly–Gly	3.17	3.21	15.03	7.51
	8.05	Gly–Gly	3.50	3.51	13.71	7.63
	8.28	Gly–Gly	3.96	3.90	12.36	7.75
Cocaine	5.03	HAc	2.28	2.25	21.37	4.82
	6.25	MES	2.28	2.27	21.21	6.09
	7.11	MOPS	2.29	2.30	20.92	6.95
	7.53	MOPS	2.33	2.36	20.39	7.36
	7.82	Gly–Gly	2.41	2.43	19.83	7.65
	8.28	Gly–Gly	2.62	2.65	18.22	7.99
	8.69	Gly–Gly	2.96	2.94	16.34	8.23
	8.81	His	3.43	3.38	14.23	8.45
	9.06	His	3.83	3.91	10.79	8.61
	9.33	His	4.49	4.45	10.81	8.74
Amylocaine	5.03	HAc	2.13	2.10	22.78	4.84
	6.25	MES	2.15	2.14	22.42	6.10
	7.00	MOPS	2.23	2.25	21.33	6.83
	7.53	MOPS	2.46	2.50	19.22	7.28
	7.86	Gly–Gly	2.77	2.83	17.06	7.55
	8.05	Gly–Gly	3.03	3.07	15.66	7.68
	8.28	Gly–Gly	3.43	3.40	14.21	7.80
	8.45	Gly–Gly	3.69	3.64	13.20	7.89
Procaine	4.72	HAc	2.13	2.09	22.98	4.53
	6.60	MES	2.10	2.10	22.94	6.46
	7.53	MOPS	2.17	2.15	22.36	7.39
	8.14	Gly–Gly	2.23	2.25	21.43	7.94
	8.39	Gly–Gly	2.34	2.34	20.58	8.15
	8.72	His	2.62	2.62	18.41	8.47
	9.01	His	2.88	2.94	16.38	8.68
	9.19	His	3.19	3.19	15.11	8.79
	9.33	His	3.42	3.40	14.19	8.86

TABLE II (*continued*)

LA	pH_L	Buffer	R_E^{exptl}	R_E^{theor}	U_{eff}	pH_S
Tropacocaine	5.03	HAc	2.12	2.07	23.22	4.85
	6.25	MES	2.10	2.08	23.10	6.12
	7.53	MOPS	2.13	2.10	22.85	7.40
	8.12	Gly–Gly	2.14	2.14	22.50	7.95
	8.69	Gly–Gly	2.27	2.29	21.03	8.42
	9.06	His	2.55	2.57	18.69	8.80
	9.33	His	2.83	2.82	17.09	8.97
	9.55	His	3.02	3.05	15.75	9.09
	9.83	His	3.34	3.33	14.42	9.20
	10.12	Ala	4.23	4.22	11.38	9.43

tration of the non-ionized free base in the zone increases with increasing pH_L. The non-ionized form of some bases is poorly soluble in water and may precipitate in the zone at a certain pH. With a common concentration of the leading electrolyte of 0.01 *M*, diperodone precipitates at about pH_L 7.0, diocaine at pH_L 7.4, cinchocaine at pH_L 7.7, psicaine-neu at pH_L 7.8, bupivacaine at pH_L 8.1 and leucinocaine at pH_L 8.3. The pH_L values at which the sample precipitates can be increased by decreasing the leading electrolyte concentration; therefore, at higher pH_L of the leading electrolyte, analysis should be performed with a lower concentration of the leading electrolyte.

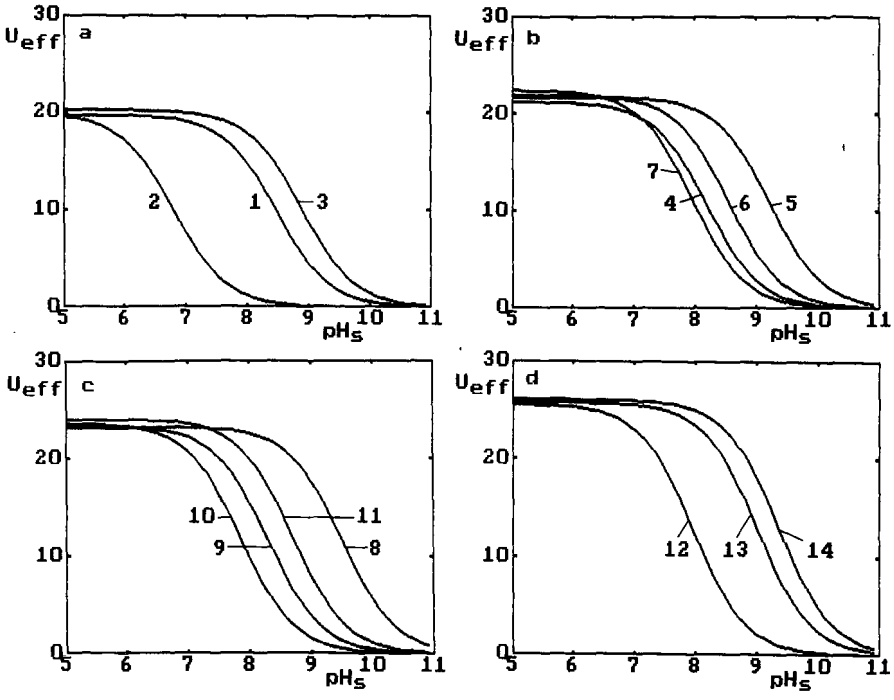

Fig. 1. Mobility curves for the local anaesthetics. U_{eff} = effective mobility (10^{-9} m^2 V^{-1} s^{-1}), pH_S = pH of the sample zone. (a) 1 = Cinchocaine; 2 = diperodone; 3 = diocaine; (b) 4 = bupivacaine; 5 = leucinocaine; 6 = psicaine-neu; 7 = trimecaine; (c) 8 = β-eucaine; 9 = tetracaine; 10 = lidocaine; 11 = cocaine; (d) 12 = amylocaine; 13 = procaine; 14 = tropacocaine. The U_{eff} and pK values are not corrected for the ionic strength.

TABLE III

CALCULATED LIMITING IONIC MOBILITIES, U^0, AND THERMODYNAMIC ACID DISSOCIATION CONSTANTS, pK_A (25°C)

U^0 in 10^{-9} m^2 V^{-1} s^{-1}; pK_{lit} = dissociation constant from literature; σ = standard deviation of a single measurement.

Compound	U^0	σ	pK_A	σ	pK_{lit}
Cinchocaine	19.7	0.1	8.47	0.08	8.31[a]
Diperodone	19.9	0.3	6.79	0.07	8.44[a]
Diocaine	20.2	0.1	8.88	0.34	–
Bupivacaine	21.2	0.1	8.19	0.02	–
Leucinocaine	21.7	0.1	9.21	0.05	9.4[b]
Psicaine-neu	21.9	0.1	8.54	0.09	–
Trimecaine	22.4	0.2	7.95	0.02	7.96[a]
β-Eucaine	23.2	0.1	9.50	0.02	9.35[a]
Tetracaine	23.3	0.2	8.29	0.02	8.5[b]
Lidocaine	23.6	0.2	7.85	0.02	7.84[a]
Cocaine	24.0	0.2	8.69	0.02	8.4[b]
Amylocaine	25.5	0.2	7.96	0.02	8.09[a]
Procaine	25.7	0.2	9.01	0.02	8.98[a]
Tropacocaine	26.0	0.2	9.36	0.01	9.9[b]

[a] From ref. 19.
[b] From ref. 18.

ACKNOWLEDGEMENTS

Dr. Zdeněk Stránský of Palacký University, Olomouc, Czechoslovakia, is thanked for kindly providing the samples of local anaesthetics.

REFERENCES

1 *Pharmacopée Francaise*, X ed., Adrapharm, Paris, 1982.
2 H. Klein, *Drug Res.*, 32 (1982) 795.
3 S. Fanali, F. Foret and P. Boček, *J. Chromatogr.*, 330 (1985) 436.
4 Z. Stránský, Z. Chmela, P. Peč and L. Šafařík, *J. Chromatogr.*, 342 (1985) 167.
5 Z. Chmela, J. Čižmárik and Z. Stránský, *Pharmazie*, 40 (1985) 731.
6 Z. Chmela, *Thesis*, Palacký University, Olomouc, 1987.
7 T. Hirokawa and Y. Kiso, *J. Chromatogr.*, 252 (1982) 33.
8 T. Hirokawa, M. Nishino and Y. Kiso, *J. Chromatogr.*, 252 (1982) 49.
9 T. Hirokawa and Y. Kiso, *J. Chromatogr.*, 257 (1983) 197.
10 T. Hirokawa and Y. Kiso, *J. Chromatogr.*, 260 (1983) 225.
11 T. Hirokawa, M. Nishino, N. Aoki, Y. Kiso, Y. Sawamoto, T. Yagi and J. Akiyama, *J. Chromatogr.*, 271 (1983) D1.
12 T. Hirokawa, T. Gojo and Y. Kiso, *J. Chromatogr.*, 369 (1986) 59.
13 T. Hirokawa, T. Gojo and Y. Kiso, *J. Chromatogr.*, 390 (1987) 201.
14 B. Gaš, M. Demjaněnko and J. Vacík, *J. Chromatogr.*, 192 (1980) 253.
15 B. Gaš and J. Vacík, *Chem. Listy*, 74 (1980) 652.
16 J. Vacík, J. Zuska and I. Muselasová, *J. Chromatogr.*, 320 (1985) 233.
17 *Sigma Catalog*, Sigma, St. Louis, MO, 1990.
18 A. Albert and E. P. Serjeant, *The Determination of Ionization Constants*, Chapman & Hall, London, New York, 1984.
19 D. D. Perrin, *Dissociation Constants of Organic Bases in Aqueous Solutions*, Butterworths, London, 1965.

Journal of Chromatography, 596 (1992) 271–275
Elsevier Science Publishers B.V., Amsterdam

CHROM. 24 023

Short Communication

Phenylboronic acid as a versatile derivatization agent for chromatography of ecdysteroids

Jaroslav Píš* and Juraj Harmatha

Institute of Organic Chemistry and Biochemistry, Czechoslovak Academy of Sciences, Flemingovo náměstí 2, 166 10 Prague (Czechoslovakia)

(First received November 8th, 1991; revised manuscript received January 21st, 1992)

ABSTRACT

Phenylboronic acid can react with the diol group to form a cyclic boronate. This reagent forms stable boronates with ecdysteroids possessing a 20,22-diol group in quantitative yield. The stability of these boronates enables the presence of a 20,22-diol group in ecdysteroids to be detected on the basis of their changed chromatographic properties. On the basis of this reaction, simple and efficient thin-layer and high-performance liquid chromatographic methods were developed.

INTRODUCTION

Ecdysteroids are significant hormones controlling the mechanism of moulting and metamorphosis of arthropods. They regulate whole series of their important physiological functions. The steroid character of these substances and their unusually broad distribution in living organisms (especially in plants) indicates that they may also have further, so far undiscovered, biological functions. The ecdysteroids from plants (phytoecdysones) [1] occur in a richer structural variety than zooecdysones [2]. They are usually more hydroxylated, either in the free form or in an ester or glycosidic form. They are nearly always present in complex mixtures of one or two main constituents and of several additional minor derivatives or analogues showing some small structural variations. The composition of the main and minor constituents is often changed in the course of phylogenetic development and, moreover, their content varies in the different organs of the plant. It is therefore important to have suitable simple and specific methods for the rapid detection and facile identification or characterization of these substances in complex mixtures of plant extracts. One such method is based on the use of the rapid and quantitative reactivity of phenylboronic acid with the diol group in the ecdysteroid molecule [3].

The usefulness of boronic acids has been demonstrated in carbohydrate chemistry [4]. Methaneboronic acid [5], phenylboronic acid [6] and ferroceneboronic acid [7] have been used for the gas chromatographic–mass spectrometric analysis of bifunctional compounds. Diphenylborate–ethanolamine complex has been used for the isolation of catecholamines from body fluids [8]. Phenylboronic acid has been used for the protection of 1,2- and 1,3-diols [9] and in the organic synthesis of chiral compounds [10]. It produces cyclic boronates. The stability of the boronates depends on the nature of the diols used. Many boronates are moisture sensitive and unstable under protic conditions. More hin-

0021-9673/92/$05.00

dered diols form more hydrolytic stable boronates. Different solvents can be used for the preparation of boronates. Their choice depends on the solubility of the reacted diol. Common solvents used for this reaction are pyridine, tetrahydrofuran, dimethylformamide (DMF) and acetone. Water is liberated in the course of the esterification reaction, hence molecular sieves or water scavengers such as 2,2-dimethoxypropane are usually added to the reaction mixture for the preparation of moisture-sensitive boronates.

With ecdysteroids, phenylboronic acid has been used for the protection of the diol system in the side-chain of cyasterone [11]. Other aromatic boronic acids, *e.g.*, phenanthreneboronic acid [12] and dansylaminophenylboronic acid [13], have been used as fluorescence labels in the analysis of ecdysteroids. Phenylboronic acid immobilized on silica gel has been used for the solid-phase extraction of ecdysteroids [14]. Ecdysones frequently contain two diol systems, one in the 2,3-position and the other in the 20,22-position of the side-chain. Phenylboronate is formed exclusively from the diol in the side-chain (Fig. 1), even if an excess of reagent is present in the reaction mixture. The reaction is quantitative and ecdysteroid boronates are unusually stable under protic conditions. The derivatization reaction results in a change in the chromatographic behaviour of reacted compounds. This property can be utilized for simple checking of the presence of the 20,22-diol system in the ecdysteroid molecule based on chromatographic methods.

EXPERIMENTAL

Chemicals

Dichloromethane and methanol (Lachema, Brno, Czechoslovakia) were redistilled and water was deionized and redistilled. Ecdysteroids, *i.e.*, 20-hydroxyecdysone-2,3-acetonide (**I**), ponasterone A (**II**), 20-hydroxyecdysone-20,22-acetonide (**III**), polypodine B (**IV**), ecdysone (**V**) and 20-hydroxyecdysone (**VI**), were isolated from *Blechnum spicant* L. [15].

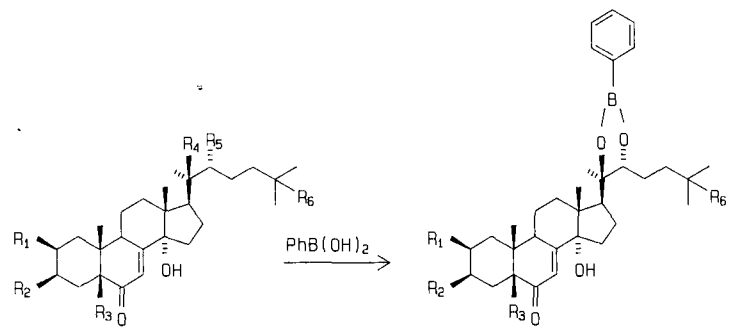

	R_1	R_2	R_3	R_4	R_5	R_6
I	A		H	OH	OH	OH
II	OH	OH	H	OH	OH	H
III	OH	OH	H	A		OH
IV	OH	OH	OH	OH	OH	OH
V	OH	OH	H	H	OH	OH
VI	OH	OH	H	OH	OH	OH

	R_1	R_2	R_3	R_6
VII	A		H	OH
VIII	OH	OH	H	H
IX	OH	OH	OH	OH
X	OH	OH	H	OH

A= $(CH_3)_2C$ <O, O>

Fig. 1. Structures of ecdysteroids and their phenylboronate derivatives.

Phenylboronic acid (phenyldihydroxyborane, benzeneboronic acid) was prepared according to a common procedure [16].

Preparation of reference compounds, boronates ***VII–X***

All boronates were prepared according to the following general procedure. Ecdysteroid (3–8 mg) was dissolved or suspended in a suitable solvent (methanol, DMF or acetone). Phenylboronic acid (1.2 equiv.) was added and the reaction mixture was stirred for 5–10 min or, when acetone was used, up to dissolution and then for an additional 5 min. After evaporation of the solvent, the reaction mixture was subjected to normal-phase high-performance liquid chromatography (HPLC), giving pure boronate in 80–90% yield. Identification of the reference boronates **VII–X** was accomplished by IR, mass and ^{1}H NMR spectroscopy [17].

Chromatography

Thin-layer chromatography (TLC) was performed in a glass chromatography tank containing an appropriate solvent. The atmosphere in the tank was allowed to presaturate before performing chromatographic separations. Merck silica gel 60 HPTLC aluminium sheets and Merck silica gel RP-8 reversed-phase HPTLC plates were used. The silica gel sheets were developed in methanol–chloroform (15:85, v/v) and the reversed-phase plates in methanol–water (70:30, v/v). The developed chromatograms were revealed by the induced fluorescence under UV light after spraying with sulphuric acid [18].

HPLC experiments were performed on a liquid chromatograph consisting of two Knauer Model 64 HPLC pumps and a Knauer variable-wavelength monitor. Samples were injected through a Rheodyne Model 7125 sampling valve. A Separon SGX (7 μm) silica gel column (250 mm × 4 mm I.D.) was used with dichloromethane–methanol–water (88:11:1, v/v/v) for isocratic elution at a flow-rate of 1.5 ml/min.

Procedure for TLC

Ecdysteroids dissolved in methanol were applied to the TLC plate, each compound as two spots. After evaporation of the solvent from the sample spots, an acetone solution of phenylboronic acid was applied to the second sample spot of each ecdysteroid. After 5 min the TLC plates were developed with a suitable solvent.

Procedure for HPLC

A solution of ecdysteroids **I–VI** in the mobile phase was used for the derivatization reaction. A dichloromethane solution of phenylboronic acid (up to 10 equiv.) was added to the solution of ecdysteroids containing *ca.* 15 μg of each compound. After shaking, the reaction mixture was allowed to react for 5 min and was then injected into the HPLC system.

Methanol and methanol–water (3:1, 1:1, 1:3 and 1:9, v/v) solutions of a crude extract containing 20-hydroxyecdysone (*ca.* 11%) from roots of *Leuzea carthamoides* (Willd.) were treated with a methanolic solution of phenylboronic acid (20 equiv. based on 20-hydroxyecdysone content). The reaction mixture was allowed to react for 15 min and was then injected into the HPLC system.

RESULTS AND DISCUSSION

TLC analysis

The reactivity of the side-chain diol-containing ecdysteroids with the phenylboronic acid on the sorbent surface was sufficiently fast and quantitative to provide unambiguous results. R_F values from silica gel plates are summarized in Table I. If a diol is present in the side-chain (compounds **I**, **II**, **IV** and **VI**), a difference between the R_F value of the original ecdysteroid and that of the ecdysteroid after reac-

TABLE I

R_F VALUES OF ECDYSTEROIDS AND THEIR BORONATES ON A SILICA GEL PLATE DEVELOPED WITH METHANOL–CHLOROFORM (15:85, v/v) AND DETECTED BY SPRAYING WITH SULPHURIC ACID

Ecdysteroid	R_F	Compound after reaction	R_F
I	0.51	**VII**	0.72
II	0.40	**VIII**	0.64
III	0.51	**III**	0.51
IV	0.27	**IX**	0.49
V	0.28	**V**	0.28
VI	0.22	**X**	0.42

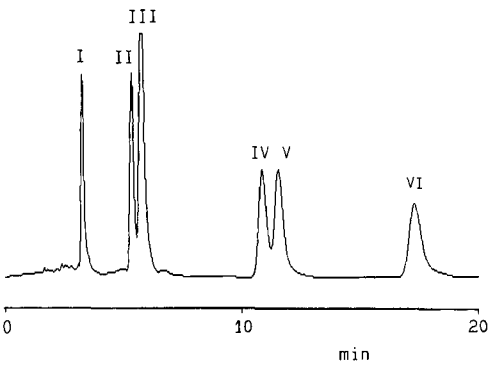

Fig. 2. Separation of ecdysteroids **I–VI** by silica HPLC.

tion was observed. With the reversed-phase RP-8 plates, boronates exhibit a shift of spots in comparison with the parent ecdysteroids. However, the shape of the boronate spots exhibited considerable deformation.

HPLC analysis

The HPLC separation of six ecdysteroids on a silica gel column is demonstrated on Fig. 2. Four of them, *viz.*, **I, II, IV** and **VI**, contain a diol in the side-chain and hence they are able to react with phenylboronic acid. The results of this small-scale reaction are demonstrated in Fig. 3. The presence of the diol function can be recognized from the total disappearance of the original ecdysteroid peaks. New peaks related to the boronates formed appear at shorter retention times. The relative elution order

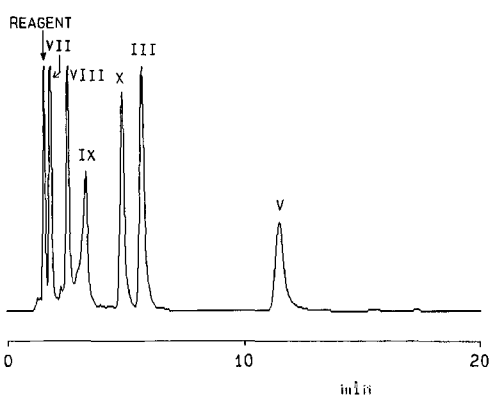

Fig. 3. Separation of ecdysteroids after reaction with phenylboronic acid by silica HPLC. Unreactive ecdysteroids, **III** and **V**; boronates formed, **VII–X**.

of the boronates is the same as that of the original ecdysteroids. The derivatization reaction is very rapid and in principle it could be carried out directly in the sample loop. Its quantitative course is limited here, however, by the reduced possibility of mixing the reaction components.

All efforts to perform such HPLC analyses in the reversed-phase mode failed, probably owing to the limited stability of the prepared boronates under these conditions. For *Leuzea carthamoides* extract the results were satisfactory when methanol was used because in this solvent reaction was complete. Equilibrium between free 20-hydroxyecdysone and its boronate occurred in water-containing solutions. The boronate-to-ecdysteroid ratio depends on the water content in reaction mixture. In methanol–water solution (10:90, v/v) only a 30% yield of the boronate was achieved.

In both TLC and HPLC analyses, the use of the normal-phase mode was more advantageous. The results of TLC analysis were equally conclusive as those of HPLC analysis, but the TLC method is less time consuming. Both methods have several advantages. They are fairly rapid and simple and they afford important structural information from microgram amounts of material. The information can be obtained directly by analysing complex mixtures, without isolation of the pure compounds.

REFERENCES

1 R. Lafont and D. H. S. Horn, in J. Koolman (Editor), *Ecdysone from Chemistry to Mode of Action*, Georg Thieme, Stuttgart, 1989, p. 39.
2 H. H. Rees, in J. Koolman (Editor), *Ecdysone from Chemistry to Mode of Action*, Georg Thieme, Stuttgart, 1989, p. 28.
3 J. Píš, J. Harmatha and K. Sláma, in I. Hrdý (Editor), *Insect Chemical Ecology, Proceedings of the Conference on Insect Chemical Ecology, Tábor, August 1990*, SPB Academic Publishing, The Hague, 1991, p. 227.
4 R. J. Ferrier, *Adv. Carbohydr. Chem. Biochem.*, 35 (1978) 31.
5 S. Takatsuto, B. Ying, M. Morisaki and N. Ikekawa, *J. Chromatogr.*, 239 (1982) 233.
6 C. F. Poole and A. Zlatkis, *J. Chromatogr.*, 184 (1980) 99.
7 C. J. W. Brooks, W. J. Coole and D. J. Robins, *Heterocycles*, 28 (1989) 151.
8 F. Smedes, J. C. Kraak and H. Poppe, *J. Chromatogr.*, 231 (1982) 25.
9 T. W. Greene, *Protective Groups in Organic Synthesis*, Wiley, New York, 1981.
10 D. S. Matteson, *Acc. Chem. Res.*, 21 (1988) 294.
11 D. Guédin-Vuong, Y. Nakaniti and G. Ourisson, *Croat. Chem. Acta*, 58 (1985) 547.

12 C. F. Poole, S. Singhawangcha, A. Zlatkis and E. D. Morgan, *J. High Resolut. Chromatogr. Chromatogr. Commun.*, 1 (1978) 96.
13 N. Ikekawa, *Trends Anal. Chem.*, 9 (1990) 337.
14 I. D. Wilson, E. D. Morgan and S. J. Murphy, *Anal. Chim. Acta*, 236 (1990) 145.
15 J. Píš, M. Budĕšínský and J. Harmatha, *Phytochemistry*, submitted for publication.
16 F. R. Bean and J. R. Jonson, *J. Am. Chem. Soc.*, 54 (1932) 4115.
17 J. Píš, J. Hykl, M. Budĕšínský and J. Harmatha, in preparation.
18 M. W. Gilgan and M. E. Zinc, *Steroids*, 20 (1972) 95.

Journal of Chromatography, 596 (1992) 276–280
Elsevier Science Publishers B.V., Amsterdam

CHROM. 24 046

Short Communication

Analytical studies of isorhoeadine and rhoeagenine in petal extracts of *Papaver rhoeas* L. using high-performance liquid chromatography

Jean-Pierre Rey*, Joël Levesque and Jean-Louis Pousset

Laboratoire de Pharmacognosie, Faculté de Médecine et de Pharmacie, 34 Rue du Jardin des Plantes, B.P. 199, 86005 Poitiers Cedex (France)

François Roblot

Laboratoire de Pharmacognosie, Faculté de Pharmacie, Rue J.B. Clément, 92296 Chatenay-Malabry (France)

(First received October 29th, 1991; revised manuscript received January 28th, 1992)

ABSTRACT

A low-pressure liquid chromatographic method on silica gel 60, with chloroform containing 0–1% (v/v) of methanol as eluent, is described that allows the isolation of isorhoeadine from the total alkaloids of petals of *Papaver rhoeas* L. A preparative high-performance liquid chromatographic (HPLC) method with a LiChrosorb Si 60 column, using chloroform containing 0–5% (v/v) of methanol (isocratic and then linear gradient) as mobile phase, is described that allows the isolation of rhoeagenine from a few fractions issuing from the previous low-pressure liquid chromatographic run. Finally, a selective analytical HPLC method with a Superspher Si 60 column using chloroform–methanol (90:10, v/v) containing 0.1% of trifluoroacetic acid as mobile phase and UV detection at 292.5 nm is described that allows the determination of isorhoeadine and rhoeagenine in red poppy extracts. In comparison with a classical chloroformic alkaloid extraction of petals from Maine et Loire (France) (total alkaloid efficiency = 0.203% dry material), a weak aqueous alcoholic acidic extract (30% ethanol) (0.216%) and an aqueous acidic extract (0.123%) of the same material, the amount of isorhoeadine is 71.1, 42.4 and 10.5 mg/g total alkaloids, respectively, and the amount of rhoeagenine is 629.7, 424.2 and 117.3 mg/g total alkaloids, respectively. Hence, the aqueous alcoholic acidic extract seems to be the most appropriate for conceiving a red poppy remedy.

INTRODUCTION

Further to our study of the application of high-performance liquid chromatography (HPLC) to the analysis of medicinal plant extracts with sedative properties, we have examined the components of *Papaver rhoeas* L. There have been numerous investigations into the alkaloidal constituents of this plant [1] and over 30 alkaloids have been isolated. It appears that *Papaver rhoeas* L. is variable in its alkaloid content and that different chemotypes exist [2]; the major alkaloid isolated proved to be rhoeadine [3,4], N-methylasimilobine [5] or rhoeagenine [6], depending on the plant source. The minor alkaloids are mainly protopine, isorhoeadine, isorhoeagine and papaverrubines [7]. Numerous studies on the rhoeadine–papaverrubine group of *P. rhoeas* L. have been made using thin-layer chromatography (TLC) [4,8–12], but no work has been reported on the determination of these alkaloids

0021-9673/92/$05.00

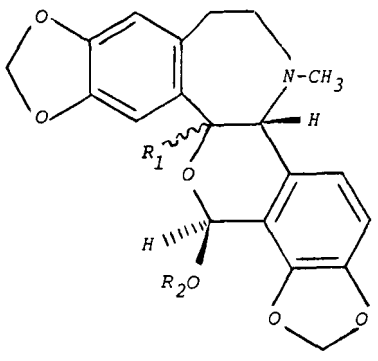

Rhoeagenine : R_1 = —H ; R_2 = H

Isorhoeadine : R_1 = ⁞⁞⁞ H ; R_2 = CH_3

using HPLC. We describe here a quantitative HPLC method for the determination of rhoeagenine and isorhoeadine, which can be used as specific tracers in petals of the plant.

EXPERIMENTAL

TLC

Silica gel Si 60 F_{254} plates were obtained from Merck (Darmstadt, Germany). The mobile phase was cyclohexane–diethylamine (80:20, v/v) and detection was effected with Dragendorff's reagent [12].

HPLC

A Varian Model 5000 chromatograph was used, equipped with a Rheodyne Model 7125 injector and a photodiode-array detector (Merck L 3000) under computer control (Merck HPLC Manager). Analyses were conducted at 20°C.

Preparative HPLC was carried out with a LiChrosorb Si 60 column (250 × 10 mm I.D., particle size 7 μm) (Merck). Two solvents were used, (A) chloroform and (B) methanol. The elution profile was as follows: 0–40 min, 100% A (isocratic); 41–46 min, 1% B in A (isocratic); 47–51 min, 2% B in A (isocratic); 52–61 min, 2–5% B in A (linear gradient). A flow-rate of 4 ml/min and UV detection at 280 nm were applied.

Analytical HPLC was carried out on a Superspher Si 60 normal-phase column (125 × 4 mm I.D., particle size 4 μm) (Merck), used with a LiChrospher Si 60 precolumn (4 × 4 mm I.D., particle size 5 μm) (Merck). The mobile phase was chloroform–methanol (90:10, v/v) containing 0.1% of trifluoroacetic acid (TFA) at a flow-rate of 1 ml/min. The injection volume was 10 μl and UV detection at 292.5 nm was applied.

Petal alkaloid extraction

A 500-g amount of petals [harvested in Maine et Loire (France)], dried at room temperature and finely powdered, was moistened with dilute ammonia solution and kept for 2 h before Soxhlet extraction with chloroform (5 l). The organic solution was evaporated under reduced pressure at 40°C to a final volume of about 100 ml, and then extracted with 5 × 50 ml of 0.25 *M* sulphuric acid. The acidic layers were mixed and filtered. After alkalinization with ammonia (pH 10), they were extracted with 4 × 50 ml of chloroform.

The organic layers were washed with 70 ml of distilled water, filtered and evaporated under reduced pressure, affording a residue (1.015 g) corresponding to the total alkaloid fraction A (0.203% dry material).

An alkaloid extraction was also applied to another batch of plant material [harvested in Vienne (France)]. The extraction procedure was the same as above (total alkaloid efficiency = 0.237% dry material).

Petal extract preparation

Aqueous alcoholic acidic extract. A 25-g amount of dried petals (Maine et Loire batch) were heated under reflux with 250 ml of 30% ethanol containing 250 mg of tartaric acid for 2 h and then filtered to afford the extract. For the extraction of the alkaloid of this extract, the ethanol was evaporated under reduced pressure until condensation of water. After alkalinization with ammonia (pH 10), the solution was extracted with 4 × 50 ml of chloroform. The organic layers were washed with 70 ml of distilled water, filtered and evaporated to dryness under reduced pressure (total alkaloid efficiency = 0.216% dry material).

Aqueous acidic extract. A 25-g amount of dried petals (Maine et Loire batch) was heated under reflux with 250 ml of distilled water containing 250 mg of tartaric acid for 2 h and then filtered to afford

the extract. This extract was directly alkalinized with ammonia (pH 10) and then extracted with 4 × 50 ml of chloroform. The organic layers were washed with 70 ml of distilled water, filtered and evaporated to dryness under reduced pressure (total alkaloid efficiency = 0.123% dry material).

Isorhoeadin isolation

A 500-mg amount of the total alkaloid fraction A diluted with chloroform (5 ml) was placed on a column (200 × 20 mm I.D) containing 20 g of silica gel 60 (particle size 0.063–0.2 mm) for low-pressure column chromatography (Merck) and 50-ml fractions were collected. Elution was effected with pure chloroform (100 ml) for fractions I and II (3 mg) and with chloroform–methanol (99:1, v/v) (450 ml) for fractions III (18.6 mg), IV–X (324 mg) and XI (8 mg).

The product of fraction III, crystallized in ethanol, afforded 11 mg of pure compound. ^{1}H NMR spectrometry (Brucker AC 200 P NMR spectrometer), mass spectrometry (MS) (Nermag R 1010 C mass spectrometer), melting point determination, UV spectrophotometric analysis and TLC allowed its identification as isorhoeadine: m.p. 161°C [11, 13]; ^{1}H NMR spectra identical with the literature [13,14]; electron impact MS, *m/z* 383 ($M^{+\cdot}$), 368 (100), 352 (10), 177 (96) [15]; UV, λ_{max} [chloroform–methanol–TFA (90:10:0.1, v/v/v)] 244 and 292.5 nm; TLC, R_F = 0.65.

Rhoeagenin isolation

The whole of fraction IV–X was diluted with 1.5 ml of chloroform and then injected on to the preparative HPLC column. Fractions of 4 ml were recovered according to the following scheme: pure chloroform (160 ml), fractions 1–40; chloroform–methanol (99:1, v/v) (24 ml), fractions 41–46; chloroform–methanol (98:2, v/v) (20 ml), fractions 47–51; chloroform–methanol (95:5, v/v) (40 ml), fractions 52–61.

The product was checked using analytical HPLC. Fractions 13–43, mixed, evaporated to dryness and crystallized in ethanol, gave 96 mg of pure compound. ^{1}H NMR spectrometry, melting point determination, UV spectrophotometric analysis and TLC allowed its identification as rhoeagenine: m.p. 236°C [11,13,16]; ^{1}H NMR spectra identical with the literature [13,17]; electron impact MS, *m/z* 369 ($M^{+\cdot}$, 10), 206 (100), 192 (79), 177 (12), 163 (100) [13,15,17]; UV, λ_{max} [chloroform–methanol–TFA (90:10:0.1, v/v/v) 245 and 292.5 nm; TLC, R_F = 0.36.

RESULTS AND DISCUSSION

In contrast to our work on the separation of alkaloids using reversed-phase HPLC [18], we adopted normal-phase HPLC on Superspher Si 60 with chloroform–methanol (90:10, v/v) containing 0.1% of TFA, which resulted in a considerable improvement in the chromatographic profile.

For quantitative analysis, the calibration graphs show a linear correlation from 0.1 to 2 mg/ml between the amounts of isorhoeadine and rhoeagenine injected and the intensity of the absorption at

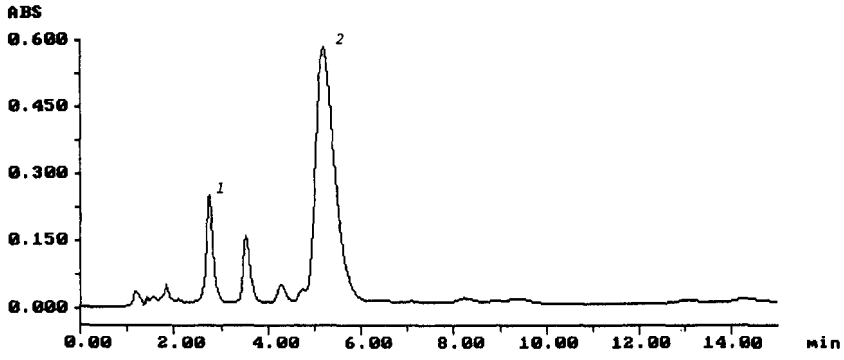

Fig. 1. Chromatogram of a total alkaloid fraction of petals of *Papaver rhoeas* L. (Maine-et-Loire). Peaks: 1 = isorhoeadine; 2 = rhoeagenine. Conditions: column, Superspher Si 60 (125 × 4 mm I.D.; particle size 4 μm); precolumn, LiChrospher Si 60 (4 × 4 mm I.D.; particle size 5 μm); mobile phase, chloroform–methanol (90:10, v/v) containing 0.1% TFA; flow-rate, 1 ml/min; UV detection at 292.5 nm.

TABLE I

VARIATION OF ISORHOEADINE AND RHOEAGENINE CONTENTS WITHIN DIFFERENT PETAL EXTRACTS OF *PAPAVER RHOEAS* L.

Quantitative parameters: $\bar{x}$ = mean (n = 5); S.D. = standard deviation; R.S.D. = relative standard deviation.

Extract	Total akaloid efficiency (% dry material)	Isorhoeadine				Rhoeagenine				Isorhoeadine/ rhoeagenine ratio
		$\bar{x}$ (mg/g total alkaloids)	S.D. (mg/g total alkaloids)	R.S.D. (%)	$\bar{x}$ (mg per 100 g dry material)	$\bar{x}$ (mg/g total alkaloids)	S.D. (mg/g total alkaloids)	R.S.D. (%)	$\bar{x}$ (mg per 100 g dry material)	
Petals (Vienne)	0.237	123.4	2.8	2.26	29.25	754.2	5.6	0.74	178.74	0.16
Petals (Maine et Loire)	0.203	71.1	1.9	2.67	14.43	629.7	3.9	0.62	127.83	0.11
Aqueous alcoholic acidic extract	0.216	42.4	0.9	2.12	9.16	424.2	2.8	0.66	91.63	0.09
Aqueous acidic extract	0.123	10.5	0.2	1.9	1.29	117.3	2.8	2.38	14.43	0.09

292.5 nm [correlation coefficient (r^2) = 0.9968 for isorhoeadine and 0.9837 for rhoeagenine]. Five determinations were carried out on different extracts in order to test the accuracy and precision of the method in terms of standard deviation and relative standard deviation. The determination of the two alkaloids was attempted on the total alkaloid fraction of petals [Vienne and Maine et Loire (Fig. 1)], aqueous alcoholic acidic and aqueous acidic extract (Maine et Loire). Quantitative analysis gave the results summarized in Table I.

If we consider that the classical procedure for the extraction of the alkaloids (involving Soxhlet extraction with chloroform) gives the real amount (100%) of isorhoeadine and rhoeagenine contained in the red poppy petals, we can calculate that during the preparation of the aqueous alcoholic acidic extract we extracted 63.5% of the total amount of isorhoeadine and 71.7% of the total amount of rhoeagenin in the petals. Also, during the preparation of the aqueous acidic extract, we extracted only 8.9% of the total amount of isorhoeadine and 11.3% of the total amount of rhoeagenine in the petals. Hence the most efficient process for conceiving a red poppy liquid remedy seems to be a weak aqueous alcoholic preparation (30% ethanol) containing 1% of tartaric acid (dry material).

Quantitative studies on various samples of petals from different sources (Vienne and Maine-et-Loire) demonstrated the existence of chemotypes in this genus, correlated with a variable alkaloid ratio (0.16 and 0.11).

In conclusion, the proposed method allows the simultaneous isocratic separation of isorhoeadine and rhoeagenine in petals of *Papaver rhoeas* L. and can be used in their routine determination in drugs.

ACKNOWLEDGEMENTS

Thanks are due to Laboratoire Pharmaceutique Florina (Valanjou), Sevres-flore (Chemillé) and Agrocing (Toulouse) for providing financial support.

REFERENCES

1 F. Santavy, *Alkaloids (N.Y.)*, 12 (1970) 339 and 17 (1979) 395.
2 A. Nemeckova, F. Santavy and D. Walterova, *Collect. Czech. Chem. Commun.*, 35 (1970) 1733.
3 Y. N. Kalav and G. Sariyar, *Planta Med.*, 55 (1989) 488.
4 J. Slavik, L. Slavikova and J. Bochorakova, *Collect. Czech. Chem. Commun.*, 54 (1989) 1118.
5 S. El-Masry, M. G. El-Ghazooly, A. A. Omar, S. M. Khafagy and J. D. Philipson, *Planta Med.*, 41 (1981) 61.
6 V. Preininger, V. Simanek, O. Gasic, F. Santavy and L. Dolejs, *Phytochemistry*, 12 (1973) 2513.
7 V. Preininger, *Alkaloids (N.Y.)*, 29 (1986) 1.
8 A. Nemeckova, F. Santavy and D. Walterova, *Collect. Czech. Chem. Commun.*, 35 (1970) 1733.
9 F. Santavy, J. Hrbek and K. Blaha, *Collect. Czech. Chem. Commun.*, 32 (1967) 4452.
10 J. D. Philipson, O. O. Thomas, A. I. Gray and G. Sariyar, *Planta Med.*, 41 (1981) 105.
11 M. Maturova, D. Pavlaskova and F. Santavy, *Planta Med.*, 14 (1966) 22.
12 A. Baerheim Svendsen and R. Verpoorte, *Chromatography of Alkaloids, Part A: Thin-Layer Chromatography (Journal of Chromatography Library*, Vol. 23A), Elsevier, Amsterdam, 1983, pp. 181, 209 and 214.
13 C. T. Montgomery, B. K. Cassels and M. Shamma, *J. Nat. Prod.*, 46 (1983) 441.
14 F. Santavy, J. L. Kaul, L. Hruban, L. Dolejs, V. Hanus, K. Blaha and A. D. Cross, *Collect. Czech. Chem. Commun.*, 30 (1965) 3479.
15 L. Dolejs and V. Hanus, *Tetrahedron*, 23 (1967) 2997.
16 S. Pfeifer and I. Mann, *Pharmazie*, 23 (1968) 82.
17 G. Sariyar and J. D. Philipson, *Phytochemistry*, 19 (1980) 2189.
18 J. P. Rey, J. Levesque, J. L. Pousset and F. Roblot, *J. Chromatogr.*, 587 (1991) 314.

Journal of Chromatography, 596 (1992) 281–284
Elsevier Science Publishers B.V., Amsterdam

CHROM. 24 018

Short Communication

Role of metal ions in the ligand-exchange separation of amino acids

D. Sud, H. S. Hothi and B. S. Pannu*

Department of Chemistry, Punjab Agricultural University, Ludhiana-141 004 (India)

(First received October 2nd, 1991; revised manuscript received January 17th, 1992)

ABSTRACT

Amberlite IR-120 resin was impregnated with transition metal ions such as Mn(II), Fe(II), Fe(III), Cu(II), Zn(II) and Mo(VI) and used for the ligand-exchange separation of amino acids available in the hydrolysates of toria and mustard oilcakes. Among the various metal ions studied, Mn(II) and Fe(II) cannot be employed for separation. The elution volume and selectivity of amino acids with the metal forms of the resin decrease in the order Cu(II) $\approx$ Fe(III) > Mo(VI) > Zn(II).

INTRODUCTION

Ligand-exchange chromatography has been employed for the separation and purification of amino acids [1,2]. The establishment of ligand-exchange equilibrium between the resin and the external solution depends on numerous factors, *e.g.*, the nature of the support, the composition of the eluent, the complex-forming ability of amino acids towards the cation present and the structure of the molecule, *i.e.*, the nature, number, position and properties of the functional groups they contain.

The influence of the eluent composition and the nature of the ion exchanger has been discussed by Doury-Berthod *et al.* [3]. In this work, the influence of the nature of the metal cation on the ligand-exchange separation of amino acids was studied. Amberlite IR-120 impregnated with transition metal ions such as Mn(II), Fe(II), Fe(III), Cu(II), Zn(II) and Mo(VI) was used for the ligand-exchange separation of amino acids in the hydrolysates of toria and mustard oilcakes.

EXPERIMENTAL

The mustard and toria oilcakes, after removal of residual oil and toxic materials, were hydrolysed with 6 *M* hydrochloric acid at 110°C to yield a mixture of amino acids and peptides. Amberlite IR-120 resin was converted into the metal form resin by stirring with 0.1 *M* solution of the chlorides or sulphates of Mn^{2+}, Fe^{2+}, Fe^{3+}, Cu^{2+} and Zn^{2+} for 24 h; with Mo^{6+}, molybdic acid solution in dilute nitric acid was used.

The operation of the column was the same as reported earlier [4]. Glass columns (90 cm × 0.9 cm I.D.) were packed with the metal forms of the resin to a depth of 60 cm. The resin was then equilibrated with 0.1 *M* ammonia solution until the effluent pH was *ca.* 10. About 8–10 h are required for equilibration of the column. The flow-rate was set to 5–6 drops per min or 5 ml in 10 min.

A known amount of the sample after adjusting its pH to 9.5–10 with concentrated ammonia solution was loaded on to the top of column. The sample was

0021-9673/92/$05.00

allowed to flow into the resin and elution was started immediately with 0.1 *M* ammonia solution, followed by elution with 1, 2 and 3 *M* ammonia solution. Generally, 25 ml of each of the first three solutions were used but the elution was continued with 3 *M* ammonia solution up to complete elution of the amino acids. However, when using 2 *M* ammonia solution with the copper column for the hydrolysate of toria oilcake and 1 *M* ammonia solution with the zinc column for the hydrolysate of mustard oilcake, the total volume of eluent applied had to be increased to 26 ml as the elution of the respective amino acids was still continuing. The eluates were collected in the order of five fractions each of 2 ml, ten fractions each of 1 ml and ten fractions each of 0.5 ml.

Thin-layer chromatography (TLC) of all of the eluate fractions was carried out on silica gel G-coated plates by using modified ninhydrin reagent [5] for colour development and the total volumes required for the respective amino acids were determined. The elutions were repeated with the required volumes for the respective amino acids to arrive at the final results given in Tables I and II.

RESULTS AND DISCUSSION

Amberlite IR-120 resin, containing sulphonic acid groups as its active sites, binds transition metal ions by the formation of ionic bonds. Ligand-exchange equilibrium for amino acid separations on a ligand-exchange column containing a metal form of the resin has been reported earlier [4]. The crude proteinaceous matter obtained from toria and mustard oilcakes on acid hydrolysis with 6 *M* hydrochloric acid yielded a mixture of amino acids and peptides. The amino acids present in the hydrolysates were detected by TLC. The hydrolysed samples were applied to columns containing Mn(II), Fe(II), Fe(III), Cu(II), Zn(II) and Mo(VI) forms of the resin. Generally the peptides were eluted as metal chelates in the first 20 ml. The amino acids were subsequently eluted with 0.1, 1, 2 and 3 *M* ammonia solutions.

When Mn(II) and Fe(II) forms of the resin were used in the column after application of an amino acid mixture, the resin turned black on addition of ammonia solution. The eluted solution gave a precipitate of metal hydroxide, indicating degrada-

TABLE I

LIGAND-EXCHANGE CHROMATOGRAPHY OF HYDROLYSATE OF TORIA OILCAKE

Free amino acids from ligand-exchange columns containing resin in the Cu(II), Zn(II), Fe(III) and Mo(VI) forms.

Ammonia solution eluent concentration (*M*)	Cu(II) column		Zn(II) column		Fe(III) column		Mo(VI) column	
	Elution volume (ml)	Amino acid eluted	Elution volume (ml)	Amino acid eluted	Elution volume (ml)	Amino acid eluted	Elution volume (ml)	Amino acid eluted
0.1	25	Glutamic acid + aspartic acid	14	Glutamic acid + asparic acid	18	Glutamic acid + aspartic acid	17	Glutamic acid + aspartic acid
1	20	Methionine	10	Methionine	15	Methionine	14	Methionine
	5	Cystine	8	Phenylalanine	10	Phenylalanine	10	Phenylalanine
			7	Histidine				
2	15	Cystine	10	Cystine	10	Histidine	10	Lysine
	11	Phenylalanine	15	Lysine	15	Cystine	10	Cystine
							5	Histidine
3	15	Lysine	20	Arginine	18	Lysine	5	Histidine
	15	Histidine			20	Arginine	18	Arginine
	16	Arginine						

tion of the metal form of the resin. The elution volume and the corresponding amino acids eluted with different ligand-exchange columns containing Fe(III), Cu(II), Zn(II) and Mo(VI) are reported in Tables I and II.

The elution volumes are different for the same amino acids for the hydrolysates of toria and mustard oilcakes. The metal ion loading of the resin was the same in both instances. This difference in the elution volumes is due to the different amounts of amino acids present in two types of oilcake.

The order of elution of amino acids for both toria and mustard oilcakes for the Cu(II) form of the resin is glutamic acid ≈ aspartic acid > methionine > cystine > phynylalanine > lysine > histidine > arginine. For the Mo(VI) form of the resin, the sequence remains the same except that cystine is eluted after lysine. The Zn(II) and Fe(III) forms of the resin show the trend glutamic acid ≈ aspartic acid > methionine > phenylalanine > histidine > lysine > arginine. The general trend of the elution sequence is that a group of acidic amino acids (glutamic acid and aspartic acid) are eluted first, followed by a group of neutral amino acids (methionine, phenylalanine) and a group of basic amino acids (lysine, histidine and arginine). In all instances except with the Cu(II) column cystine is eluted in the group of basic amino acids. This order is in agreement with that reported previously [3,6].

The results showed that the general elution sequence of amino acids does not change appreciably. However, the basic amino acids show more differentitated behaviour. The elution volumes and thereby the selectivity of ligand-exchange chromatography are greatly affected. The elution volumes are notably smaller with the Zn(II) form of the resin. The decreases in the retention volume and in the selectivity that are observed on passing from the Cu(II) to the Zn(II) form of the resin have been reported [7,8] for the separation of aliphatic amines. The chromatographic behaviour for the separation of three amino acids, glycine, alanine and leucine, has been discussed [3]. The elution volume when using the Mo(VI) form of the resin was lower than those with the Cu(II) and Fe(III) forms, but greater than that with the Zn(II) form. With the Fe(III) form of the resin, the elution volume for some of the amino acids is greater and for others it is less than that with the Cu(II) form of the resin. Generally, the acidic amino acids are eluted in a smaller volume

TABLE II

LIGAND-EXCHANGE CHROMATOGRAPHY OF HYDROLYSATE OF MUSTARD OILCAKE

Free amino acids from ligand-exchange columns containing resin in the Cu(II), Zn(II), Fe(III) and Mo(VI) forms.

Ammonia solution eluent concentration (*M*)	Cu(II) column		Zn(II) column		Fe(III) column		Mo(VI) column	
	Elution volume (ml)	Amino acid eluted	Elution volume (ml)	Amino acid eluted	Elution volume (ml)	Amino acid eluted	Elution volume (ml)	Amino acid eluted
0.1	25	Glutamic acid + aspartic acid	13	Glutamic acid + asparic acid	22	Glutamic acid + aspartic acid	18	Glutamic acid + aspartic acid
1	15	Methionine	11	Methionine	13	Methionine	12	Methionine
	10	Cystine	7	Phenylalanine	12	Phenylalanine	10	Phenylalanine
			8	Histidine				
2	10	Cystine	10	Lysine	12	Histidine	10	Lysine
	10	Phenylalanine	10	Cystine	13	Lysine	10	Histidine
	5	Lysine	5	Arginine				
3	10	Lysine	15	Arginine	20	Cystine	12	Cystine
	10	Histidine			24	Arginine	15	Arginine
	20	Arginine						

with the Fe(III) form of the resin. The elution volumes and the selectivity of amino acids with the metal forms of the resin decrease in the order Cu(II) $\approx$ Fe(III) > Mo(VI) > Zn(II).

The differences in the chromatographic behaviour of the different metallic forms of the resin are probably due to the differences in the stabilities of the mixed complexes formed by amino acids with the metal cations. The order is in accordance with the values of the stability constants of the metal complexes reported for various amino acids.

REFERENCES

1 H. F. Bellinger and N. R. M. Buist, *J. Chromatogr.*, 87 (1973) 513.
2 H. F. Walton, in J. A. Marinsky and Y. Marcus (Editors), *Ion Exchanger and Solvent Extraction, a Series of Advances*, Vol. 4, Marcel Dekker, New York, 1973, p. 121.
3 M. Doury-Berthod, C. Poitrenaud and B. Tremillon, *J. Chromatogr.*, 179 (1979) 37.
4 D. Sud and B. S. Pannu, *J. Indian Chem. Soc.*, 67 (1990) 931.
5 E. D. Moffat and R. I. Lytle, *Anal. Chem.*, 31 (1959) 926.
6 M. Maeda, A. Tsuji, S. Ganno and Y. Onishi, *J. Chromatogr.*, 77 (1973) 434.
7 H. F. Walton, *J. Chromatogr.*, 102 (1974) 57.
8 H. F. Walton, *Sep. Purif. Methods*, 4 (1975) 189.

Journal of Chromatography, 596 (1992) 285–289
Elsevier Science Publishers B.V., Amsterdam

CHROM. 24 012

Short Communication

Estimation of tobacco blend compositions using closed-loop stripping analysis and stepwise multiple linear regression and partial least-squares techniques

B. Lebeau

Philip Morris Holland BV, Marconilaan 20, 4622 RD Bergen op Zoom (Netherlands)

W. E. Hammers*

Department of Analytical Molecular Spectrometry, Utrecht University, Sorbonnelaan 16, 3584 CA Utrecht (Netherlands)

(First received October 14th, 1991; revised manuscript received January 14th, 1992)

ABSTRACT

Multiple linear regression and partial least-squares techniques were applied to closed-loop stripping analysis results for flavours from tobacco blends. The merits of this approach for the determination of blend compositions were evaluated.

INTRODUCTION

Closed-loop stripping analysis (CLSA) was introduced by Grob [1] in 1973, and has been developed for the determination of volatile organic compounds at the ng/l level in potable water [1–4]. CLSA in a slightly modified version can also be applied to volatile organic compounds in solid biological materials [5,6]. The closed system consists of a membrane pump, a thermostated sample compartment and an active carbon filter. The volatile components from the sample are transported continuously by a stream of (pre-heated) gas to the carbon filter where they are adsorbed. The adsorbates are eluted from the filter with a suitable solvent, and are analysed by gas chromatography (GC).

Heinzer *et al.* [6] applied CLSA to divide virginia tobaccos into three quality classes on the basis of headspace GC fingerprints, using principal component analysis and discriminant analysis. The carbon trap was eluted with carbon disulphide and cold on-column injection was applied without a pre-column. Heinzer *et al.* reported that the performance of the GC column irreversibly diminished and ascribed this problem to contamination by a relatively large amount of stripped fatty acids.

The aim of this work was to evaluate the GC analysis of tobacco blends for the purpose of production and taste quality control. First, the CLSA–GC method applied by Heinzer *et al.* [6] was modified to overcome the problem of column contamination. Second, multiple linear regression (MLR) and partial least-squares (PLS) techniques [7–10] were applied for calibration (and cross-validation).

0021-9673/92/$05.00

EXPERIMENTAL

Chemicals and characterization of blends

N-Methylbis(trifluoroacetamide) (MBTFA) and Deriva-sil were supplied by Chrompack (Middelburg, Netherlands) and carbon disulphide, dichloromethane and methanol by J. T. Baker (Deventer, Netherlands).

Batches of burley, virginia and oriental tobacco were subjected to a single casing treatment. EXTO is an "expanded" tobacco [11]; the expanded stems are the (treated) main veins of virginia tobacco leaves. The water content of these tobacco samples was determined with ISO Method 6488. Next, the samples were milled to fine powders. A total of ten calibration blends (code 01–10) and five individual tobaccos (code 11–15) were prepared on a dry weight basis. The compositions of the blends were chosen at random within practical ranges: burley 17.7–51.6%, virginia 8.6–32.1%, oriental 7.2–25.4%, EXTO 4.3–33.0% and stems 1.0–10.7%.

Apparatus and procedures

The experiments were conducted with a CLSA system according to Grob (see Fig. 1a), equipped with a glass sample compartment for solid samples and a filter holder (Brechbühler, Schlieren, Switzerland). Throughout 1 g of blend was analysed. The temperatures of the sample compartment and the heating block were 37 ± 1 and 40°C, respectively. The flow-rate of the stripping gas (air) was within the range 1.0–2.5 ml/min (according to the manufacturer's specification), and the strip time was 30 min. The filter holder contained 1.5 mg of finely powdered active carbon between stainless-steel screens. The solutes were quantitatively eluted from the filter with two 1-μl volumes of dichloromethane by moving the plunger of an injection syringe (see Fig. 1b) up and down ten times. The eluates were stored in closed 100-μl vials at −18°C. The filter was regenerated by consecutively sucking through 2 ml of carbon disulphide, methanol and dichloromethane, and was dried under vacuum.

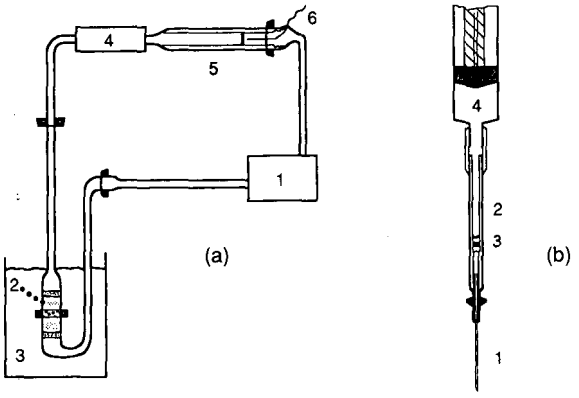

Fig. 1. (a) Scheme of the CLSA apparatus for solid samples. 1 = Membrane pump; 2 = sample compartment; 3 = thermostated water-bath; 4 = heating block; 5 = filter holder; 6 = thermocouple. (b) Design for elution from the carbon filter. 1 = Stainless-steel needle; 2 = filter holder; 3 = carbon filter; 4 = syringe (2 ml) with plunger.

The analyses were executed with an HP 5890 gas chromatograph, equipped with a split injector, a flame ionization detector and an HP 3396 integrator (Hewlett-Packard, Amstelveen, Netherlands). The quartz insert of the split injector was filled with tightly compressed glass-wool to minimize peak broadening. The splitting ratio was 1:10 and the sample size was 5 μl. These conditions were about optimum as far as minimum solute deterioration in the hot injector, amount of sample entering the GC column and extent of contamination of the GC column by strongly retained solutes are concerned. The applied CP Sil-8-CB fused-silica capillary (50 m × 0.25 mm I.D., 95% dimethyl–5% phenylsiloxane, layer thickness 0.23 μm) and the empty fused-silica precolumns (1.5 m × 0.25 mm I.D.) were supplied by Chrompack (Middelburg, Netherlands). After 50 injections the analytical column was flushed through with methanol and the precolumn was replaced. The flow-rates of the carrier gas (helium), septum purge gas, vent gas, make-up gas, hydrogen and air were 1.3 (at 60°C), 3.6, 14, 38, 36 and 270 ml/min, respectively. The injector and detector temperatures were 275 and 300°C, respectively. The oven temperature was linearly programmed from 60°C (injection) to 235°C at 2.5°C/min.

To avoid possible decomposition of thermo-labile constituents [6], the extracts were treated with MBTFA, giving trifluoroacetyl derivatives of primary and secondary amines [12]. Derivasil was applied to convert hydroxyl, amido and amino groups to trimethylsilyl derivatives [13]. These reactions were conducted in either carbon disulphide or dichloromethane.

Ten blends and five individual tobaccos were examined. Each of these was analysed twice by CLSA–GC, giving a total of 30 data series, each consisting of 42 relative peak area data (denoted as the 42/30 set)[a]. To validate the results obtained with MLR and PLS, 28 data series were used for calibration, whereas the two remaining (randomly chosen) data series were used to compute the corresponding single-blend compositions [7]. This procedure was repeated till all 30 blend compositions were computed. Mean-blend compositions were calculated from the results for two single compositions of blends with identical composition. In general, a large number of calibration samples was required for MLR. Therefore, stepwise Max R multiple linear regression [14] was applied in this work. In this technique, more or less characteristic peaks for the various tobaccos are selected, which reduced the required amount of input data. In PLS the number of calibration samples must be at least equal to the number of components to be determined. In general, a larger number is recommended for complex samples in order to compensate for unexpected sources of variation of a chemical and/or statistical nature. The stepwise Max R MLR software (SAS) was supplied by the SAS Institute (Hilversum, Netherlands), and the PLS software (Unscrambler II) by Oliemans, Punter & Partners (Utrecht, Netherlands).

RESULTS AND DISCUSSION

The derivatization reactions appeared to result in the formation of unsoluble residues after evaporation of the solvent. Such evaporation tests were also applied to the untreated extracts. Those in carbon disulphide gave a persistent, unsoluble precipitate on the vial wall after heating at 200°C.

This was not observed when dichloromethane was used as the solvent. Therefore, dichloromethane was used, and derivatization was not applied. The CLSA–GC procedure outlined above appeared to be adequate. Up to 50 samples could be analysed without significant decline of the column performance.

Inspection of the chromatograms revealed that all the blends examined had 8 resolved peaks (higher than ten times the noise level) in common. The relative net retention times of these peaks were calculated, and the peak areas formed the basic 81/30 data set. First, the repeatability of the CLSA–GC results was determined by analysing a representative blend six times. The relative standard deviations (R.S.D.) ranged from 3 to 140%, the lower ones corresponding to large peaks, and the large ones to small peaks, as expected. The median R.S.D. was 11.4%.

In order to improve the precision of the data input, relative peak areas were calculated and R.S.D. values were recalculated. Next, data with R.S.D. $> 12\%$ were not used in the statistical analyses. In addition, peaks having similar relative peak areas in two or more individual tobaccos were omitted to eliminate redundant information from the data base. In this manner 42 peaks were selected. The mean and the median of the R.S.D. data of the relative peak areas were $7.5 \pm 2.7\%$ and 8.0%, respectively. Thus, $R.S.D._a = 8\%$ may be considered as the estimate of the analytical precision (*i.e.*, including sub-sampling errors) of the 42/30 data set.

The impact of the correlation between the relative peak area data for the five individual tobaccos was evaluated with PLS. The 42/30 data set was used. Mean results from computed single compositions (as outlined under Experimental) are given in Table I. If no correlation were to occur between the data series for the tobaccos and the experimental errors were to be negligible, a composition of about 100% would be predicted for each of the tobaccos. This is approximately the case, except for virginia lamina and stems, which cannot be distinguished. This can be ascribed to the fact that the examined stems originated from virginia tobacco leaves. Thirty-seven out of 42 relative peaks area data for these tobaccos appear to be correlated ($r = 0.9256$). The data input for these constituents cannot simply be combined to overcome this problem, because the concentrations of virginia and stems strongly determine the taste of a blend. As percentage compositions are computed, it needs no comment that correlation effects also have an adverse impact on the other results in Table I. Therefore, it will be examined whether such effects can be diminished by omitting the data series for the individual tobaccos, which results in the 42/20 data set.

In order to examine the quality of the PLS results,

[a] The data input is available from the authors on request.

TABLE I

MEAN PLS RESULTS FOR INDIVIDUAL TOBACCOS, USING THE 42/30 DATA SET

Code	Real (R) and computed (C) compositions (%)									
	Burley		Virginia		Oriental		EXTO		Stems	
	R	C	R	C	R	C	R	C	R	C
11	100	85.8	0	1.6	0	5.4	0	2.6	0	4.6
12	0	−5.3	100	88.0	0	11.3	0	0.3	0	5.7
13	0	−15.8	0	11.4	100	98.0	0	3.4	0	3.0
14	0	−10.8	0	1.4	0	4.6	100	99.1	0	5.7
15	0	36.5	0	114.6	0	−78.4	0	−26.1	100	53.4

mean-blend compositions were calculated from single-blend results, using the 42/30 data set (as outlined under Experimental). For each of the five blend constituents these results were compared with the real compositions. The largest positive and negative deviations thus obtained are presented as range limits in Table II. These ranges are a measure of the predictive reliability. This reliability appears to improve when the 42/30 instead of the 81/30 data set is used, but no further improvement is achieved with the 42/20 data set. Obviously, correlation effects persist in the 42/20 data set.

The predictive precision was calculated for each blend constituent as the square root of the pooled variance of the two computed results for blends of identical composition. These precision data are given in Table II. The average precision for the five blend constituents appears to improve from 7.1% for the 81/30 set to 4.4% for the 42/30 and 42/20 sets.

PLS and MLR results for two single blends and mean results from single blends with an identical composition are given in Table III. The results from the 81/30 data set appear to be poor, as expected, whereas those from the 42/30 and 42/20 data sets are equivalent. On average, the MLR and PLS methods appear to give similar predictive reliabilities. However, note that the sum of the MLR results is not equal to 100%, which is a weak point in this method. Further, it is illustrated in Table III that poor predictions can incidentally be obtained for single-blend data (for instance, the burley content of blend 07.1, computed with PLS from the 42/30 data set); the mean result for burley in the 07 blend is more accurate. Using the 42/30 and 42/20 dats sets, the mean deviation from the real percentages is $\pm 3.0\%$. It is noted that for taste quality control absolute deviations of $\leqslant 2\%$ are desirable.

Finally, it will be estimated to what extent correla-

TABLE II

MEAN PLS RESULTS FOR THE PREDICTIVE RELIABILITY (RANGE) AND PRECISION, USING THE 81/30, 42/30 AND 42/20 DATA SETS

Set	Parameter	Burley	Virginia	Oriental	EXTO	Stems
81/30	Range	−7.4; 7.0	−17.9; 16.0	−6.7; 4.2	−3.9; 5.2	−9.0; 7.6
	Precision	7.4	10.3	4.5	5.1	4.0
42/30	Range	−4.5; 7.9	−7.2; 6.0	−4.4; 3.9	−5.0; 9.6	−7.2; 3.5
	Precision	6.7	4.0	3.0	4.9	1.4
42/20	Range	−4.1; 2.9	−4.6; 7.4	−6.4; 4.8	−5.7; 10.6	−7.4; 4.5
	Precision	2.7	3.3	6.4	6.0	1.6

TABLE III

PLS AND MLR RESULTS FOR THE BLENDS 03.2 AND 07.1, AND MEAN RESULTS FOR THE 03 AND 07 BLENDS, USING THE 81/30, 42/30 AND 40/20 DATA SETS

Data input	Real and computed compositions (%)				
	Burley	Virginia	Oriental	EXTO	Stems
Composition 03	26	23.9	26.0	18.9	4.6
Blend 03.2					
81/30 PLS	21.9	33.8	23.9	15.1	5.3
42/30 MLR	33.8	12.8	22.0	20.0	5.0
42/30 PLS	30.8	18.8	26.4	17.7	6.3
42/20 PLS	26.4	20.8	26.0	22.7	4.1
Blends 03					
42/30 PLS	22.1	23.7	24.0	23.0	7.4
42/20 PLS	25.8	23.0	22.2	23.6	5.4
Composition 07	31.1	10.7	22.9	31.7	3.6
Blend 07.1					
81/30 PLS	41.4	−17.0	18.2	42.2	15.2
42/30 MLR	30.6	18.9	17.0	29.4	2.0
42/30 PLS	18.5	16.6	21.6	35.2	8.1
42/20 PLS	32.5	16.0	19.0	27.1	5.4
Blends 07					
42/30 PLS	29.1	15.0	22.0	28.1	5.9
42/20 PLS	31.6	18.1	21.0	26.0	3.4

tion between the relative peak-area data for the various tobaccos adversely affected the predictive precision of the PLS results. First, it is assumed that R.S.D.$_a$ = 8% for all blend constituents. Second, it is assumed for convenience that the analysis errors propagate unaltered into the final results (which is probably too pessimistic an assumption). On this basis, the standard deviations, s_a, can be calculated from the real composition data given in Table III. It was verified with the Kolmogorov–Smirnov test [15] that the differences between the computed and real percentages for single-blend results (using the 42/30 and 42/20 data sets) do not deviate significantly from a normal distribution. Combination with the precision data (here denoted as s_p) obtained from the 42/30 data set presented in Table II gives s_c/s_p $[\geqslant (1 - s_a^2/s_p^2)^{\frac{1}{2}}] \geqslant 0.9$, where s_c is the standard deviation due to correlation effects. Therefore, it can be concluded that correlation effects, rather than analytical precision, determine the predictive precision (and reliability) of the PLS (and MLR) results for tobacco blend analysis.

CONCLUSIONS

Tobacco flavours can be analysed satisfactorily with the CLSA–GC technique if split injection is applied and dichloromethane is used to elute these compounds from the carbon filter. The median R.S.D. of the relative areas of 42 selected peaks is 8%, which is acceptable in ultra-trace analysis.

CLSA–GC in combination with PLS can be successfully applied to identify individual tobaccos (burley, virginia, oriental and EXTO), but virginia tobacco leaves cannot be distinguished from its stems owing to the correlation between the peak area data. Correlation effects predominantly determine the reliability and precision of the computed blend composition. Using a 42/30 (or a 42/20) data set, and PLS or stepwise MLR, the means of computed results for two identical blends provide more reliable estimates and show, on average, a deviation of ±3.0% from the real percentages of the blend constituents. The mean precision of the computed percentages is 4.4%.

ACKNOWLEDGEMENTS

The authors are indebted to Dr. M. Gerritsen (University of Nijmegen, Netherlands) for the execution of the PLS computations, and to Drs. A. Spijkers (Philip Morris Holland) for his contribution to the MLR computations.

REFERENCES

1 K. Grob, *J. Chromatogr.*, 84 (1973) 255.
2 K. Grob and G. Grob, *J. Chromatogr.*, 90 (1974) 303.
3 K. Grob, K. Grob, Jr. and G. Grob, *J. Chromatogr.*, 106 (1975) 299.
4 K. Grob and F. Zürcher, *J. Chromatogr.*, 117 (1976) 285.
5 E. Lorbeer, M. Mayr, B. Hausmann and K. Kratzel, *Monatsh. Chem.*, 113 (1984) 1107.
6 F. Heinzer, H.-P. Maître, M. Rigaux and J. Wild, *Beitr. Tabakforsch. Int.*, 14 (1988) 93.
7 S. Wold, *Technometrics*, 20 (1978) 397.
8 W. Lindberg, J.-Å. Persson and S. Wold, *Anal. Chem.*, 55 (1983) 643.
9 M. Sjöström, S. Wold, W. Lindberg, J.-Å. Persson and H. Martens, *Anal. Chim. Acta*, 150 (1983) 61.
10 H. Martens and T. Naes, *Multivariate Calibration*, Wiley, New York, 1989.
11 Philip Morris, *US Pat.*, 822 793 (1977).
12 M. Donike, *J. Chromatogr.*, 78 (1973) 273.
13 J. F. Klebe, H. Finkbeiner and D. M. White, *J. Am. Chem. Soc.*, 88 (1966) 3390.
14 G. Seber, *Linear Regression Analysis*, Wiley, New York, 1977.
15 W. J. Dixon and F. J. Massey, Jr., *Introduction to Statistical Analysis*, McGraw-Hill, New York, 3rd ed., 1969, pp. 346 and 550.

Journal of Chromatography, 596 (1992) 290–293
Elsevier Science Publishers B.V., Amsterdam

CHROM. 24 043

Short Communication

Determination of topanol antioxidants in methacrylates using capillary gas–liquid chromatography

Ian D. Smith* and David G. Waters

SmithKline Beecham Pharmaceuticals, Old Powder Mills, Leigh, Tonbridge, Kent TN11 9AN (UK)

(First received September 6th, 1991; revised manuscript received January 24th, 1992)

ABSTRACT

This paper presents a method to identify and determine topanol A and topanol O antioxidants in methylmethacrylate and 11-bromoundecylmethacrylate. The method is both simple and rapid. Analysis is performed on a 10 m × 0.53 mm I.D. HP-1 capillary gas chromatography column with a temperature gradient and a high carrier gas flow-rate (16.5 ml/min). Quantitation is by internal standardisation. Validation of the method is described for both topanols at concentrations of approximately 50 ppm in methylmethacrylate and 250 ppm in 11-bromoundecylmethacrylate.

INTRODUCTION

Methylmethacrylate is supplied with an antioxidant to inhibit spontaneous polymerisation. The antioxidant, either topanol A (2-*tert.*-butyl-4,6-dimethylphenol) or topanol O (2,6-di-*tert.*-butyl-4-methylphenol), has been added at a concentration of approximately 50 ppm. Methylmethacrylate is used in the preparaton of a cross-linked polymethacrylate and the antioxidant is carried into the intermediate product (11-bromoundecylmethacrylate) and concentrated approximately 5-fold to about 250 ppm. The structures of the analytes are shown in Fig. 1.

It was necessary to be able to identify which of the two topanols had been added, and to determine the concentration in methylmethacrylate and 11-bromoundecyl-methacrylate.

A number of methods have been reported in the literature, with a variety of sample matrices and by a number of techniques. These include the analysis of BHT (butylated hydroxytoluene, or topanol O) in transformer oil by high-performance liquid chromatography (HPLC) [1], derivatisation followed by packed-column gas chromatography (GC) and HPLC [2], determination in soaps [3] and in soybean oil [4] by packed-column GC, and in chewing gum by capillary-column GC [5]. However, none of these were suitable for the required analysis, so a new method was developed. It was decided to use 2,4,6-tri-*tert.*-butyl phenol (see Fig. 1) as internal standard to improve the precision of analysis, and to employ a wide-bore capillary GC column to take advantage of the well-known high sample capacity and good efficiency.

EXPERIMENTAL

Chemicals

2,6-Di-*tert.*-butyl-4-methylphenol (99%), 2-*tert.*-

0021-9673/92/$05.00

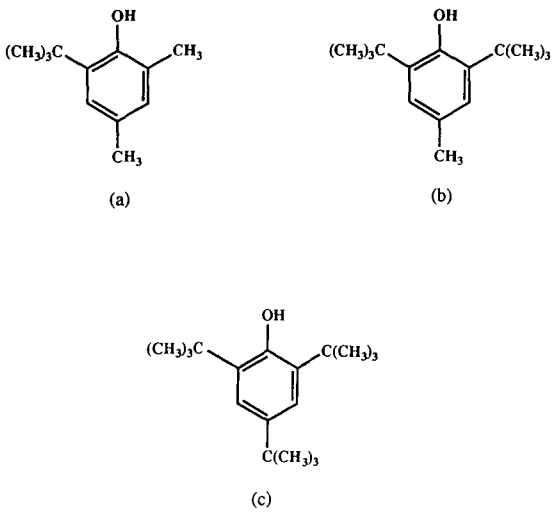

Fig. 1. Structures of (a) topanol A, (b) topanol O and (c) the internal standard.

butyl-4,6-dimethylphenol (99%), and 2,4,6-tri-*tert.*-butylphenol (97%) were all supplied by Aldrich. Dichloromethane was HPLC grade, supplied by Romil.

Instruments

GC analysis was performed on a Varian Model 3400 gas chromatograph, equipped with a Varian Model 8035 autosampler, a Varian Model 1093 septum programmable injector used in on-column mode and a flame ionisation detector. The GC column was a Hewlett-Packard HP-1 (methyl silicone), 10 m × 0.53 mm I.D., 2.65 μm film thickness. The injector temperature was 250°C, the detector temperature 260°C. The oven temperature programme was slightly different for the two sample matrices. For methylmethacrylate samples, it was 70°C for 3 min, then up to 150°C at 15°C/min, and held at 150°C for 12 min. For 11-bromoundecylmethacrylate samples, it was 70°C for 3 min, then up to 150°C at 15°C/min, and held at 150°C for 5 min, then up to 250°C at 30°C/min and held at 250°C for 5 min as a purge step to ensure the complete elution of all the sample components. The carrier gas was helium, at a flow-rate of 16.5 ml/min (measured at 70°C by a bubble flow meter). The injection volume was 0.3 μl.

Data collection and processing was performed using a Perkin-Elmer LIMS/CLAS 2000 data system. Least-squares regression analysis and plotting of graphs were performed using Cricket Software's "CricketGraph".

Procedures

Methylmethacrylate analysis. The internal standard solution was prepared at a concentration of 0.1 mg/ml. A standard solution was prepared with concentrations of 0.005 mg/ml for both of the topanols and of the internal standard.

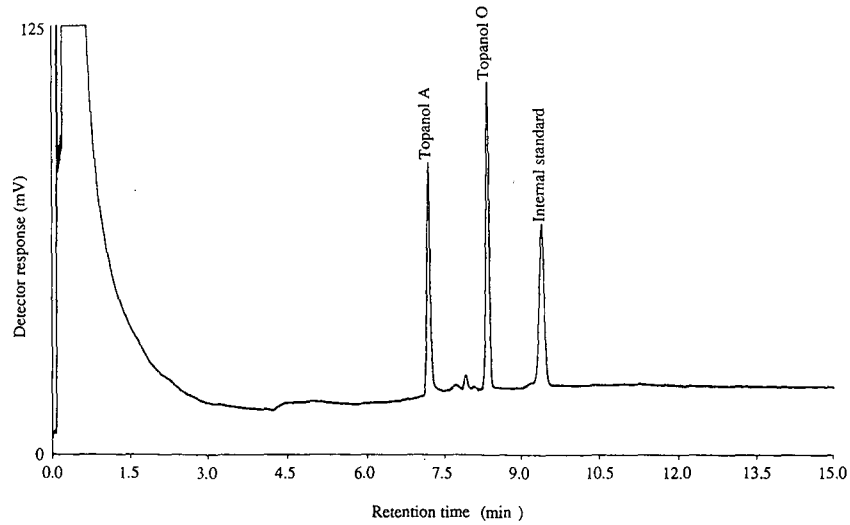

Fig. 2. Chromatogram of the 50-ppm standard solution, showing both the topanol peaks and the internal standard peak.

Sample solutions were prepared by dissolving 1 g of sample and 1.00 ml of internal standard solution in 10 ml of dichloromethane, giving a sample concentration of approximately 100 mg/ml.

Sample and working standard solutions were analysed in duplicate.

11-Bromoundecylmethylacrylate analysis. The internal standard solution was prepared at a concentration of 0.5 mg/ml. A working standard solution was prepared with concentrations of 0.025 mg/ml for both of the topanols and of the internal standard.

Sample solutions were prepared by dissolving 2 g of the sample and 1.00 ml of the internal standard solution in 20 ml of dichloromethane, giving a sample concentration of approximately 100 mg/ml.

Sample and working standard solutions were analysed in duplicate.

Calculation of results. The chromatograms were integrated and the areas of the topanol and internal standard peaks found. The concentration of topanol in the sample was determined using the conventional ratio calculation.

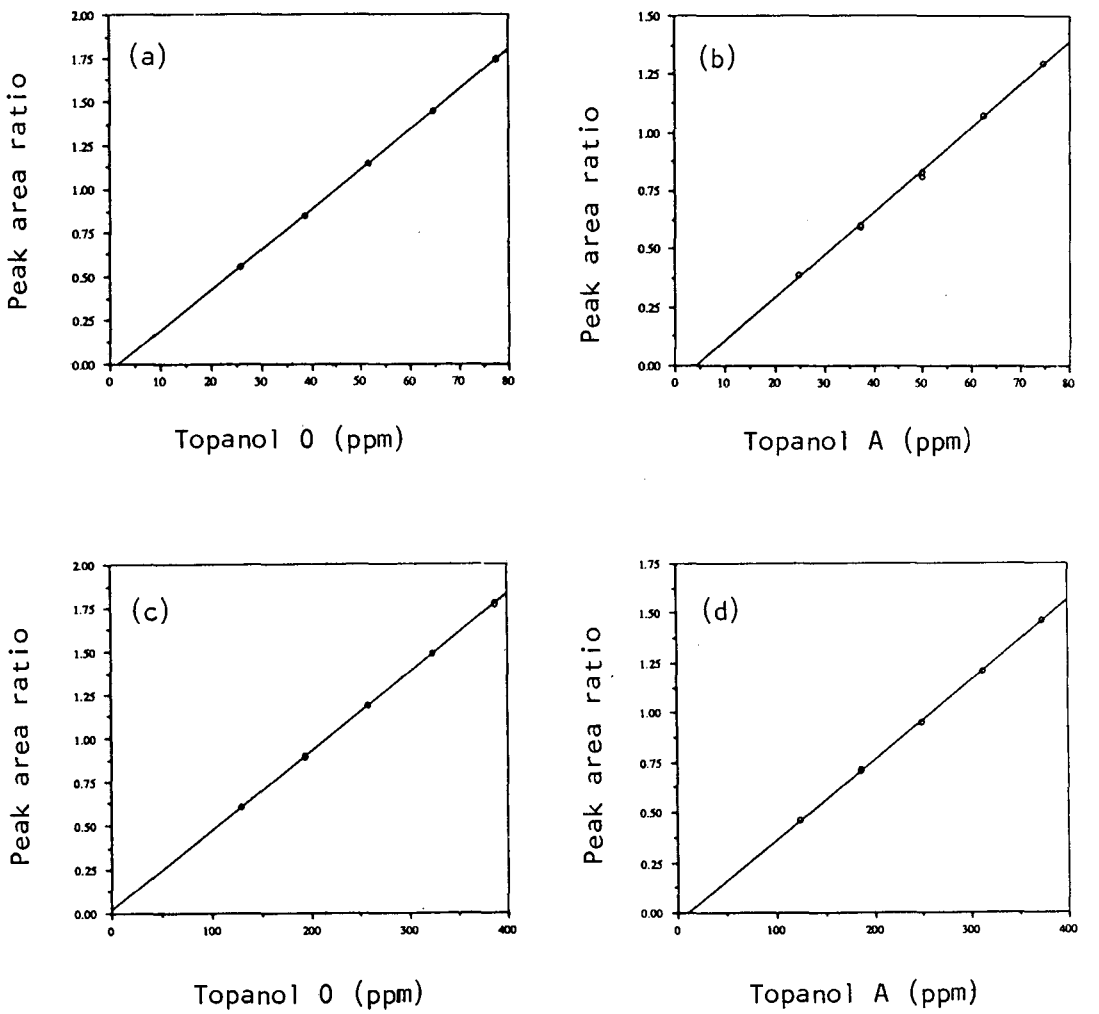

Fig. 3. Plots of the linearity of the peak area ratio against concentration for (a) topanol A and (b) topanol O over the range 25–75 ppm, and (c) topanol A and (d) topanol O over the range 125–375.

Validation experiments. The linearity of response of the method was examined by two injections at each of five concentrations over the ranges 25 to 75 ppm and 125 to 375 ppm. These ranges represent 50 to 150% of the nominal standard concentration of topanol for methylmethacrylate and 11-bromoundecylmethacrylate respectively.

The stabilities of both solutions were assessed by comparison with freshly prepared solutions after 4 and again after 7 days storage in the dark at 4°C. The sample stability was assessed by analysing a freshly prepared sample solution and then reanalysing against freshly prepared standards after 24 h storage in the dark at 4°C.

The precision of replicate injections was examined by making 10 injections of the same standard solution.

RESULTS AND DISCUSSION

The method described gave well resolved peaks with good efficiency in a total run time of less than 10 min. A chromatogram of the 50-ppm standard is shown in Fig. 2.

The peak area ratio response was found to be linear for both topanols over the concentration range examined. Plots of peak area ratio against concentration are shown in Fig. 3. The correlation coefficients (r) were all 0.999 or better.

Standard solutions were found to be stable on storage in the dark at 4°C for up to 7 days, and sample solutions for at least 24 h.

The precision of replicate injections were found to be quite acceptable for trace level assays. At 50 ppm, topanol A gave a peak area ratio relative standard deviation (R.S.D.) of 5.6%, topanol O, 4.1%. At 250 ppm the R.S.D. for topanol A was 5.8% and topanol O 3.2%. These results give confidence limits ($p = 0.05$) for topanol O of $\pm$ 1.2 ppm at 50 ppm and $\pm$ 5.0 ppm at 250 ppm.

Methylmethacrylate eluted with the solvent peak, and no other sample-related peaks have been observed in chromatograms of methylmethacrylate samples. The 11-bromoundecylmethacrylate elutes after the internal standard, and a number of sample-related peaks have been seen in chromatograms from samples of this compound. These are low-level impurities in the samples, and although they run close to the topanol O and internal standard peaks, there is no evidence of co-elution or interference. There is a minor impurity in the 2,4,6-tri-*tert*.-butylphenol, which elutes between the two analyte peaks and is well resolved from both.

CONCLUSION

The methods presented are simple and rapid, allowing both the confirmation of the identity of the antioxidant and its determination at low levels. The method has acceptable reproducibility, as shown by the relatively low R.S.D. values and is linear over the ranges examined.

REFERENCES

1 C. Laumarre and A. Gendron, *J. Chromatogr.*, 464 (1989) 448.
2 T. Mizutani, K. Tajima, N. Okino and K. Yamamoto, *J. Chromatogr.*, 333 (1985) 171.
3 L. Sedea and G. Toninelli, *J. Chromatogr. Sci.*, 19 (1981) 290.
4 D. B. Min and D. Schweizer, *J. Food Sci.*, 48 (1983) 73.
5 M. J. Greenberg, J. Hoholick, R. Robinson, K. Krubis, J. Groce and L. Weber, *J. Food Sci.*, 49 (1984) 1622.

Journal of Chromatography, 596 (1992) 294–298
Elsevier Science Publishers B.V., Amsterdam

CHROM. 24 085

Short Communication

Rapid determination of free tryptophan in plant samples by gas chromatography–selected ion monitoring mass spectrometry

Lech Michalczuk

Department of Botany, University of Maryland, College Park, MD 20742 (USA)

Krystyna Bialek and Jerry D. Cohen*

Horticultural Crops Quality Laboratory, Beltsville Agricultural Research Center, Agricultural Research Service, US Department of Agriculture, B050 HH4 BARC-west, 10300 Baltimore Avenue, Beltsville, MD 20705-2350 (USA)

(First received November 11th, 1991; revised manuscript received February 6th, 1992)

ABSTRACT

An isotope dilution assay for plant tryptophan is described. The method consists of solid-phase extraction techniques, the one-step formation of the N-acetyl methyl ester derivative, followed by purification by C_{18} high-performance liquid chromatography and analysis by gas chromatography–selected ion monitoring mass spectrometry. The method can be used effectively to measure free tryptophan in plant samples as small as 10 mg fresh weight.

INTRODUCTION

The biosynthetic pathway to the amino acid tryptophan is closely linked to the metabolism of an important plant growth regulator, indole-3-acetic acid (IAA). In order to effectively study IAA biosynthesis in plants, it is essential to have effective methods for quantification and mass spectral analysis of low levels of both IAA and tryptophan. We have previously described methods for the analysis of plant IAA by quantitative mass spectrometry (MS) [1,2]. However, only a few methods for amino acid analysis by gas chromatography (GC)–MS have considered the difficult problem of sample preparation from plant tissues. Most prior efforts have tended to stress derivatization procedures and conditions for separation of mixtures of amino acids by GC [3–7]. Samples of vegetative plant tissues such as leaves, shoots, or roots contain a multitude of native compounds which coextract with tryptophan, thus necessitating extensive purification. Since, like other indolic compounds, tryptophan is a notably labile compound, purification procedures often cause significant losses [8]. Indeed, recoveries of less than 5% have been noted [3]. For our work on indole metabolism in plant tissues we have developed a quantitative mass spectral isotope dilution assay which utilizes disposable sample preparation columns and a single step of high-performance liquid chromatography (HPLC) prior to GC–selected ion monitoring (SIM) MS analysis. The procedure provides a quick and efficient way to

accurately measure tryptophan levels in a few mg (fresh weight) of plant material.

EXPERIMENTAL[a]

Leaf tissue from a Rock Elm (*Ulmus thomasii* Sarg.), 0.01 to 1.0 g, was frozen with liquid nitrogen and ground, while frozen, with a mortar and pestle. The ground sample was then homogenized in 5 to 8 times the tissue volume of isopropanol–0.2 *M* imidazole buffer, pH 7.0 (65:35). A radioactive tracer, [5-^{3}H]tryptophan (0.5 kBq; Amersham, 1 TBq/mmol) and an internal standard of [2,4,5,6,7-$^2H_5$]-tryptophan (98.5% isotope enrichment, MSD Isotopes; 0.01 to 1.0 μg), were added and the sample was left at 4°C for 1 h for isotope equilibration. After 1 h, the extract was centrifuged for 5 min at 10 000 *g*. The pellet was washed three times with isopropanol–imidazole buffer and the pellet discarded. The combined supernatants were then evaporated *in vacuo* to approximately one third of the initial volume in order to remove the organic phase. Water-insoluble compounds which precipitated were removed by centrifugation. In experiments where the full spectrum of endogenous tryptophan was to be obtained for confirmation of identity, the addition of the deuterated standard was omitted. The supernatant was applied to an 8-ml bed volume column of Dowex 50W-X2, 200–400 mesh, equilibrated with 1 *M* HCl. After the sample was applied, the column was washed with three volumes of distilled water. The sample was then eluted with three bed volumes of 2 *M* NH_4OH. The alkaline eluate was evaporated *in vacuo* to approximately one third of the initial volume and was passed through a BakerBond spe amino disposable extraction column (J.T. Baker, pre-equilibrated with 2 ml of methanol followed by 2 ml of distilled water). Under these conditions, tryptophan was not retained on the column. The column was washed with 3 ml of distilled water and the combined eluent was evaporated to dryness *in vacuo* on a rotary evaporator in a 10-ml evaporation flask. The oily residue was dehydrated by multiple azeotropic distillations *in vacuo*; first with absolute ethanol, then with dichloromethane. Immediately after the last distillation from dichloromethane, 1 ml of anhydrous methanol (dehydrated by distillation from magnesium activated with iodine) and 0.5 ml of acetic anhydrice (Supelco) were added and the evaporation flask was closed tightly with a PTFE-sleeved glass stopper and clip. The contents were mixed for 1 min on a vortex mixer and put into a heating block set at 65°C. After 1 h the methanol and acetic anhydride were evaporated under vacuum. The residue was dissolved in 1 ml of distilled water and applied to a Fisher PrepSep C_{18} disposable column. The column was washed with 5 ml of distilled water and the sample was eluted with 2 ml of acetonitrile. The acetonitrile was evaporated to dryness. The residue was dissolved in 100 μl of methanol–water (50:50) and injected onto a Waters NovaPak C_{18} column (15 cm × 3.9 mm) connected to a Waters 600MS HPLC pumping system. The column was eluted with methanol–water (30:70) and the retention time for the N-acetyl methyl ester of tryptophan was 10.4 min. Fractions containing radioactivity were collected, evaporated to dryness and redissolved in 10 μl of ethyl acetate. GC–MS analysis was done on a Hewlett-Packard 5890 gas chromatograph connected to a 5917A mass selective detector. The gas chromatograph was equipped with a 15 m × 0.237 mm DB-1701 fused-silica capillary column (J & W Scientific) and helium was used as carrier gas at 1 ml/min. A 1-μl injection was made in the splitless mode with GC conditions as follows: injector temperature 250°C, initial oven temperature 140°C for 1 min, followed by a ramp at either 20 or 30°C/min up to 280°C and hold for 2 min. Under these conditions the retention time for the N-acetyl methyl ester of tryptophan was 6.07 or 7.83 min, depending on the temperature ramp rate. For quantitative analysis of tryptophan, ions at *m/z* 130 and 135 (unlabeled and labeled quinolinium ions) and at 260 and 265 (unlabeled and labeled molecular ions) were monitored.

RESULTS AND DISCUSSION

One objective of this work was to develop a relatively quick and efficient method for purification of tryptophan from small amounts of plant material

[a] Mention of a trademark, proprietary product, or vendor does not constitute a guarantee or warranty of the product by the United States Department of Agriculture, and does not imply its approval to the exclusion of other products or vendors that may also be suitable.

for analysis by GC–MS. Crude extracts from different plant samples (leaves, carrot cell suspension, bean hypocotyls) contained from 20 to 100 mg of soluble solids per gram of extracted material. The two ion-exchange preparative columns removed the bulk of the impurities (with essentially quantitative recovery of radioactive tracer), but samples at this step were still too contaminated for high-resolution HPLC under the conditions necessary for elution of underivatized tryptophan. Thus, the partially purified sample was derivatized. Among the many possible amino acid derivatives showing improved properties for reversed-phase HPLC analysis described in the literature [9], the most promising for use on very small samples was the concerted formation of stable N-acyl alkyl esters. Such compounds are stable under the conditions necessary for further purification and are also directly suitable for analysis by GC. Derivatization decreased the polarity of the molecule such that reversed-phase chromatography using simple alcohol–water mixtures became an effective purification technique. In addition, the derivatives are relatively simple in structure, thus facilitating final interpretation of the spectral results. Using a microscale modification of the procedure described by Mee *et al.* [10] for the single step acetylation and methylation of several amino acids using a mixture of anhydrous methanol and acetic anhydride, we were able to obtain good yields of derivatized tryptophan even in complex plant extracts. A large excess of the reagents allowed the effective derivatization of crude samples and the excess of acetic anhydride consumed small traces of water retained in the oily residues. At 65°C, derivatization was essentially quantitative after 35–45 min (as determined by thin-layer chromatography of aliquots taken out during the course of the reaction). The reaction produced about 90% of N-acetyl methyl ester (Fig. 1, peak A) and about 10% of the N,N-diacetyl methyl ester of tryptophan (Fig. 1,

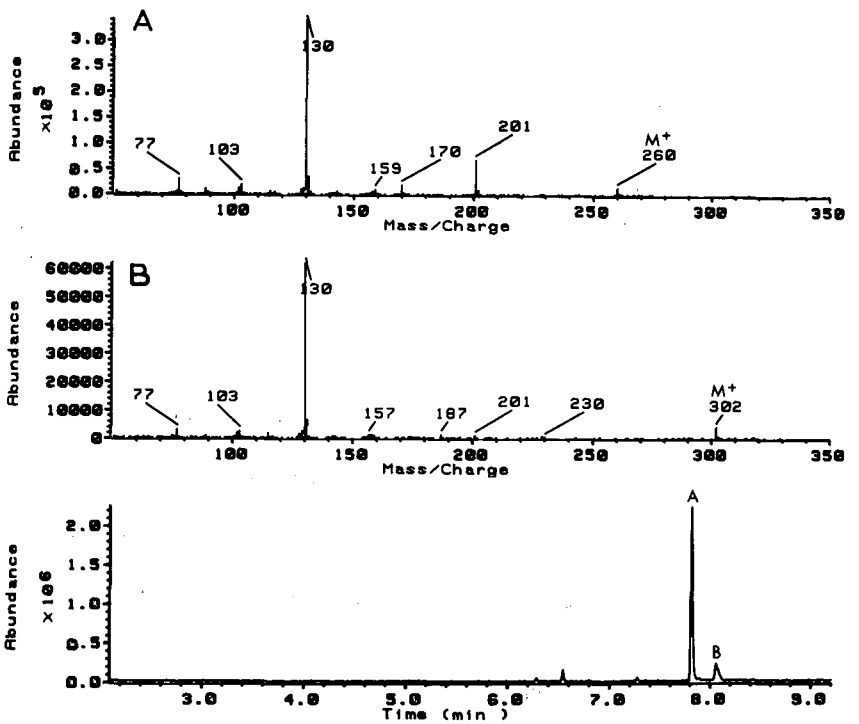

Fig. 1. Reconstructed ion chromatogram (lower frame) from the GC–MS analysis of tryptophan derivatized as described in text to form the mono- and diacetyl methyl ester. The chromatographic peak and the averaged spectrum of the primary reaction product, N-acetyl-tryptophan methyl ester, are labeled A. Under the conditions described only minor amounts of the diacetyl-tryptophan methyl ester are formed, as shown by the peak and averaged spectrum labeled B.

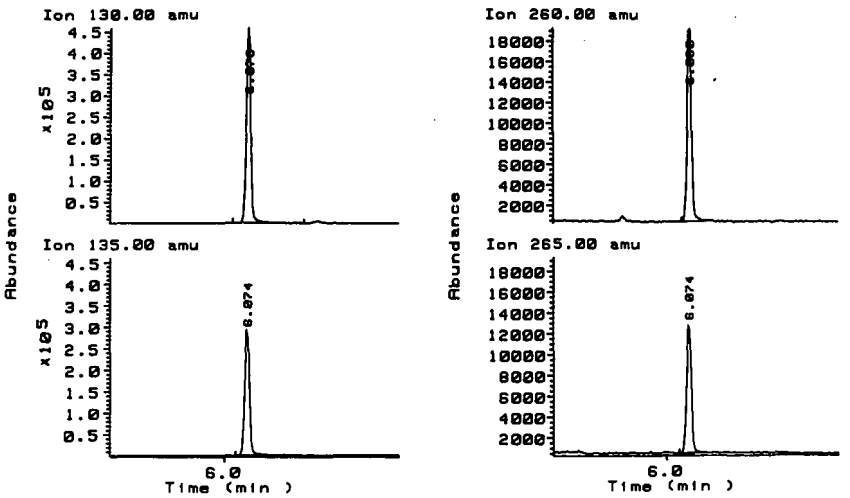

Fig. 2. Selected ion chromatograms for tryptophan isolated from leaf tissue. Ions at *m/z* 130 and 260 are the quinolinium and molecular ions from the native, plant derived, tryptophan while ions at 135 and 265 are from the [$^2H_5$]tryptophan internal standard.

peak B). After HPLC, the derivatized sample was sufficiently pure such that no major peaks, aside from derivatized tryptophan, were detectable by GC–SIM-MS.

A second objective of this study, once suitable purification and derivatization methods were developed, was the application of stable isotope dilution analysis to measure tryptophan in plant samples. For quantification of isolated and derivatized plant tryptophan by GC–SIM-MS two ion pairs were chosen: the quinolinium ion, characteristic for 3-substituted indoles (*m/z* 130 for the naturally occuring compound and *m/z* 135 for the internal standard) and the molecular ion (*m/z* 260 and 265 for the natural and deuterated compounds, respectively). Because the internal standard was labeled at high enrichment with five deuterium atoms on the indole ring, the ions derived from the endogenous compound and from the internal standard were separated by five atomic mass units and there was no overlapping of peaks derived from the endogenous compound and internal standard. Typical SIM traces, as shown for the sample of Rock Elm (*Ulmus thomasii* Sarg.) leaf tissue, are in Fig. 2.

The recovery of tryptophan, based on the radioactive tracer, was 50 to 60%, depending on sample size. The method has proven to be highly reproducible and has been applied to analyze low levels of tryptophan in a wide variety of plant samples including leaves from trees, seedlings of cereal grasses, and legume seedlings. In all of these plant materials, samples of 10 mg fresh weight were clearly sufficient for analysis. The precision of the technique is only limited by the accuracy of weighing the tissue, addition of the internal standard and integration of selected ion peaks. In our hands, variation of replicate samples was usually less than 2%. Thus, this method provides a convenient, sensitive and accurate technique for the routine analysis of tryptophan from complex plant samples.

ACKNOWLEDGEMENTS

This work was supported by grants from the US–Israel Binational Agricultural Research and Development Fund (US-1362-87), USDA-CRGO Plant Growth and Development (89-37261-4734) and by funds from the USDA Agricultural Research Service.

REFERENCES

1 J. D. Cohen, B. G. Baldi and J. P. Slovin, *Plant Physiol.*, 80 (1986) 14.
2 K-H. Chen, A. N. Miller, G. W. Patterson and J. D. Cohen, *Plant Physiol.*, 86 (1988) 822.
3 C. J. Biermann, C. M. Kinoshita, J. D. Marlett and R. D. Steele, *J. Chromatogr.*, 357 (1986) 330.
4 R. J. Early, J. R. Thompson, G. W. Sedgwick, J. M. Kelly and R. J. Christopherson, *J. Chromatogr.*, 416 (1987) 15.

5 P. Hušek and M. Macek, *J. Chromatogr.*, 113 (1975) 139.
6 T. P. Mawhinney, R. S. R. Robinet, A. Atalay and M. A. Madson, *J. Chromatogr.*, 358 (1986) 231.
7 M.J. Zagalak, H.-Ch. Curtius, W. Leimbacher and U. Redweik, *J. Chromatogr.*, 142 (1977) 523.
8 P. Felker, *Anal. Biochem.*, 76 (1976) 192.
9 D. R. Knapp, *Handbook of Analytical Derivatization Reactions*, Wiley, New York, 1979, p. 242.
10 J. M. L. Mee, J. Korth, B. Helpern and J. B. Lewis, *Biomed. Mass Spectrom.*, 4 (1977) 178.

Author Index

PUBLICATION SCHEDULE FOR 1992

Journal of Chromatography and *Journal of Chromatography, Biomedical Applications*

MONTH	O 1991–F 1992	M	A	M	J	
Journal of Chromatography	Vols. 585–593	594/1 + 2 595/1 + 2	596/1 596/2 597/1 + 2	598/1 598/2 599/1 + 2 600/1 600/2	602/1 + 2	The publication schedule for further issues will be published later.
Cumulative Indexes, Vols. 551–600						
Bibliography Section		610/1			610/2	
Biomedical Applications	Vols. 573 and 574	575/1 575/2	576/1	576/2 577/1	577/2	

INFORMATION FOR AUTHORS

(Detailed *Instructions to Authors* were published in Vol. 558, pp. 469–472. A free reprint can be obtained by application to the publisher, Elsevier Science Publishers B.V., P.O. Box 330, 1000 AH Amsterdam, The Netherlands.)

Types of Contributions. The following types of papers are published in the *Journal of Chromatography* and the section on *Biomedical Applications*: Regular research papers (Full-length papers), Review articles and Short Communications. Short Communications are usually descriptions of short investigations, or they can report minor technical improvements of previously published procedures; they reflect the same quality of research as Full-length papers, but should preferably not exceed five printed pages. For Review articles, see inside front cover under Submission of Papers.

Submission. Every paper must be accompanied by a letter from the senior author, stating that he/she is submitting the paper for publication in the *Journal of Chromatography*.

Manuscripts. Manuscripts should be typed in double spacing on consecutively numbered pages of uniform size. The manuscript should be preceded by a sheet of manuscript paper carrying the title of the paper and the name and full postal address of the person to whom the proofs are to be sent. As a rule, papers should be divided into sections, headed by a caption (*e.g.*, Abstract, Introduction, Experimental, Results, Discussion, etc.). All illustrations, photographs, tables, etc., should be on separate sheets.

Introduction. Every paper must have a concise introduction mentioning what has been done before on the topic described, and stating clearly what is new in the paper now submitted.

Abstract. All articles should have an abstract of 50–100 words which clearly and briefly indicates what is new, different and significant.

Illustrations. The figures should be submitted in a form suitable for reproduction, drawn in Indian ink on drawing or tracing paper. Each illustration should have a legend, all the *legends* being typed (with double spacing) together on a *separate sheet*. If structures are given in the text, the original drawings should be supplied. Coloured illustrations are reproduced at the author's expense, the cost being determined by the number of pages and by the number of colours needed. The written permission of the author and publisher must be obtained for the use of any figure already published. Its source must be indicated in the legend.

References. References should be numbered in the order in which they are cited in the text, and listed in numerical sequence on a separate sheet at the end of the article. Please check a recent issue for the layout of the reference list. Abbreviations for the titles of journals should follow the system used by *Chemical Abstracts*. Articles not yet published should be given as "in press" (journal should be specified), "submitted for publication" (journal should be specified), "in preparation" or "personal communication".

Dispatch. Before sending the manuscript to the Editor please check that the envelope contains four copies of the paper complete with references, legends and figures. One of the sets of figures must be the originals suitable for direct reproduction. Please also ensure that permission to publish has been obtained from your institute.

Proofs. One set of proofs will be sent to the author to be carefully checked for printer's errors. Corrections must be restricted to instances in which the proof is at variance with the manuscript. "Extra corrections" will be inserted at the author's expense.

Reprints. Fifty reprints of Full-length papers and Short Communications will be supplied free of charge. Additional reprints can be ordered by the authors. An order form containing price quotations will be sent to the authors together with the proofs of their article.